UNIVERSITAT DE BARCELONA

Analysis and coordination of different mechanisms controlling tube elongation during the development of the embryonic system in *Drosophila melanogaster*

Ivette Olivares Castiñeira

Departamento de Genética, Microbiología y Estadística
Programa de Doctorado de Genética (HDK0S)
Facultad de Biología
Universidad de Barcelona

Analysis and coordination of different mechanisms controlling tube elongation during the development of the embryonic tracheal system in *Drosophila melanogaster*

Memoria presentada por

Ivette Olivares Castiñeira

Para optar al grado de

DOCTOR por la Universidad de Barcelona

Tesis dirigida por

Marta Llimargas Casanova
En el Instituto de Biología Molecular de Barcelona (IBMB)-
Consejo superior de investigaciones Científicas (CSIC)

Marta Llimargas Casanova
Directora

Pedro Martínez Serra
Tutor

Ivette Olivares Castiñeira
Autora

ACKNOWLEDGEMENTS

M'agradaria donar les gràcies a totes aquelles persones que de més i de menys han contribuït durant aquests 4 anys, sense la seva ajuda i suport aquest difícil camí no hauria estat el mateix.

Primer de tot vull donar les gràcies a la meva directora, la Marta Llimargas, per donar-me l'oportunitat d'endinsar-me en aquest món de la investigació, tan complicat i feixuc però alhora tan fascinant. Agrair-te tot el que he après tan a nivell de treball com de persona i gràcies per fer-me créixer personalment i professionalment. Agradecer también a la segunda persona que más importante ha sido para mi durante esta etapa, a ti Anni. Sin tu incondicional ayuda nada hubiera sido lo mismo. Tanto a nivel laboral, en el que me has ayudado muchísimo, como personal hemos pasado muy buenos momentos. Nuestras risas infinitas por tonterías (zapatos de pelo), nuestra adición a comprar cosas por internet (bolsos, zapatos, relojes, pulseras…), ponernos de acuerdo con la ropa casi cada día, el apoyo mutuo y la complicidad con la que venir cada día al trabajo se ha hecho mucho más llevadero. También agradecer a dos personas que siempre han estado ahí para ayudarme, Nico y Esther. A ti Nico por tu gran ayuda con los CRISPR y en todo lo molecular en general. Sin ti nada saldría en el lab, siempre tienes alguna solución para todo y gracias por animar siempre el laboratorio. A ti Esther por ayudarme siempre con cualquier problema en el lab, por el apoyo que siempre me has dado, por las risas y por nuestras salidas fuera del laboratorio, roma, cursas, perritos. Echaré de menos al equipo Running y nuestros super desayunos.

Agrair al meu company de taula durant aquests quatre anys, Guillem. Gràcies per les bones converses, pels riures, per compartir els mateixos maldecaps de la tesi i per ser un excel·lent company de tesi, bona sort en la nova etapa. A Ettore por ser la super nueva incorporación. Aunque no vayamos a compartir muchos años, al menos los que sí han sido para ver que eres muy paciente y trabajador y en los momentos de desespero también me has dado tu apoyo. Mucha suerte en tu tesis, seguro que te irá genial.

Muchas gracias también a todas esas personas que encontré al principio y que por desgracia ya no están. Pili, fuiste como una madre para todos nosotros, siempre preocupándote por todos y también quiero agradecerte las risas en el lab y todo el apoyo que tuve por tu parte. A mis chicas, Arzu y Lorena, aunque estemos lejos nunca olvidaré nuestras noches en la rosa negra, nuestras risas, mojitos y momentos en los que me sentí muy contenta de haberos conocido. Espero que en algún momento nos volvamos a ver. A todos aquellos que ya no están pero que también formaron parte de estos años, Guille, Pablo, Paula, Oscar y Gonzalo por las risas y buenos momentos en la flyroom, Kyra, Delia y Ale por ser los italianos más divertidos y por pasar muy buenos momentos en el lab, a la Marina, per ser una super estudiant i pels bons moments i riures que vàrem passar, i la Neus, la millor tècnic que podíem haver tingut. Va ser un plaer poder coincidir amb tu.

Agradecer a todos los miembros del laboratorio de Jordi Casanova y Marta, al Jordi pels llargs labmeetings preguntant y debatint, al Marc per la seva ajuda en els nostres projectes, a Juanjo por siempre ayudarme en cualquier duda que he tenido en los experimentos y por

las risas en la flyroom y a Sofia por su incondicional ayuda, a Sara, Xavi, Bea, Fridi, Sandra y a Yolanda porque sin ti el lab sería un caos.
A las chicas de Gerardo, Marta per ajudar-me també amb els CRISPRs i pels riures al café, a la Núria per compartir riures, roba, viatges i bons moments, a Laura, Sara y Aikaterini.

I després de tots vosaltres, vull agrair a la meva família que sempre m'han donat força i un somriure en els moments difícils. Als meus pares, Eduard i Núria, per estar sempre al meu costat i donar-me el suport i el millor consell. Sense vosaltres no hauria estat el mateix però sé que sempre estareu al meu costat. També a la meva avia que sé que estarà orgullosa de mi.
A los padres de Ruben, Juan y Palmira, por todo el apoyo recibido y por darme las fuerzas necesarias para no decaer nunca. A la Manoli, Josep, Anna i Núria per preocupar-vos sempre per mi i preguntar com portes la tesi?
A tots els meus amics de Roda i del Palcam, per tots els anys que fa que ens coneixem i gràcies per donar-me sempre l'empenta i el suport, per estar al meu costat i per continuar sent amics després de tants anys.
Por último, y una de las personas más importantes de mi vida, agradecer a Ruben el apoyo recibido cada día, los ánimos incesantes en los momentos más difíciles y agobiantes de la tesis, por empujarme a realizar todo aquello que quiero y darme ese poder y fuerza para realizarlo. Gracias infinitas porque sin ti todo hubiera sido más difícil y gracias por tu amor incondicional.

Per a Eduard, Núria i Ruben….

INDEX

1. INTRODUCTION 1
1.1 *Drosophila* tracheal system as a model to study tubulogenesis 1
1.2 Overview of the embryonic tracheal development 1
1.3 The genetic program controlling tracheal development 3
1.4 Mature branching pattern 3
1.5 Tracheal tube architecture 4
1.6 Cellular organization of tracheal system 7
1.7 Tracheal tube maturation: tube elongation and expansion 8
1.7.1 Mechanisms that regulate tube growth 9
1.7.2 Circumferential enlargement 11
1.7.3 Axial elongation 12
1.7.3.1 Modification of the aECM 12
1.7.3.2 Crb plays a key role in tube size control 14
1.7.3.3 Src kinases control axial elongation 16
1.8 Epidermal growth factor receptor 17
1.8.1 EGFR activity in the tracheal system 18
1.8.2 EGFR signalling pathway 19
1.8.3 EGFR ligands 20
1.8.4 Nuclear factors 21
1.9 Endocytic routes 23
1.9.1 The Retromer complex 25
1.9.2 The retromer complex and apical polarity trafficking 26
1.9.3 Trafficking of luminal cargoes 28
1.9.4 Rab GTPases 28

2. OBJECTIVES 33

3. MATERIAL AND METHODS 37
3.1 *Drosophila* strains 37
3.2 Immunohistochemistry 39
3.3 Antibodies 40
3.4 Image acquisition and processing 41
3.5 Morphometric analysis 41
3.5.1 Tube size quantifications 41
3.5.2 Cell junctions length 42
3.5.3 Crb intensity levels 42
3.5.4 Crb subcellular accumulation 42
3.5.5 Crb anisotropy accumulation 42
3.5.6 Crb Serp colocalization 43
3.5.7 Analysis of cargoes in endosome 43
3.5.8 Cell number 43
3.6 FRAP assay 43
3.7 Time-lapse imaging 44
3.7.1 Vesicle dynamics 44
3.7.2 Crb apical subcellular accumulation 44
3.8 Quantifications and statistics 44

4. RESULTS 47
4.1 EGFR requirement in tracheal tube size 47

4.1.1 The modulation of EGFR activity controls tube length 47
4.1.2 Cell number and cell shape 49
4.2 EGFR activation in tube size control 50
4.2.1 The role of Spi in the control of DT elongation 50
4.2.2 The activity of Vein and keren in tracheal formation 52
4.3 The requirement of the RAS-MAPK pathway in tube size control 54
4.3.1 EGFR controls tube size by the RAS-MAPK pathway 54
4.3.2 The nuclear requirement of EGFR signalling in tube size 55
4.4 EGFR mechanism of tube size regulation 58
4.4.1 EGFR controls Serp accumulation in the aECM 58
4.4.2 EGFR controls Crb accumulation in the DT 60
4.5 Crb apical subcellular accumulation 62
4.5.1 Crb subcellular accumulation during tracheal formation 64
4.5.2 Crb subcellular accumulation depends on its endocytosis 66
4.6 Crb apical localisation and recycling pathways 68
4.6.1 The role of Rab4 in Crb recycling 68
4.6.2 The role of RE-Rab11 in Crb recycling 71
4.7 Serp and Crb localise in common sorting endosomes 73
4.7.1 Serp and Crb recycling mutually affect each other 75
4.8 EGFR is required for the proper organisation of Serp-Crb endosomes 78
4.9 EGFR affects WASH complex localisation 79
4.10 Crb anisotropic accumulation in DT cell junctions 83
4.10.1 Crb anisotropically accumulation in the control 83
4.10.2 Crb anisotropic accumulation is decreased in the Src42A^{DN} mutant embryos 86
4.11 Constitutively activation of Src42A affects Crb junctional accumulation and Serp luminal deposition 89

5. DISCUSSION 95
5.1 EGFR restricts tube elongation in the trachea 95
5.2 A role for EGFR in endocytic traffic regulation 97
5.3 The regulation of Crb localisation in the trachea 98
5.4 The regulation of Crb anisotropic accumulation in DT cell junctions 101
5.5 A possible connection between Src42A activity and intracellular trafficking 102

6. CONCLUSIONS 105

7. BIBLIOGRAPHY 109

8. APPENDICES 125
8.1 List of abbreviations 125
8.2 Movie legends 128
8.3 Summary 129
8.4 Resumen en castellano 131
8.5 Published papers 132

1. INTRODUCTION

1. INTRODUCTION

1.1 *Drosophila* tracheal system as a model to study tubulogenesis

A major goal of developmental biology is to understand organ formation. The branched tubular network is one of the most common structural designs used in organ formation, and it is present in organs such as the lung, kidney and the vascular system. These organs carry out essential functions such as the transport of gases or body fluids. The morphogenesis of branched tubular structures is known as tubulogenesis.

Drosophila melanogaster has been proven to be an excellent model for identifying the underlying molecules and mechanisms of many aspects for development and disease. As with all multicellular organisms, *Drosophila* contains a variety of tubular organs such as the salivary gland, the tracheal system (respiratory organ) and the Malpighian tubules (the excretory system). Since the mechanisms of tube formation are conserved from worms to humans (Andrew and Ewald 2010) and it is difficult to analyse these structures in mammalian systems, due to their complexity, the *Drosophila* tracheal system has emerged as a good model to study tubulogenesis. The tracheal system of *Drosophila*, a highly branched tubular network, is a vey well-described system for understanding the molecular and cellular underpinnings of tube formation. Furthermore, the huge amount of genetic tools and cellular approaches helps to understand in detail the formation of branched structures.

1.2 Overview of the embryonic tracheal development

The tracheal system is established during embryonic development when a group of epithelial cells are determined to become part of the tracheal system as ten ectodermal placodes (or clusters) on each side of the stage (stg) 9 embryo (Manning and Krasnow, 1993, Affolter and Caussinus 2008, Maruyama and Andrew 2012, Schottenfeld et al. 2010, Uv et al. 2003, Loganathan et al. 2016). Subsequently, at stg 10 of embryogenesis, these cells on either side of the embryo invaginate in an ordered choreography to form the internalised tracheal sacs through an apical constriction mechanism. This structure generates the luminal cavity, which is subsequently expanded and remodelled during the branching process. Later, at stg 11, the around 40 tracheal cells of each placode undergo the final round of mitotic division resulting in 80 cells per tracheal segment (metamere). Thereafter, subsets of cells within each sac begin to migrate towards specific directions in a stereotypical manner to form the distinctive branches visible from stg 12 onwards. At stg 13-14, through cell rearrangements, and cell shape changes, tracheal cells undergo a distinct sequential programme of branch sprouting, directed branch outgrowth and branch fusion. These buds elongate to form branches of distinct cellular architecture, ranging from multicellular tubes to fine branches. From stg 14 onwards, an interconnection of the

metameric, branched units at distinct fusion points occurs. Meanwhile, terminal tracheal cells at the branch tips extend the luminal space into individual cell extensions, which adopt tree-like structures and reach every cell. The air enters the trachea through specialized openings, the spiracles, and at the tip of the terminal branches, gas is exchanged with the surrounding tissue once the tracheal system becomes physiologically active at the end of the embryogenesis (Affolter and Caussinus 2008) (Fig.1).

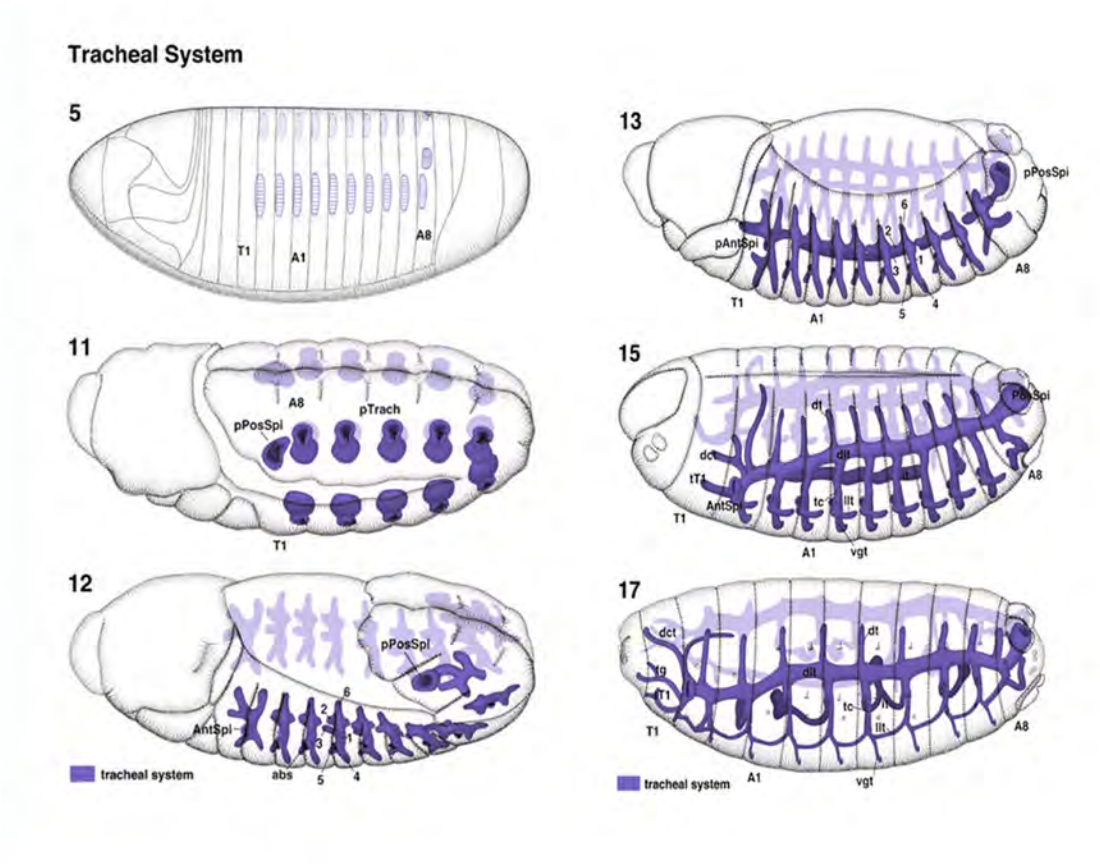

Figure 1. Development of embryonic *Drosophila* tracheal system. There are ten tracheal placodes at each side of the embryo at stage 10. Tracheal cells undergo apical constriction and starts to invaginate to form internalized tracheal sacs at stage 11. From stage 12, subsets of cells bud towards different directions giving rise to the different branches that will continue extending as development proceeds. From stage 14, the tracheal cells will mediate branch fusion with contralateral or adjacent branches, forming a continuous tubular tracheal network until the end of embryogenesis (From Atlas of Drosophila Development by Volker Hartenstein).

1.3 The genetic program controlling tracheal development

The genetic program and the signalling pathways underlying tracheal development have been extensively studied for the last years. Tracheal cell specification requires a combination of transcription factors, including *trachealess* (*trh*), *ventral veinless* (*vvl*) and *knirps/knirps-related* (Affolter and Shilo 2000). Once the tracheal placodes are formed, the cells invaginate by apical constriction to form internalized tracheal sacs (Isaac and Andrew 1996, Llimargas and Casanova 1999), in a process that requires the expression of Trh (Isaac and Andrew 1996, Wilk et al. 1996). In Trh mutants, tracheal primordia fail to accumulate apical actin and do not constrict, remaining at the surface of the embryo. Therefore, the invagination of the tracheal pits is associated with an accumulation of actin at the cell surfaces and both invagination and actin accumulation are dependent on *trh* activity (Isaac and Andrew 1996, Llimargas and Casanova 1999). *Trh* controls invagination partly through the transcriptional activation of *rhomboid* (*rho*) (Boube et al. 2000, Zelzer and Shilo 2000), which encodes a protein essential for the processing of the Epidermal Growth Factor ligand (EGF ligand) (Lee et al. 2001). However, in *rho* mutants tracheal invagination is only partially affected, indicating that additional pathways may function downstream of Trh to control internalization. In this respect, a role for the apical determinant Crumbs (Crb) in tracheal invagination was proposed (Letizia et al. 2011).

Upon invagination, the migration of specific tracheal branches along distinct trajectories requires the Fibroblast Growth Factor (FGF)/ Breathless (Btl) signalling pathway (Sutherland et al. 1996). Subsequent branch sprouting and outgrowth occurs without cell division as cells migrate towards neighbouring cells or towards tissues that express sources of the Btl ligand Branchless (Bnl) and attractant signal of the Fibroblast Growth Factor Receptor (Fgfr). Therefore, Bnl/Fgf secretion controls the migratory behaviour and the direction of tracheal cell movement (Sutherland et al. 1996). Cells at the tip of the tracheal branches, called tip cells, appear to be highly dynamic and send out filopodia and lamelopodia in response to Btl/Fgfr signalling, thereby regulating cytoskeleton dynamics (Okenve-Ramos and Llimargas 2014a, b, Ribeiro et al. 2002). In the absence of Fgfr signalling, cells remain in the sac-like shape, and filopodia and lamelopodia are not seen (Ribeiro et al. 2002), demonstrating that Bnl/Fgf signalling regulates both motility and the directionality of tracheal cell movement in the embryo. The Fgf signalling leads to phosphorylation and activation of the Ras/Mitogen-Activated Protein Kinase (MAPK) cascade, which in turn regulates the expression of several target genes to control cell behaviour (Affolter and Caussinus 2008).

1.4 Mature branching pattern

The tracheal system is a complex structure that consists of interconnected metameric units of different-sized tubes that extend over the entire embryo until the end of the embryogenesis. Different branches can be distinguished in the mature embryonic tracheal

system (Fig.2A,B,C). The dorsal trunk (DT) extends along the anterior-posterior axis of the embryo and forms the major tracheal tube. The dorsal branches, (DBs) extend towards the dorsal midline. DBs of each side fuse with their contralateral ones at the dorsal midline. The transverse connective (TC) sprouts from the DT and extends ventrally. The visceral branches (VBs) sprout from the TC and extend internally towards the gut. A lateral trunk (LT) forms parallel to the DT. The ganglionic branches (GBs) extend from the TC and reach the ventral nerve cord. Finally, the group of cells that remain near the site of the invagination form the spiracular branches (SBs) (Manning and Krasnow, 1993).

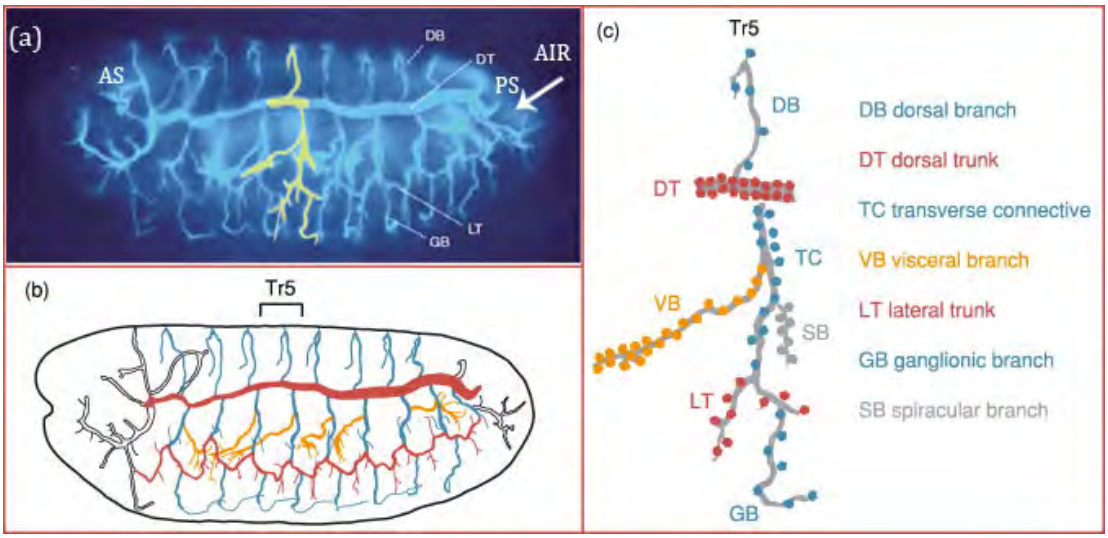

Figure 2. Structure of a tracheal metamere. **(A, B)** Lateral view of the embryonic tracheal system of *Drosophila*. Abbreviations: Anterior and posterior spiracle (AS, PS). **(C)** A schematic representation of a single tracheal metamere. The main branches are indicated: the dorsal trunk (DT); dorsal branch (DB); transverse connective (TC), visceral branch (VB); lateral trunk (LT); ganglionic branch (GB); spiracular branch (SB). Adapted from (Uv et al. 2003).

1.5 Tracheal tube architecture

Each tracheal branch within a metamere has fixed cell numbers (Samakovlis et al. 1996) and characteristic tubular dimensions (Beitel and Krasnow 2000). We can classify the tracheal branches into four major types according to their size and cellular architecture (Uv et al. 2003):

Type I tubes, such as the DT (the major branch of the trachea) and the majority of TC (the stalk connecting all of the tracheal branches within each metamere), are multicellular tubes. In these tubes, several cells are connected by intercellular junctions and surround an extracellular central lumen.

The type II tubes, such as the LT, GB, DB and VB, are narrower and multicellular. These tubes comprise a linear arrangement of single cells whose apical surfaces surround an extracellular lumen. Cells connect with themselves through autocellular junctions and with their neighbours through intercellular junctions. The main function of type I and II tubes are to transport gases.

Type III tubes interconnect type I and type II tubes of the adjacent or contralateral tracheal metameres to mediate luminal branch fusion and form a continuous network. They are composed of tubular protrusions of single cells attached to each other, resulting in seamless tubes without intracellular junctions. Meanwhile, the two fusion cells connect themselves by intercellular junctions and form an intracellular lumen.

Type IV tubes, such as the lateral ganglionic (LG) branches, are highly branched intracellular cytoplasmic extensions that form in terminal cells at the tips of the tubes. Their main function is to contact target tissues for gas exchange (table1, Fig.3A,B,C).

Table1. Types of tracheal tubes. Abbreviations used: DT: Dorsal trunk, TC: Transverse connective, LT: Lateral trunk, GB: Ganglionic branch, DB: Dorsal branch, VB: Visceral branch and LG: Lateral ganglionic. Adapted from (Zuo et al. 2013).

Type	Cellular make-up surrounding the central lumen	Tracheal tubes	Connections of cells surrounding the lumen	Lumen
I	Multicellular	**DT, TC**	Intercellular junction	Extracellular
II	Multicellular	**LT, GB, DB, VB**	Autocellular junction	Extracellular
III	Tubular protrusions of single cells	**Connect type I and II (fusion cells)**	Seamless, no intracellular junction	Intracellular
IV	Intracellular cytoplasmic extension	**LG (terminal cells)**	Seamless, no intracellular junction	Intracellular

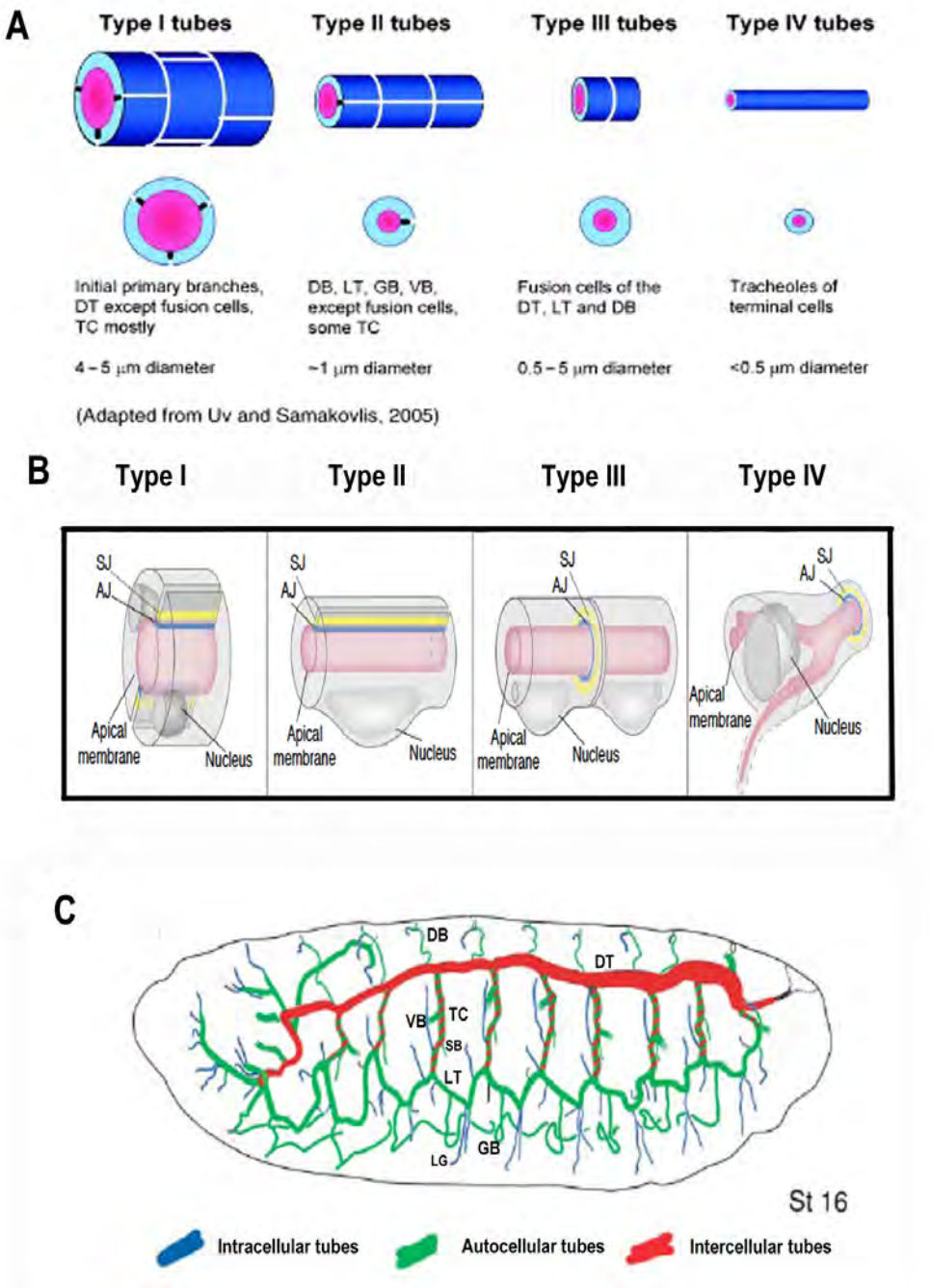

Figure 3. Types of tracheal tubes. **(A)** Scheme representation shows the types of tubes that form in the *Drosophila* trachea, indicating which type of tube is found in each branch. The lumen is shown in pink, with the apical membrane in dark pink. The basal surface is dark blue and the cytoplasm is lighter blue. Adapted from (Kerman et al. 2006, Tonning et al. 2005)**. (B)** Four distinct cellular types of tubes. Abbreviations used: AJ: Adherens junctions, SJ: Septate junctions. Adapted from (Uv et al. 2003). **(C)** Schematic overview of the different patterns of tubes. Intracellular tubes are shown in blue, autocellular tubes in green and intercellular in red. Abbreviations used: DT: Dorsal trunk, TC: Transverse connective, LT: Lateral trunk, GB: Ganglionic branch, DB: Dorsal branch, VB: Visceral branch, LG: Lateral ganglionic and SB: Spiracular branch. Adapted from (Ribeiro et al. 2004).

1.6 Cellular organization of tracheal system

The *Drosophila* trachea is a ramifying network of epithelial tubes. The tracheal cells have features characteristic of typical epithelial such as apicobasal polarity, maintenance of tissue integrity via cell-cell and cell-extracellular matrix adhesions, a basement membrane and the capacity for directed secretion. The development of the tracheal system involves dramatic tissue remodelling, including cell rearrangements and cell shape changes. Remarkably, during remodelling cells that form the tracheal tubes remain attached to one another maintaining their epithelial integrity and polarity. A single layer of polarized epithelial cells composed of apical and basal membrane domains forms the embryonic tracheal tube. The apical membrane of the tracheal cells faces the luminal cavity filled with an apical extracellular matrix (aECM)[1] whereas, the basolateral membrane is in contact with neighbouring cell or either basal membrane (Fig.4).

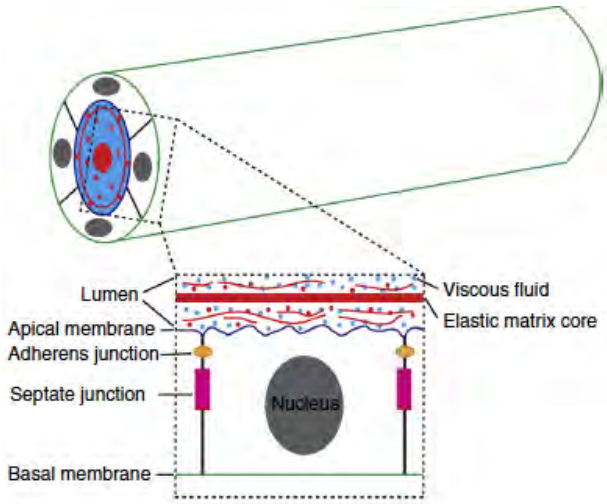

Figure 4. Schematic representation of tracheal epithelial cells. Top: epithelial cells surrounding the tracheal luminal space by its apical side. Bottom: single epithelial cell facing the apical membrane to the lumen. Inside the lumen, aECM is formed by a viscous fluid and an elastic matrix core. From (Dong and Hayashi 2015).

Epithelial cells contact each other through junctional structures that serve to link the cells and provide structural support, prevent the diffusion of membrane proteins and lipids, and provide barrier functions. Apical and basal regulators are associated with distinct membrane domains:

Adherens junctions (AJ) contain E-cadherin (E-Cadh) and Armadillo (βCatenin) form a cell-cell adhesive belt around the apical membrane, known as the Zonula adherens (ZA) that segregate the apical and basolateral membrane domains. Just apical to the ZA lies the

[1] **Apical Extracellular Matrix (aECM)**: It is an extracellular scaffolding matrix that provides mechanical support for tissue assembly and organ shape. It is mainly constituted of secreted transmembrane proteins and polysaccharides, fibrous structural proteins, fluids and signalling molecules, forming an organized meshwork closely associated with the cell membrane (Labouesse, 2012). aECM is present both at the basal and apical surfaces of epithelia.

Subapical region (SAR), also described as marginal zone. The SAR is defined by the presence of Crb and Par complexes, which have an important role in establishing epithelial polarity (Knust and Bossinger 2002). The Septate Junctions (SJs), equivalent to the tight junctions in vertebrates, are found below the AJs at the basolateral membrane. The SJ functions as the diffusion barrier that controls the exchange of solutes between epithelial cells. The SJ is composed of several protein complexes. (Laprise and Tepass 2011, Swanson and Beitel 2006, Wu et al. 2004). The most apical part of the plasma membrane forms an apical free membrane or region (AFR) and in the tracheal cells it faces directly the extracellular space contacting the tube lumen (Fig.5A).

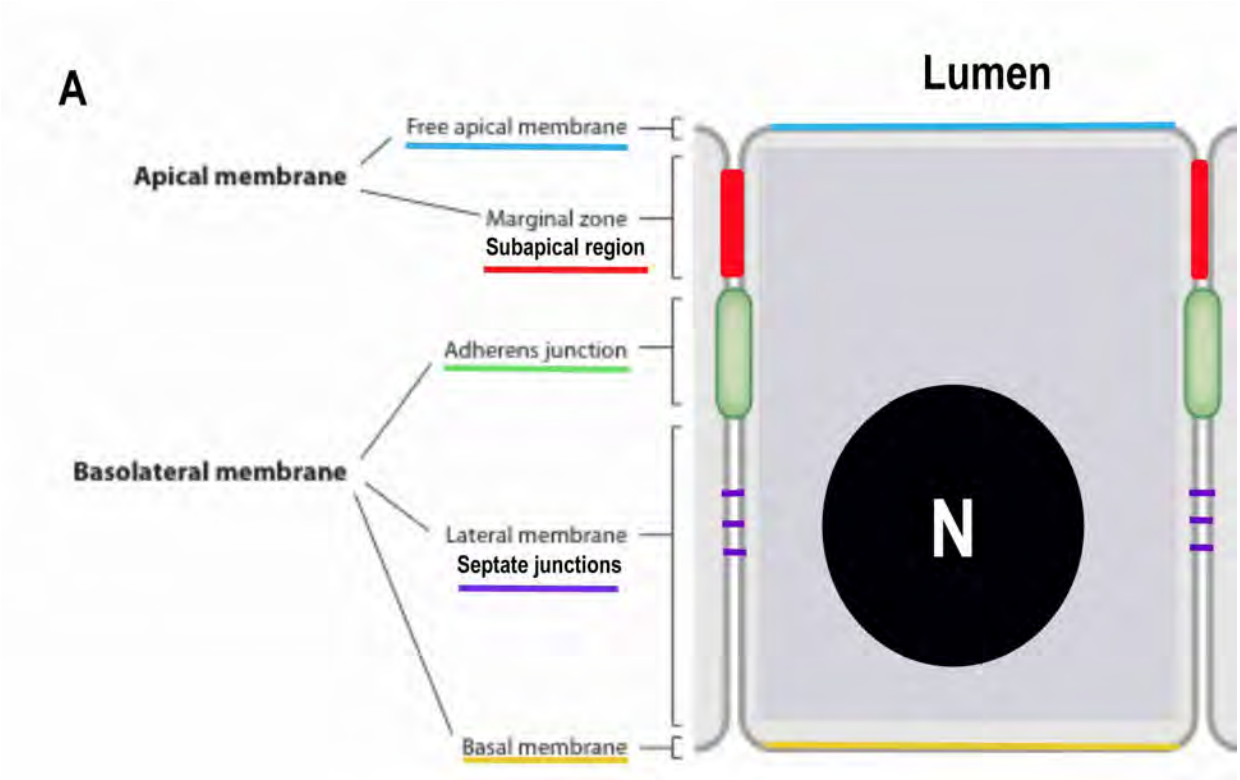

Figure 5. Organization of the *Drosophila* epithelial cells. (A) Scheme of *Drosophila* epithelial cell. The tracheal cells are epithelial cells with polarized plasma membrane associated with two membrane domains: Apical and basolateral membrane. The apico-basal polarity region of these cells is maintained through interactions between apical polarity regulators and basolateral polarity regulators. Adapted from (Tepass 2012).

1.7 Tracheal tube maturation: tube elongation and expansion

After a morphogenetic phase in which the branches form by branching morphogenesis, tracheal branches undergo a process of maturation (Tsarouhas et al. 2007). This branch maturation process includes the acquisition of the correct size concerning length and diameter, unique to each type of branch (Ghabrial A. et al. 2003) and required for proper tube function. The DT is one of the most extensively studied branches in the context of tube size control and geometry regulation (Beitel and Krasnow 2000).

1.7.1 Mechanisms that regulate tube growth

The tracheal tubes have to be constructed with an optimal shape for the efficient circulation of gas. In *Drosophil*a, the growth of embryonic tracheal tubules proceeds in two dimensions, by axial elongation and diameter expansion. Maintaining a constant tube diameter and fitting axial length, which are controlled by distinct genetic programs and cellular mechanisms (Beitel and Krasnow 2000), are two key requirements for proper tube function (Fig.6A,B,C).

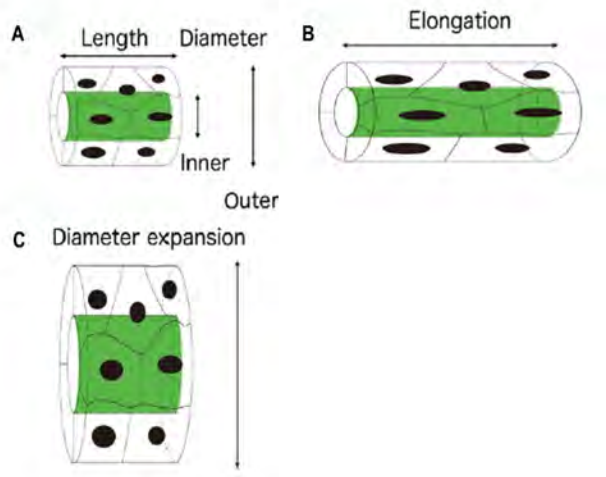

Figure 6. Schematic drawings of DT elongation and expansion. **(A, B, C)** Scheme representing the DT axial extension (tube elongation) along the long axis and the diameter expansion (tube dilatation, circumferential) increasing the circumference of the lumen cavity. Luminal space is labelled in green. Cell outline and nucleus are drawn in black line and filled circle, respectively. Adapted from (Hayashi and Dong 2017).

The aECM, which fills the entire tube lumen, is essential for the generation of these two growth forces. The aECM is formed by various proteins and polysaccharides secreted from the tracheal cells (Devine et al. 2005, Tonning et al. 2005). The components of the aECM include: chitin, chitin deacetylation domain proteins (serpentine/Serp and vermiform/Verm), chitin associated proteins (2A12/Gasp and Obstructor-A/Obst-A), and zona pellucida (ZP) domain proteins (Dumpy/Dp and Piopio/Pio) (Table2, Fig.7). These components span a wide range of molecular sizes and are distributed in unique patterns, suggesting that aECM is a complex of various structural elements.

Table 2. Apical ECM components. Abbreviations used: ZP: Zona pellucida, AP: Anterior-Posterior. From (Dong and Hayashi 2015)

aECM	Molecule characteristics	Expression Stg	Luminal pattern	Tracheal tube phenotype in mutants	References
Chitin	Chitin	From stg 13 to 16	AP axis orientated fibers	Tube over-elongation/irregular diametric expansion	(Tonning et al. 2005)
Serp	Chitin deacetylase	From stg 12 and start to fade from stg 15	Diffusible in the lumen	Tube over-elongation	(Dong et al. 2014a, Forster et al. 2010, Luschnig et al. 2006, Wang et al. 2006)
Verm	Chitin deacetylase	From stg 12 and start to fade from stg 15	Diffusible in the lumen	Tube over-elongation	(Luschnig et al. 2006, Wang et al. 2006)
Obst-A	Chitin associated protein	From stg 13 onward	Diffusible in the lumen	Tube over-elongation/defects of tube diametric expansion	(Petkau et al. 2012, Tiklova et al. 2013)
2A12	Chitin associated protein	From stg 13 onward	Diffusible in the lumen	Defects of tube diametric expansion	(Tiklova et al. 2013)
Dp	ZP domain protein	From stg 11 onward	Affinity to apical membrane with a dense and elastic core	Tube over-elongation/defects of tubular integrity	(Dong et al. 2014a, Wilkin et al. 2000)
Pio	ZP domain protein	From stg 11 and start to fade from stg 14	Affinity to apical membrane with a dense core	Defects of tubular integrity	(Jazwinska et al. 2003)

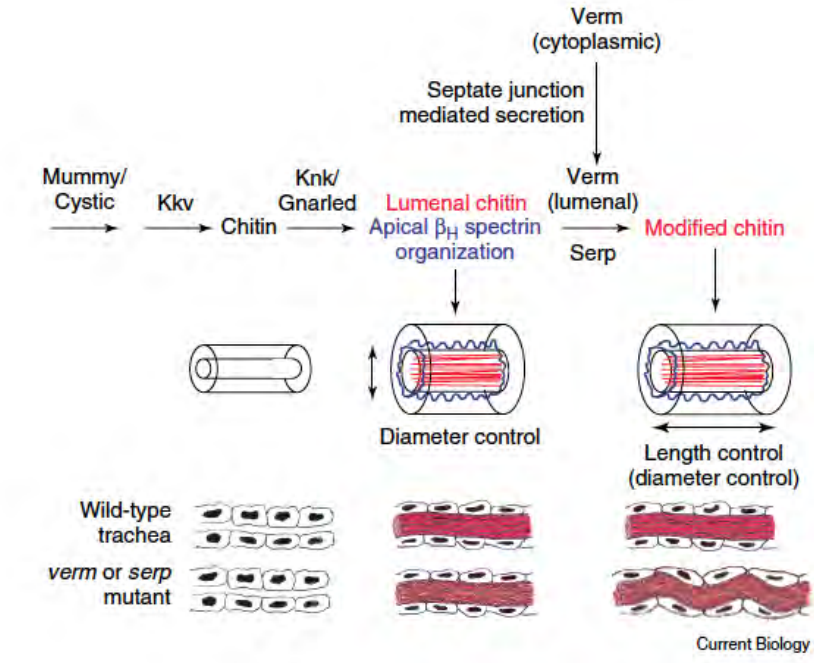

Figure 7. Model for the tracheal tube size control in *Drosophila*. The expansion of the diameter of the tracheal tubes from narrow to longer takes place during the embryogenesis by the transient chitin fibrils matrix (red) that is also required for the normal organization of the apical β_H spectrin cytoskeleton (blue). Septate junctions mediate the Verm and Serp secretion, which is required for the subsequent modification of chitin matrix, to prevent enlarges of the tracheal cells and tubes. From (Swanson and Beitel 2006).

1.7.2 Circumferential enlargement

The deposition of the aECM in the luminal space is associated with the onset of a diametrical expansion of the tube (Forster et al. 2010). This diametrical expansion is carried out in a defined time interval between embryonic stages 14-15. Different luminal proteins present in the tracheal cell cytoplasm are secreted into the lumen by different vesicle trafficking COPI (Coat complex protein I) (Armbruster and Luschnig 2012, Jayaram et al. 2008) and COPII-mediated complexes (Coat complex protein II) (Norum et al. 2010) (COPI: γCOP, σCOP; COPII: sec23, sec24, sar1, sec13) and by the Diaphanous-dependent secretory pathway (Massarwa et al. 2009). All these secretory pathways are required for the deposition of aECM components and the addition of apical membrane, leading to expansion of the intraluminal space (Fig.8).

Furthermore, the chitin fibrils are deposited along the tube lumen and coordinate uniform tube expansion. In the absence of chitin synthesis, the lumen is expanded in an irregular manner causing tube dilations (Tonning et al. 2005). Thus, the chitin cable coordinates the behaviour of the tracheal cells that surround it, and stabilizes the epithelium during diametric expansion (Schottenfeld et al. 2010).

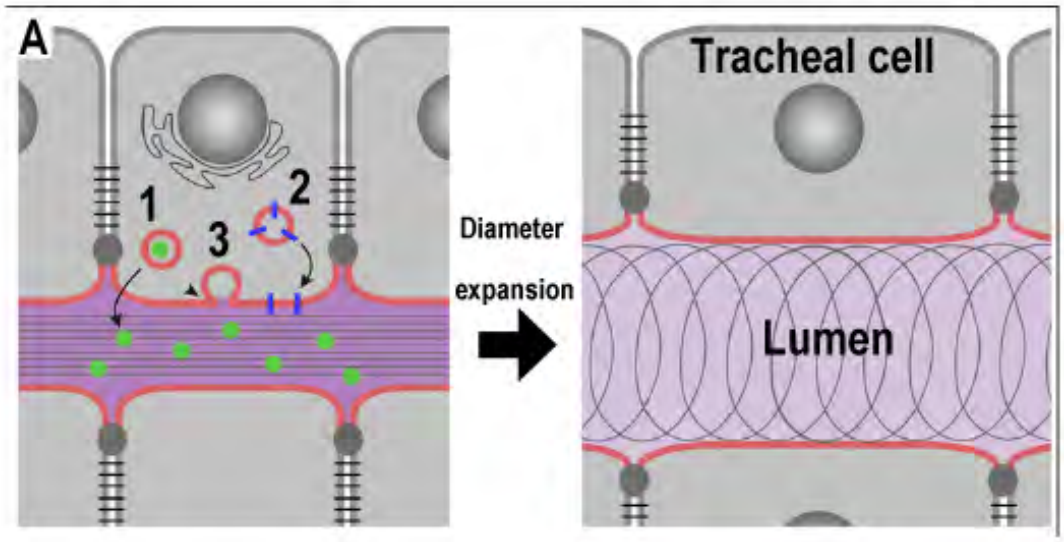

Figure 8. Model with the secretion roles implicated in tracheal tube expansion. (A) Secretory activity mediates tracheal lumen expansion by (1) soluble secreted proteins in the lumen, (2) membrane proteins delivered to the apical cell surface and (3) membrane material released into the lumen cavity required for the proper diameter expansion. From (Forster et al. 2010). Moreover, the chitin fibrils inside the lumen send signal to the epithelial cells to organize the luminal diameter (Swanson and Beitel 2006).

1.7.3 Axial elongation

Following diametrical expansion the tube grows axially until the end of the tracheal development. Studies using tube elongation defective mutants (Beitel and Krasnow 2000, Ghabrial A. S. et al. 2011) have shown that axial growth requires Septate junctions (Llimargas et al. 2004, Paul et al. 2003, Wang et al. 2006, Wu et al. 2004), the subapical protein complex (Dong et al. 2014a, Laprise et al. 2010), planar cell polarity (Chung et al. 2009) and the maintenance of chitin deacetylases and Src kinase levels (Forster and Luschnig 2012, Luschnig et al. 2006, Nelson et al. 2012, Wang et al. 2006) Disruption of all these processes, with the exception of maintenance of Src kinase levels, leads to over-elongated tubes. However, the exact molecular mechanisms that cause tube over-elongations remain uncharacterized.

1.7.3.1 Modification of the aECM

The proper organization and modification of the aECM is required to restrict tube over-elongation. When the remodelling of the chitin polymer is compromised due to a loss of function of the secreted chitin deacetylases (Serp amb Verm) (Luschnig et al. 2006, Wang et al. 2006), the tracheal tubules exceed their normal length and show convoluted patterning. Therefore, such over-elongated tube phenotype suggests that an axial elongation force is present in the tracheal cells and that aECM restricts the excess elongation.

Chitin undergoes a deacetylation reaction resulting in the exposure of an amino group that converts insoluble chitin into a biologically compatible form with a rigid structure, the chitosan (Kim, 2011). The modification of the chitin cable is essential to restrict tube over-elongation. Serp and Verm, secreted proteins which contain both chitin binding and deacetylase domains, are putative chitin deacetylases present in the tracheal lumen and their function is required to restrict tracheal tube length (Fig.9E,F) (Luschnig et al. 2006, Wang et al. 2006). The lack of chitin modification by the absence of Serp and Verm leads to an over-elongated and convoluted DT at stages 15-16 of tracheal development, while there is little or no effect in the diameter of the DT (Fig.9A-D, F). This suggests that tube length is controlled separately from diameter by modulation of physical properties of the chitin ECM (Luschnig et al. 2006) (Fig.9F).

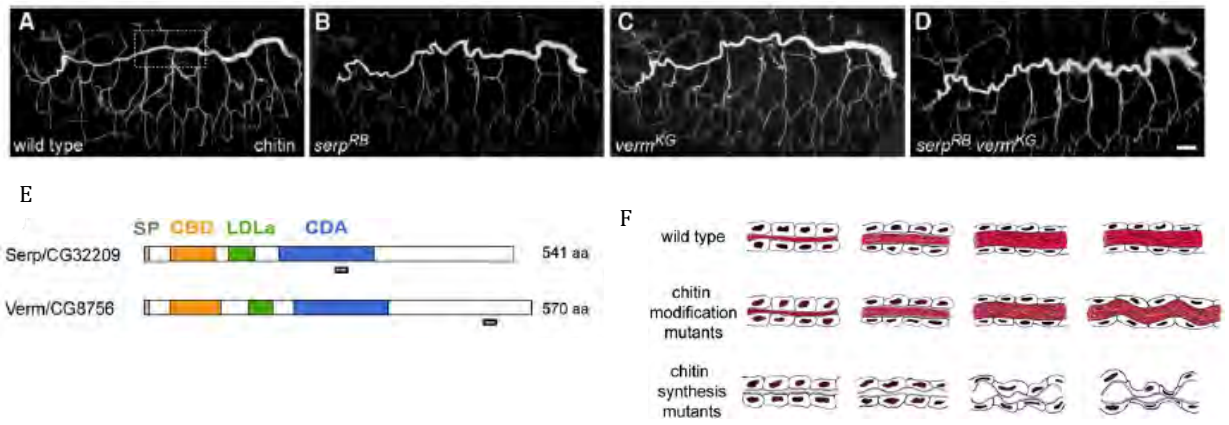

Figure 9. Serpentine and Vermiform, chitin deacetylases. Adapted from (Luschnig et al. 2006).
(A-D) Stage 16 embryos showing genotypes immunostained with a fluorescent chitin binding protein labelling the tracheal lumen. **(B,C)** Single Serp and Verm mutant display a slightly convoluted DT compared to the control **(A)**. **(D)** In double mutants Serp-Verm, display a strong phenotype of elongated and tortuous DT. The diameter is not affected in the mutant conditions.
(E) Scheme showing the protein domains of Serp and Verm: Sp, N-terminal signal peptide; CBD, Chitin Binding Domain; LDLa, LDL receptor type A ligand binding motif; and CDA, Chitin deacetylase domain.
(F) Summary of the different roles of chitin regulating diameter versus tube length. In the top panels is shown the DT expansion of wild-type embryos. Middle panels show the requirements for *serp* and *verm* chitin modification in the regulation of tube length. Lower panels show the requirement of the presence of chitin for tube diameter regulation and tube stability. In chitin modification mutants the chitin cylinder and the lumen tube are longer and convoluted, whereas in chitin synthesis mutants, the chitin cylinder is absent and tubes are not dilated properly.

Serp and Verm are first detected at early stage 13 embryos in the cytoplasm of tracheal cells. Later on, the two proteins accumulate in the lumen and at the apical membrane. Maintenance of Serp in the lumen requires recycling through the endocytic pathway, through a Rab9-mediated retrograde[2] trafficking process (Dong et al. 2013); see below in chapter 1.9.3. In addition, Serp is also transcytosed[3] from the fat body to the tracheal lumen being retained there through chitin association (Dong et al. 2014b). These mechanisms ensure the optimal accumulation of Serp in the lumen, facilitating the remodelling of the aECM to balance the continuous elongation of tracheal tubes. The transcytosis and retrograde pathways are specific for Serp protein and do not act on other luminal proteins such as Verm or Pio (Dong et al. 2014b, Dong et al. 2013).

[2] **Retrograde trafficking pathway**: transport of cargoes from the endosomes to the trans-Golgi network (TGN) (Dong et al. 2013).

[3] **Transcytosis**: a type of transcellular transport in which the cargoes are transported across the interior of the cell. It is a key process to facilitate protein translocation across epithelial barriers (Dong et al. 2014b)

1.7.3.2 Crb plays a key role in tube size control

The Crb transmembrane protein, a component of the SAR, is a key regulator of apical polarity in *Drosophila* epithelial cells (Tepass 2012, Tepass and Knust 1990, Tepass et al. 1990). Crb contains one large extracellular domain, which is composed of 29 epidermal growth factor (EGF)-like repeats and four laminin-A globular-domain-like repeats. The cytoplasmic domain, called the intra domain, consists of two highly conserved regions, the C-terminal PSD-95/Disc-large/ZO-1 (PDZ)-binding motif ERLI, and a 4.1/ezrin/radixin/moesin (FERM)-binding domain. The intra domain is responsible for the interaction with different proteins, like Stardust, Patj and Lin-7, with which it forms a complex, and also connects with the apical βH-spectrin (βH), the actin cytoskeleton and basolateral polarity complexes (Bulgakova and Knust 2009) (Fig.10A,B). Loss of Crb causes severe defects in epithelial polarity and AJ integrity (Bulgakova and Knust 2009, Tepass et al. 2001).

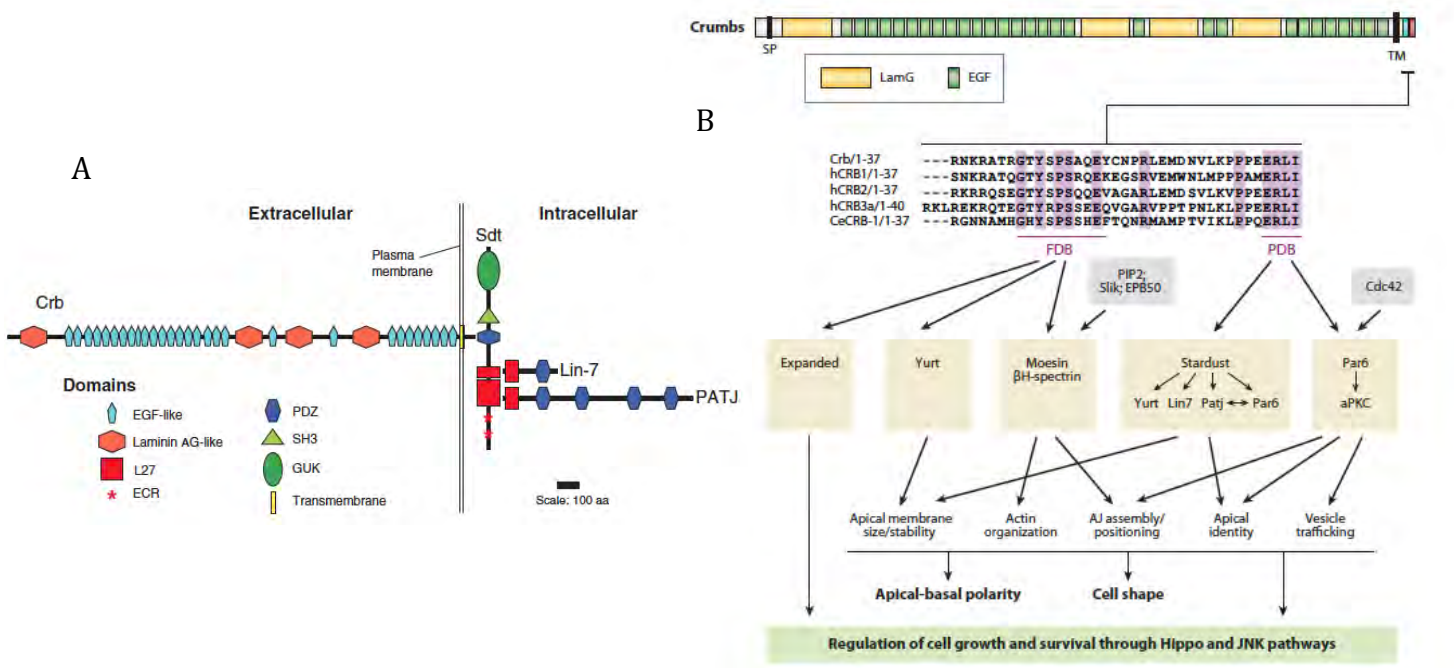

Figure 10. *Drosophila* Crb protein complex and Crb protein domains.
(A) Scheme of the core proteins of *Drosophila* Crb complex. Crb complex is formed by four components: Crb, Stardust (Sdt), PATJ and Lin-7. From (Bulgakova and Knust 2009).
(B) Molecular interaction of Crb protein domains. The cytoplasmic tail of Crb protein has two conserved motifs: a FERM domain binding site (FDB) and a PDZ-domain binding site (PDB) that interact with several partners in order to regulate different processes such as the formation, structure and maintenance of the apical domain of epithelial cells to establish the apico-basal polarity, epithelial cell shape, and the regulation of cell proliferation and survival. From (Tepass 2012).

During tracheal tube elongation, Crb overexpression causes overexpansion of the apical domain and this leads to an increased DT length (Dong et al. 2014a, Laprise et al. 2010, Laprise et al. 2006) (Fig.11). High levels of Crb are detected during the invagination of the tracheal placodes, being reduced as tracheal development proceeds (Letizia et al.

2011) suggesting that Crb accumulation in the apical membrane has to be controlled in order to allow correct DT length.

At late stages, Crb plays a key role in controlling the length and diameter of the DT through negative regulatory interactions with the FERM proteins Yurt (Yrt) and Coracle (Cora). Crb regulates the apical membrane size at the same time that controls tracheal tube length. Apical and basolateral epithelial polarity proteins interact with each other in order to regulate the tracheal tube length independently of the aECM requirement (Laprise et al. 2010) (Fig.11).

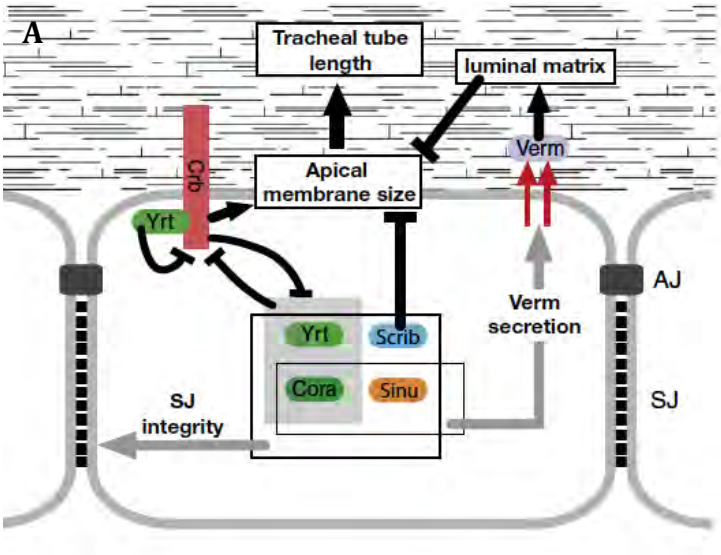

Figure 11. Model of interactions between Crb with Yrt and Cora related with the tube length regulation. The apical polarity protein Crb is controlling epithelial tube size through the interaction with Yrt and Cora, two SJ-associated polarity proteins. From (Laprise et al. 2010).

In *shrub*[4] mutants, Crb is lost from the apical membrane and forms huge cytoplasmic aggregates at late stages. It has been proposed that the loss of *shrub,* an ESCRT-III component, causes defective Crb turnover, leading to Crb mislocalization and misregulation, which induces apical membrane overgrowth. In *shrub* mutants, the DT is over-elongated and bent in a sinusoidal pattern with no changes in tube diameter (Dong et al. 2014a) (Fig.12).

[4] ***Shrub:*** ESCRT III-mutant**.** Endosomal sorting complex required for transport (ESCRT) is cytoplasmic machinery required for membrane deformation, internalization and scission (Wollert et. 2009). In *Drosophila* the *Shrub* gene encodes Vps32, a subunit of ESCRT III, which regulates endocytotic sorting of membrane-associated proteins leading to lysosomal degradation (Hori et al. 2011).

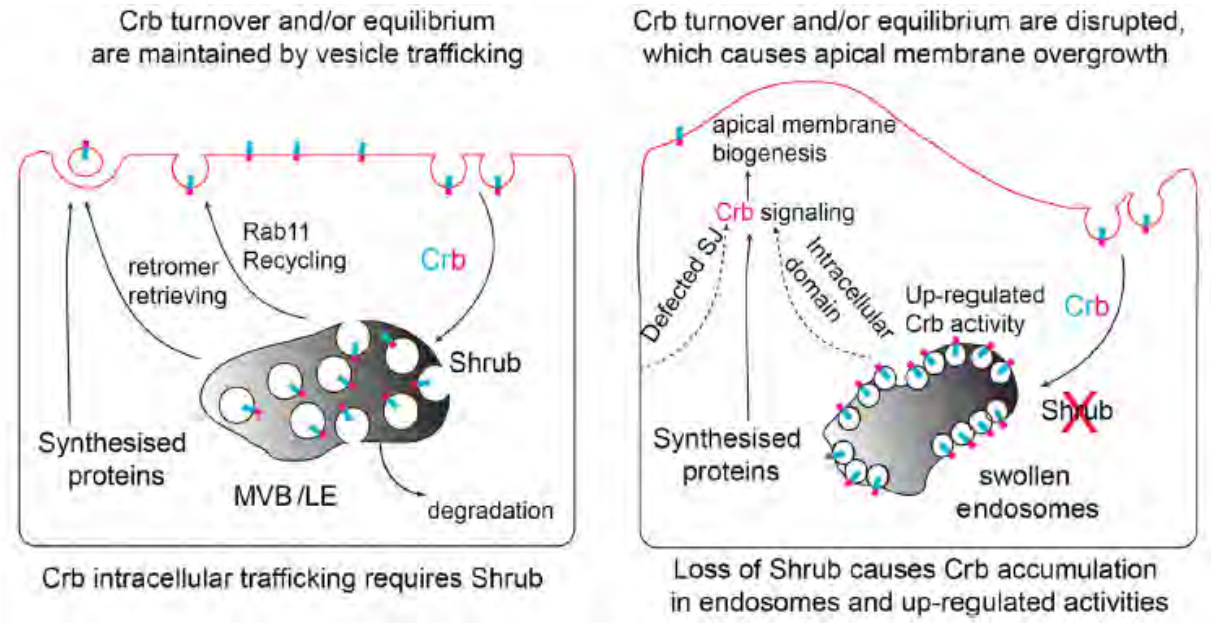

Figure 12. Scheme showing Shrub's control of apical membrane biosynthesis through the regulation of Crb activity. The left panel shows the WT conditions where the balance between Rab11 and the Retromer – mediated recycling and degradation pathways controls Crb activity. In the right panel, the loss of Shrub causes Crb to accumulate in enlarged endosomes promoting a Crb overactivation, which induces the synthesis of the apical membrane, resulting in apical membrane overgrowth. From (Dong et al. 2014a).

1.7.3.3 Src kinases control axial elongation

Src-family kinases have a role in the control of tube size in mammalian epithelial and endothelial tubular systems. Moreover, Src proteins associate with the cytoskeleton and adherens junctions (Thomas and Brugge 1997). It has been shown that in *Drosophila,* Src42A also plays a key role in tracheal tube length control (Forster and Luschnig 2012, Nelson et al. 2012). The downregulation of Src42A produces a reduction of tube length, while the overexpression leads to elongated tubes. The results indicated that Src42A is required to increase DT length and that its activity is required autonomously in the trachea for DT elongation (Fig.13A,B). It was proposed that Src42A acts together with Daam, a Diaphanous-related formin (Aspenstrom et al. 2006), in controlling DT apical growth. *dDaam* mutants display a short and thicker DT length, similar to *Src42A* mutants, suggesting that dDaam and Src42A control together directional apical surface growth (Nelson et al. 2012). A fine analysis at the cellular level indicated that in Src42A mutants the cell's apical surface is significantly reduced and the surface axial extension is biased toward a more circumferential axis, compared to control. This revealed a clear effect of Src42A in polarised cell shape changes. In addition, it was proposed that Src42A affects E-Cadh recycling at AJs (Forster and Luschnig 2012).

In summary, Src42A regulates tube length by an anisotropic mechanical force that impinges on expansion along the longitudinal axis (anterior-posterior axis). This is achieved by regulating AJs remodelling (Forster and Luschnig 2012) and by polymerization of actin through the formin DAAM leading to axial apical expansion (Nelson et al. 2012).

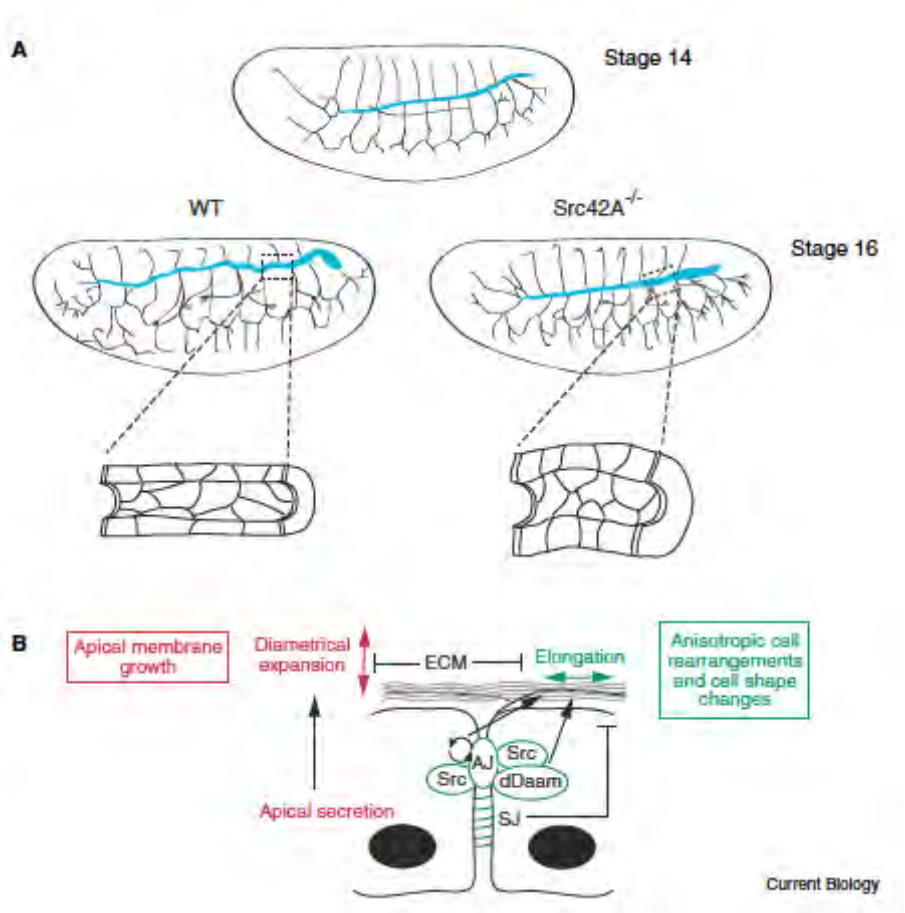

Figure 13. Model for the regulation of Src in *Drosophila* tracheal tube expansion. From (Ochoa-Espinosa et al. 2012)
(A) DT elongation stars at mid-stage of the embryogenesis. In the absence of Src42A, DT expansion is disrupted and display short DT phenotype.
(B) Src initiates the elongation of tubes by the regulation of cell rearrangement and anisotropic growth of the apical surface, whereas the aECM and SJ proteins are required to prevent an overelongation of the tubes. Src42A mediates the cell changes by the induction of adherens junction turnover. At the same time, Src42A promotes the axial elongation of apical surfaces united with dDaam/formin. The circumferential expansion is carried out in a Src42A-independent manner.

1.8 Epidermal growth factor receptor

The Epidermal Growth Factor Receptor (EGFR), a Tyrosine Kinase Receptor (RTK), triggers one of the principal conserved signalling pathway operating in development and homeostasis. During development, EGFR signalling controls important aspects such as migration, differentiation, proliferation, cell growth and survival. In addition, a miss-regulation of EGFR activity can lead to cancer and metastasis. Given its relevance, it is crucial to identify the whole plethora of EGFR activities and the downstream molecular machinery that leads to the different cellular outcomes.

1.8.1 EGFR activity in the tracheal system

Roles for EGFR during tracheal development have already been proposed. EGFR is required for tracheal invagination and to maintain the epithelial integrity.

EGFR signalling controls the initiation of apical constriction, cell rearrangements and cell migration allowing invagination. In the absence of EGFR signalling, the cells of tracheal placodes remain at the surface of the embryo and consequently an abnormal tracheal tree is formed. This is consistent with an EGF-dependent activation of MAPK cascade in the tracheal placode at stg 10 (Llimargas and Casanova 1999). Additionally, EGFR controls the activity of the RhoGTPase *Rho1* during tracheal invagination by regulating the RhoGTPase-Activating Protein (RhoGAP), encoded by *crossveinless-c* (cv-c), that affects the actin-myosin apical distribution. Hence, the EGFR pathway regulates cytoskeleton organization through the regulation of *cv-c* and *Rho1*, which, in turn, modify the apical actin required for the correct invagination and proper tracheal development (Fig.14A) (Brodu and Casanova 2006).

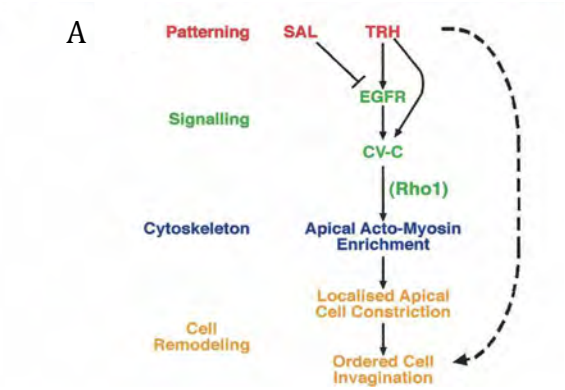

Figure 14. **Model for the regulation of tracheal cells invagination. (A)** Trh induces and organizes tracheal invagination triggering EGFR signalling. EGFR activity is responsible for the proper tracheal invagination. *Sal*, a partner of tracheal invagination, is expressed in the dorsal half of the placodes. Its role is, at least in part, to downregulate EGFR signalling activity. Once EGFR is activated, *cv-c* controls the actin organization. Proper actin assembly, display a well-localized actin rings in the apical region, which leads to a proper apical cell constriction From (Brodu and Casanova 2006).

EGFR pathway has also been to maintain tracheal branch epithelial integrity through activation of the canonical MAPK pathway, but independently of the nuclear transcription factor Pointed. Downregulation of the EGFR pathway results in loss of tube integrity, whereas upregulation leads to increased tissue stiffness. This regulation of tissue integrity correlates with differences in the accumulation of E-cadh at cell-cell junctions (Cela and Llimargas 2006).

1.8.2 EGFR signalling pathway

The EGFR is one of the most versatile RTK known and it has been extensively studied. EGFR functions in a wide range of cellular processes such as cell fate determination, cell proliferation, cell migration and apoptosis. Several positive and negative regulators modulate EGFR activity (Adamson 1990, Dominguez et al. 1998, Schweitzer and Shilo 1997, Sibilia et al. 1998).

EGFR is a transmembrane protein containing an extracellular ligand-binding domain, a single membrane-spanning domain, and a cytoplasmic protein tyrosine kinase domain (Fig.15). At the plasma membrane, the un-stimulated EGFR is present as a monomer. Upon binding of an extracellular ligand, the receptor undergoes dimerization resulting in trans-autophosphorylation of its cytoplasmic domain. The ligand-binding domain is identifiable in the glycosylated extracellular domain by the presence of conserved cysteine-rich clusters. The cytoplasmic domain contains a juxtamembrane region required for signal attenuation by protein kinase C (PKC), and is followed by the tyrosine kinase domain (Src homologous domain 1-SH1-). The latter is the most conserved region and mediates auto-phosphorylation of the carboxy-terminal tail on six tyrosine residues, located in the non-catalytic tail. The phosphorylation of these residues allows recruitment of various adapter proteins with a Src homology domain 2 (SH2) or phosphotyrosine binding domain (PTB). In addition, EGFR can be phosphorylated by other kinases such as PKC in order to regulate its distribution at the membrane. The carboxy-terminal tail contains motifs for receptor internalization and degradation. After ligand binding, EGFR is endocytosed rapidly for signal attenuation.

In *Drosophila*, there is a single gene encoding EGFR, called DER (Bogdan and Klambt 2001). DER signalling is used broadly and throughout different contexts such as in development and growth (Schweitzer and Shilo 1997, Wasserman and Freeman 1997).

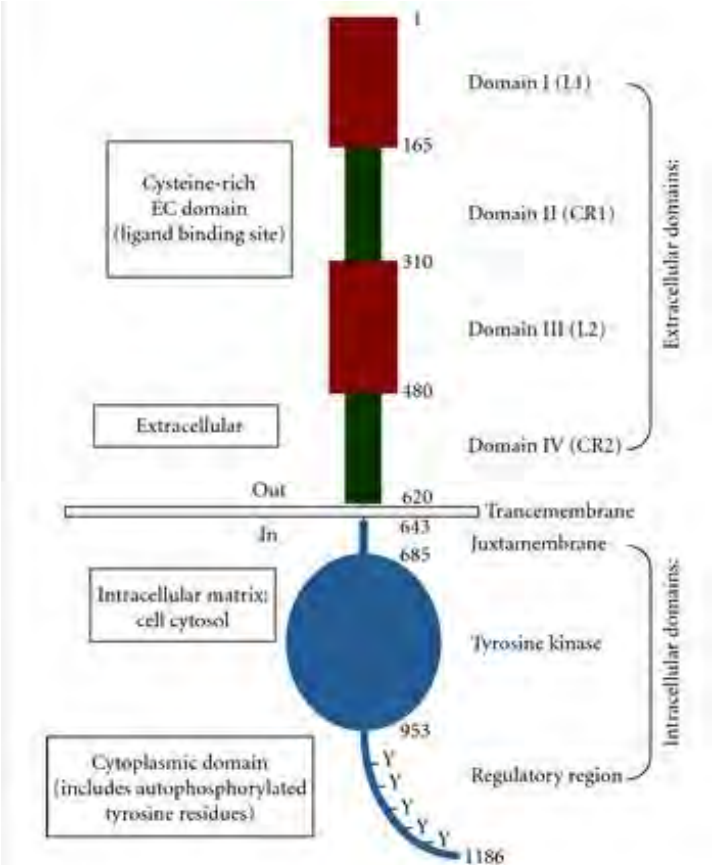

Figure 15. Overview of the EGFR domains. EGFR is a monomer composed of 1186 amino acids. Its extracellular domain is characterized by two cysteine-rich motifs where the ligand binds. Then is followed by a transmembrane domain. The intracellular domain is composed of a juxtamembrane domain, a tyrosine kinase domain and a regulatory region domain (Flynn et al. 2009).

1.8.3 EGFR ligands

In *Drosophila* there are four active EGFR ligands: Spitz (Spi), Vein (Vn), Gurken (Grk) and Keren (Krn) (Fig.16,1). The main activating ligand is Spi, a membrane-tethered EGF ligand that resembles the mammalian ligand transforming growth factor -α (TGF-α) (Freeman 1994, Rutledge et al. 1992, Schweitzer et al. 1995a, Tio and Moses 1997, Tio et al. 1994). The full-length Spi is unable to transduce the signal and must be processed into an active, soluble form. The precursor of Spi is transported from the endoplasmic reticulum to the Golgi compartment by Star (a transmembrane protein) in order to be processed (Kolodkin et al. 1994). Once Spi is in the Golgi compartment it is cleaved at its transmembrane domain by Rhomboid-1 (Rho1), an intramembrane serine protease (Urban et al. 2001).

There are two other membrane-tethered EGFR ligands in *Drosophila*: Grk and Krn. Grk is restricted to oogenesis, being expressed in the oocyte and signaling to the EGFR expressing follicle cells leading to egg polarization (Gonzalez-Reyes et al. 1995, Neuman-Silberberg and Schupbach 1993). It has been suggested that Grk, like Spi, requires post-translational activation in order to signal (Ghiglione et al. 2002). Rho2, a member of the

rhomboid family, is expressed in the oocyte and may carry out Grk processing (Guichard et al. 2000). Krn is highly similar in structure to Spi and was identified originally by the *Drosophila* Genome Project. The processing of Krn is regulated in an analogous manner to Spi, by Star and Rho proteins (Reich and Shilo 2002, Urban et al. 2002).

The last activating ligand is Vn, which resembles the vertebrate Neuroregulin. Unlike the other ligands, Vn is a secreted ligand, which possesses an inherently weaker activation capacity and is used in tissues where low levels of EGFR activation are required (Schnepp et al. 1996, Schnepp et al. 1998). Vn is required for muscle attachment cell fate (Yarnitzky et al. 1997) and also induces several distal cell fates in the leg (Campbell 2002, Galindo et al. 2002).

Argos (Aos) is a secreted ligand that has a single EGF-like domain with an expanded B-loop. It was initially assumed that Aos binds to EGFR through its EGF-like domain, functioning as a competitive inhibitor (Freeman et al. 1992, Jin et al. 2000, Schweitzer et al. 1995b). However, it was later found that Aos is associated predominantly with Spi and prevents Spi binding, EGFR dimerization and consequently EGFR activation (Klein et al. 2004).

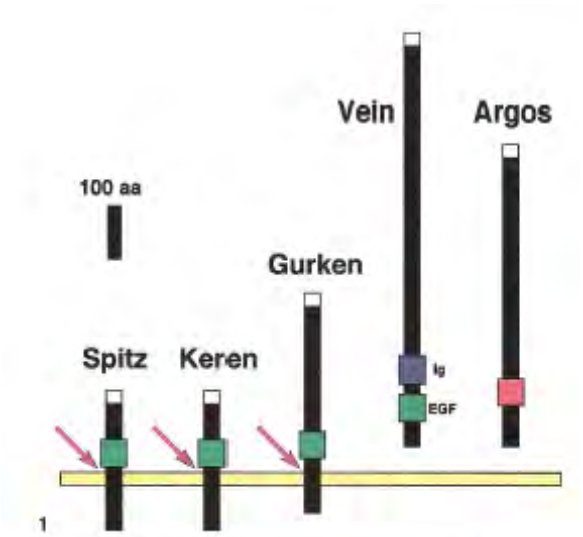

Figure 16. EGFR ligands.
(1) Activating and inhibitory *Drosophila* epidermal growth factor receptor (EGFR, DER) ligands. Four activating ligands and one inhibitory ligands of EGFR have been described. Spi, Krn and Grk are produced as transmembrane precursors that have to be cleaved (pink arrow) to generate the active ligand and to be secreted. Vn is generated as a secreted protein. Aos is produced as a secreted protein and binds to Spi protein to prevent EGFR signalling. From (Shilo 2003).

1.8.4 Nuclear factors

EGFR signals through the MAPK pathway, one of the most conserved signalling cascades in multicellular organisms (Chen R. E. and Thorner 2007). Upon EGFR dimerization, the cytoplasmic domain leads to a trans-phosphorylation of the tyrosine residues contained in the tyrosine kinase domain (Arkhipov et al. 2013). This recruits

different adaptor proteins; in particular, the cytoplasmic growth factor receptor bound protein 2 (Grb2). Subsequently, Grb2 recruits the Guanine exchange factor Son Of Sevenless (SOS) that activates the membrane associated Ras. Ras, then, initiates a cascade of phosphorylation of the three kinases: Raf, MAPKK (MEK) and MAPK (ERK or *Rolled* in *Drosophila*) (Futran et al. 2013, Sopko and Perrimon 2013, Wortzel and Seger 2011) (Fig.17). The activity of MAPK (ERK) is negatively regulated by MAPK phosphatase 3 (MKP3), which dephosphorylates the critical threonine and tyrosine residues of MAPK (Kim et al. 2004).

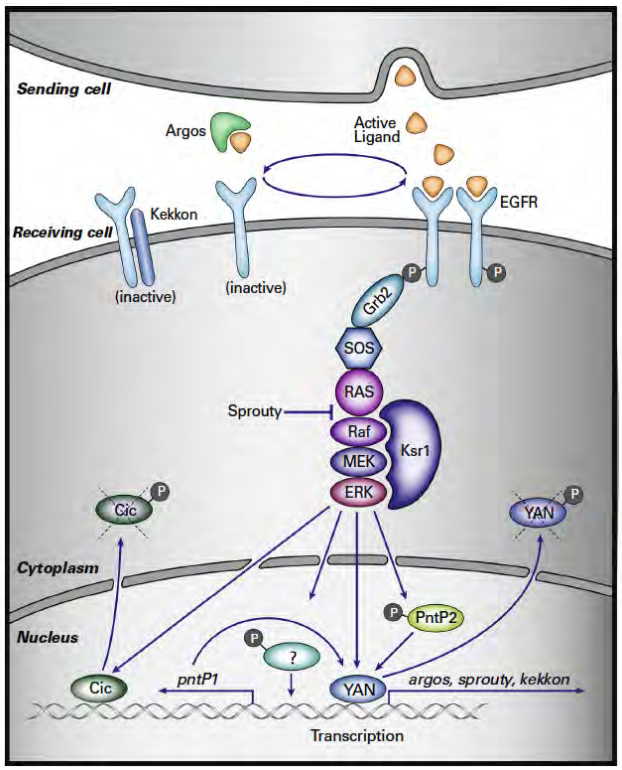

Figure 17. EGFR canonical signalling pathway. Ligands bind to EGFR on the cell surface, which upon dimerization trigger its canonical signalling pathway involving Sos/Ras/Raf/MEK/MAPK pathway. Ksr1 (Kinase suppressor of Ras), a scaffold protein, regulates the Raf/MEK/MAPK activity increasing the efficiency of signalling. The main transcriptional output of the signalling pathway is mediated by the ETS protein Pointed (Pnt). The isoform PntP2 is activated mainly by MAPK phosphorylation, while the second isoform, PntP1, is constitutively active and its transcriptionally regulated by MAPK. In addition, Yan a constitutive repressor protein that competes for Pnt-binding sites, is removed from the nucleus and degraded upon phosphorylation by MAPK. Capicua (Cic), an HMG-box protein, is another repressor that is removed from the nucleus and degraded by the MAPK phosphorylation. Additional downregulation of the pathway is mediated by Sprouty and Kekkon, which attenuate the signalling maintaining the signalling pathway in check. From (Shilo 2014).

MAPK has a wide variety of substrates both nuclear and cytoplasmic (Fig.17). The cytoplasmic substrates are non-transcriptional factors that affect other cell biological processes such as cell migration (Gabay et al. 1997, Sutherland et al. 1996), although not much is known about these substrates. The role of the nuclear substrates is better known. Two principal nuclear transcriptional substrates have been described to transduce the

MAPK canonical signal: the ETS-domain protein Pointed (Pnt), which is one of the major activators of transcription downstream of RTKs, and the transcriptional repressor Yan. Pnt is produced in two forms. PntP2 is directly activated by MAPK phosphorylation upon EGFR activation. In contrast, PntP1 is a constitutively active form but requires MAPK transcriptional induction (Brunner et al. 1994, Gabay et al. 1996, Klambt 1993, O'Neill et al. 1994, Scholz et al. 1993).

MAPK also regulates nuclear transcription through the phosphorylation and inactivation of the transcriptional repressors like Yan/Anterior open (Aop) and Capicua (Cic). Yan is an ETS-domain protein that lacks the transcription activation domain and blocks the binding of Pnt. Upon MAPK phosphorylation, Yan is exported to the cytoplasm and degraded (Lai and Rubin 1992, Rebay and Rubin 1995, Tootle et al. 2003). Cic is an HMG-box protein whose phosphorylation by MAPK leads to its inactivation and nuclear export (Astigarraga et al. 2007).

1.9 Endocytic routes

Endocytic recycling is critical for many basic processes like signalling, polarity, cell adhesion, migration, cytokinesis or nutrient uptake. Cells internalise cargoes such as extracellular material, ligands, lipids or membrane proteins and return them back to the plasma membrane or to the extracellular space, ensuring their correct localisation and function, thereby coordinating the endocytic recycling with the endocytic uptake. Following endocytosis from the plasma membrane, internalized cargoes first reach the early sorting endosome. The sorting endosome acts as the main platform by which endocytic cargoes are sorted and further transported to their final destination through different specific pathways. Cargoes targeted to degradation will be transported from the sorting endosome to the late endosome (LE), which is also known as the multivesicular body[5] (MVBs), and then to the lysosome. Alternatively, cargoes can be recycled back to membrane or the extracellular space. In these cases, cargoes can either undergo a retrograde transport to the TransGolgi Network (TGN), which allows access to the secretory pathway or they can recycle to the plasma membrane from the sorting endosome using a direct route or an indirect one through the recycling endosome (RE) (Grant and Donaldson 2009, Hsu et al. 2012). Different Rabs proteins (see also chapter 1.9.4) are associated with and control each of these trafficking steps. For instance, Rab5 mediates internalisation to early endosomes (EE), Rab4 is associated with a short-loop recycling pathway back to the plasma membrane, Rab9 is associated with a retrieval pathway from the endosomes to the TGN and Rab11 is associated with the recycling to the cell surface through RE (Bhuin and Roy 2014, Wandinger-Ness and Zerial 2014) (Fig.18).

Cargo retrieval to the TGN or to the membrane usually relies on the presence of sorting signals in the cargoes that are recognized by specific coat complexes. This interaction facilitates the partition of cargoes into different discrete domains in the sorting

[5] **Multivesicular Body**: an endocytic intermediate organelle in the lysosomal degradative pathway that contains small vesicles and is surrounded by a limiting membrane (Grant and Donaldson 2009).

endosomes. The subsequent tubulations, which eventually detach from these endosomes, become trafficking vesicles delivered to distinct intracellular routes. One of these coat complexes is the retromer complex (Burd and Cullen 2014, Gallon and Cullen 2015, Seaman et al. 2013, Wang and Bellen 2015).

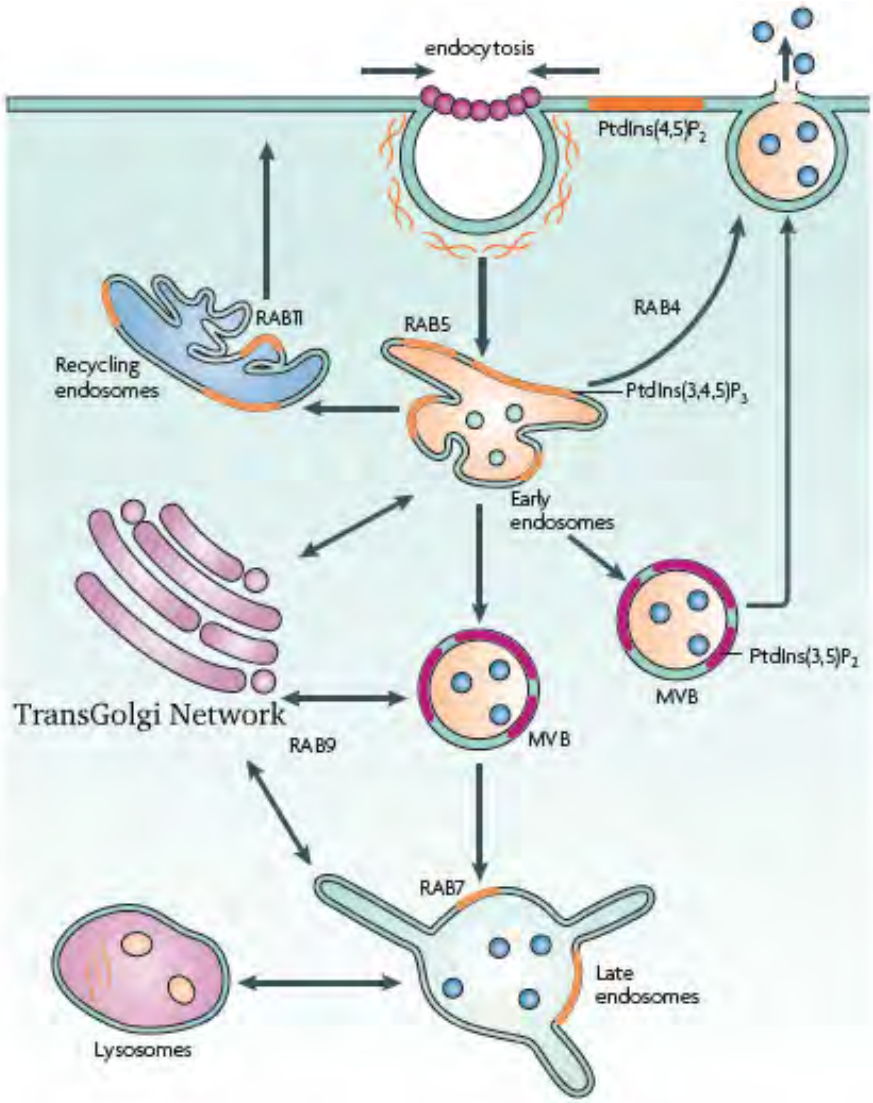

Figure 18. Overview of endosomal sorting pathways. Once proteins are internalized, they are sorted into the early endosomes, which are characterized by the presence of the Rab GTPase Rab5. Afterwards, endosomes maturate and switch between Rab5 and Rab7, which mediate the conversion of these endosomes to late endosomes. Also, in many cases, exist an intermediate organelle called MVB that mediates the cargo transfer to the lysosomes. Proteins can also be directly recycled back from EE to the plasma membrane by Rab4 GTPase. Recycling of other proteins to the cell surface occurs through RE, marked by Rab11. Rab9 carries out cargo delivered from the endosomes to the TGN. From (Rajendran et al. 2010).

1.9.1 The Retromer complex

The retromer complex is a conserved protein complex originally identified in yeast. The retromer regulates endosomal sorting and trafficking by rescuing cargoes from degradation and mediates two trafficking pathways: the retrograde transport from the endosomes through the TGN, and a direct delivery from endosomes to the plasma membrane (Burd and Cullen 2014, Gallon and Cullen 2015, Seaman et al. 2013, Wang and Bellen 2015). The retromer is a key component of the endosomal protein sorting machinery and operates by recognising specific membrane proteins or cargoes that are concentrated into discrete domains of the sorting endosome membrane to transport them to their appropriate destination. Moreover, the retromer complex regulates the subcellular localization of proteins and prevents its lysosomal degradation (Seaman 2012).

The retromer complex contains a Vps26-Vps29-Vps35 trimer (termed the cargo-selective complex, CSC) (Burd and Cullen 2014), which forms a stable structure that is absolutely required for retromer activity (Arighi et al. 2004, Seaman 2004). The CSC is regarded as the core of the retromer complex.

The retromer complex associates with different proteins, like sorting nexins (Snx). The association of the CSC with Snx proteins determines cargo selection and the trafficking route, i.e to the TGN or to the plasma membrane (Burd and Cullen 2014, Gallon and Cullen 2015, Seaman et al. 2013, Wang and Bellen 2015). Moreover, the small GTPase Rab7a and the Snx3, which associate with the Vps35 subunit, have been implicated in mediating the proper recruitment of the CSC to the membrane (Harterink et al. 2011b, Rojas et al. 2008, Seaman 2012, Seaman et al. 2009). In addition, the retromer associates with the WASH[6] complex, which promotes the formation of branched actin networks on endosomes and generates discrete actin patches that facilitates cargo sorting and stabilization of the retromer tubule formation and scission (Seaman et al. 2013) (Fig.19,1,2).

[6] **WASH**: (Wiskott-Aldrich Syndrome Protein and Scar Homolog): actin nucleation-promoting factors that regulate the actin nucleating properties of the Arp2/3 complex (Campellone and Welch 2010). WASH associates with a regulatory complex composed of FAM21 (family sequence similarity 21), SWIP, strumpellin and CCDC53 (coiled-coil domain containing protein 53) (Gomez and Billadeau 2009, Derivery et al., 2009).

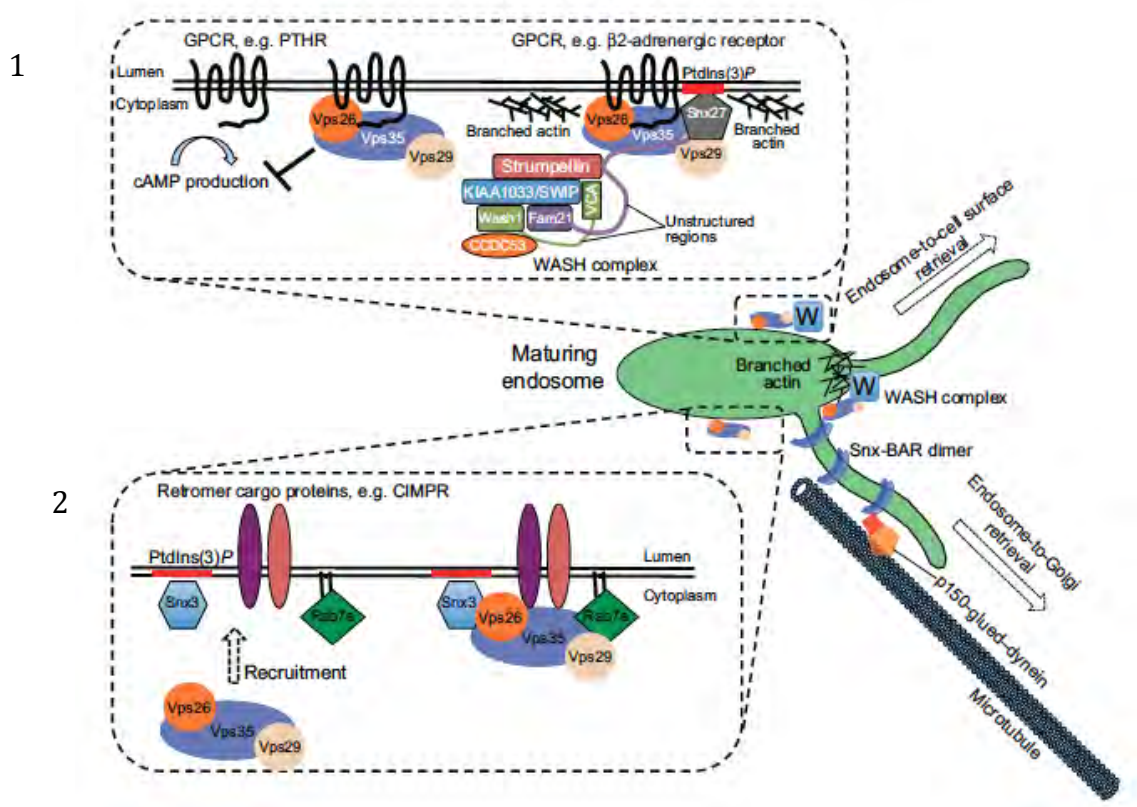

Figure 19. Scheme showing the retromer complex pathways during regulation of the endosomal protein sorting trafficking. In this scheme is depicted a general overview of the two retromer recycling pathways. At the bottom **(2)** is shown an example of retromer retrieval pathway from EE to TGN. The CSC is recruited to the endosomal membrane mediated by Snx3 and Rab7a. The CSC recruits WASH complex to mediate the production of actin patches on the surface of the endosomes. Above **(1)** is shown an example of a direct pathway from EE to cell surface. Once the CSC is recruited to the endosome membrane, together with Snx27 and the WASH complex. It regulates the cargo specific route from the endosomes to cell surface. From (Seaman 2012).

In summary, the core complex acts as a recruiting hub in endosomal sorting and trafficking, which coordinates the cargo uptake/enrichment and actin polimerization to achieve cargo sorting into recycling pathways rather than lysosomal degradation. The Snx and other retromer-associated proteins, in combination with the CSC, provide functional diversity and spatiotemporal regulation of retromer-mediated trafficking pathways (Burd and Cullen 2014, Mukadam and Seaman 2015).

1.9.2 The retromer complex and apical polarity trafficking

The retromer complex regulates several biological processes, such as lysosome maturation (Arighi et al. 2004, Seaman 2004), polymeric IgA transcytosis (Verges et al. 2004), Wingless (Wnt) secretion (Belenkaya et al. 2008, Franch-Marro et al. 2008, Harterink et al. 2011a, Port et al. 2008), apoptotic cell clearance (Chen D. et al. 2010) and the efflux of the phytohormone auxin (Jaillais et al. 2007). However, how the retromer regulates apical-basal polarity in epithelial cells remains unknown.

Recent studies have suggested a link between the retromer complex and Crb recycling. In the follicle epithelium, during both oogenesis and embryogenesis, loss of *Vps35* disrupts the epithelial cell layering, and apical markers such as Crb and Patj are lost from the membrane (Pocha et al. 2011, Zhou et al. 2011). Moreover, overexpression of Crb rescues both cuticle loss and polarity defects in *Vps35* mutant embryos (Zhou et al. 2011), suggesting a role for the retromer in Crb recycling and prevention of its lysosomal degradation (Fig.20). Additionally, wing imaginal discs mutant for Scribble (Scrib), a regulator of basolateral membrane identity, show defective retromer-dependent sorting of Crb (de Vreede et al. 2014). Thus, the retromer complex is a hub that coordinates and sorts different polarity proteins to the correct domains at the plasma membrane. This key role of the retromer in recycling apical proteins determines the establishment of epithelial cell polarity.

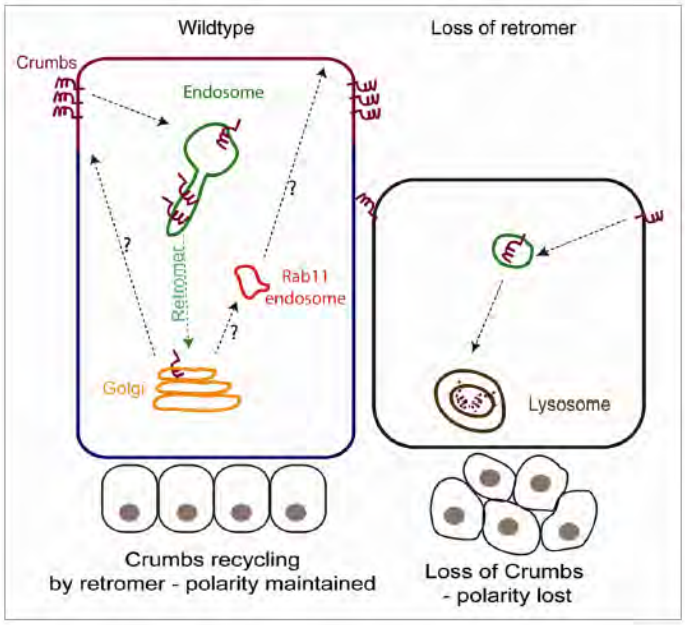

Figure 20. Trafficking of Crb in Wild type and Retromer-deficient conditions. In Wild type, Crb is located in the apical domain (purple) and absent from the basolateral domain (blue). After Crb endocytosis, it is retrieved from endosomes to the apical membrane by the Retromer, although, the specific pathways by which Crb is recycled to the apical domain remain unclear. Presumptive recycling pathways are: First, transport of endocytosed Crb through the TGN to the apical domain. Second, direct or indirect traffic, by Rab11 recycling endosomes. Loss of Retromer activity, leads to a reduction of Crb retrieval from the endosomes, so that Crb is delivered to the lysosomes to be degraded. This results in a strong reduction of Crb levels and severe defects in the epithelial polarity. From (Pocha and Wassmer 2011).

Crb recycling has also been shown to require other alternative pathways. For instance, Rab11 regulates Crb trafficking in the *Drosophila* embryonic ectoderm (Roeth et al. 2009), and the Exocyst 84 (Exo84) has a role in the apical localization of Crb (Blankenship et al. 2007).

1.9.3 Trafficking of luminal cargoes

Although the majority of retromer cargoes are transmembrane proteins, the retromer can also traffic luminal proteins. A clear example in *Drosophila* is Serp, which as previously explained is a deacetylase protein released into the lumen to regulate DT length during tracheal tube morphogenesis. Serp is internalized in Rab5 EE and transported to the TGN using the retrograde pathway that ensures its luminal recycling. This is coordinated by the retromer/WASH together with the small GTPase Rab9. A disruption of retromer activity in *vps35* mutant embryos and Rab9 mutant embryos causes an increase in DT length (Dong et al. 2013) (Fig.21).

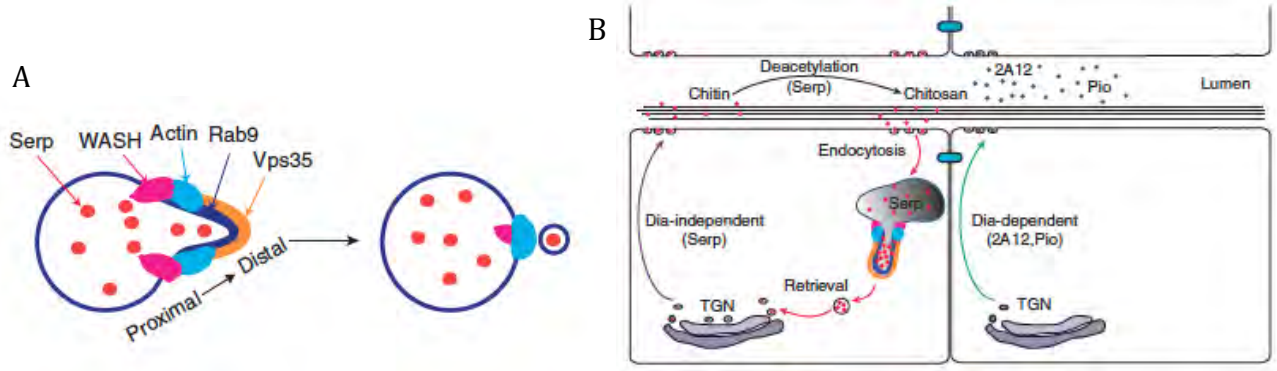

Figure 21. Serpentine recycling regulated by the retromer, Rab9 and WASH. (A) Scheme of the composition and organization of the retrieval machinery for the budding of the vesicles containing Serp**.** Serp is inside the vesicle and WASH, Rab9 and Vps35 are localized at he endosomal membrane. **(B)** At late stage of *Drosophila* tracheal development, Serp is endocytosed by Rab5 and sorted out into the endosomal-budding membranes enriched with WASH, actin, Rab9 and Vps35. Then, it is recycled back to the lumen by the TGN. From (Dong et al. 2013).

1.9.4 Rab GTPases

It is well established that Rab proteins are master regulators of the retromer-mediated vesicular transport and of cargo intracellular trafficking in general. Rabs are small GTPases of the Ras superfamily that are essential components of the intracellular trafficking routes. Through recruitment of effectors, Rab proteins regulate the cargo sorting, vesicle budding and transport of vesicles along cytoskeleton fibrils. Moreover, Rabs regulate vesicle tethering, docking and fusion with the target membrane. The activity of Rab proteins is subject to cycles of GTP binding (Rab-GTP, active) and hydrolysis to GDP (Rab-GDP, inactive), regulated by the guanine-nucleotide exchange factors (GEFs) and GTPase-activating proteins (GAPs) (Barr 2013, Pfeffer 2013, Wandinger-Ness and Zerial 2014). Most of the Rab proteins are ubiquitous in their expression while some have a more restricted tissue/cell type specific distribution (Chavrier et al. 1991, Ullrich et al. 1996). Irrespective of the tissular pattern of accumulation, Rab proteins are predominantly localized to the membranes of traffic vesicles and to specific compartments. For instance, Rab5 is associated with EEs (Gruenberg et al. 1989) mediating the endocytic internalization

of the cargo from the plasma membrane to the EEs (Christoforidis et al. 1999, Murray et al. 2002) and early endosome fusion (Gorvel et al. 1991). Rab4 is also localized to EE (Van Der Sluijs et al. 1991). Unlike Rab5, Rab4 mediates a fast recycling route from EEs directly back to the plasma membrane as well as directing the sorting of cargo to the endocytic-recycling compartment (ERC) (van der Sluijs et al. 1992). Recently, Rab4 has been associated with the Retromer complex (Maxfield and McGraw 2004). Rab11 is localized to the REs (Ullrich et al. 1996) and the TGN (Urbe et al. 1993), and regulates transport from the ERC to the plasma membrane, or traffic between the TGN and ERC (Ullrich et al. 1996, Wilcke et al. 2000). Rab9 is involved in the trafficking of cargoes from the LEs to the TGN in a retrieval pathway (Dong et al. 2013) and it is associated with the retromer complex. Rab7 is involved in the transport from EEs to LEs and serves as marker for LEs (Feng et al. 1995, Wichmann et al. 1992).

2. OBJECTIVES

2. OBJECTIVES

Tracheal tube growth is a finely regulated process that ensures the proper formation and physiological activity of the tracheal system. Several mechanisms have been shown to regulate the elongation of the embryonic tracheal tubes. However, in spite of the extensive knowledge obtained so far, we still lack a complete understanding of the exact molecular mechanisms at play and of how the different mechanisms are coordinated. The general aim of this work was to gain further insights into the mechanisms controlling tube elongation and the interactions between these different mechanisms.

The specific objectives of this work are the following:

1. **Analysis of the role of EGFR in tube elongation.**

We have identified a previously uncharacterised role for EGFR in regulating the length of the main tracheal branch. The specific goals to characterise this new role of EGFR are:

1. 1- Phenotypic characterisation of the role of EGFR in tracheal tube size.

1.2- Analysis of the activation of EGFR during the regulation of tracheal tube size

1.3- Analysis of the contribution of the canonical Ras-MAPK pathways to tracheal tube size control

1.4- Identification of the molecular mechanism/s downstream of EGFR that regulates tube size.

2. **Analysis of the mechanism mediated by Crb controlling tube length.**

The apical determinant Crb has been shown to regulate tracheal tube elongation by regulating the apical membrane growth. However, it remained unclear how the Crb-mediated apical membrane growth is biased to the axial direction. The specific goals to characterise this role of Crb are:

2.1- Analysis of the accumulation of Crb during tracheal tube elongation.

2.2- Analysis of the regulation of Crb accumulation during tracheal tube elongation.

2.3- Analysis of the molecular mechanism/s involved in Crb regulation.

3. **Investigate the interactions and coordination of the different mechanism controlling tracheal tube elongation.**

3. MATERIAL AND METHODS

3. MATERIAL AND METHODS

3.1 *Drosophila* strains

Unless stated otherwise, all the *Drosophila Melanogaster* strains were raised at 25ºC under standard conditions and all the overexpression and the RNA interference (RNAi) experiments were carried out, using GAL4/UAS system, at 29ºC (Brand and Perrimon 1993). *btlGal4* alone or *btlG4>UASSrcGFP* (where the expression of Src membrane protein fused with GFP mark tracheal cells) were used to drive the overexpression of the transgenes in all tracheal cells from invagination onwards. *AbdBGal4* was used to drive expression in the posterior part of the embryo. The mutant chromosomes were balanced over CyO, TM3 or TM6, marked with P[w^+, *wg-lacZ*], P[w^+, *ftz-lacZ] or* P[w^+, *Ubx-lacZ]* respectively to recognize the homozygous mutant embryos.
The strain y^1w^{118} was used as wild type (wt) strain. The fly strains used in this study are listed and described in table 3.

Table 3. Fly strains used during the study. Abbreviations used: Chr: Chromosome number; **BDSC**: Bloomington *Drosophila* Stock Center. **VDRC**: Vienna *Drosophila* Resource Center.

UAS constructs	Chr.	Description	Origin/Reference
UAS-Egfr^{DN}	II	UAS construct. Dominant negative allele of EGFR gen (truncated C-terminal aminoacids of the transmembrane domain)	(Freeman 1996)
UAS-Egfr^{CA} (λTop)	X	UAS construct of a constitutive active form of EGFR. This construct carries a λ dimerization domain, which is independent of ligand binding and therefore is always active.	(Queenan et al. 1997)
UAS-Rab5^{DN} (UAS-Rab5^{S43N})	III	UAS construct. Expresses a dominant negative Rab5 protein under UAS control	BDSC 42704
UAS-Rab5^{CA} (UAS-Rab5^{Q88L})	III	UAS construct. Expresses activated Rab5 under UAS control	BDSC 43335
UAS-Rab4^{DN}-YFP (UAS-Rab4^{S22N}-YFP)	III	UAS construct. Expresses a dominant negative, YFP-tagged Rab4 protein under UAS control.	BDSC 9769
UAS-Rab4^{DN}-YFP (UAS-Rab4^{S22N}-YFP)	II	UAS construct. Dominant negative form of Rab4 carrying a YFP marker.	BDSC 9768
UAS-Rab4^{CA} (UAS-YFP-Rab4^{Q67L})	III	UAS construct. Expresses a constitutively active form, YFP-tagged Rab4 protein.	BDSC 9770
UAS-Rab11^{DN}-YFP (UAS-Rab11^{S25N}-YFP)	II	UAS construct. Dominant negative form of Rab11 carrying a YFP marker.	BDSC 9792
UAS-Crb^{FL}	II	Overexpression of Crb full-length protein.	Gift from E. Knust
UAS-Src-DN	III	UAS construct: Transgene contains a point mutation (lysine at position 295 has been replaced by methionine	Kindly provided by S. Luschnig

		(K295M)), at the catalytic centre of the kinase domains that abolish catalytic activity.	
UAS-Src-CA	II	UAS construct: Transgenic transposon that contains an amino acid replacement: Y511F producing constitutively active form of Src42A.	Kindly provided by S. Luschnig
UAS-Argos	I;II	UAS construct. Transposable element expressing Argos.	BDSC 5363
UAS-Spitz	III	UAS construct. Transgenic transposon that produces Secreted Spitz protein.	(Schweitzer et al. 1995)
UAS-SEM	III	UAS construct. Constitutive active form of MAPK (amino acid replacement)	(Martin-Blanco 1998)
UAS-PntP1	III	Expresses the P1 form of pnt under the control of UAS.	BDSC, 869
UAS-Yan^{Act2}	II	UAS construct. Constitutive active form of Yan. (All MAPK consensus sites were mutated).	(Rebay and Rubin 1995)
UAS-Serp-CBD-GFP	II	Transgene that includes the signal peptide and the chitin-binding domain (CBD) o Serp ligated along with a GFP sequence.	Kindly provided by S. Luschnig
NSM801 (MKP3)	III	UAS construct. Overexpression of MKP3. GS element insertion of line 801 to 75F6.	(Gomez et al. 2005)

Mutant Alleles	Chr	Class	Origin/Reference
VnC221	III	Hypomorphic mutant allele	BDSC, 2460
Vn γ4	III	Amorphic mutant allele	(Simcox et al. 1996)
Df (3L) Krn$^{9\text{-}6\text{-}A}$	III	Hypomorhic mutant allele of Keren (P-element activity)	BDSC, 51333 (McDonald et al. 2006)
Grk^{HF}	II	Null mutant allele	(Butchar et al. 2012)
Spi^{2A}	II	Null mutant allele	(Butchar et al. 2012)
Vn^{L6}	III	Null mutant allele	(Butchar et al. 2012)
Krn^{27}	III	Null mutant allele	(Butchar et al. 2012)
Crb^{11A22}	III	Amorphic mutant allele	Gift from E. Knust
Serp^{RB}	III	Amorphic mutant allele.	Kindly provided by S. Luschnig
Yan^{e2d}	II	Amorphic mutant allele	(Rogge et al. 1995)

RNAi constructs	Chr	Description	Origin/Reference
UASSpi^{RNAi}	III	Transgenic RNAi. Expresses dsRNA for RNAi of spi under UAS control.	BDSC 34645
UASVn^{RNAi}	II	Transgenic RNAi. Contains phiC31-based transgene with a defined insertion site. Expresses dsRNA for RNAi of Vn under UAS control.	VDRC 109437

Knock in	Chr	Description	Origin/Reference
Crb^{GFP}-C	III	Knock in (Endogenous promoter) generating a Crb-GFP tagged functional protein.	Kindly provided by Y. Hong
Crb^{Cherry}	II	Knock in (Endogenous promoter) generating a Crb-Cherry tagged functional protein.	Kindly provided by Y. Hong
Rab4^{EYFP}	II	Knock in (Endogenous promoter) generating a Rab4 tagged functional protein.	BDSC 62542

GAL4 drivers	Chr	Description	Origin/Reference
BtlGal4	II	GAL4 fused to *btl* promoter	Marcus Affolter
AbdBGal4	III	GAL4 fused to *AbdB* promoter	E. Sanchez
TubGal4	III	GAL4 fused to *tubulin* promoter (General driver)	BDSC, 42732
TwistGal4	III	GAL4 fused to *twist* promoter (Mesodermal expression)	(Martin-Bermudo et al. 1997)
DaGal4	II	GAL4 fused to *da* promoter (Ectodermal expression)	(Wodarz et al. 1995)

3.2 Immunohistochemistry

Immunostainings were performed on embryos (collected from 13 to 18 hours on agar plates) dechorionated in 100% bleach for 2 minutes and rinsed with triton 0.1%. Embryos were collected and fixed for 20 minutes (except for E-Cadh staining, for which embryos were fixed for 10 minutes) in 4% formaldehyde in PBS (0.1M NaCl, 10 mM phosphate buffer, pH7.4) and heptane to generate holes in the viteline membrane. After removing the bottom phase, which contains PBS and formaldehyde, 2ml of methanol (to remove the viteline membrane) was added and the tubes were vigorously shacked for 20 seconds. The bottom phase contains the devitelinated embryos. The embryos were transferred into new tubes and washed for 1 hour in three changes of PBT (PBS with 0,1% Triton X-100) containing 0.5% Bovine Serum Albumine (BSA) for 20 minutes. Primary antibody incubations were performed in PBT-0.5%BSA overnight at 4ºC. Embryos were then washed for 1 hour in three changes of PBT-0.5%BSA of 20 minutes each. Secondary antibody incubations were performed for 2-3 hours at room temperature (RT) at 1:300 in PBT-0.5%BSA in the dark. Embryos were washed for 1 hour in three changes of PBT and mounted in Fluoromount-G (Southern Biotech). Primary and secondary antibodies dilutions are listed in Table 4.

For Dextran injections we used Rhodamine-labelled 10 KDa dextran injections for an in vivo endocytosis assay and were performed as described in (Lamb et al. 1998, Tsarouhas et al. 2007). Embryos of stage 13 carrying *btlG4-UASSerp-CBD-GFP* (control), *btlG4-UASSerp-CBD-GFP;EGFR^{DN}* and *btlG4-UASSerp-CBD-GFP;EGFR^{CA}* were dechorionated in 100% bleach for 2 minutes and rinsed with triton 0.1%. Embryos were transfer to in an agar plate and lined up. Afterwards, they were transferred on a glass coverslip with injection glue (containing double-stick tape and heptane) and desiccated in a closed container containing silica gel for 10 min. The embryos were then covered with oil 10-S Voltalef (VWR) and incubated at 29ºC during 5 hours. Rhodamine B-labelled dextran (10,000MW, Invitrogen) was then injected and the embryos were examined on a TCS-SPE.

3.3 Antibodies

Table 4. Antibodies and stains used in the study. Abbreviations used: Developmental Studies Hybridoma Bank (DSHB).

Name	Antigen	Species	Dilution	Origin
Stains				
CBP	Chitin	-	1:300	Produced by N.Martín in J.Casanova's lab
Primary antibodies				
Anti-EGFR extracellular domain	EGFR extracellular domain	Mouse	1:500	Sigma
Anti-Crb (Cq4)	Crb	Mouse	1:20	DSHB
Anti-E-Cadh (DCAD2)	De-Cadherin	Rat	1:100	DSHB
Anti-Wash P3	WASH	Mouse	1:50	DSHB
Anti-Serp	Serp	Rabbit	1:300	Generously provided by S. Luschnig
Anti-Rab11	Rab11	Rabbit	1:2000	Generously provided by T. Tanaka
Anti-Rab5	Rab5	Guinea pig	1:1000	Generously provided by T. Tanaka
Anti-Uif	Uif	Guinea pig	1:500	Generously provided by R. Ward
Anti-GFP	GFP	Rabbit	1:600	Moleculars Probes and Roche
Anti-GFP	GFP	Goat	1:600	Moleculars Probes and Roche
Anti-βgal	βgal	Chicken	1:300	Abcam

Secondary antibodies				
Alexa 488		Donkey	1:300	Jackson ImmunoResearch
Alexa 561		Donkey	1:300	Jackson ImmunoResearch
Alexa 647		Donkey	1:300	Jackson ImmunoResearch
Cy2		Donkey	1:300	Jackson ImmunoResearch
Cy3		Donkey	1:300	Jackson ImmunoResearch
Cy5		Donkey	1:300	Jackson ImmunoResearch

3.4 Image acquisition and processing

Fluorescence confocal images of fixed embryos were obtained with Leica TCS-SPE system using 20x and 63x (1.40-0.60 oil) objectives. Unless otherwise indicated, images shown are maximum projections of Z stacks sections (0.2-0.4 µm).

Images were imported mainly into Fiji (ImageJ 1.47n. (Schindelin et al. 2012)) for measurements and adjustments. The figures were assembled with Adobe Photoshop CS5.

3.5 Morphometric analysis

3.5.1 Tube size quantifications

Confocal projections of *wild-type* and mutant embryos were used to analyse the length of the embryonic dorsal trunk (DT) stained with CBP in stage 16 embryos. We traced two paths using the freehand line selection tool of Fiji software between the junction DT/Transverse Connective (TC) from metamere 4 to 9, one following DT curvature and a straight one. DT length was expressed as the ratio between the real path and the straight line. A ratio of 1 reflects a straight DT.

Moreover, to check that the extra-long tubes are not due to a defective embryo size, we also measured the total length of the embryo drawing a straight line from the most anterior part to most posterior region. The length of other branches, such as DB and TC, was also measured in metamere 5 and the DT diameter was measured in the region between metameres 7 to 8. All measurements were expressed in µm (Fig.22A,B).

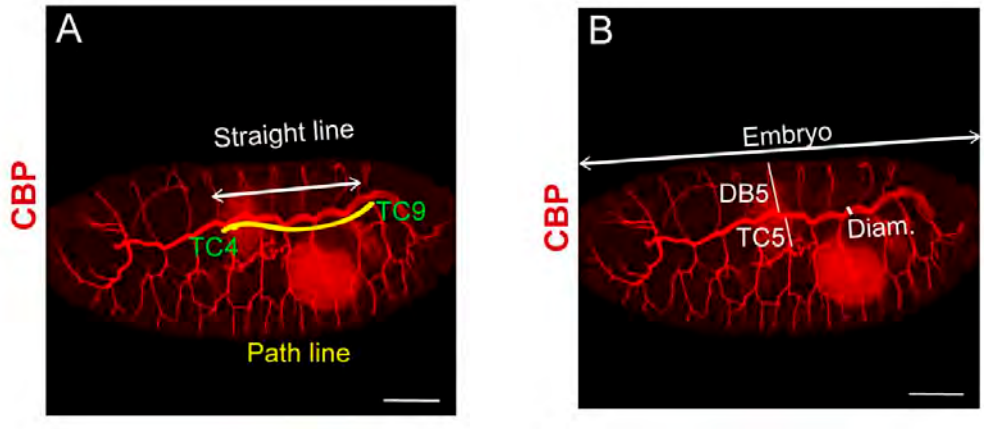

Figure 22. Example of the branch length measurements. (A) The path length between the junctions DT/TC from metameres 4 to 9 was measure by tracing two lines through the tube, one following the DT curvature (yellow line) and a straight one (white line). **(B)** The total embryo size was measured by tracing a straight line between the distances from the most anterior part to the most posterior part. We quantified the length of DB5, TC5 and the DT diameter was measured in the region between tracheal metameres 7 and 8. Scale bar 50 µm.

3.5.2 Cell junctions length

Cell junctions were classified according to the angles (tube axis set to 0º), considering axial junctions those oriented 0º±30º and circumferential junctions 90º±30º. The freehand line selection tool of Fiji software was used to measure the length of the junctions. The length of cell junctions was expressed in μm.

3.5.3 Crb intensity levels

Projections of confocal sections that include MT and a piece of DT were used for the analysis. *EGFR^{DN}/EGFR^{CA}* transgenes were expressed in the tracheal cells by means of *btlGal4*, which is not expressed in the MT. We measured the mean levels pixels in each structure using the freehand line selection tool of Fiji, tracing a line including the whole tube (line with 60 for DT and line with 10 for MT). Fluorescence intensity of Crb in the DT was normalised to the Crb levels in MT in each embryo. We compared the ratio of Crb levels in the trachea/MT among the experimental conditions and the internal control *wild-type* embryos.

3.5.4 Crb subcellular accumulation

We quantified the total levels of Crb (using the Sum Fluorescence Intensity projection in Fiji) in different apical subcellular domains. We selected individual cells from the region of the DT between metameres 7 and 9, and generated projections of few sections to include only the whole cell or a small number of them. We quantified Crb in SAR by outlining the cell contour (using E-Cadh to visualise it) and Crb in AFR by drawing a freehand section inside the cell. We expressed the subcellular accumulation as the ratio between SAR/AFR.

3.5.5 Crb anisotropy accumulation

Images of DT fragments between metameres 7 to 9 of stage 16 embryos were taken to analyse the Crb accumulation in cell junctions and evaluate the anisotropy. After setting the longitudinal tube axis to 0º, cellular junctions were identified as axial (LCJ) (those oriented 0º±30º) or circumferential (CCJ) junctions (oriented 90º±30º). The “maximal Z projection” tool of Fiji software was performed for E-Cadh channel images to follow all the cellular junctions properly. To obtain the total accumulation of Crb from the different stacks we generated a projection using the Sum Fluorescence Intensity projection tool in Fiji software. To measure the total fluorescence in each cell junctions we obtained the raw intensity density (the sum of all pixels values from the different stacks in the selected junction) using the polygon selection tool of Fiji software. The fluorescence of Crb was normalised to the length of each junction. We expressed the Crb anisotropic accumulation as the ratio between Axial/Circumferential accumulation and as the sum of all pixels per junctional length.

3.5.6 Crb Serp colocalization

Colocalisation analysis was performed using the ImageJ plugin Colocalisation highlighter, considering colocalisation when the ratio of fluorescence intensities between red and green channels was above 0.5. Those fluorescence intensities above the threshold appear in a binary image colour as white (colocalised points). From this mask, we selected manually each vesicle with colocalisation with the wand tool in Fiji and added it in the ROI Manager. Thereafter, to analyse the colocalisation, a ratio between the number of pixels (integrated density) of one channel that colocalises with the marker in the other channel and the total number of pixels above the threshold measured for each channel was measured.

3.5.7 Analysis of cargoes in endosome

For each region of DT analysed, we counted in each stack the number of endosomes containing Crb and Serp, Crb alone and Serp alone. We analysed the proportion of each type of endosome.

3.5.8 Cell number

To count cell number, embryos were stained with anti-Uif, anti-laminin A and DAPI to label apical and basement membrane, and the nuclei of tracheal cells. To analyse the cell number, we counted in each stack the nuclei from the region of the DT between metameres 7 and 8 in stage 15-16 embryos. Images were obtained with Leica DMI6000 TCS-SP5 laser confocal microscope 63x/1.4 NA oil using a 405 nm diode laser.

3.6 FRAP assay

Embryos carrying *btl*Gal4;Crb^{GFP}-*C* (i.e *control*) and *btl*Gal4;Crb^{GFP}-*C*/UAS-Src42A^{DN} (i.e mutant) were collected at 29ºC. Embryos were mounted and lined up on Menzel-Gläser cover slips with oil 10-S Voltalef (VWR) and covered with a membrane (YSI membrane kit). FRAP was carried out on a Zeiss Lsm780 Confocal and Multiphoton System. The ZEN 2.1 SP3 of the Zeiss Confocal Software was used for data acquisition. The 488 nm emission line of an Argon laser was used for excitation. We selected embryos at the appropriate stage (Stg 14-15) lying in a lateral position. We performed 10 pre-bleach scans with the 63x objective with a 1.5 zoom. These pre-bleach scans covered several Z-sections (1µm thick, 4 sections) in order to image the Crb accumulation in cell junctions that lie at different focal planes. Regions-of-interest (ROIs) of the same size were selected in longitudinal and circumferential junctions. After 10 pre-bleach scans, bleaching was performed at these ROIs. Post-bleach scans were obtained immediately after bleaching at every 10 seconds and during 10-20 minutes. Average projections of the Z-sections were exported for each time point and these were assembled into a movie using Fiji software (movie 5A, B; movie 6A, B).

Fluorescence intensity in the ROIs was measured at each time point with Fiji software intensity plot profile tool. To calculate the half-time ($t_{1/2}$) and the mobile fraction (M_f) the normalised FRAP values were fitted into curves using the Igor-Pro software.

3.7 Time-lapse imaging

Life imaging was performed on a Zeiss Lsm780 Confocal and Multiphoton System. Dechorionated embryos were mounted and lined up on a Menzel-Gläser cover slips with oil 10-S Voltalef (VWR) and covered with a membrane (YSI membrane kit). In all movies we used an Oil 63x/1.4 NA objective. To visualize time-lapse movies, maximal intensity projections are shown.

3.7.1 Vesicle dynamics

For movie 2, *Rab4*^{EYFP} and *Crb*^{Cherry} were used to visualize Rab4 and Crb accumulation in vivo at stage 14. For movies 3-4, *Crb*^{Cherry} and *BtlG4-UASSerp-CBD-GFP* constructs were used to visualize Crb and Serp vesicle dynamics at stage 14, respectively. Images were taken continuously in a single Z-stack during 2 (movie 2), 3,5 (movie 3) or 6 (movie 4) min with a 2,5 zoom. For these movies a 488/514 nm Argon laser was used.

3.7.2 Crb apical subcellular accumulation

To visualize Crb apical subcellular accumulations, the *Crb*^{GFP} construct was used. Images were taken every 2 minutes during 2,30 hours in a 20 Z-stacks of 0,5 µm and with a zoom=2, from early stage 14 to stage 15. For this movie a 950nm Multiphoton laser MaiTai HP DS was used.

3.8 Quantifications and statistics

Total number of cells/embryos/junctions is provided in text and figures. Error bars in bar graphics denote standard error (s.e). Measurements are imported and treated into the STATA 12.1 software; where boxplots were generated, and treated into excel software 14.7.1, where histograms were generated. Statistical analyses were performed using STATA 12.1 software and *P*-values were obtained with an unpaired two-tailed Student's t-test. Differences were considered significant when $p<0,05$. In graphics; * $p<0,05$, ** $p<0,01$, *** $p<0,001$.

4. RESULTS

4. RESULTS

4.1 EGFR requirement in tracheal tube size

4.1.1 The modulation of EGFR activity controls tube length

Previous analysis described roles of the EGFR pathway in regulating invagination and the integrity of tracheal branches (Brodu and Casanova 2006, Cela and Llimargas 2006, Llimargas and Casanova 1999, Nishimura et al. 2007). Besides the previously described defects, we noticed that at late embryonic stages the size and shape of the tracheal tubes were abnormal when EGFR was downregulated or constitutively activated in the tracheal cells. For this and all subsequent experiments, EGFR downregulation was achieved by expressing a dominant negative form of the receptor in tracheal cells by means of the btlGa4 line, and the constitutive activation, by expressing a constitutively active form of the receptor. From now on I will refer to these combinations as $EGFR^{DN}$ mutants and $EGFR^{CA}$ mutants, respectively. A convoluted dorsal trunk (DT) in $EGFR^{DN}$ (Fig.23B,B') conditions, and a shorter one in an $EGFR^{CA}$ conditions (Fig.23C,C') was observed when compared to the control (Fig.23A,A').

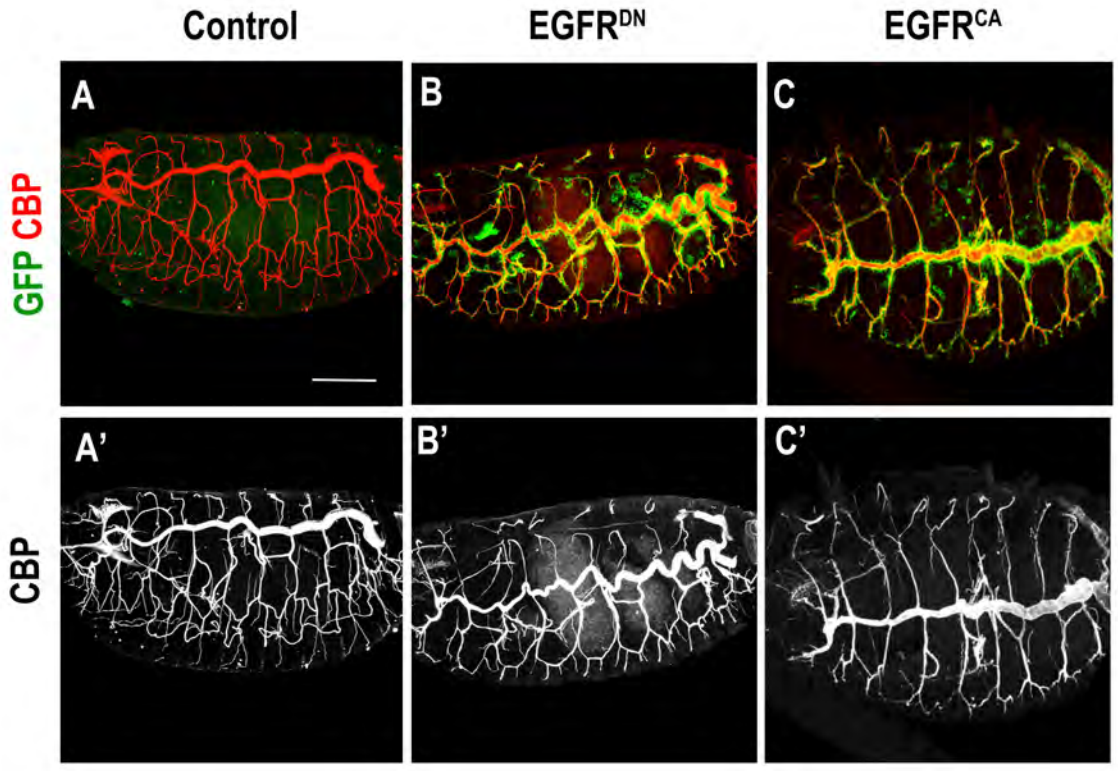

Figure 23. EGFR regulates DT length. **(A-C)** Lateral views of stage 16 embryos stained for CBP (Red, lumen) and GFP (Green). Compare DT length in $EGFR^{DN}$ (*BtlGal4-UASsrcGFP-UASEGFR^{DN})* to the control *(UASEGFR^{DN})* and to $EGFR^{CA}$ (*BtlGal4-UASsrcGFP-UASEGFR^{CA}).* **(A'-C')** Shows only CBP staining. Scale bar 50 μm.

The tube length phenotype was quantified. DT length was expressed as the ratio of the length measured following the DT path between metameres 4 and 9 and a straight line between the two points (see Material and Methods for details). The length of other branches, like the Dorsal Branch 5 (DB5) and the Transverse Connective 5 (TC5) was also measured and expressed as the total length following the path expressed in µm. The diameter of the DT in the metamere 7-8 was also measured. The quantification indicated a clear elongation of the DT in EGFR^{DN} (22,6% longer than the sibling control embryos), while the embryo size did not change (Fig. 24A,A',A''). A mild reduction in DT length was noticed in EGFR^{CA} (3%) (Fig.24A,A'), which correlated with a diametrical enlargement of the tubes in EGFR^{CA} embryos (Fig.24A''). The length of the rest of the branches was unchanged (Fig.24 A''), indicating a specific role of the EGFR in regulating the size of the DT.

A

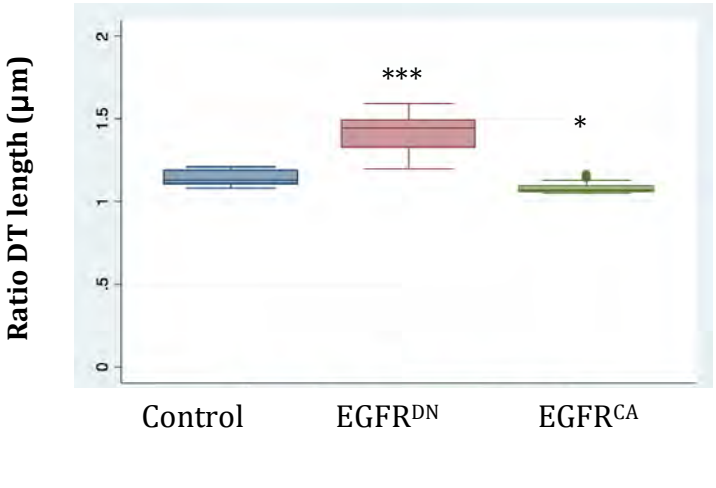

A'

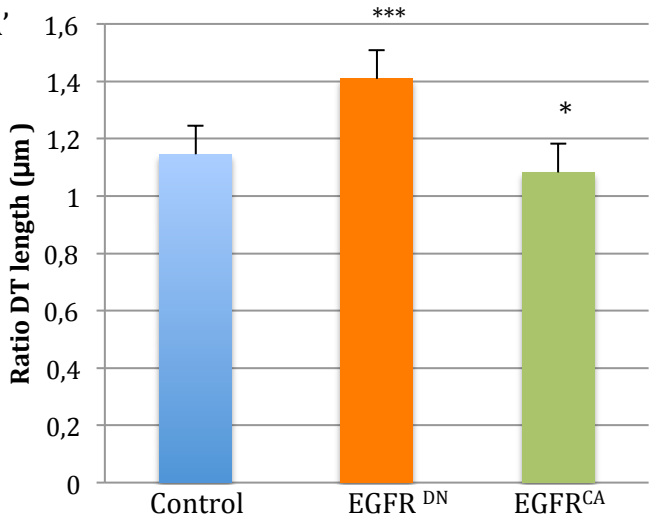

A''

	Control	EGFR^{DN}	pValue	Control	EGFR^{CA}	pValue
DB5	21.918 µm	18.041 µm	0.966	21.918 µm	17.983 µm	0.485
TC5	48.186 µm	45.052 µm	0.0705	48.186 µm	42.893 µm	0.0514
Diameter (MT7-8)	8.472 µm	7.622 µm	0.3285	8.472 µm	12.761 µm	0.0109
Embryo size	336.336 µm	335.485 µm	0.895	336.336 µm	337.843 µm	0.573

Figure 24. Quantifications of the branch length in control and EGFR mutants. **(A-A')** Box plot and histogram of DT ratio length. Compared to the control, EGFR^{DN} DT length is longer and EGFR^{CA} is shorter. Control n=26, EGFR^{DN} n= 16, EGFR^{CA} n=21. ***p < 0.001 and * p<0.05 by unpaired two-tailed student's t-test. Error bars indicate s.e.m. **(A'')** Table shows the quantifications of DB5, TC5, diameter and size in µm. pvalue was obtained by unpaired two-tailed student's t-test.

4.1.2 Cell number and cell shape

The tube enlargement found in EGFR^{DN} mutants could be due to an increase in cell number. To evaluate this possibility the number of cells in metamere 7-8 of the DT were counted. Cell numbers was roughly similar in mutant and control (25,5 cells in control embryos, n=4; and 26 cells in EGFR^{DN}, n=3 embryos), indicating that this was not the cause of tube enlargement. The shape of the DT cells was analysed, as it has been documented that cell morphology impinges on tube size and shape (Forster and Luschnig 2012, Nelson et al. 2012). Cell shape differences were clearly detected. In EGFR^{DN} mutant cells were elongated along the anterioposterior axis (Fig.25B) while cells were abnormally oriented diametrically in EGFR^{CA} (Fig.25C). The length of the axial cell junctions and of the circumferential junctions was measured in control and mutants embryos. There was a clear bias towards an enlargement of the axial junctions in EGFR^{DN} and a significant bias towards a reduction in EGFR^{CA} (Fig.25D).

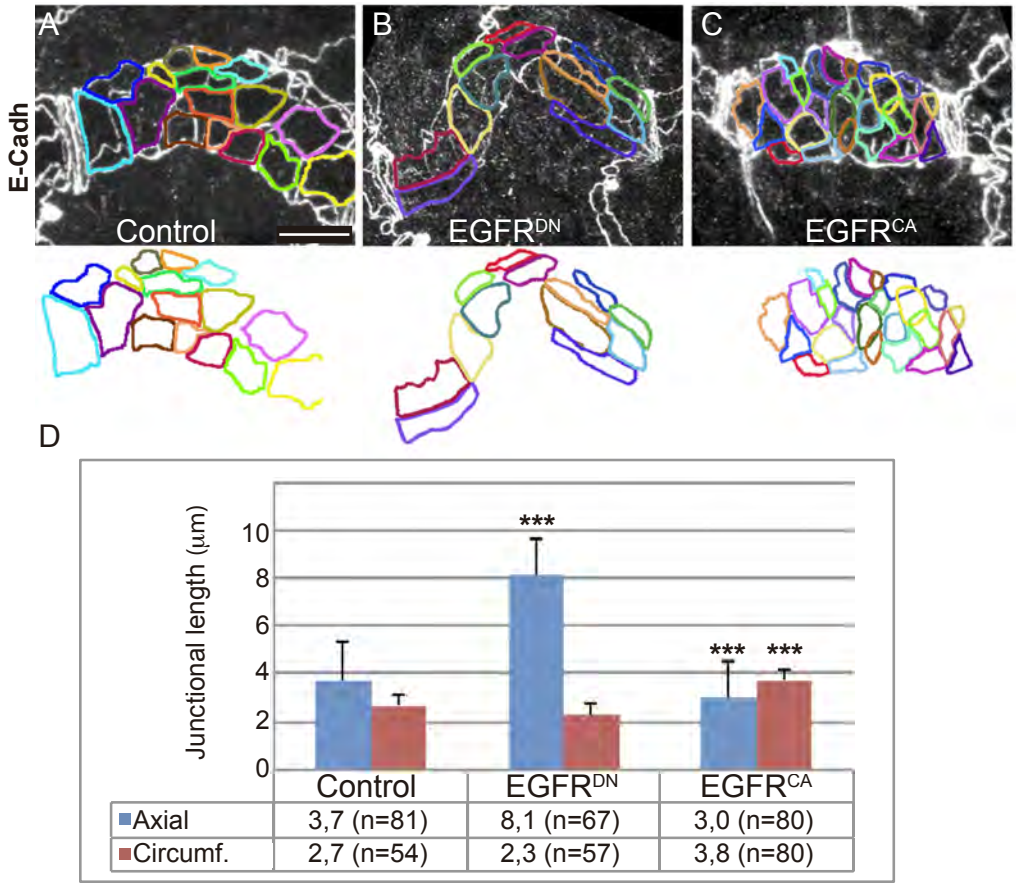

Figure 25. Cell shape and cell junction quantification in Control and EGFR mutants. **(A-C)** Single tracheal metamere of stage 16 embryos stained for E-Cadherin that shows the apical shape. The apical outline of the cells is drawn in colours. In EGFR^{DN} embryos the cells are more elongated axially whereas in EGFR^{CA} the cells display a narrow shape. Scale bar 7,5 µm**. (D)** Histogram showing the quantifications of the junction length in µm. N =3 in all experimental conditions. ***$p < 0.001$ by unpaired two-tailed student's *t*-test. Error bars, s.e.m.

Altogether these results indicate that the EGFR activity prevents the excessive DT length and regulates the morphology of DT cells.

4.2 EGFR activation in tube size control

4.2.1 The role of Spi in the control of DT elongation

To investigate how is EGFR activated, the contribution of the different EGFR ligands in the context of tube size regulation was analysed. Four ligands, Spitz (Spi), Keren (krn), Gurken (Grk) and Vein (Vn), have been shown to activate EGFR in different contexts (Perrimon et al. 2012, Shilo 2003, 2005). Three of them, namely Spi, Grk and Krn require a post-translational activation to be active, while Vn is a secreted ligand that does not require any modification (Schnepp et al. 1996). As Grk is only expressed during the oogenesis, we did not analyse its contribution to tracheal formation.

Spi is the principal active ligand for EGFR during *Drosophila* embryogenesis and is responsible for most EGFR activities (Rutledge et al. 1992). Due to these pleiotropic effects it was not possible to determine tube size in Spi mutants. As an alternative approach, the downregulation of Spi using a RNAi was tested. The expression of spiRNAi in the tracheal cells did not produce a comparable DT elongation to that of $EGFR^{DN}$ (Fig.26C). RNAiSpi was also expressed in a generalised pattern using tubulinG4. This produced also a DT overelongation (Fig.26B), although milder than that of $EGFR^{DN}$, about a 5% longer than the control (Fig.26D). These results suggest that Spitz coming from different sources (tracheal and non-tracheal cells) would activate EGFR in the tracheal cells to control tube elongation.

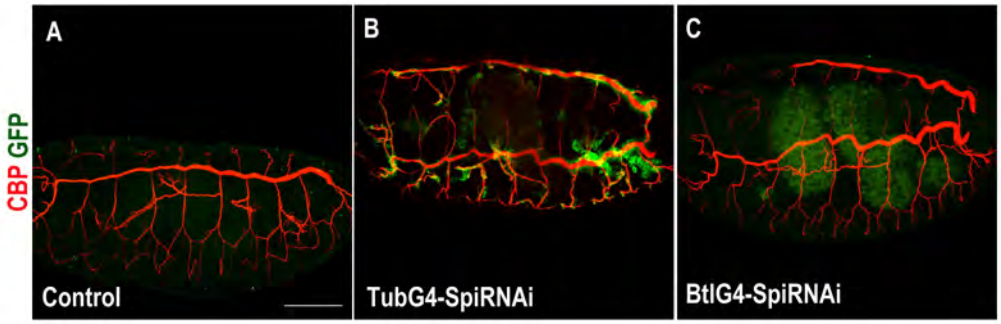

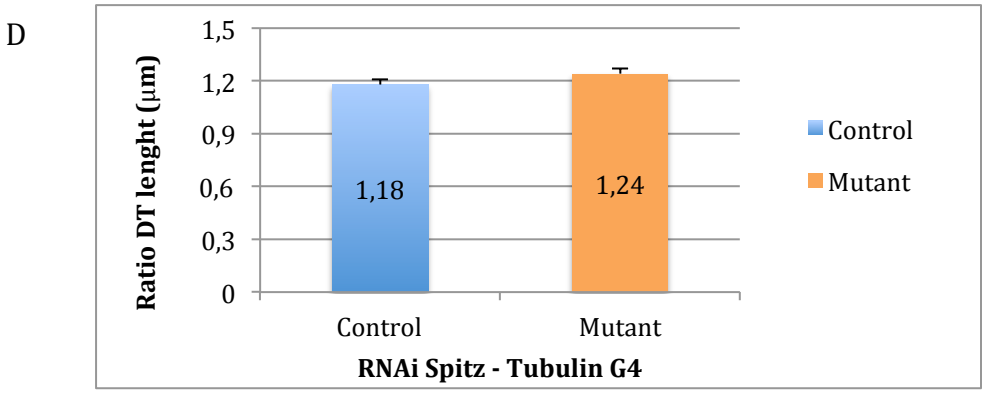

Figure 26. Downregulation of Spi did not produce clear tube size defects. (A-C) Lateral views of stage 16 embryos of indicated genotypes stained for CBP (red) and GFP (green). Note that expressing the SpiRNAi in the tracheal cells did not produce clear tube size defects **(D).** Expressing SpiRNAi in a generalised pattern (using a TubG4) produced an overelongation of the DT, although the phenotype is milder than in a $EGFR^{DN}$ and there are no clear significant differences compared to control. SpiRNAi n= 36, Control n= 18 embryos. Scale bar A-C 50 µm.

Argos (aos) has been shown to compete with Spi preventing Spi binding to the receptor thereby preventing the EGFR dimerization that triggers the signal (Klein et al. 2004). Thus, the overexpression of Aos acts and is used as a loss of Spi activity. The expression of aos in tracheal cells produced clear tube size defects, which resembled those of $EGFR^{DN}$ (17,4% n= 38 embryos) (Fig.27A-D). This result indicates that aos expressed in tracheal cells acts blocking EGFR ligand activation, strongly suggesting a capital role of Spi in activating EGFR to control tube length.

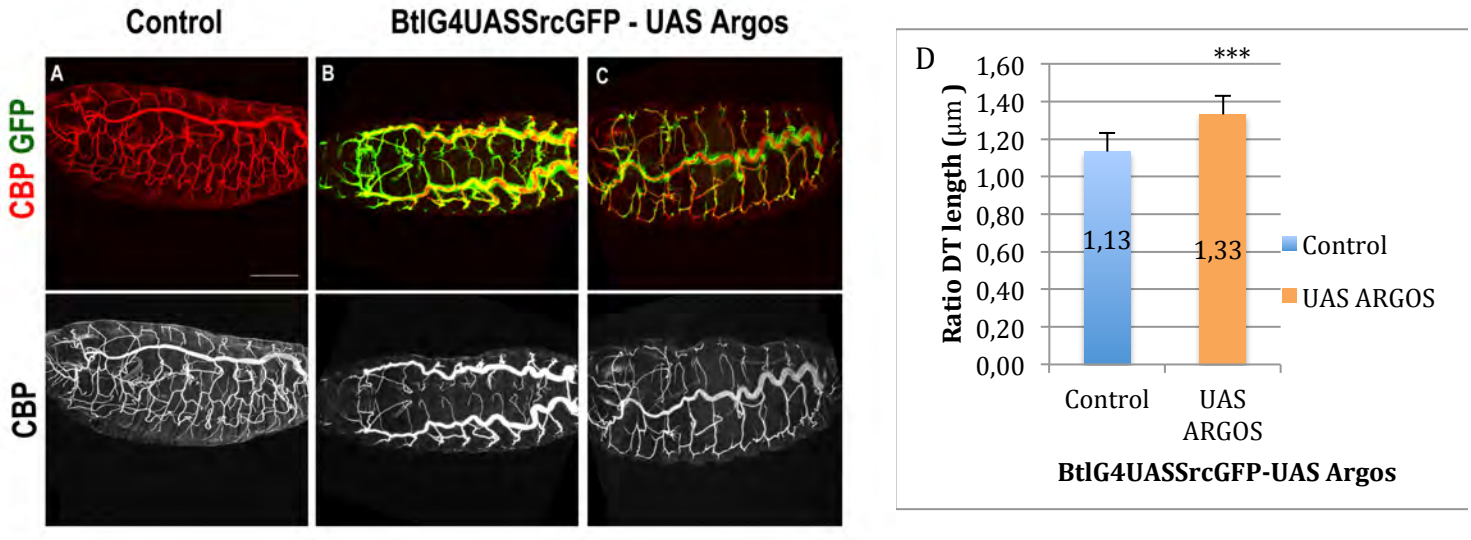

Figure 27. Aos expression in the tracheal cells produced clear tube size defects. (A-C) Lateral views of stage 16 embryos of indicated genotype stained for CBP (red) and GFP (green). Note that the expression of aos in tracheal cells produced clear tube size defects. **(D)** Quantification of the ratio DT length indicates significant differences when aos is expressed in the tracheal cells compared to control. ***$p < 0.001$ by unpaired two-tailed student's *t*-test. Error bars, s.e.m. Scale bar A-C 50 µm.

The overexpression of Spi was also analysed. The phenotype was comparable to that of EGFR^{CA}, indicating that Spi can activate the receptor in the tracheal cells (Fig.28A-C).

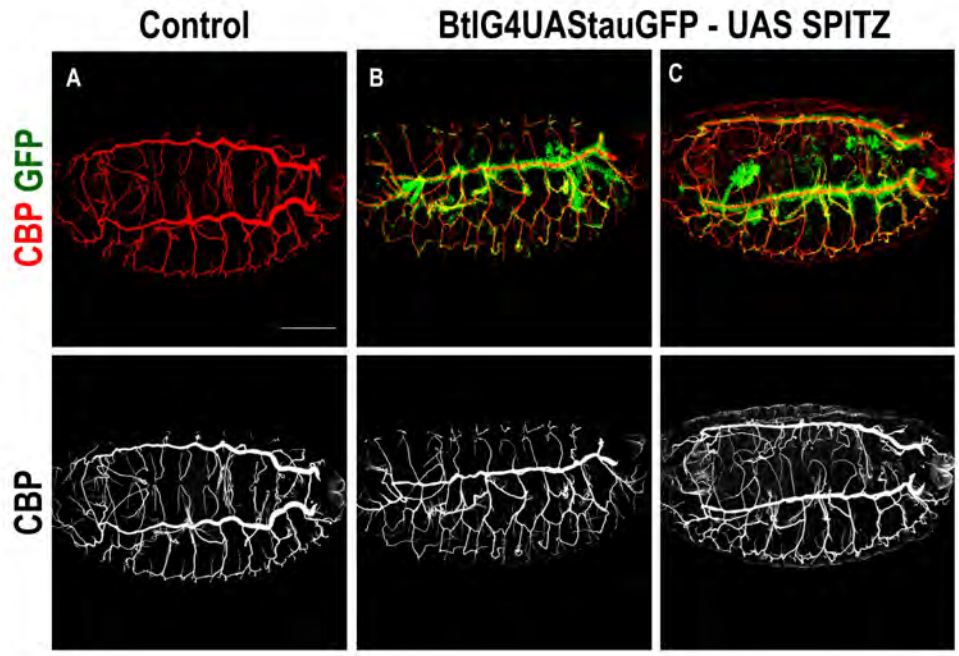

Figure 28. The overexpression of Spi produced a similar phenotype to that of EGFR^{CA}. (A-C) Lateral views of stage 16 embryos of indicated genotype stained for CBP (red) and GFP (green). Note that the overexpression of Spi in the tracheal cells produced a phenotype of shorter tubes comparable to that of EGFR^{CA}. Scale bar 75 μm.

Altogether these results strongly suggest that spi acts as the ligand that activates EGFR in the tracheal system.

4.2.2 The activity of Vein and keren in tracheal formation

The possible requirement of other EGFR ligands, in particular Vein and keren, was also evaluated. The loss of function of Vein in tracheal formation was analysed using a hypomorphic mutant allele (VnC221) or a null allele (Vn γ4), which produced no tracheal defects (Fig.29A-E). In addition, Vein RNAi was expressed in the tracheal cells (using btlGal4) or in a general pattern (using DaG4, TwistG4 and TubG4) but no tracheal defects were detected in any of these conditions either (Fig.29C-H). Similarly, single mutants for Keren (hypomorphic mutant allele) did not produce tracheal defects (Fig.29I, J).

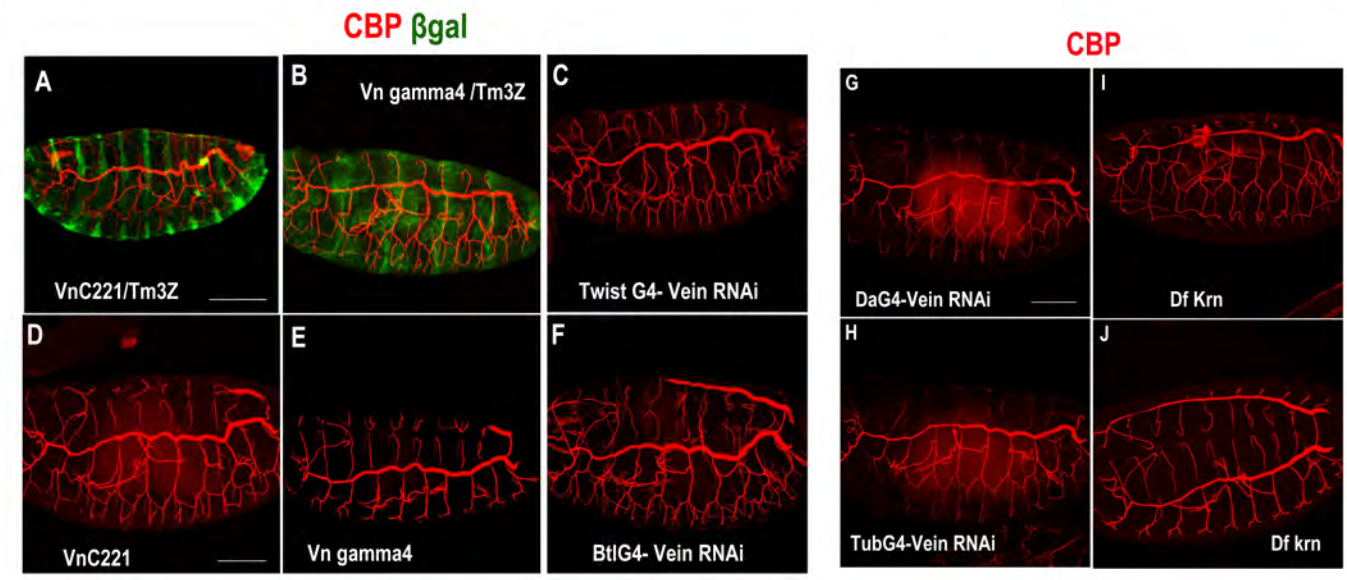

Figure 29. Vn and Krn mutant function is not required for tube size control. **(A-J)** Lateral views of stage 16 embryos of indicated genotype stained for CBP (red) and βGal (green). Note that no tube size defects were detected in any of these mutant conditions. Scale bar A 75 μm and B-J 50 μm.

Finally, we tested the absence of Vn and Krn activity at the same time, to determine whether they could act redundantly. We did not observe tracheal defects (Fig.30C,D).

In addition, we analysed the absence of all EGFR ligands (null mutants alleles, Vn^{L6}, Krn^{27}, Grk^{HF} and Spi^{2A}) to completely block the receptor activation. In Spi mutant embryos the tracheal system is strongly affected (Fig.30A,B). Due to these pleiotropic effects, we generated a similar effect as Spi mutant by the overexpression of aos. The embryos expressing the overexpression of aos tended to show tube size defects, whereas the Vn Krn activity seemed to not participate in the phenotype (Fig.30E-H).

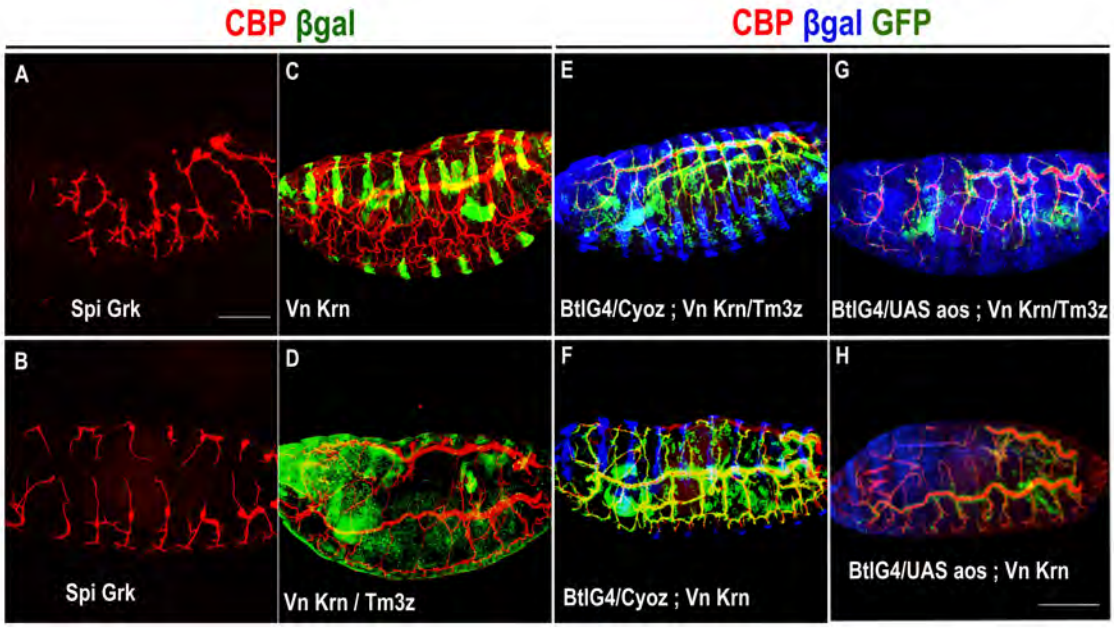

Figure 30. The absence of all EGFR ligands did not cause tube size defects. (A-H) Lateral views of stage 16 embryos of indicated genotype stained for CBP (red), βGal (green, blue) and GFP (green). Scale bar A-G 50 μm and H 75 μm.

Altogether these results indicate that Vn, Krn and Grk are not required to activate EGFR during tracheal formation.

4.3 The requirement of the RAS-MAPK pathway in tube size control

The contribution of known downstream mediators of EGFR signal in tracheal tube elongation was analysed to understand EGFR activity. EGFR transduces the signal mainly thought the RAS-MAPK pathway, also during the maintenance of epithelial integrity in tracheal formation (Cela and Llimargas 2006).

4.3.1 EGFR controls tube size by the RAS-MAPK pathway

The central element of the MAPK pathway, MAPK (known as rolled, rl in *Drosophila*), was downregulated by means of a mutant MAPK allele (rlI3) or using the overexpression of a MAPK negative regulator (i.e. the MAP Kinase Phosphatase 3, MKP3 (Kim et al. 2004). Under these conditions, the tracheal tubes became elongated to a similar extend to that of $EGFR^{DN}$ mutants (28,04% n=25) (Fig.32A-D). In contrast, when a constitutively activated form of the MAPK was expressed (UAS-Sem), the tubes resembled those found in $EGFR^{CA}$ mutants (2,6% n=20) (Fig.31A-D).

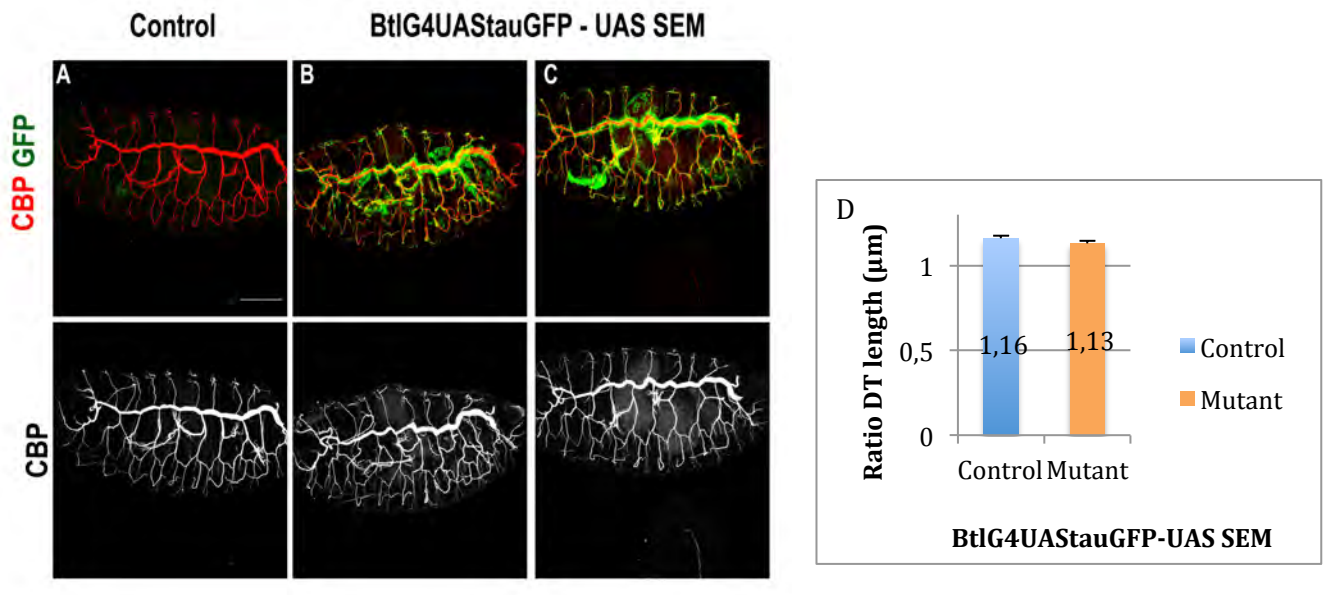

Figure 31. The constitutively active form of MAPK produced a short tube phenotype similar to that of $EGFR^{CA}$. (A-C) Lateral views of stage 16 embryos of indicated genotype stained for CBP (red) and GFP (green). Note that a constitutively form of the MAPK expressed, the tubes resemble those found in $EGFR^{CA.}$ **(D)** Quantification shows a reduction in the tube length when the MAPK is over activated, similar to that of control. Scale Bar 50 µm.

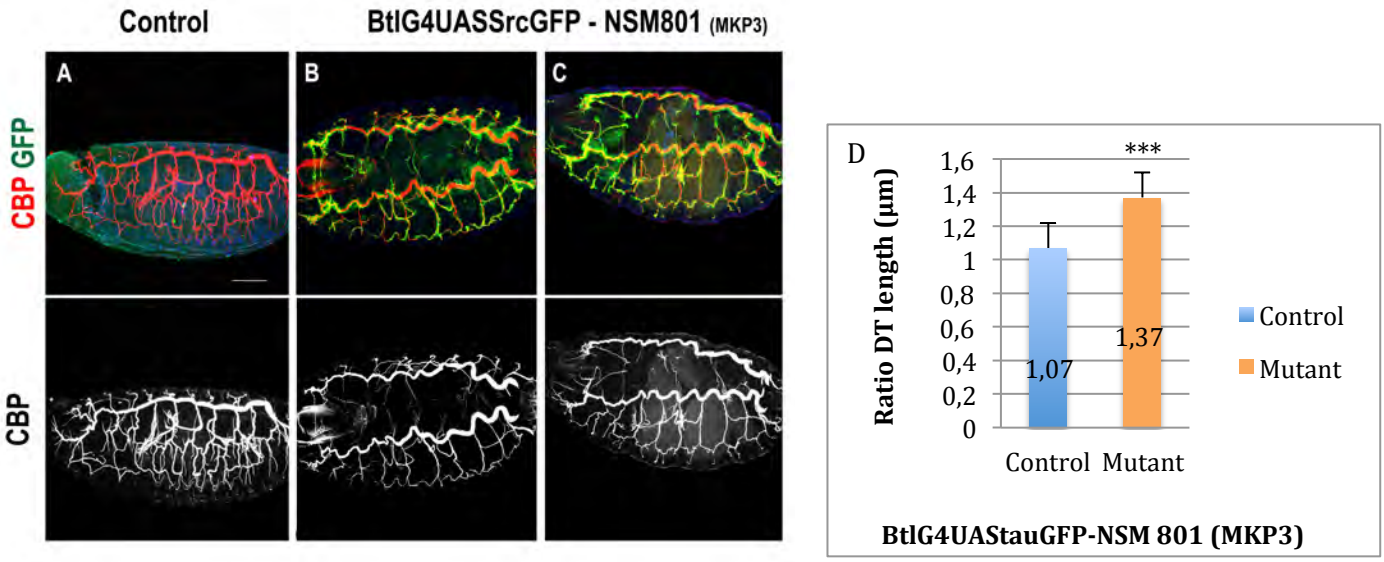

Figure 32. The downregulation of MAPK activity lead to an enlargement of the tracheal tubes. (A-C) Lateral views of stage 16 embryos of indicated genotype stained for CBP (red) and GFP (green). Note that using the overexpression of a MAPK negative regulator (MKP3), the tracheal DT became elongated to a similar extend to that of $EGFR^{DN}$. **(D)** Quantification shows a significant elongation of the DT when MAPK is downregulated compared to control. ***$p < 0.001$ by unpaired two-tailed student's *t*-test. Error bars, s.e.m Scale bar 50 µm.

Altogether, these results strongly suggest that the EGFR signal controls tube size through the canonical RAS-MAPK pathway.

4.3.2 The nuclear requirement of EGFR signalling in tube size

The canonical MAPK pathway typically transduces the signal through the activation of nuclear transcription factor effectors (Futran et al. 2013, Wortzel and Seger 2011). To better understand EGFR activity we asked whether tube elongation was mediated by known transcriptional effectors of the pathway.

Pnt is one of the major transcriptional activators of the pathway. The PntP2 isoform is directly activated by MAPK phosphorylation, while a second isoform, PntP1, is constitutively active but transcriptionally regulated by MAPK (Shilo 2014). The requirement of Pnt in tube elongation, assessed by means of a null allele (PntD88), could not be analysed due to pleiotropic effects. In addition, a PntP2-lacZ reporter indicated that this isoform was not expressed in the tracheal cells and therefore it was not analysed further. PntP1 overexpression in tracheal cells produced defects in tube fusion (Fig.33white arrow), however, no clear defects in tube size were observed. These results suggest that Pnt is not required to transduce the EGFR signal that controls tube elongation.

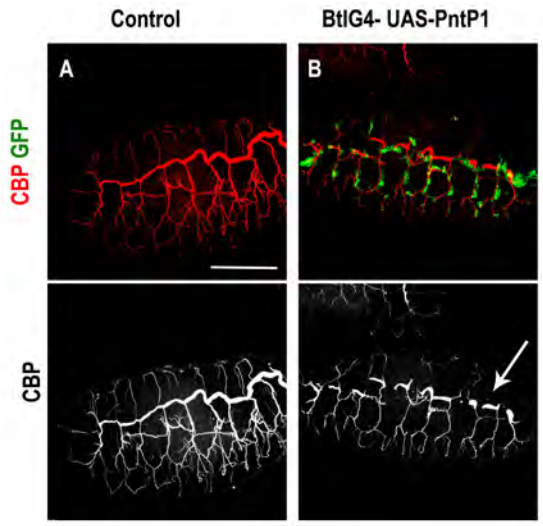

Figure 33. Tracheal fusion defects in an overexpression form of PntP1. **(A-B)** Lateral views of stage 16 embryos of indicated genotype stained for CBP (red) and GFP (green). Note that the overexpression of PntP1 led to a DT fusion defects, but no defects in tube size were detected. Scale bar 50 μm

The MAPK pathway also controls the activity of transcriptional repressors (Futran et al. 2013, Wortzel and Seger 2011), like Yan. Yan is a constitutive repressor that competes for Pnt-binding sites, and hence blocks the binding of Pnt. Phosphorylation of Yan by MAPK leads to its translocation from the nucleus and its degradation (Lai and Rubin 1992, Rebay and Rubin 1995, Tootle et al. 2003). The contribution of Yan to the tracheal control of tube size was analysed. The overexpression of Yan in tracheal cells showed clear DT fusion defects, but no defects in tube size (Fig.34A-C).

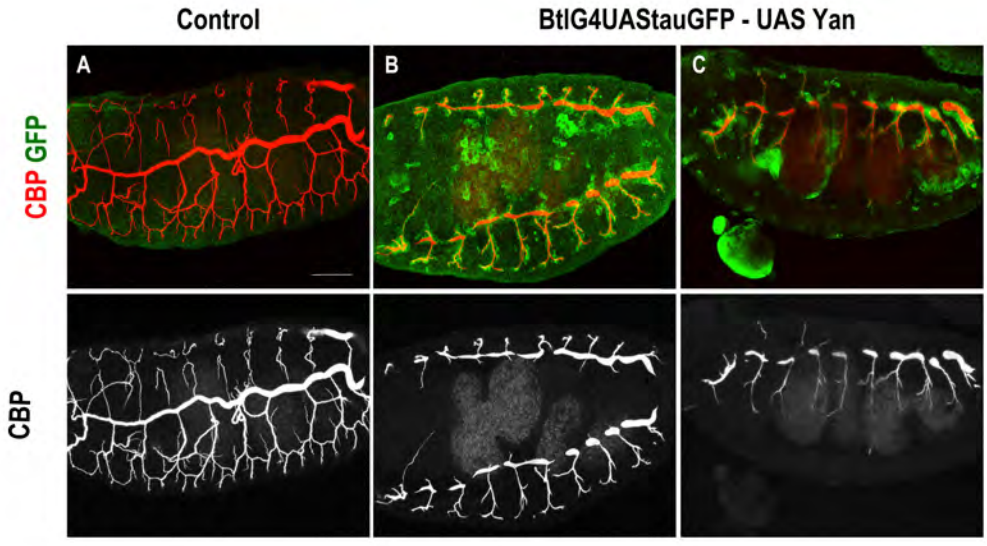

Figure 34. Tracheal fusion defects in an overexpression form of Yan. **(A-C)** Lateral views of stage 16 embryos of indicated genotype stained for CBP (red) and GFP (green). Note that the overexpression of Yan led to a DT fusion defects, but no defects in tube size were detected. Scale bar 50 μm

On the contrary, the absence of Yan activity (using an amorphic mutant allele, Yan^{E2D}) produced defects in tube size (Fig.35A-C,D). Indeed, we noticed that these tube size defects were due to a head involution defect during embryogenesis, which left less space inside the embryo for the normal tracheal system development. The head segments failed to migrate as far as internally as they ought and thereby, they were crowded into the anterior tip of the head without reaching their final position inside the embryo. Although the tracheal network did not develop correctly, the embryo size did not change either (Fig.35E).

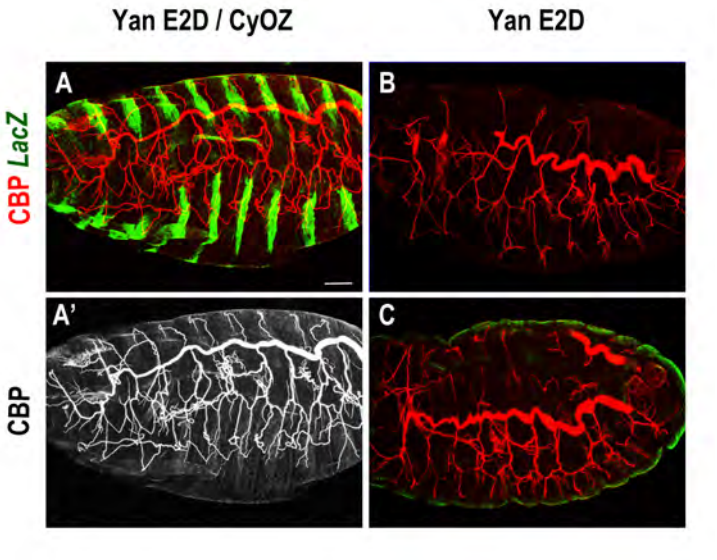

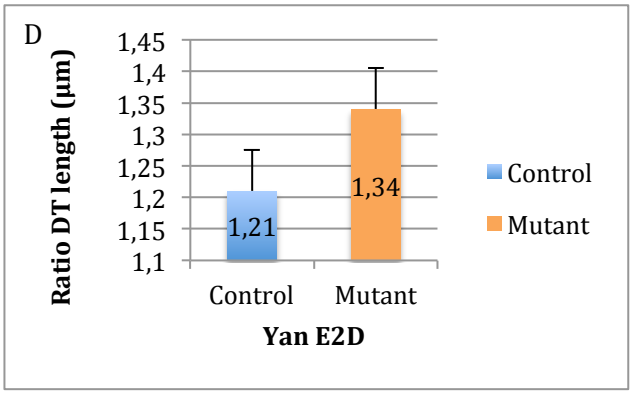

E

	Embryo size	Head involution (From the most anterior tip of the head until the tracheal system)
Yan E2D / CyOZ	443.347,7 µm	93.311,9 µm
Yan E2D (HM)	453.614,3 µm	144.365,2 µm

Figure 35. Mutant allele of Yan did not produce tube size defects. (A-C) Lateral views of stage 16 embryos of indicated genotype stained for CBP (red) and βGal (green). **(D)** Quantification of the ratio DT length indicated an enlargement of the tube in Yan mutants compared to control, but this phenotype is due to a head involution defect. **(E)** Quantification from the most anterior tip of the head to the first tracheal branches and embryo size quantification. Scale bar 50 µm.

Altogether, these results strongly suggest that the most canonical nuclear targets of EGFR signalling, Pnt and Yan, do not seem to be implicated in the control of tube size.

4.4 EGFR mechanism of tube size regulation

Longitudinal growth of tracheal tubes depends on intrinsic cell properties such as Crumbs-dependant (Crb) apical membrane growth (Dong et al. 2014, Laprise et al. 2010) and pSrc-dependant polarised cell shape changes (Forster and Luschnig 2012, Nelson et al. 2012). In addition, it also depends on extrinsic mechanical forces exerted by the aECM (apical extracellular matrix) that counteracts and restricts tube elongation. In particular, it was shown that the chitin filament needs to be properly organised and modified by chitin-associated proteins like the chitin deacetylases Verm and Serp to prevent excessive growth (Luschnig et al. 2006, Wang et al. 2006). We evaluate whether EGFR was regulating any of these mechanisms.

4.4.1 EGFR controls Serp accumulation in the aECM

The chitin binding protein Serp is required for restricting the excessive tracheal tube elongation by the regulation of the structural properties of the chitin filament (Luschnig et al. 2006, Wang et al. 2006). Hence, in the absence of Serp, the tracheal tube overelongate, showing a very similar phenotype to that of the $EGFR^{DN}$. This prompted us to analyse a possible relationship between EGFR and Serp.

Serp is first secreted in the cytoplasm of the tracheal cells at embryonic stage 13 (Fig.36A green arrow). From stage 14 until stage 16, Serp is secreted and accumulated in the lumen of the tracheal tubes (Fig.36B,C pink arrows), colocalising with the chitin filament (Luschnig et al. 2006). In addition, Serp also accumulates from early stages in the apical membrane of the tracheal cells that surround the DT, lining the lumen (Fig.36B,C blue arrows).

The accumulation of Serp when $EGFR^{DN}$ was expressed in the trachea was analysed. At early stages, Serp was detected in the cytoplasm of the tracheal cells (Fig.36D green arrow), in the lumen and in the apical membrane of the cells (Fig.36E,F pink and blue arrows), as in the control. However, at late stages, there was a decrease of Serp accumulation in the lumen (Fig.36F pink arrow), although the accumulation in the apical membrane did not decrease (Fig.36F blue arrow).

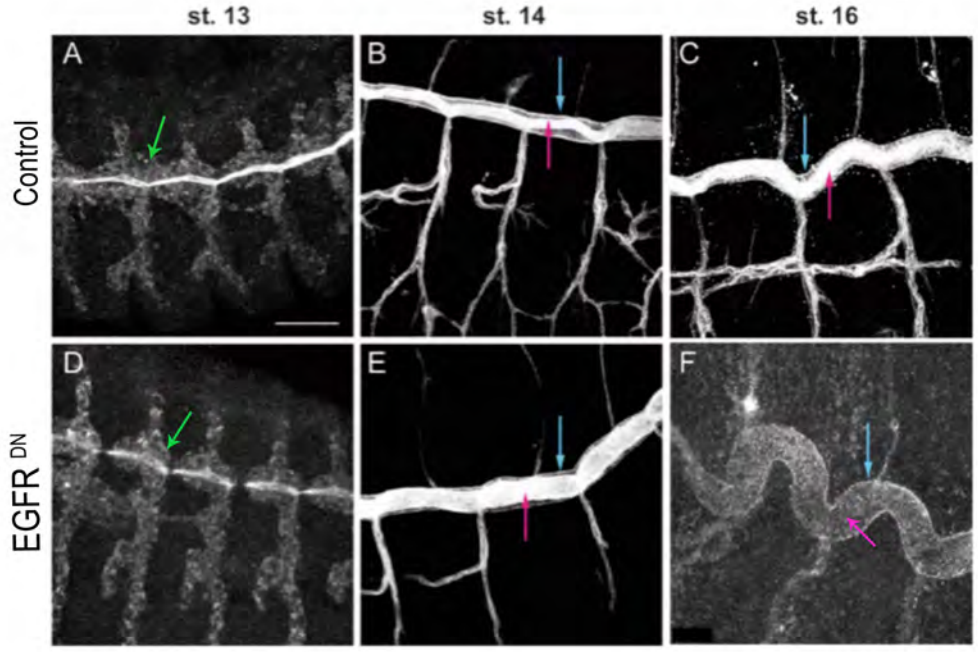

Figure 36. EGFR regulates the luminal accumulation of Serp. (A-F) Lateral views of control embryos and embryos carrying *BtlG4-UAS-EGFR^{DN}* stained with Serp antibody at indicated stages. From early stages Serp can be detected in the lumen (pink arrows) and in the apical membrane of the tracheal cells (blue arrows). When EGFR is downregulated, Serp accumulation in the lumen substantially decreases with time, but remains detectable in the apical membrane of the tracheal cells (blue arrow in F). Scale bar 25 μm.

This was especially clear when we expressed EGFR^{DN} in the posterior part of the tracheal system (Fig.37A-B').

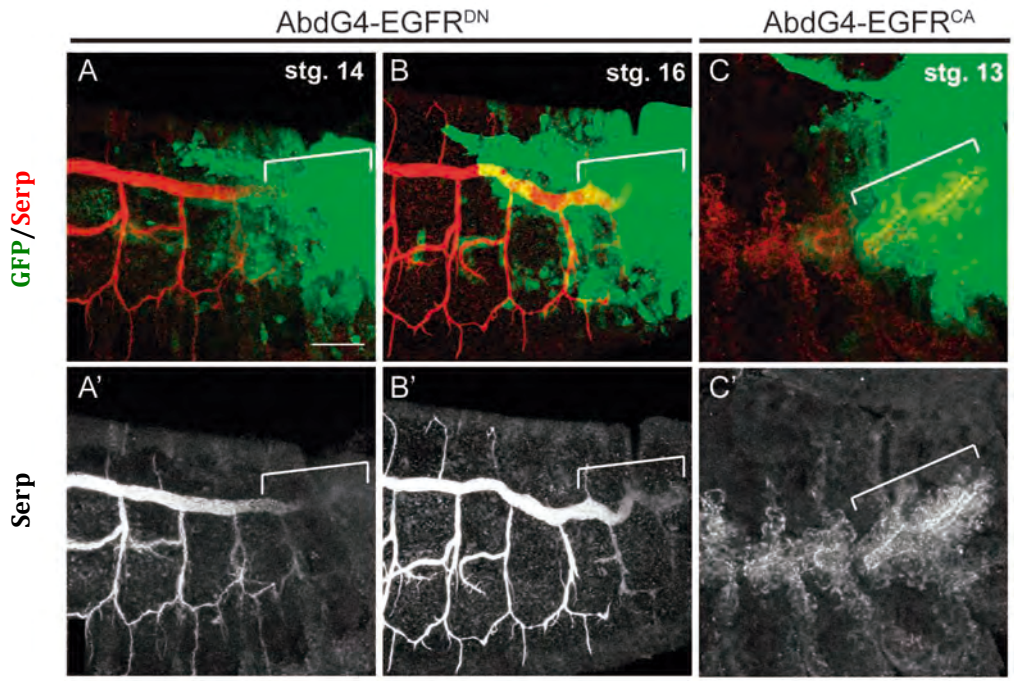

Figure 37. Luminal accumulation of Serp expresses in *AbdB* conditions. (A-C) Lateral views of embryos at the indicated stages carrying *AbdBGal4-UASGFP* stained with Serp antibody (red or white) and GFP (green). Note the difference of Serp luminal accumulation in the Abd domain (marked by white bracket) in the different EGFR mutant conditions. Scale bar 25 μm.

The expression of EGFR^{CA} had a mild effect on Serp accumulation, which seemed to starts accumulating in the lumen slightly earlier than in the control (Fig.38D,E pink arrow; Fig.37C,C'), while at later stages Serp remained strong in the lumen and in the apical membrane (Fig.38F pink and blue arrows).

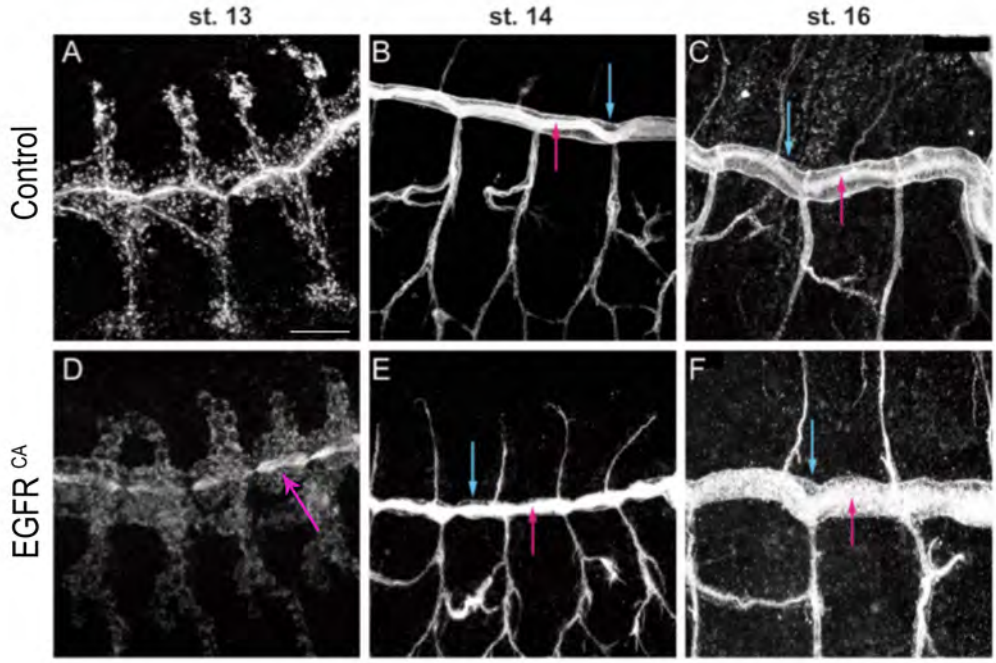

Figure 38. Accumulation of Serp in EGFR^{CA}. (A-F) Lateral views of control embryos and embryos carrying *BtlG4-UAS-EGFR^{CA}* at indicated stages stained with Serp antibody. From early stages, Serp is already detected in the lumen (pink arrows) and in the apical membrane of the tracheal cells (blue arrows). When EGFR is constitutively activated, Serp is accumulated slightly earlier and high levels of Serp are detected in the lumen. Scale bar 25 μm.

As Serp has been shown to control tube elongation and we find that EGFR controls its luminal accumulation, we propose that EGFR controls tube size at least in part by regulating Serp accumulation in the DT.

4.4.2 EGFR controls Crb accumulation in the DT

The activity of *crb* also correlates with tube elongation. The overexpression of *crb* (Laprise et al. 2010) or the increase of Crb activity (Dong et al. 2014) leads to an overproduction of apical membrane that results in overelongated tubes. In line with these reports, previous results showed that Crb levels decrease at late stages (Letizia et al. 2011) consistent with the idea that Crb is finely regulated to prevent excessive growth.

Hence, Crb accumulation in the different EGFR mutant conditions was analysed. When EGFR^{DN} was expressed in the trachea, Crb normally localised apically throughout all the tracheal development. Nevertheless, the accumulation of *crb* was brighter and sharper compared to the control (Fig.39A-C).

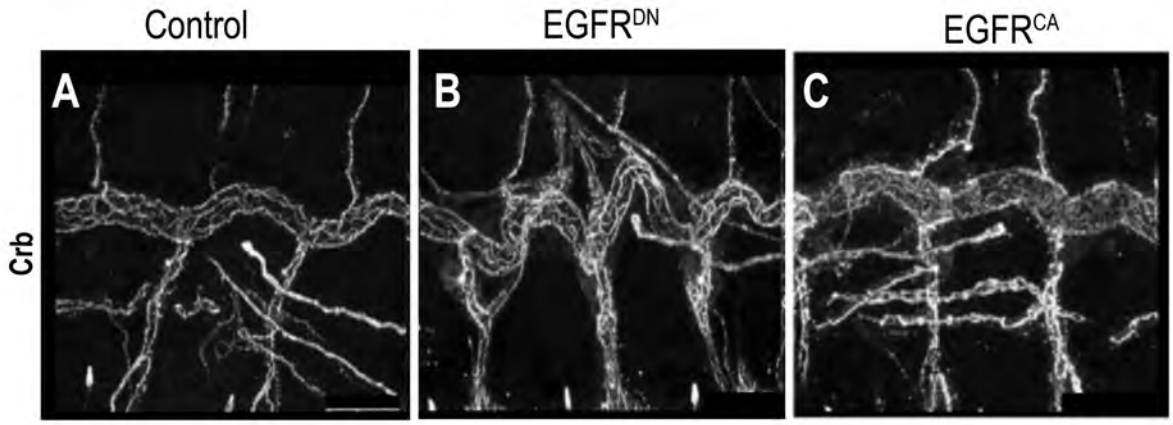

Figure 39. EGFR controls Crb accumulation in the DT. (A-C) Lateral views of 16 embryos stained for crb antibody. Note that Crb is accumulated higher in EGFR mutant conditions (*BtlG4-UAS-EGFR^{CA}; BtlG4-UAS-EGFR^{DN})* compared to control. Scale bar 25 µm.

To confirm this observation, the levels of Crb in the DT of stage 16 embryos were analysed. For each embryo, Crb levels in the trachea were normalised the value to the levels in Malphigian tubules (MT), which did not expressed EGFR^{DN}. In EGFR^{DN} embryos the levels of Crb in the trachea were higher than in the control sibling embryos (Fig.40A,B,D). The levels of Crb in the DT were also analysed in stage 16 embryos expressing EGFR^{CA} in tracheal cells. The levels of Crb were also higher than in the control embryos (Fig.40A,C,D).

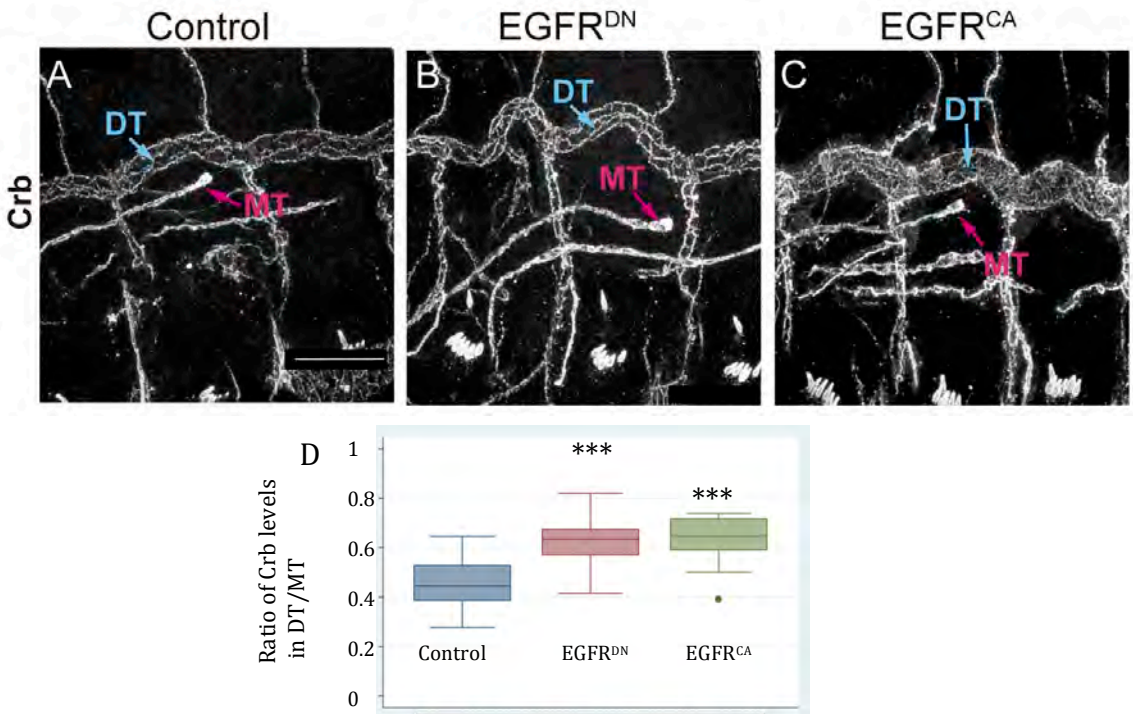

Figure 40. EGFR regulates Crb levels in the DT. (A-C) Lateral views of stage 16 embryos stained for Crb. Images show the DT of 3 tracheal metameres (Blue arrows) and the MT to compare and quantify Crb levels (pink arrows). MT do not express EGFR constructs (using *BtlG4-UAS-EGFR^{CA}; BtlG4-UAS-EGFR^{DN}).* Scale bar 25 µm. **(D)** Quantification of Crb levels. The ratio significantly increases in EGFR mutants, indicating higher levels of Crb in the DT. Control n= 35, EGFR^{DN} n= 34, EGFR^{CA} n= 16. ***$p < 0.001$ by unpaired two-tailed student's *t*-test.

Overall, these results indicate that EGFR activity regulates Crb levels in the DT. Because Crb has been shown to promote apical membrane growth at late stages of tracheal formation, we propose that EGFR triggers its function in part through the regulation of Crb levels.

4.5 Crb apical subcellular accumulation

Despite the apparently similar phenotype of increased Crb levels in $EGFR^{DN}$ and $EGFR^{CA}$, a closer evaluation of Crb accumulation indicated clear differences between EGFR mutant conditions. We found that Crb localised in different apical subcellular domains in the different EGFR mutant conditions.

At stage 16 $EGFR^{DN}$ embryos, Crb was well defined in the Subapical region (SAR) (Fig.41B,B'), as in the control (Fig.41A,A'). The SAR corresponds to the most apicolateral region of the membrane that connects adjacent epithelial cells (Fig.41E, red; F, red). The accumulation of Crb in the SAR outlines the cell contour, as it does the accumulation of E-Cadherin (E-Cadh), which accumulates in the Adherents Junctions (AJ), positioned just below the SAR (Fig.41F green). On the contrary, in $EGFR^{CA}$ mutant conditions, the accumulation of Crb in the SAR appeared blurred and faint, while Crb seemed very conspicuous in the Apical free region (AFR) (Fig.41C, C'). The AFR is the most apical region of the membrane, which is in direct contact with the tracheal lumen (Fig.41E blue; F blue). This abnormal accumulation was particularly conspicuous in certain regions of the DT, randomly distributed but more frequent in the posterior regions. These regions with more delocalised Crb accumulation in the SAR, correlated with cell surfaces elongated circumferentially and with a circumferential enlargement of the DT tube (arrow in Fig.41C).

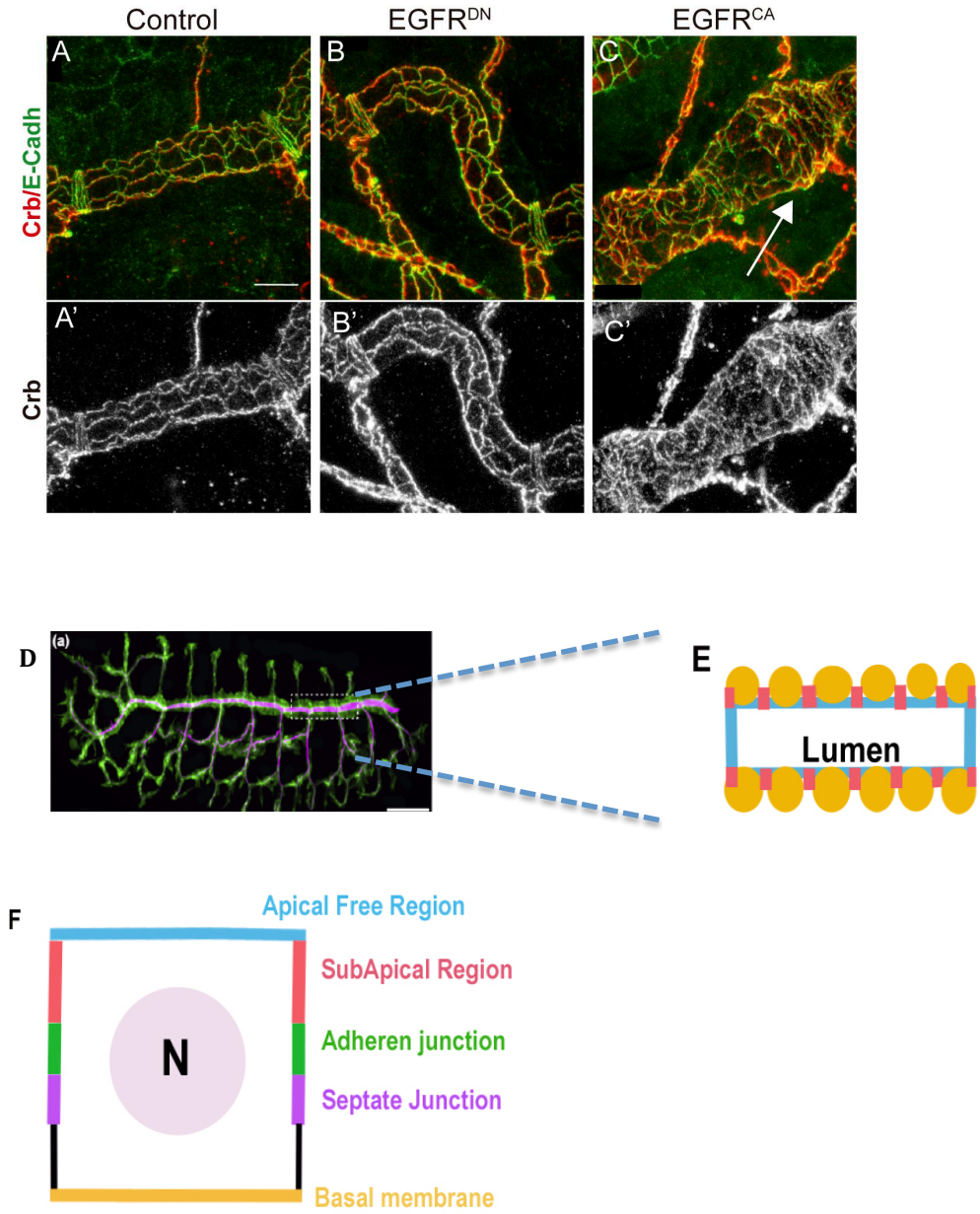

Figure 41. Crb subcellular accumulation in the apical membrane indicates clear differences between EGFR mutants' conditions. (A-C') Details of one single tracheal metamere of stage 16 embryos of indicated genotypes stained for E-Cadh (green) and Crb (red, white). Scale bar 7,5. **(D)** Image representing the tracheal system in a control embryo. **(E)** The scheme represents a fragment of the DT in an apical view showing the tracheal cells (orange) surrounding the luminal cavity by its apical side (blue). **(F)** Scheme of a single cell showing the membrane domains. The apical region of the tracheal cells faces the lumen of the tube (blue). Crb accumulates in the apical free region (AFR, blue), in direct contact with the lumen, and in the Subapical region (SAR, red), contacting two adjacent cells. E-Cadh accumulates basal to the SAR, in AJs (green).

To evaluate this observation, the ratio of Crb levels in the SAR versus AFR in individual cells of control and mutant EGFR conditions was quantified. The analysis indicated that while the ratio in $EGFR^{DN}$ was not very different from the control (Fig.42A,B) (suggesting that Crb is increased in all apical regions), it was significantly different in $EGFR^{CA}$, with less enrichment of Crb in the SAR and more accumulation of Crb in the AFR (Fig.42A,B).

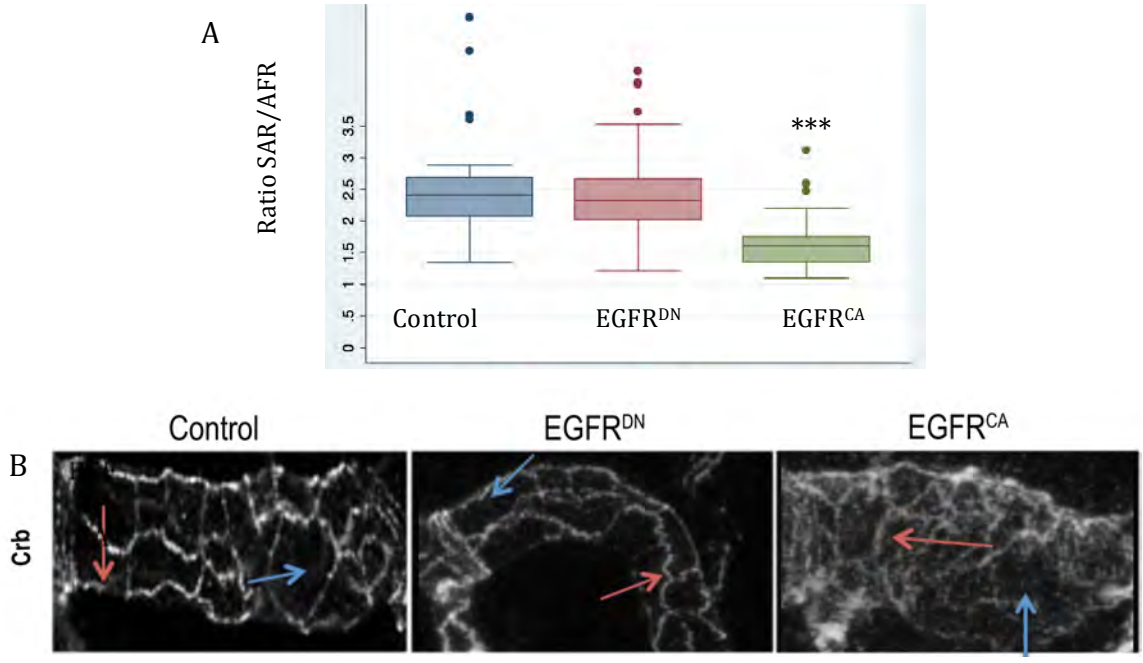

Figure 42. Crb can accumulate in different subcellular domains in the apical membrane of EGFR mutant conditions. (A) Quantification of the ratio of Crb subcellular accumulation in SAR vs AFR. Note that in an $EGFR^{CA}$, Crb enrichment in the SAR is significant decreased. Control n= 25 cells from 5 embryos, $EGFR^{DN}$ n= 41 cells from 9 embryos and $EGFR^{CA}$ n= 53 cells of 11 embryos. ***$p < 0.001$ by unpaired two-tailed student's *t*-test. **(B)** Details of one single tracheal metamere of stage 16 embryos of indicated genotypes stained for Crb. Panels show an example used to evaluate Crb subcellular accumulation in the AFR (blue arrows) and the SAR (red arrows).

Altogether our results show that Crb can accumulate in different subcellular domains in the apical membrane of tracheal cells and suggest that EGFR activity can regulate this accumulation.

4.5.1 Crb subcellular accumulation during tracheal formation

Since the previous results indicated that Crb can localise in different apical regions of the membrane, we further investigated this subcellular localisation of Crb during the tracheal development. Due to its homogenous and distinct pattern, E-Cadh was used to follow the cell outline of DT cells (Fig.43A-E). The analysis of the accumulation of Crb indicated a dynamic pattern. At early stages Crb mainly localised in the AFR with not much enrichment in the SAR (Fig.43A-C). However, as development proceeded a progressive enrichment of Crb in the SAR was detected (Fig.43D-E; movie 1). By stage 16-17 Crb appeared neatly accumulated and could be perfectly distinguished in the SAR (Fig.43E). This progressive subcellular accumulation in the apical region, which could also be observed in Z-sections (Fig.43F-J), correlated with a stage specific accumulation and presence of Crb in intracellular vesicles. These vesicles were highly abundant and clearly detected at stage 13-14 (Fig.43A,B,C blue arrows). By the end of stage 14 and 15, these vesicles disappeared, being less frequent at stage 16 (Fig.43D,E). This inverse correlation between the presence of Crb vesicles before the enrichment in the SAR raised the possibility that these two events are related.

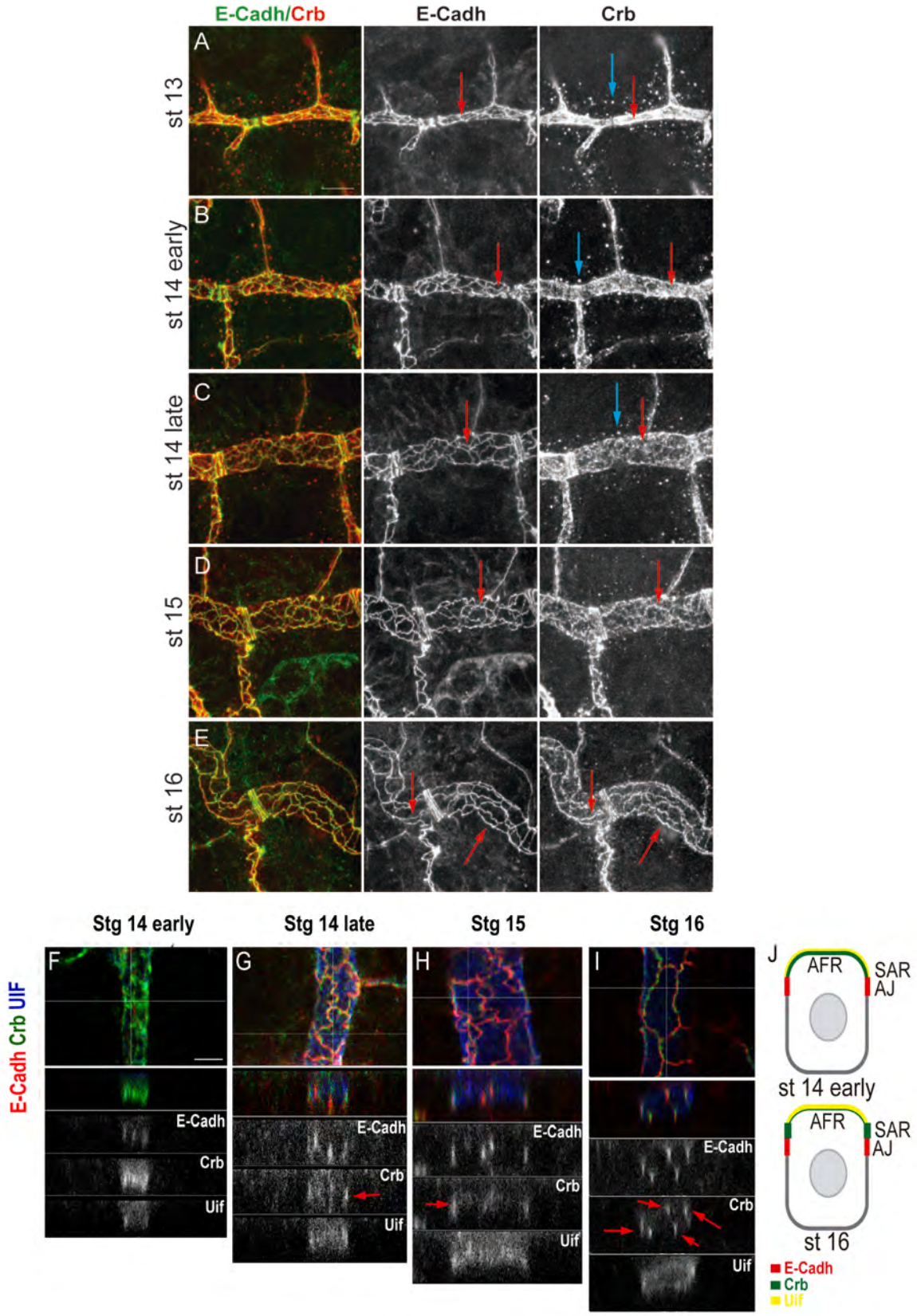

Figure 43. Subcellular accumulation of Crb during tracheal development. (A-E) Lateral views of Control embryos at indicated stages stained for E-Cadh (green, white) and Crb (red, white), showing 1-2 tracheal metameres. At early stages (14), while E-Cadh is already accumulated in the junctions (red arrows), Crb mainly accumulates in the AFR (red arrows). Crb becomes more enriched in the SAR as development proceeds (E). In addition, at early stages (14), abundant Crb vesicles were detected (blue arrows), but they decreased as development proceeds (late stages). Scale Bar 7,5 μm. **(F-I)** Z reconstructions of DTs of embryos at indicated stages stained for E-Cadh (red, white), Crb (green, white) and Uif (blue, white). The horizontal line in the

upper panel indicates the position of the Z- reconstruction. E-Cadh is always localising to the AJs, in the apicolateral membrane, visualised as lines spanning the AJs. Uif always localises in the most apical membrane. Note the transient accumulation of Crb during the development. Crb becomes more enriched in the SAR (red arrows, partially colocalising with E-Cadh) as development proceeds. Scale bar 5 μm. **(J)** Diagram representing a Z-section of a DT cell at early and late stages of the development. Uif (yellow) is accumulated in the apical region of the tracheal cells facing the lumen (AFR). E-Cadh is accumulated in AJs (red). Crb (green) first accumulates in the AFR, where Uif is accumulated, and later becomes enriched in the SAR.

4.5.2 Crb subcellular accumulation depends on its endocytosis

We investigated the nature of these vesicles. Diameter quantification indicated that they are around 0,5-0,6 μm (n= 21 vesicles from 3 different embryos), consistent with being endosomes (Gruenberg 2001). To determine the nature of these vesicles, the presence of Rab proteins, which are the master proteins implicated in intracellular trafficking and markers for different types of vesicles (Bhuin and Roy 2014, Wandinger-Ness and Zerial 2014), was determined.

Rab5 mediates traffic from the plasma membrane to early endosomes (EE) and serves as marker for EE. Crb vesicles were found to be rich in Rab5, suggesting that these are endosomes (Fig.44A).

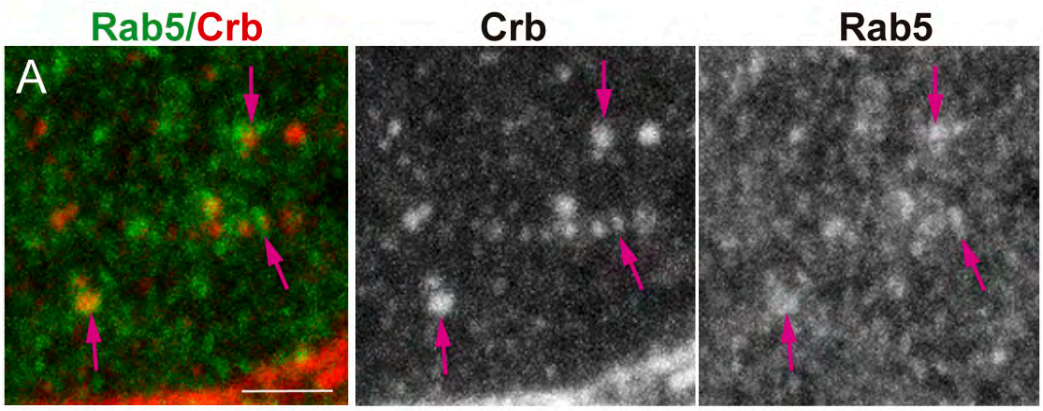

Figure 44. Crb vesicles are rich in Rab5. (A) Control embryo showing a double labelling of Rab5 (green, white) and Crb (red, white). Note that many Crb vesicles co-stain with Rab5 (pink arrows). Scale bar 2,5 μm.

To confirm that Rab5 was implicated in Crb accumulation, a dominant negative form of Rab5 was expressed in the trachea to block endocytosis. Interestingly, the 0,5-0,6 μm Crb vesicles typically found at stages 13-14, disappeared (Fig.45A).

At later stages, when the endocytosis was blocked, Crb remained high in the AFR and did not become enriched in the SAR (Fig.45B), suggesting a dynamic recycling of Crb at different apical domains dependent on internalisation.

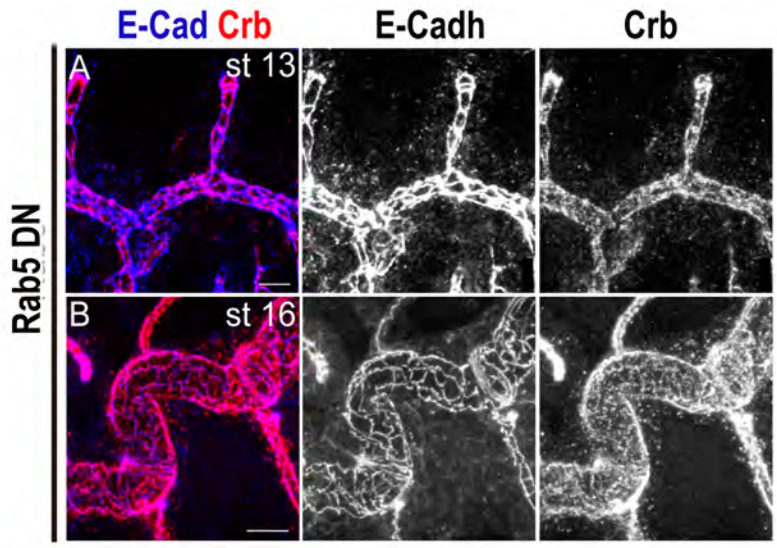

Figure 45. Crb is not enriched in the SAR in Rab5^{DN} embryos. (A, B) Lateral views of embryos with downregulated Rab5 activity at the indicated stages stained for E-Cadh (blue, white) and Crb (red, white) showing 1-2 tracheal metameres. At early stages Crb vesicles are absent **(A)**, and at late stages **(B**) Crb is not enriched in the SAR. Scale bar A 5 μm, B 7,5 μm

On the other hand, the expression of a constitutively active Rab5 protein induced the formation of enormous Crb endosomes at early stages (Fig.46A,B white arrow). In addition, at later stages, Crb was almost absent from the trachea, particularly from the DT (Fig.46C white arrow), suggesting that most Crb accumulating in the big endosomes is targeted to degradation.

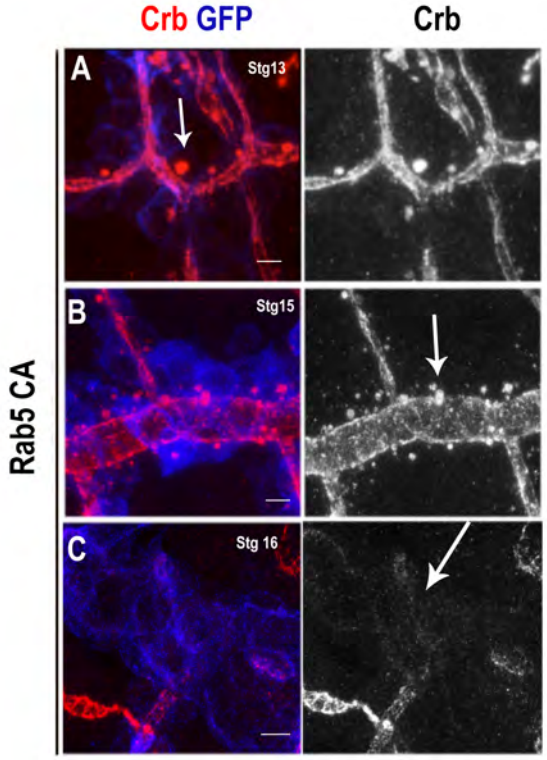

Figure 46. Crb is almost absent mainly from the DT in a Rab5 constitutively expression. (A-C) Lateral views of embryos at the indicated stages with activated Rab5 activity in the trachea stained for Crb (red, white) and GFP (blue). **(A, B)** At early stages huge Crb vesicles are detected (white arrow A, B), but at late stages **(C)** Crb is almost absent mainly from the DT region (white arrow C). A, B scale bar 5 μm and C 7,5 μm.

Altogether these results indicate that Crb undergoes a highly dynamic pattern of subcellular localisation throughout tracheal development, refining at the SAR at late stages. This pattern requires Rab5-dependent endocytosis.

4.6 Crb apical localisation and recycling pathways

All these results suggested that during the tracheal development Crb is endocytosed and likely recycled back to the SAR. In the literature, different endosomal sorting pathways control Crb trafficking regulating its activity. While a fraction of the pool of internalised Crb protein undergoes degradation (Dong and Hayashi 2015), Crb is also recycled back to the apical membrane through Recycling Endosome-Rab11 (RE-Rab11) (Roeth et al. 2009), Exo84 (Blankenship et al. 2007) or the Retromer complex (Pocha et al. 2011, Zhou et al. 2011) dependent pathways. We asked whether any of these pathways is required for Crb trafficking and recycling during tracheal development.

4.6.1 The role of Rab4 in Crb recycling

Once Crb is endocytosed by a Rab5-mediated endocytosis, Crb has to be recycled back to the apical membrane. To further characterise Crb endosomes present at early stages, we used tagged Rab proteins. A double staining for Crb/Rab4 proteins revealed that Crb endosomes were rich in Rab4 (Fig.47A1). A Rab4-YFP-tagged protein revealed that Rab4 is partially decorating the Crb endosomes (Fig.47A2, movie 2), suggesting that a pool of Crb protein accumulates in the lumen of the endosomes, likely to be directed to degradation. Nevertheless, some puncta of Crb/Rab4 colocalisation were detected, suggesting a Rab4-mediated recycling (Fig.47A1).

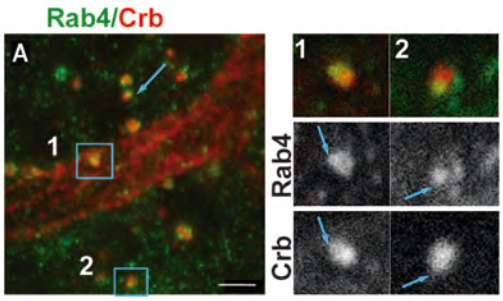

Figure 47. Crb endosomes are rich in Rab4 endosomes. **(A)** Double staining of Crb (Red) and Rab4 (using Rab4^{EYFP}-green). Examples of co-localisation of Crb/Rab4 in endosomes **(1);** and Crb localisation in the lumen of endosomes decorated by Rab4 **(2)**. Scale bar 2,5 µm.

It has been shown that Rab4 participates in a short loop endocytic pathway to directly recycle cargoes back to the plasma membrane (Gallon and Cullen 2015), and it has been associated with the Retromer complex (Temkin et al. 2011). The Retromer complex has been shown to participate in Crb recycling (Pocha et al. 2011, Zhou et al. 2011). In light of this evidence, it was hypothesised that Crb could recycle using a Rab4/Retromer dependent pathway.

In agreement with this hypothesis, it was found that when Rab4 is constitutively active, bigger vesicles containing Crb are detected at early embryonic stages (Fig.48A,B). This correlated with a poorer enrichment of Crb in the SAR at late stages (Fig.48C). These results suggested a hypothetical route of Crb recycling mainly to the AFR involving the Rab4/retromer complex.

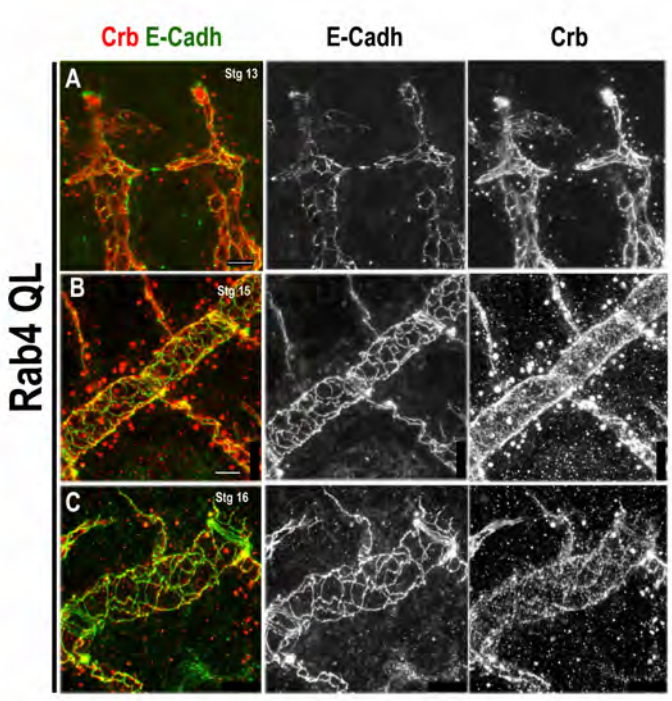

Figure 48. Crb is less enriched in the SAR in Rab4^{CA} embryos at later stages. **(A-C)** Lateral views of embryos at indicated stages expressing a constitutively form of Rab4 in the trachea stained for ECadh (green, white) and Crb (red, white). **(A, B)** Note that Crb accumulates in big endosomes at early stages. **(C)** At late stages, Crb is less enriched in the SAR. Scale bar A, B, C 7,5 µm.

A Rab4^{DN} (dominant negative of the Rab4 activity) expressed in the trachea did not produce clear defects. At early stages, Crb endosomes were normally detected close to the DT, and were indistinguishable form those in control embryos (Fig.49A). At late stages, Crb was enriched in the SAR as in the control (Fig.49B,C).

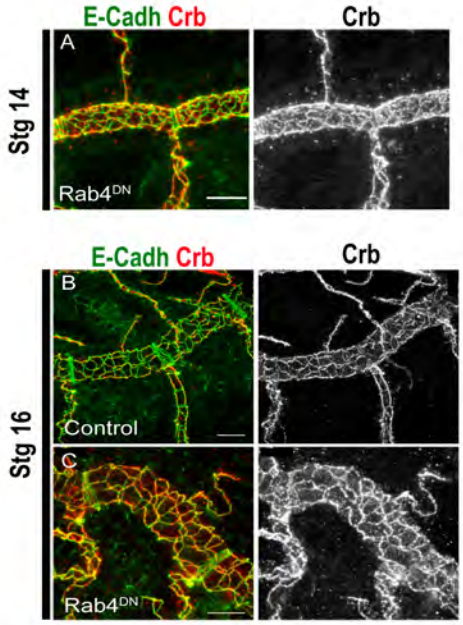

Figure 49. Accumulation of Crb in Rab4^{DN} mutants. **(A-C)** Lateral views of indicated genotypes and stages stained for Crb (red, white) and E-Cadh (green). **(A)** Note that at early stages Crb is accumulated similar as in control conditions. **(B, C)** At late stages, Crb is sharply accumulated in the SAR in Rab4^{DN} mutants. Scale bar A, B 10 µm and C 7,5 µm.

Interestingly, in EGFR^{DN} mutants, we detected an advanced enrichment of Crb in the SAR as compared to control (Fig.50A-H).

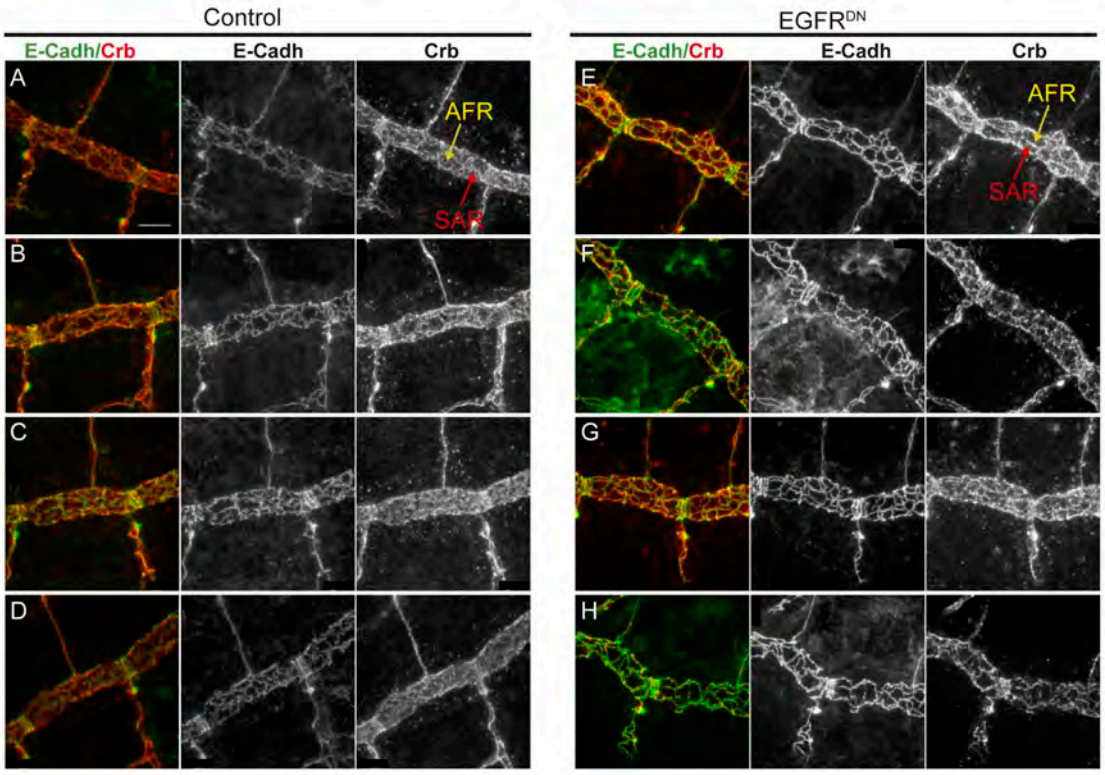

Figure 50. Advanced enrichment of Crb in the SAR in EGFR mutants. (A-H) Lateral views of representative stage 14 control embryos or embryos expressing EGFR^{DN} in the trachea stained for E-Cadh (green, white) and Crb (red, white). Note that in EGFR^{DN} mutants the enrichment of Crb in the SAR is more conspicuous at this stage as compared to control embryos. Scale bar 7,5 µm.

4.6.2 The role of RE-Rab11 in Crb recycling

To further characterize Crb trafficking in the tracheal development, we analysed the contribution of RE-Rab11 dependent trafficking on Crb accumulation. A double staining of Crb/Rab11 revealed presence of Crb vesicles co-stained for Rab11 (Fig. D 1, 2). Interestingly, these were not the endosomes detected at early stages, as they were smaller (0,28 µm, n=6 recycling endosomes from 2 different embryos), detected at later stages, and typically close to cell junctions (Fig.51D 1,2 blue arrows).

The downregulation of RE-Rab11 activity (expressing a dominant negative construct of Rab11 in the trachea) produced defects in Crb accumulation. At early stages there were no clear defects and Crb was enriched in the AFR and found in endosomes as in the control (Fig.51A). However, at late stages, Crb was not specially enriched in the SAR as much as it is in the control, whereas E-Cadh was still detected in the junctions (Fig.51B,C). To confirm the phenotype, the ratio of Crb accumulation in the SAR versus the AFR was quantified. The ratio was found to be significantly different from the control, being biased towards a depletion of Crb accumulation in the SAR (Fig.51E). This result suggested a role for the RE route for Crb recycling in the trachea.

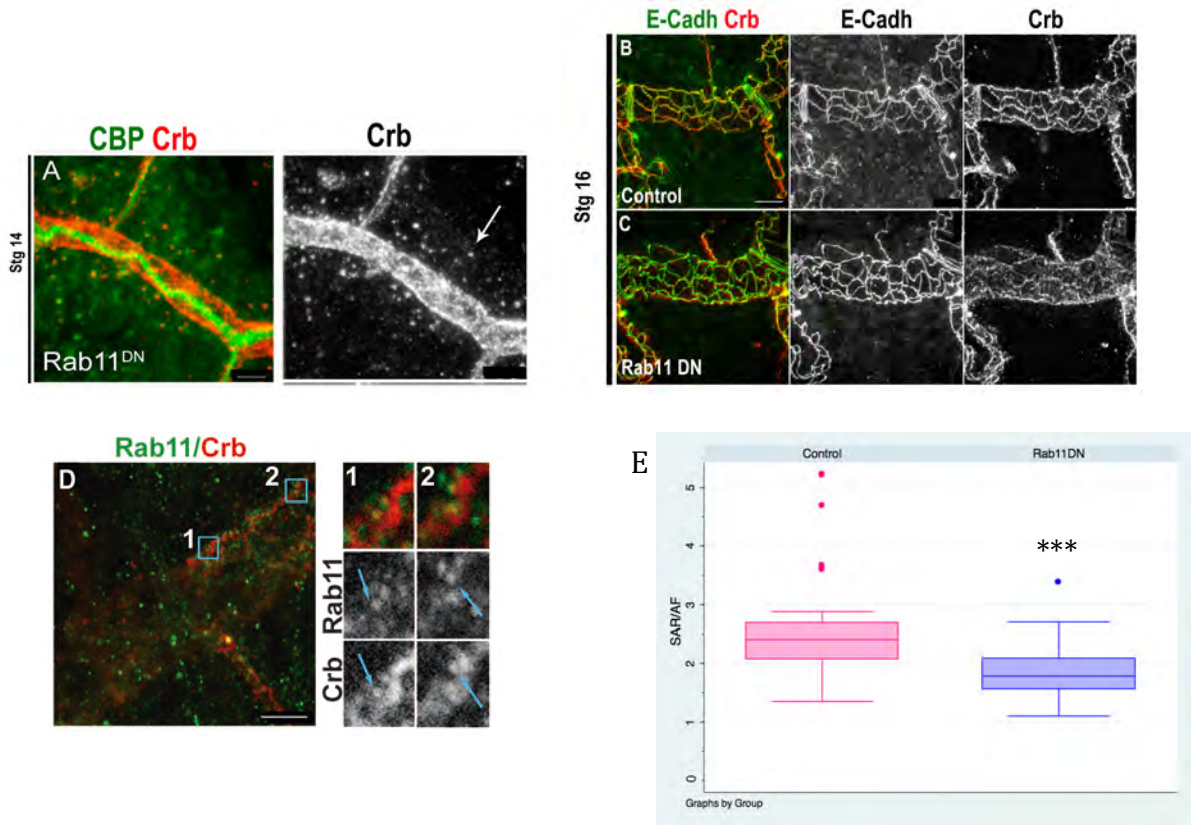

Figure 51. Trafficking of Crb through Rab11 pathway. **(A-C)** Laterals views of indicated genotypes and stages stained for Crb (red, white), E-Cadh (green, white) and CBP (green). **(A)** Note that at early stages Crb is accumulated similar to control in Rab11^{DN}, whereas, at late stages in Rab11^{DN}, Crb accumulation in the SAR decreases compared to the control **(B, C). (D)** Single confocal section of Crb (red) and Rab11 (using anti-

Rab11-Green). Note the appearance of small Crb vesicles, in contact with the junctional area, marked with Rab11 at late stages (Stage 15, blue arrows in 1 and 2). Scale bar A 10 µm; B, C 7,5 µm and D 2,5 µm. **(E)** Quantification of the ratio SAR vs AFR. When Rab11 is downregulated, the enrichment of crb in SAR decreased. Control n= 25, $Rab11^{DN}$ n= 49. ***$p < 0.001$ by unpaired two-tailed student's *t*-test

Altogether these results are consistent with a role of RE-Rab11 in recycling Crb, particularly to the SAR junctional area.

To sum up, altogether our results are consistent with a model where, after Rab5-mediated endocytosis, a pool of Crb would be retrieved from the degradation pathway to undertake different recycling routes. One of them would involve the Rab4/Retromer complex and would ensure the fast recycling route directly to the apical membrane, preferentially the AFR. On the contrary, another fraction of Crb would take a slower/longer-recycling route, which involves the RE-Rab11, and would traffic Crb from the endosome to the apical membrane, mainly to the SAR. In agreement with a role of both routes in Crb recycling, the downregulation of both proteins led to a strong decrease of Crb in apical regions, particularly in the DT (Fig.52A-C).

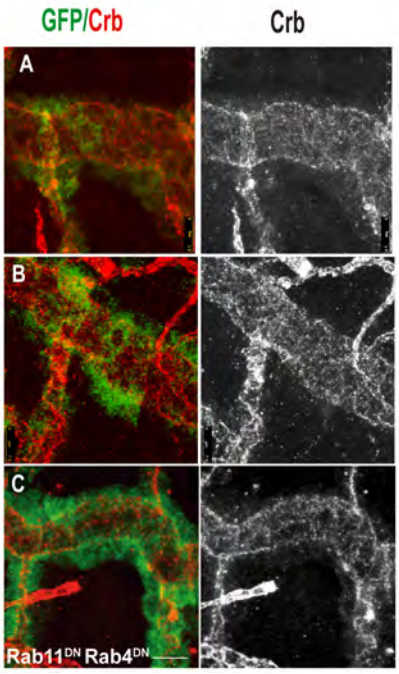

Figure 52. The downregulation of both Rab11 and Rab4 leads to a strongly decrease of Crb in apical regions. **(A-C)** Lateral views of embryos expressing $Rab11^{DN}$-$Rab4^{DN}$ in the trachea stained for Crb (red, white) and GFP (green), showing one metamere. Note that the downregulation of both proteins leads to a strong decrease of Crb in apical regions. Scale bar 7,5 µm.

4.7 Serp and Crb localise in common sorting endosomes

In the literature, Serp has been shown to undergo a specific recycling route that maintains its luminal content, which is necessary to restrict the tube elongation of the tracheal system. Serp recycling requires Rab9, the Retromer complex and WASH complex to mediate its retrograde trafficking to the lumen space through the TGN (Dong et al. 2013). Similarly, in this work we described that Crb trafficking is also regulated to maintain its apical localisation. The relative subcellular localisation of the two proteins in tracheal cells was analysed.

Serp and Crb were found to partially co-localise, indicating that they localise in common endosomes (Fig.53A). This common localisation increased as development proceeds and reached a peak at stage 14 of the embryogenesis (Fig.53A,B). Quantifications in embryos of that stage indicated that the 66% of endosomes contained both Crb and Serp, 15% contained only Crb and 18% contained only Serp (Crb/Serp$_e$, Crb$_e$ and Serp$_e$, respectively, in Fig.53A, n=194 vesicles from 5 different embryos; Fig54A-C', D). From stage 15 onwards, Crb endosomes decreased or became smaller while Serp endosomes were maintained (Fig.53C). As mentioned, Serp and Crb did not perfectly colocalise in the same endosomes, but rather they seemed sorted into different regions of a common endosome (insets in Fig.53A, B and yellow arrow in A; Fig.54A'-C', D). To confirm this observation, a co-localisation image analysis indicated around a 60% of co-localisation of Serp/Crb signal in common sorting endosomes (n=118 endosomes, from 5 different embryos). In agreement with this result, Crb and Serp are partitioned into different discrete domains in a common sorting endosome.

Life imaging using a Serp-GFP and Crb^{Cherry} showed a highly dynamic pattern of vesicles trafficking (Fig.53D, movie 3, movie 4). Endosomes were clearly detected, which contained both Crb and Serp, very often sorted into different regions. Several examples were found where Crb/Serp endosomes fused or evolved rendering Serp and Crb distinct vesicles (Fig.53D1-4), other examples showed Crb endosomes that seemed to disappear likely reflecting protein degradation (Fig.53D4-5), and other examples showed Crb or Serp localised in (distinct) tubulations or smaller vesicles, likely reflecting retrieval for recycling route (arrow in Fig.53D7).

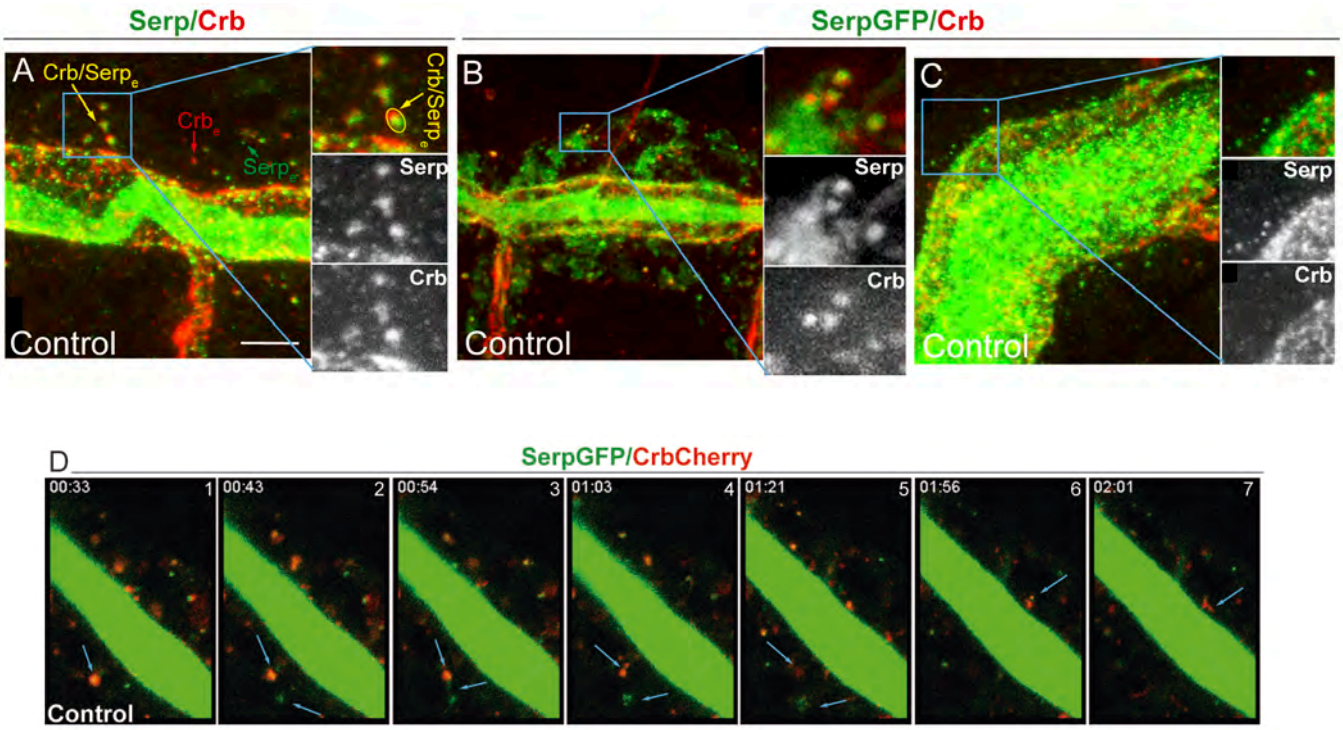

Figure 53. Serp and Crb accumulate in common endosomes. **(A-C)** Lateral views of control (A) or *BtlG4-UASSerp-CBD-GFP* (B, C) embryos stained for Crb (red, white) or Serp/GFP (green, white). **(A, B)** At stage 14, Crb/Serp (Crb/Serp$_e$) colocalise in the same endosomes, but endosomes containing only Serp or Crb (Serp$_e$ and Crb$_e$, respectively) are also found. In Crb/Serp$_e$, the two proteins are sorted into different endosomal domains (insets) but they colocalise in a region. **(C)** At stage 16, Serp endosomes are still abundant, while Crb endosomes decrease**.** Scale bar 5 μm**. (D)** Time-lapse images of vesicles dynamics of tracheal cells carrying *BtlG4-UASSerp-CBD-GFP* and Crb^{cherry}. Crb/serp endosomes are highly dynamic. Blue arrows point to an endosome from which Serp is sorted, joining another Serp containing vesicle (2-5). A fraction of Crb protein is also sorted and the rest fades (4-5). Upper blue arrow in 6-7 points to a Crb tubulation.

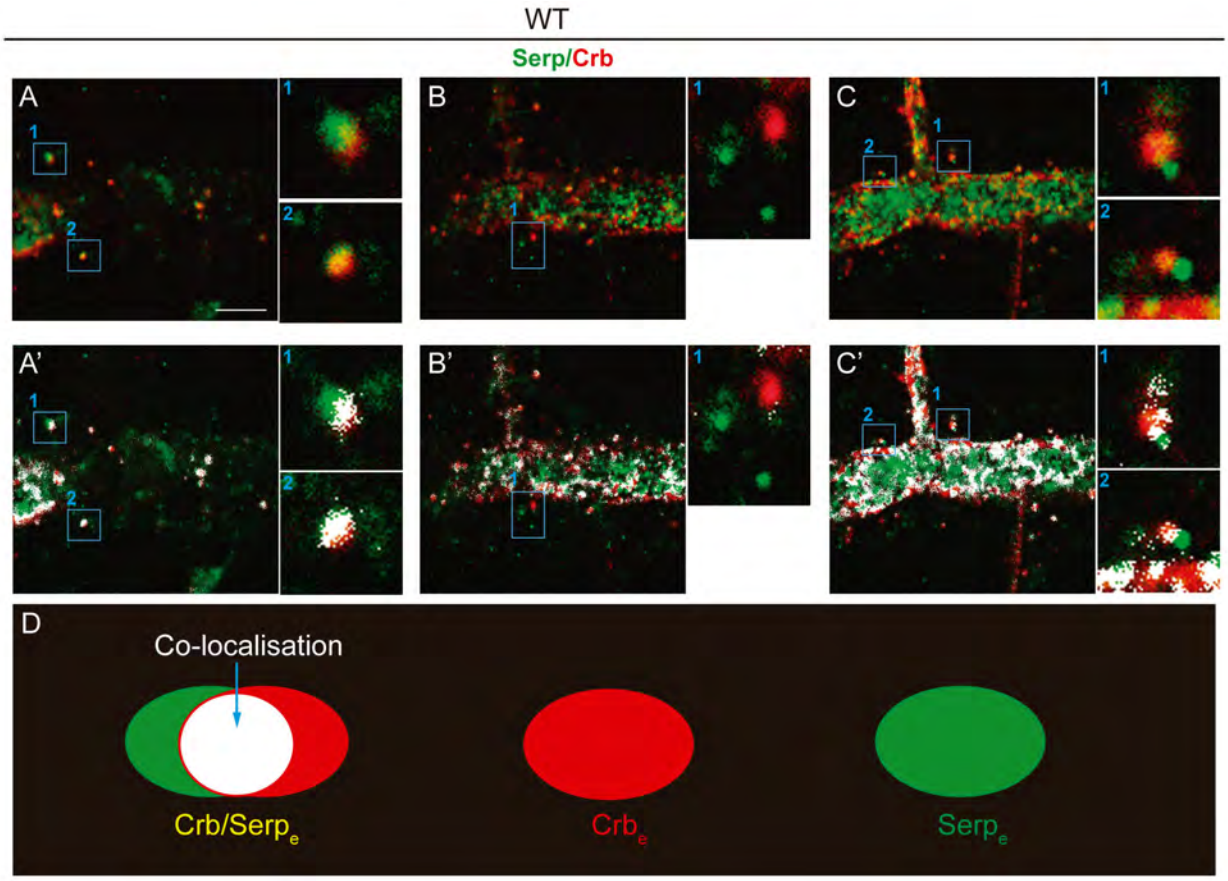

Figure 54. Accumulation of Crb and Serp in the endosomes. (A-C') Lateral views of stage 14 WT embryos stained for Crb (red) and Serp (green). Each image in A, B, C shows a single confocal stack. Panels marked with 1 and 2 correspond to the insets shown in A-C. Below, the same image is shown with a co-localisation point mask visualised in white. Note that many endosomes accumulate both proteins, but endosomes containing only Serp or Crb are also found. In endosomes with both proteins, Serp and Crb are sorted into different endosomal domains, colocalising in a region (insets). Scale bar 5 μm. **(D)** Scheme representing the different type of vesicles found (Crb/Serp$_e$, Serp$_e$ and Crb$_e$) Crb and Serp partially colocalise (white).

Altogether these results show that Crb and Serp traffic together in common sorting endosomes. They are sorted into different domains, consistent with the hypothesis that they use different retrieval recycling pathways to recycle back to their final destination.

4.7.1 Serp and Crb recycling mutually affect each other

As mentioned before, Crb and Serp localise in common sorting endosomes. As their recycling is regulated by common mechanisms, we wondered whether the recycling of one of these cargos might influence the other.

In *crb* mutants, the apico-basal polarity is strongly affected, although a rudimentary tracheal system is still formed (Tepass et al. 1990). Serp accumulation in *Crb* null mutants was analysed. *Crb* mutants still deposit chitin (Fig.55A yellow arrow), indicating the capacity of these cells to organise in a tube, to localise apically the machinery for the chitin deposition, and to secrete material into the luminal compartment. Serp accumulation in the

luminal spaces was largely decreased or absent, and only occasionally Serp was colocalising with CBP (Fig.55A blue arrow).

On the other hand, the overexpression of Crb in the tracheal tissue produced the expected apicalisation of the membranes, with a higher accumulation of CBP around the tracheal cells and the formation of an abnormal luminal compartment. Although the apical membrane was affected, all the machinery necessary to produce the chitin was able to localise at the membrane, even if it is mislocalised. Surprisingly, Serp was completely absent in the lumen of these embryos (Fig.55B).

In summary, these results suggest that Crb regulates the accumulation of Serp in a specific manner.

In *serp* mutants, Crb is found in apparently normal endosomes at stages 13-14. At later stages, Crb is also found enriched in the SAR, however, this enrichment is slightly less conspicous as compared to the sibling control embryos (Fig55C,D). This result suggested a possibe role for *serp* in Crb recycling route. Moreover, to further explore this posibility, Crb accumulation was analysed in the absence of *serp* in sensitised conditions, in particular in EGFR downregulation conditions. The phenotype was stronger, with the presence of large Crb-containing endosomes at early and late stages (st 14 and 16) (Fig.55E,F). Indeed, the enrichment of Crb in the apical domain was hardly detected at late stages (Fig.55F blue arrowhead). These results raise the possibility that Serp plays a direct or indirect role in endocytic trafficking affecting Crb recycling.

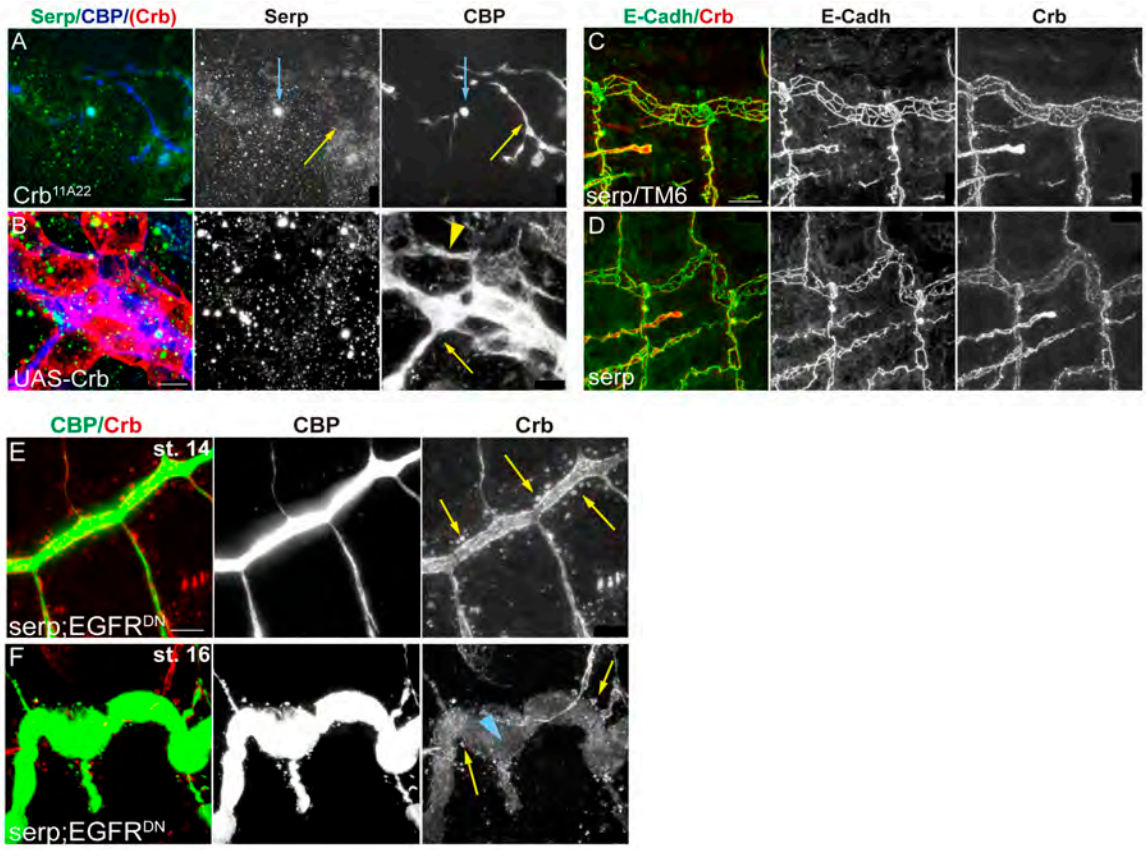

Figure 55. Crb and Serp require each other for the proper recycling. **(A, B)** Lateral views of embryos null mutants **(A)** or overexpressing *crb* **(B). (A)** In spite of *crb* absence, chitin (visualised with CBP) is well deposited in the malformed tubes (yellow arrow). Serp is only occasionally detected there (blue arrow). **(B)** When *crb* is overexpressed in the trachea it accumulates around the cells, indicating apicalisation (red in B). Chitin is deposited extracellularly, in the apical (yellow arrow) and the basal surfaces (yellow arrowhead), but Serp is completely absent. Scale bar A 10 µm, B 5 µm. **(C-D)** Lateral views of 2 tracheal metameres of stage 16 embryos stained for Crb (red, white) and E-Cadh (green, white). Note that Crb staining in the SAR is slightly compromised when *serp* is absent (D), compared to control (C). Scale bar C 10 µm. **(E, F)** Lateral views showing a portion of the DT when *serp* is absent and *EGFR* is downregulated. Note the presence of large Crb vesicles (yellow arrows) at all stages and the depletion of Crb in the apical domain of late embryos (blue arrowhead). Scale bar E 7,5 µm.

In summary, these results would be consistent with the hypothesis that Serp and Crb are endocytic cargos that in turn also regulate (directly or indirectly) the endocytic trafficking.

4.8 EGFR is required for the proper organisation of Serp-Crb endosomes

As previously mentioned, EGFR regulates both Crb apical localisation and Serp luminal accumulation. The accumulation of both proteins depends on recycling routes to maintain their levels. Therefore, it was important to investigate the requirement of EGFR in their trafficking. In the control, Serp and Crb localised in the same sorting endosome. In $EGFR^{DN}$ conditions, Crb/Serp endosomes were still found, indicating that internalisation was not impaired. This was confirmed by a live endocytosis assay (Tsarouhas et al. 2007) that showed presence of internalised rhodamine-labelled dextran in control and EGFR mutant conditions (Fig.56A,B,C).

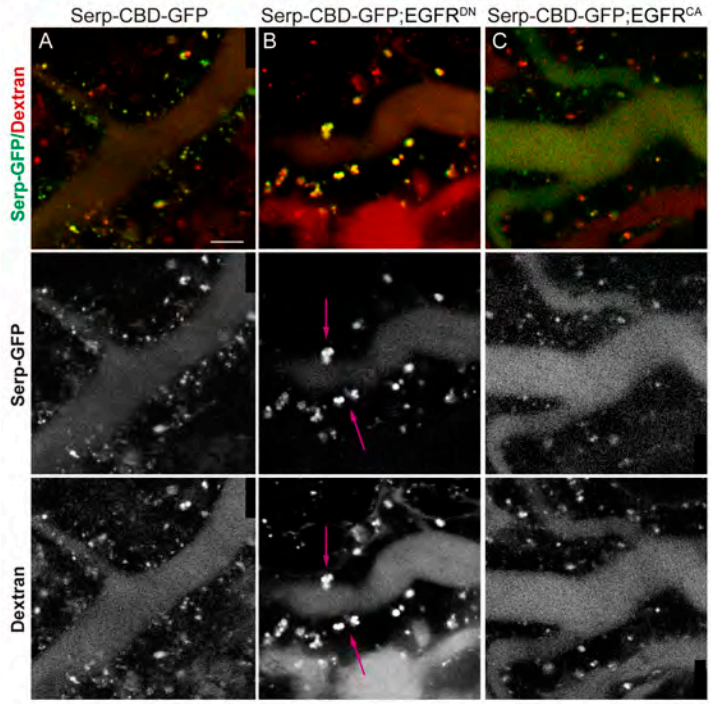

Figure 56. Live endocytosis assay. (A-C) Time-lapse images of stage 17 embryos carrying *btlG4-UASSerp-CBD-GFP* injected with rhodamine-labelled dextran in the different genetic backgrounds indicated. Intracellular dextran punctae largely colocalise with SERP-CBD-GFP containing endosomes, indicating internalisation. Note that dextran internalisation is detected in downregulation and constitutively active conditions for EGFR. Also note that SERP-CBD-GFP/Dextran containing endosomes are abnormally big compared with the control when EGFR is downregulated (pink arrows in B). Scale bar 5 μm.

However, endosomes displayed an abnormal shape and aspect. They were bigger, measuring around 1,3 μm in diameter (n=27 endosomes, from 6 different embryos). In the control, Crb/Serp normally accumulate in a well-defined region in the endosome, usually differently sorted (Fig.57A). In $EGFR^{DN}$ conditions the accumulation of both proteins was more diffused and both proteins were found intermingled, although generally still differently sorted in the endosome. Moreover, Serp and Crb were often deposited at the surface of the endosome, rather than in the lumen (Fig.57B, C), suggesting that more protein is retrieved from the degradation pathway. In addition, this result would be consistent with the fact that in EGFR mutant conditions Crb levels were higher compared to the control.

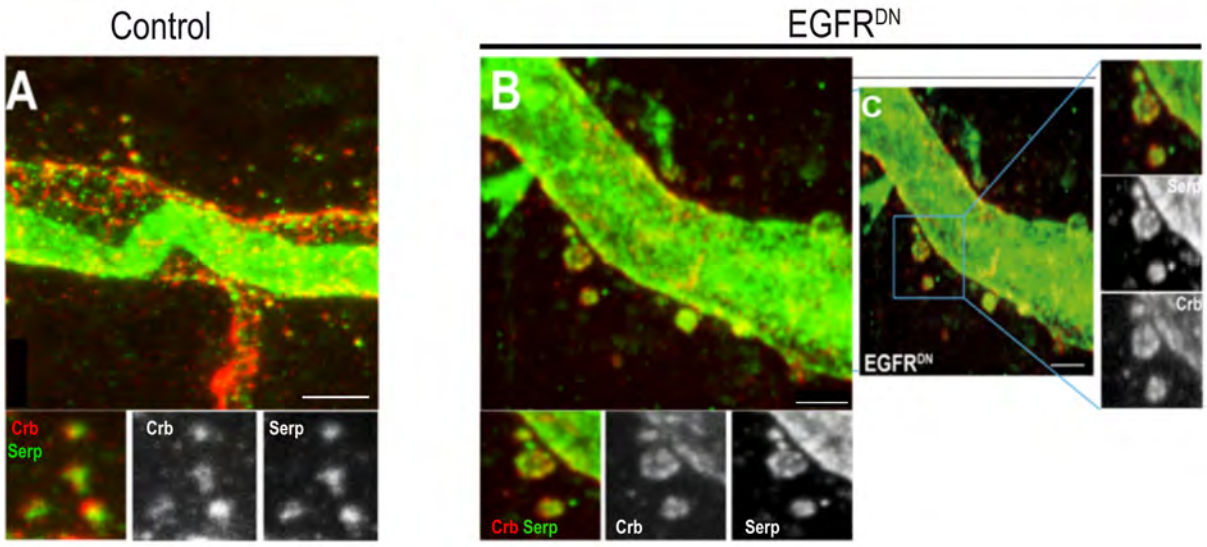

Figure 57. EGFR is required for the proper sorting of Crb and Serp in the endosomes. (A-C) Lateral views of stage 14 Control and $EGFR^{DN}$ embryos carrying *btlGal4-UASSerp-CBD-GFP* stained for Serp/GFP (green, white) and Crb (red, white). **(A)** In the control, Crb/Serp colocalise in the same endosomes, but endosomes containing only Serp or Crb ($Serp_e$ and Crb_e, respectively) are also found. In Crb/$Serp_e$ the two proteins are sorted into different endosomal domains (insets) but they colocalise in a region**.** Scale bar 5. **(B, C)** Crb/Serp endosomes are bigger when EGFR is downregulated and both proteins are abnormally localised, missorted and intermingled compared to the control. The cargoes often accumulate at the endosome surface (insets B-C). Scale bar A 5 µm; B, C 2,5 µm.

Hence, these results suggest that impairing EGFR activity results in the missorting of both cargoes, consistent with the hypothesis that EGFR is required for the proper sorting of cargoes, particularly Crb and Serp, in endosomal membranes.

4.9 EGFR affects WASH complex localisation

The Retromer complex plays a key role in Serp (Dong et al. 2013) and Crb recycling (Pocha et al. 2011, Zhou et al. 2011). We asked whether EGFR somehow controls Retromer activity.

The retromer recruits the actin-nucleator WASH complex. This complex is required for the sorting of cargo proteins into at least two distinct endosomal recycling pathways (early endosome to Golgi or early endosome to cell surface) (Gomez and Billadeau 2009). The WASH complex is important to mediate the formation of actin patches and generate discrete domains into which specific proteins are directed (Derivery et al. 2009, Puthenveedu et al. 2010). The formation of these actin fibres facilitates the budding from the endosome and the recycling of protein cargoes (Seaman et al. 2013). WASH accumulation with respect Crb and Serp in the control and EGFR mutant conditions was analysed.

In control embryos, WASH was accumulated as one or occasionally two WASH punctae partially colocalising with Serp and Crb (Fig.58A,C). In contrast, in EGFR^{DN} mutant conditions, the pattern of WASH accumulation was clearly different from the control. WASH was accumulated in many smaller punctae in the endosomes; often forming like a rosette with Serp and Crb abnormally sorted in the endosomes and intermingled (Fig.58B,D). This suggested a role for the EGFR regulating WASH dynamics on the endosome.

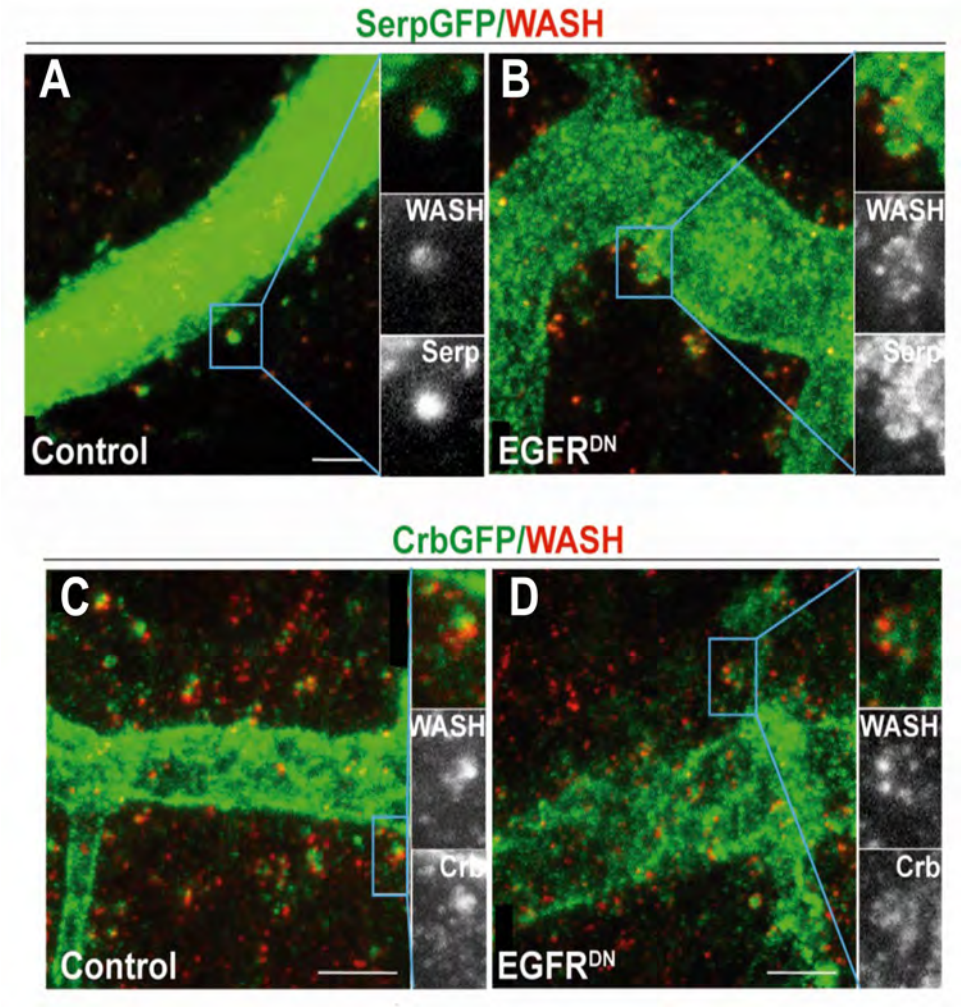

Figure 58. EGFR is required to organize the proper sorting endosomes. **(A-D)** Lateral views of stage 14 embryos stained for GFP (green) and WASH (red) carrying *btlGal4-UASSerp-CBD-GFP* (A,B) or CrbGFP (C,D). In control embryos, WASH is normally localised in one or two punctae in Crb/Serp endosomes. When EGFR was downregulated, WASH accumulated in more punctae forming like a rosette around the endosome. Scale bar A-B-D 2,5 µm, C 5 µm.

In addition, the accumulation of other markers of the Serp/Crb endosomes, like Rab4, was analysed. In EGFR^{DN}, Rab4 was not nicely and strongly decorating Crb endosomes as in the control (Fig.59C,D). Instead Rab4 accumulation was weaker and diffuse, and punctae of Crb/Rab4 colocalisation were more frequently detected than in control embryos (Fig.59A-D).

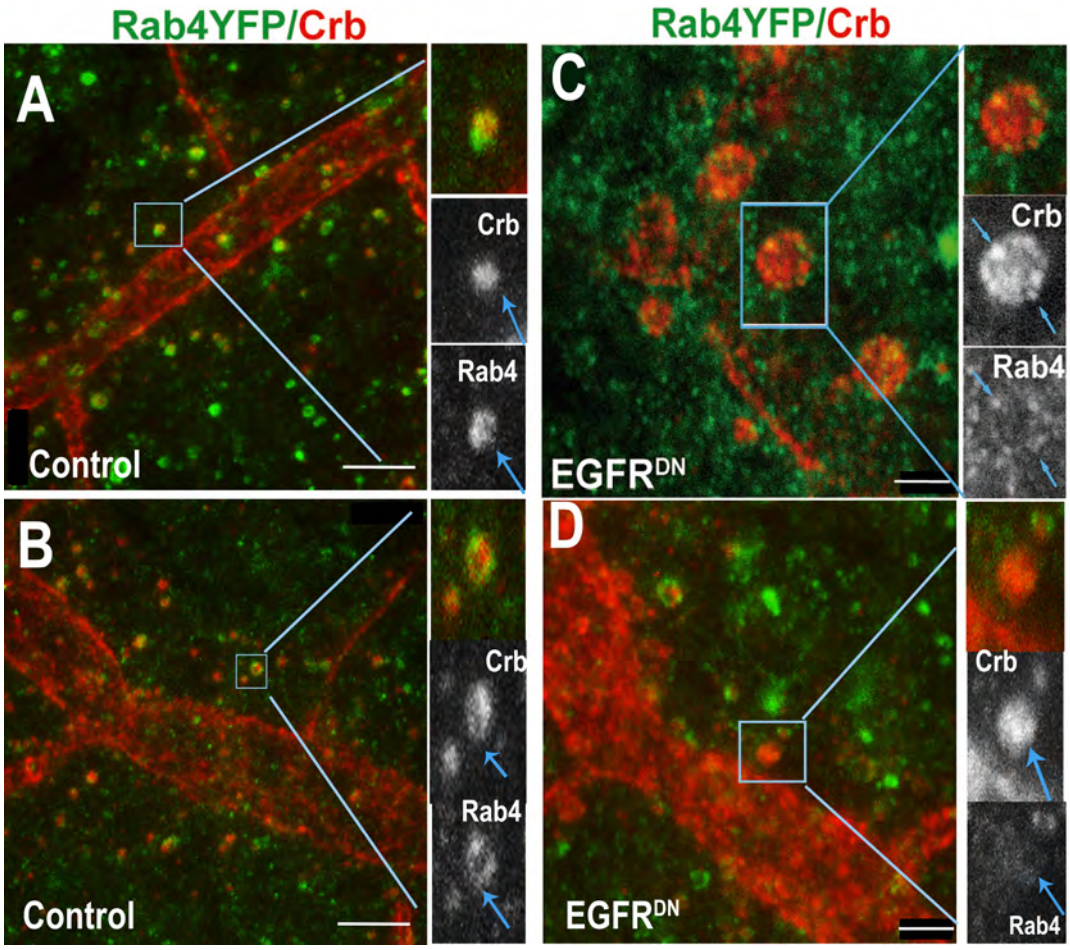

Figure 59. In EGFR^{DN} conditions Rab4 accumulation is affected. **(A-D)** Lateral views of embryos at indicated genotypes and stained for Crb (red, white) and GFP (green, white). Rab4^{EYFP} was used to visualise Rab4 accumulation. **(A)** Lateral view of a stage 14-control embryo. Note that Crb is colocalising with Rab4 (arrows insets in A). **(B)** Lateral view of a stage 14 embryo where Rab4 is decorating Crb endosomes (arrows insets in B). **(C)** Lateral view of a stage 14 embryo expressing EGFR^{DN} in the trachea. In EGFR^{DN}, Rab4 is less nicely accumulated and more frequent Crb/Rab4 punctae are detected (arrows insets in C). **(D)** Lateral view of a stage 14 embryo expressing EGFR^{DN} where Rab4 is more diffusing (arrows insets in D). Scale bar A-B 5 µm , C-D 2,5 µm.

Altogether, these results indicate that during the tracheal development, EGFR is required to organise the sorting endosome containing Serp and Crb, likely regulating their proper sorting.

Interestingly, it was found that EGFR itself also traffics in the same sorting endosomes that contain Serp and Crb (Fig.60A-D). This result raises the possibility that EGFR directly influences the traffic of the sorting endosomes that contain Serp and Crb, in which the receptor is also loaded.

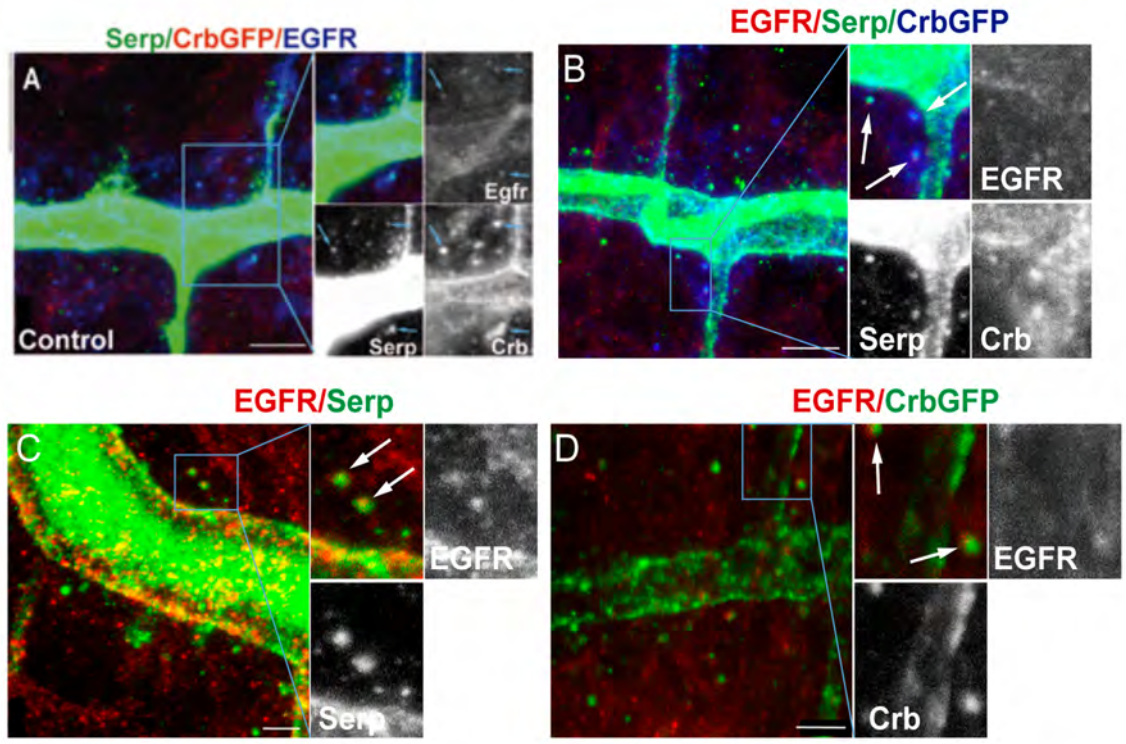

Figure 60. EGFR accumulation in Crb/Serp sorting endosomes. **(A-D)** Lateral views of stage 14 embryos stained for EGFR (red, blue, white), Serp (green, white) and GFP (red, blue, white, green; in embryos carrying Crb^{GFP} in A, B, D). Note that EGFR itself is also found very often in Crb/Serp containing endosomes (blue arrows, insets A; White arrows, insets B), and it also found only in Serp endosomes (white arrows, insets C) and Crb endosomes (white arrows, insets D). Scale bar A, B 5 μm, C, D 2,5 μm.

4.10 Crb anisotropic accumulation in DT cell junctions

Crb has been proposed to regulate tube length by promoting apical membrane growth (Laprise et al. 2010). To assess a possible correlation with longitudinal tube growth the accumulation of Crb in the DT was examined. As previously mentioned, during the stages of longitudinal DT elongation, particularly stage 15 onwards, Crb is accumulated strongly in the SAR displaying a mesh-like pattern that identifies the apical junctional domain.

Epithelial cell junctions can be classified in two types, the longitudinal/axial/horizontal cell junctions (LCJ), those with 0°±30° angle with respect the longitudinal axis of the tube, and the circumferential/transverse/vertical cell junctions (CCJ), those with 90°±30° angle with respect the longitudinal axis of the tube (Fig.61A,B).

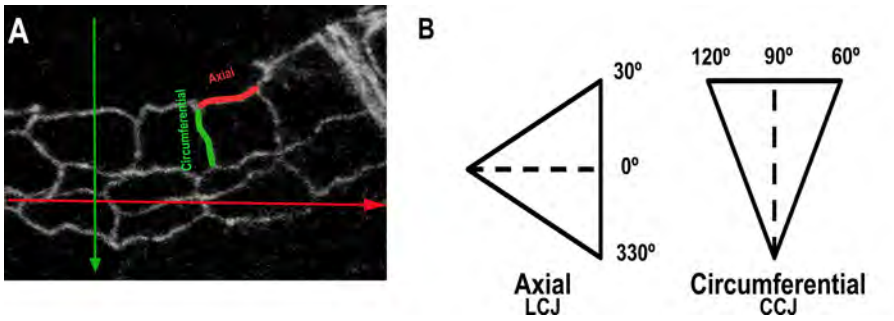

Figure 61. Axial versus Circumferential cell junctions orientation. (A) Details of a part of one DT metamere showing axial and circumferential cell junctions. **(B)** Scheme of angle axis.

4.10.1 Crb anisotropically accumulation in the control

A close evaluation of Crb accumulation revealed that it was not equally distributed among all cell junctions. Crb seemed more conspicuous in LCJ than in CCJ. In contrast, E-Cadh, a core component of AJs, seemed isotropically distributed among all cell junctions (Fig.62A-B'').

To verify this observation, a rigorous analysis and quantification was carried out. The levels of Crb and E-Cadh (total pixels/junction length) of each LCJ or CCJ from a region of the DT between metameres 7 and 9 were quantified. Quantifications indicated that E-Cadh accumulates at comparable levels in LCJ and CCJ, so the ratio of accumulation in LCJ vs CCJ was close to 1 (Fig.62C). Accumulation in LCJ was about 13% higher than in CCJ, but these differences were not significant. Crb accumulation instead was clearly biased to LCJ, where levels were around 30% higher than in CCJ (Fig.62D). A 1,5 LCJ vs CCJ ratio significantly documented this planar polarised Crb accumulation (Fig.62C).

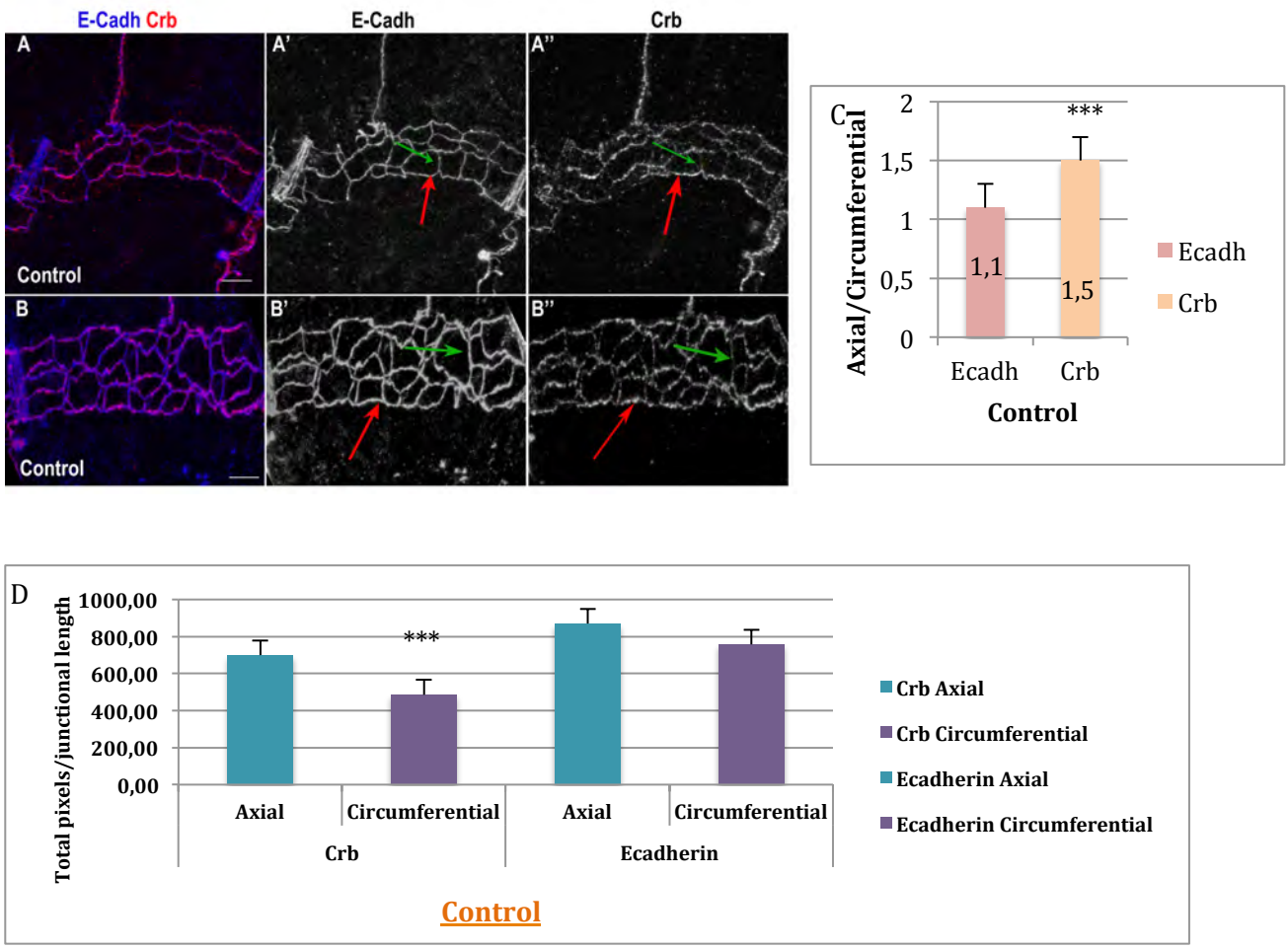

Figure 62. Crb is accumulated anisotropically in the cell junctions in the control. (A-B'') Lateral views of stage 16 embryos stained for E-Cadh (Blue, white) and Crb (Red, white). **(A'-B'')** Green arrows show circumferential junctions for E-Cadh and Crb. Red arrows show axial junctions for E-Cadh and Crb. Note that Crb is less enriched in the circumferential junctions than in the axial ones. E-Cadh is accumulated homogenously. Scale bar 7,5 µm. **(C)** Quantification of axial/circumferential ratio for E-Cadh and Crb. **(D)** Quantification of the total intensity of pixels/junctional length of Crb and E-Cadh cell junctions. N=15 control embryos were analysed, producing 254 LCJ and 314 CCJ. ***$p < 0.001$ by unpaired two-tailed student's *t*-test. Error bars, s.e.m.

Altogether, these results indicate that a larger proportion of LCJ accumulate higher levels of Crb than in CCJ. Interestingly, this transient planar polarisation of Crb accumulation that we observed at stages 15-16 correlates with an anisotropic growth of the tracheal tubes only along the longitudinal axis of the DT.

The preferential accumulation of Crb in LCJ could result from different molecular mechanisms, like specific degradation in CCJ, specific membrane stabilisation in LCJ, targeted intracellular trafficking and differential protein recycling, among others. To investigate the dynamics of Crb protein we performed FRAP (Fluorescence Recovery After Photobleaching) analysis in either LCJ or CCJ of embryos carrying a viable and functional CrbGFP allele and were compared the results.

FRAP analysis indicated that the amount of fluorescent protein mobilized during the experimental time (the mobile fraction, M_f) was significant higher in LCJ compared to CCJ, (M_f Axial= 0,7; M_f Circumferential= 0,4)(Fig.63A,C,G; movie 5A, 5B). Kymographs also represent the dynamics of FRAP processes, where the image gives an intensity line along time in the x direction and along space in the y direction for all images of a stack (Fig.63B, D).

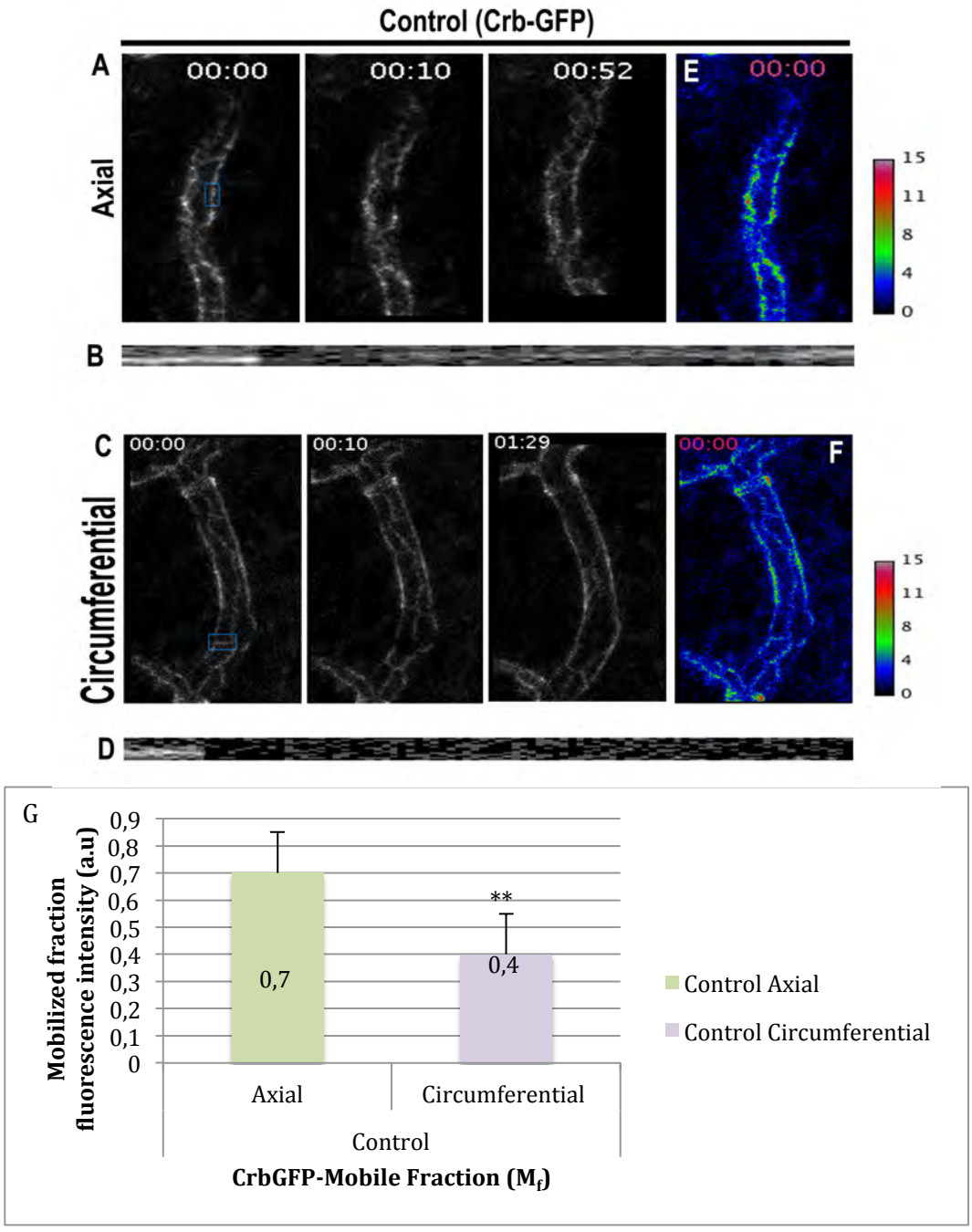

Figure 63. FRAP experiment in Axial and Circumferential control cell junctions. **(A, C)** Example of a FRAP experiment. The three images in A and B show pre-bleach, bleach and the end of recovery, respectively. **(B, D)** Kymographs of the bleached areas indicate that the fluorescence recovery is not due to lateral diffusion. On the kymograph the x coordinates report the time and the y coordinates report the space. **(E, F)** Panels show Crb-GFP signal intensities colour-coded using the heat-map shown on the right. **(G)** Quantification of the

Mobile fraction in both junctions. Note the significant difference between the mobilized fractions. Control axial n=9, control circumferential n=8. **$p < 0.01$ by unpaired two-tailed student's *t*-test. Error bars, s.e.m.

These results are consistent with a model where Crb protein would be more prone to recycle and/or traffic in LCJ than in CCJ.

4.10.2 Crb anisotropic accumulation is decreased in the Src42A^{DN} mutant embryos

To get insights into how the preferential accumulation of Crb in LCJ was achieved we turned our attention to Src42A. The activity of pSrc42A was proposed to orient membrane growth in the longitudinal/axial axis (Forster and Luschnig 2012). In Src42A loss of function conditions (either using a mutant allele or a dominant negative form of Src42A) LCJ do not expand and tubes becomes shorter (Nelson et al. 2012). The accumulation of Crb in the DT cells of embryos expressing Src42A^{DN} in the trachea was analysed. Image analysis pointed to a less conspicuous preferential accumulation of Crb in LCJ (Fig.64A-B'' axial red arrows, circumferential green arrows). To document this observation, the accumulation of Crb and E-Cadh (total pixels/junctional length) in LCJ and CCJ was quantified (Fig.64D). E-Cadh accumulated at comparable levels in LCJ and CCJ, with a 1,1 LCJ/CCJ ratio as observed in control embryos (Fig.64C). However, in contrast to control embryos, the LCJ/CCJ ratio for Crb accumulation decreased to 1,3 (Fig.64C).

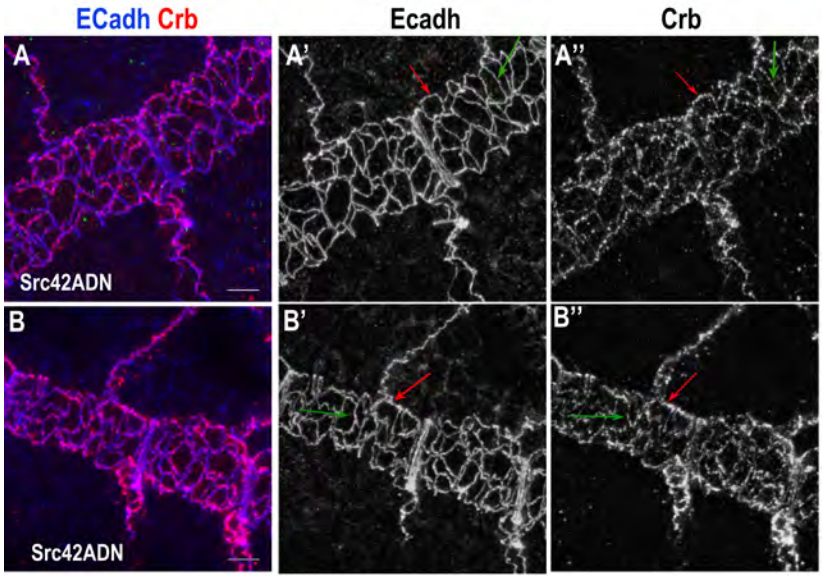

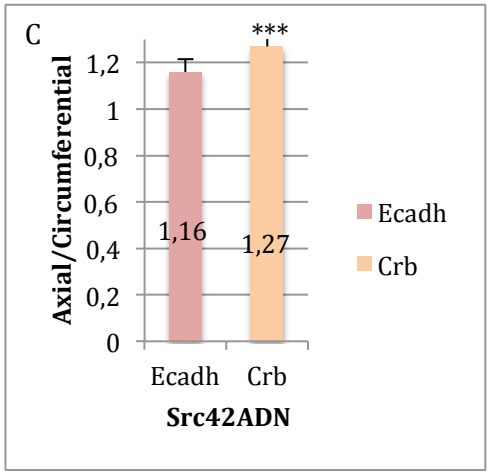

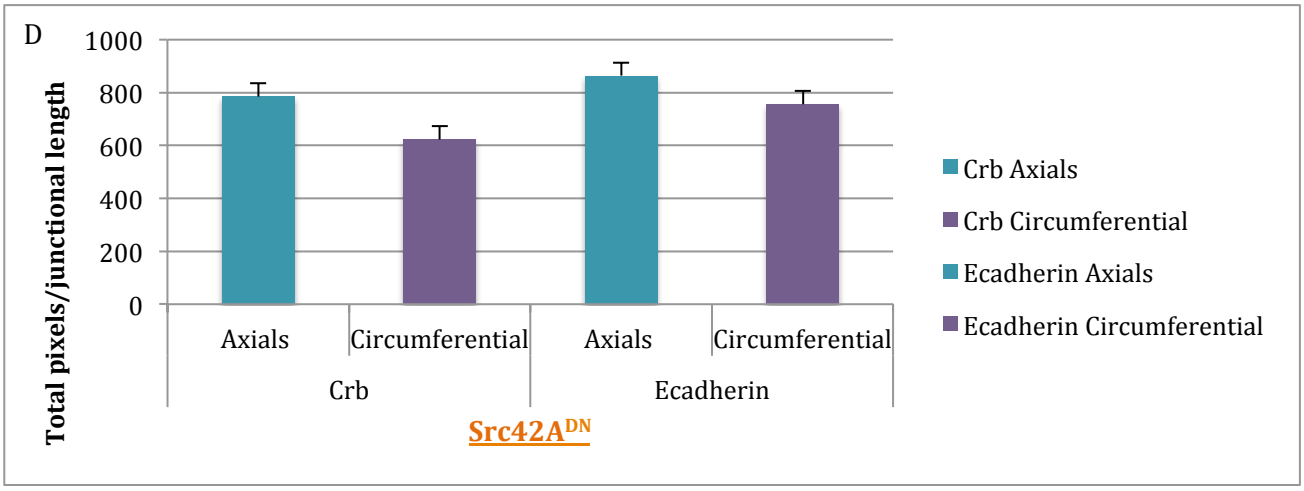

Figure 64. Crb anisotropic accumulation is decreased in Src42A^{DN} mutant embryos. **(A-B)** Lateral views of stage 16 embryos stained for E-Cadh (Blue, white) and Crb (Red, white). **(A'-B'')** Green arrows show circumferential junctions for both E-Cadh and Crb. Red arrows show axial junctions for both E-Cadh and Crb. Note that Crb anisotropic accumulation decrease and Crb is more homogenously enriched in all cell junctions. Scale bar 7,5 µm. **(C)** Quantification of the Axial/circumferential ratio for Crb and E-Cadh. **(D)** Quantification of the total intensity of pixels/junctional length of Crb and E-Cadh cell junctions. N= 15 Src42A^{DN} embryos were analysed producing 349 LCJ and 417 CCJ. ***$p < 0.001$ by unpaired two-tailed student's *t*-test. Error bars, s.e.m.

Altogether these results indicate that a decrease in Src42A activity leads to a more isotropic accumulation of Crb in cellular junctions, suggesting that Src42A contributes to Crb preferential accumulation in the LCJ.

To understand the mechanism by which Src42A may be controlling Crb accumulation, FRAP analysis in LCJ and CCJ was carried out in a Src42A dominant negative background. Strikingly, clear differences were found with respect to control, as it was observed that the M_f in LCJ and CCJ were comparable and not significantly different (M_f Axial= 0,5; M_f Circumferential= 0,522) (Fig.65A,C,G movie 6A, 6B). Kymographs also represent the dynamics of FRAP processes, where the image gives an intensity line along time in the x direction and along space in the y direction for all images of a stack (Fig.65B, D).

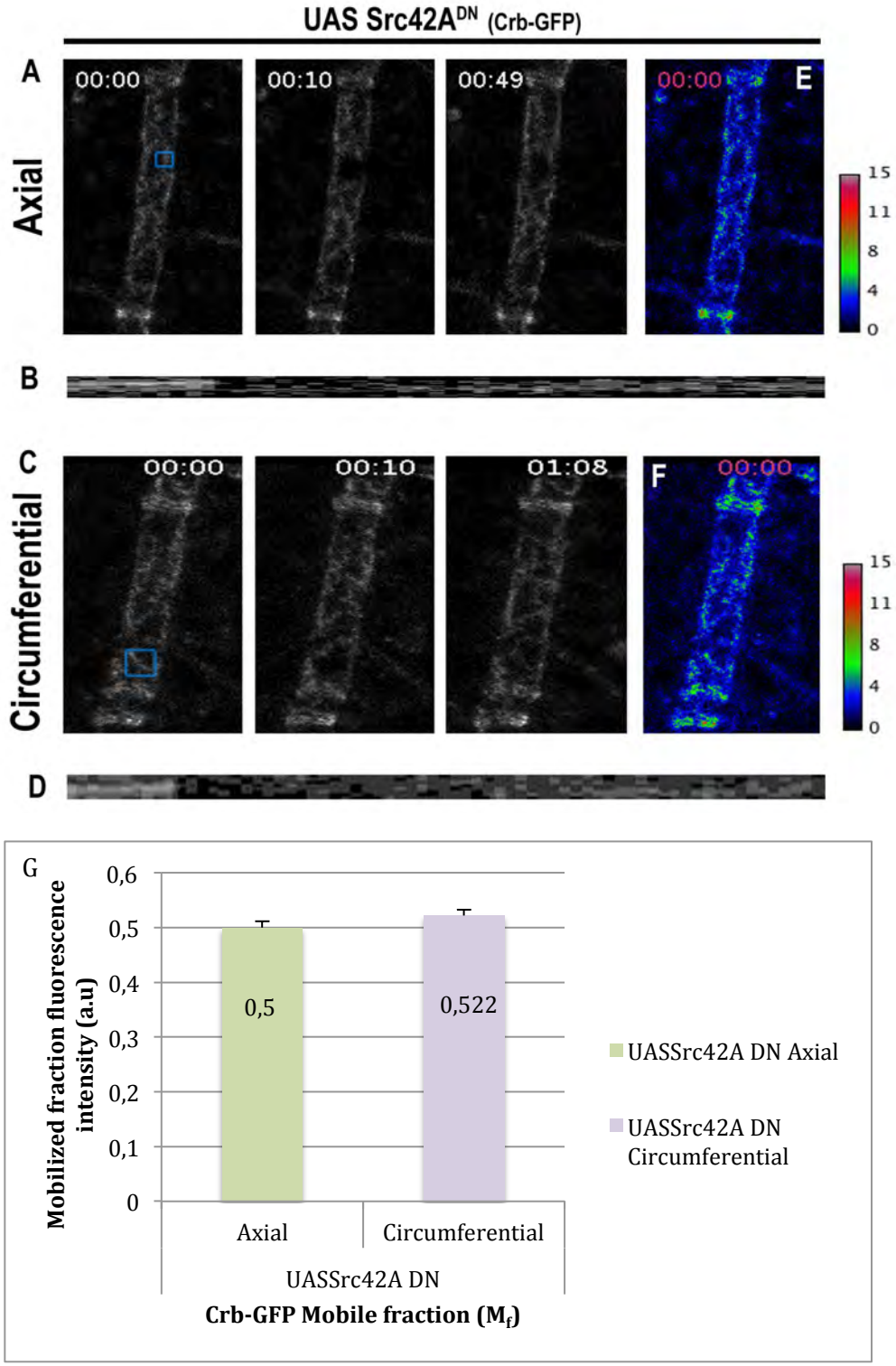

Figure 65. FRAP experiment in Axial and Circumferential Src42A^{DN} cell junctions. **(A, C)** example of a FRAP experiment. The three images in A and B show pre-bleach, bleach and the end of intensity recovery, respectively. **(B, D)** Kymographs of the bleached areas indicate that the fluorescence recovery is not due to lateral diffusion. On the kymograph the x coordinates report the time and the y coordinates report the space. **(E, F)** Panels show Crb-GFP signal intensities colour-coded using the heat-map shown on the right. **(G)** Quantification of the Mobile fraction in axial and circumferential junctions. Note that there are no significant differences between the mobilized fractions in both cellular junctions. Src42A^{DN} axial n=8, Src42A^{DN} circumferential n=9. Error bars, s.e.m.

In addition, the M_f in the LCJ of Src42A^{DN} mutant embryos was significantly lower than the M_f in the control embryos (M_f Axial Src42A= 0,5; M_f Axial Control= 0,7). On the contrary, the M_f in the CCJ of Src42A^{DN} mutant embryos was very similar to the M_f in the control (M_f Circumferential Src42A= 0,522; M_f Circumferential Control= 0,47) (Fig.66A).

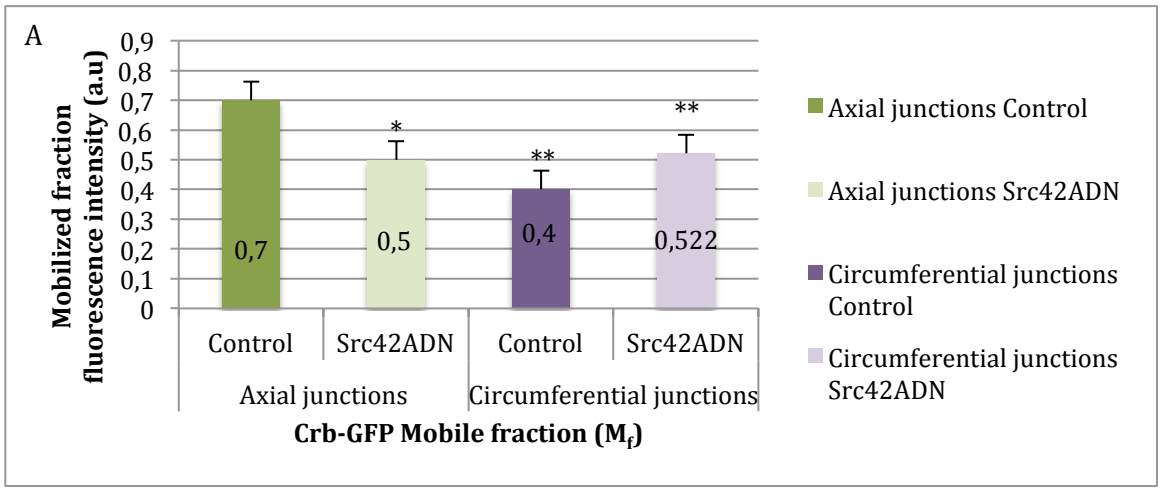

Figure 66. Frap analysis in both cellular junctions in control and Src42A^{DN} embryos. (A) Quantification of the mobile fraction in the different experimental conditions. Note that there are significant differences between the mobile fractions compared to axial control junctions. *$p < 0.05$, **$p < 0.01$ by unpaired two-tailed student's *t*-test. Error bars, s.e.m.

Altogether these results can be interpreted in a model where Src42A is more active in LCJ, as in Src42A^{DN} conditions the high M_f in LCJ observed in control embryos decreases.

4.11 Constitutively activation of Src42A affects Crb junctional accumulation and Serp luminal deposition

It was previously shown that increased levels of Src or a constitutively activated Src42A produce longitudinally elongated tracheal tubes (Forster and Luschnig 2012, Nelson et al. 2012). This phenotype could derive from the expected increased levels of Crb that would drive apical membrane expansion. Surprisingly, however, we found that Crb was strongly decreased in the SAR of DT cells (Fig.67A-C'').

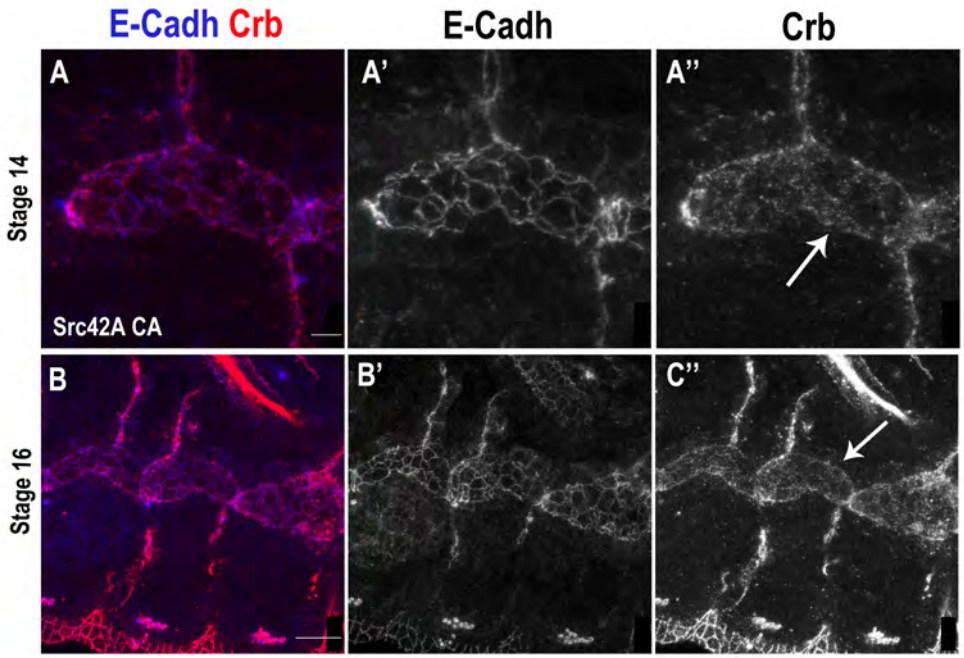

Figure 67. Crb is strongly decreased in the SAR in Src42A CA embryos. **(A-C'')** Laterals views of embryos at the indicated stages stained for Crb (red, white) and E-Cadh (blue, white). Note that Crb is strongly decreased in the SAR. Scale bar A 5 μm and B 10 μm.

This result of activated Src42A challenged the simple model where Src42A would regulate tube elongation through the control of Crb accumulation, and the notion that Crb levels regulate tube growth (Dong et al. 2014, Laprise et al. 2010). To understand tube overelongation when Src42A is constitutively activated we investigated other known tube length regulators, as it is the case of Serp (Luschnig et al. 2006, Wang et al. 2006). In conditions of $Src42A^{DN}$, Serp is well accumulated in the lumen as it is in the control (Fig.68D-E'). In contrast, we found that in $Src42A^{CA}$ Serp accumulation was abnormal. While at early stages Serp accumulated normally in the tracheal cells (Fig.68A-B', A' white arrow), at late stages Serp was completely absent from the luminal compartment (Fig.68C-C', C' white arrow).

This result may explain the tube elongation defects observed in $Src42A^{CA}$ embryos, as Serp absence leads to overelongated tubes.

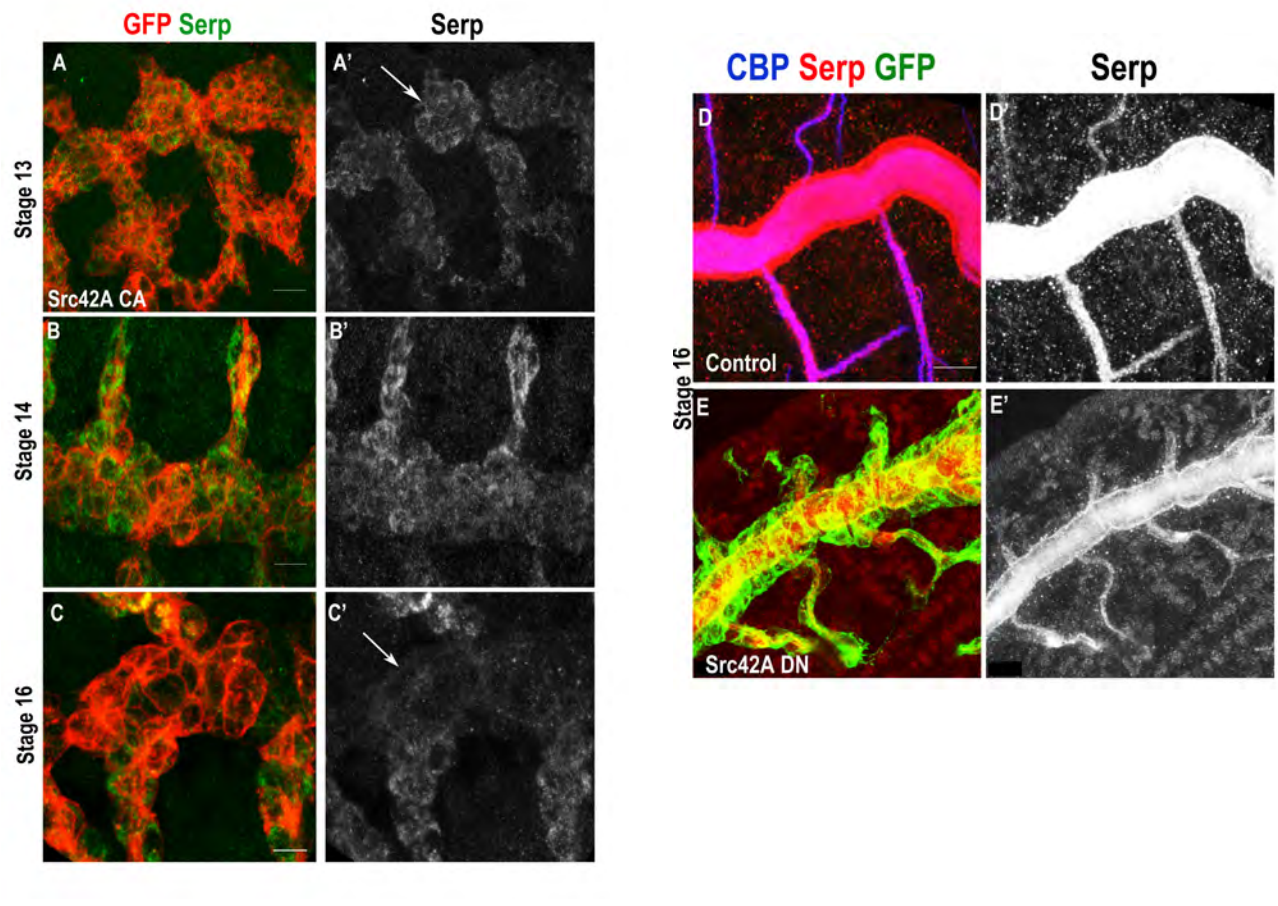

Figure 68. Constitutively active form of Src42A affects Serp luminal accumulation. **(A-E)** Laterals views of embryos at indicated genotypes and stages stained for Serp (red, white, green), GFP (green, red) and CBP (blue). **(A-C')** Note that Serp is absent from the DT lumen as development proceeds when Src42A is constitutively activated. **(D-E)** On the contrary, when Src42A activity is downregulated, Serp accumulation is maintained in the lumen as it is in the control. Scale bar A, D, E 10 μm and B, C 5 μm.

In summary, we find that during tracheal tube elongation Crb is transiently enriched in the SAR joining DT cells in a planar polarised manner. This polarised enrichment correlates with a different dynamics of Crb protein, which seems to have higher levels in longitudinal/axial than in circumferential/vertical junctions. This polarised enrichment also correlates with an anisotropic growth of the apical membrane, axially-biased, that drives the longitudinal enlargement of the tracheal tubes.

5. DISCUSSION

5. DISCUSSION

The shape and size of the various tubes within tubular organs such as the lung, vascular system, kidney and mammary gland must be finely regulated for optimal functions in delivering gases, nutrients and liquids within the entire organism. However, in spite of the relevance of this regulation, the underlying molecular and cellular mechanisms responsible for tubular organogenesis are not yet fully understood. The *Drosophila* tracheal system has emerged as an excellent in vivo model to study the molecular mechanisms employed by signalling pathways to instruct cells to form tubular structures. In addition, the tracheal system has been widely used to explore the fundamental mechanisms of tube-size regulation, as it is strictly regulated. In this study we identify a novel role for EGFR in the regulation of the tracheal tubes and investigate the molecular mechanism downstream. In addition, this work provides further insights into the different mechanisms of tube size regulation.

5.1 EGFR restricts tube elongation in the trachea

The shape of biological tubes is optimized to support efficient circulation of liquid and gas and to maintain the homeostasis. Maintaining the proper tube diameter and fitting tube length to body size are two crucial requirements for proper tube function. The embryonic tracheal system is a network composed of epithelial tubes that facilitates gas exchange from the environment to the target tissues (Affolter and Caussinus 2008, Uv et al. 2003). After the establishment of the branching pattern, tracheal branches undergo diametric expansion and axial growth to attain their final size, which is unique to each branch type (Ghabrial et al. 2003). Different studies identified the apical extracellular matrix (aECM) as a crucial regulator of tube expansion and elongation. The aECM consists of a viscoelastic matrix that restricts excessive elongation. The evidences suggest a connection between the aECM and the underlying epithelium, coordinating the apical membrane growth and cell contractility to control tube growth (Dong and Hayashi 2015). On the other hand, Crb-dependant apical membrane growth (Dong et al. 2014a, Laprise et al. 2010) and pSrc-regulated cell shape changes, also control tube length (Forster and Luschnig 2012, Nelson et al. 2012). How the aECM instructs the underlying tracheal epithelium to adjust its apical enlargement is not fully understood, although mechanical or signalling events, or a combination of both, may be required to control tube geometry. It is likely that the cell intrinsic mechanisms (i.e apical membrane expansion and/or cell shape changes) and the cell extrinsic mechanisms (i.e aECM) are coordinated rather than being two independent mechanisms controlling the same morphometric event. Indeed, some reports propose that the aECM may be anchored to the apical cell membrane through connecting proteins such as ZP proteins (Dumpy), which behaves elastically and generates mechanical tension against the stretching force of tube elongation (Dong and Hayashi 2015, Dong et al. 2014a, Jazwinska and Affolter 2004, Sakaidani et al. 2011).

This work shows that a single signalling pathway, EGFR, controls both intrinsic and extrinsic tube elongation mechanisms. This provides a possible explanation to further understand how these mechanisms are coordinated. We found that EGFR regulates the accumulation and subcellular localisation of different factors known to participate in the control of tube length, in particular the apical determinant Crb (intrinsic factor) and the chitin deacetylase Serp (extrinsic factor). Furthermore, our results suggest that the trafficking of Crb and Serp may influence each other, adding an extra layer of coordination to the system. Actually, a role for Crb in regulating endocytic trafficking has been already proposed (Nemetschke and Knust 2016). Indeed, several reports indicate that polarity proteins are both cargoes and regulators of endocytic recycling (Roman-Fernandez and Bryant 2016). In the trachea, we find that Crb seems to control Serp trafficking. In agreement with this we find that the overexpression of Crb leads to the loss of Serp in the lumen, maybe because the excess of Crb saturates the entire retromer complex recycling machinery, which preclude Serp recycling to the lumen. In turn, Serp can also influence Crb recycling. While Serp has been proposed to act as chitin deacetylase (Luschnig et al. 2006, Wang et al. 2006), it cannot be ruled out that it also plays a role in endocytic trafficking. Further experiments are required to determine whether Crb and Serp display a direct instructive role by controlling specific endocytic regulator/s, or an indirect one by altering the trafficking homeostasis, by competing for common trafficking factors or by stimulating compensatory trafficking pathways.

The interdependence of different tube length regulators may mask the exact contribution of each one to tube enlargement. Hence, a clear correlation of tube size with excess or absence of different tube length regulators may be difficult to be established. In agreement with this, it has been shown that both the absence of Serp and its overexpression gives rise to extralong tubes (Wang et al. 2006).

It was proposed that the luminal chitinous matrix may be also required to regulate tube morphogenesis by organizing the subapical cytoskeleton. The organization of the subapical β_{heavy}-Spectrin (βH), an essential apical cytoskeleton component (Thomas 2001), is disrupted in the absence of chitin synthesis, suggesting that rather than acting as a rigid matrix upon which cells are wrapped, the fibrillar chitin matrix signals the tracheal cells to reorganize their cytoskeleton in order to adjust cell shape and provide structural support (Tonning et al. 2005). Crb interacts with DMoesin and βH (Medina et al. 2002), providing a link between the Crb complex and the cortical cytoskeleton (Klebes and Knust 2000). Forces provided by the plasma membrane or by the cortical apical actin cytoskeleton could drive the expansion of the tracheal tubes. Hence, Crb could control tube size in part by the regulation of the actin cytoskeleton in the apical membrane.

In summary, the results obtained in this work show that the downregulation of EGFR activity leads to an abnormal cell shape and an overelongation of the DT. This correlates with defective Serp deposition in the lumen, which regulates the aECM, and defective Crb accumulation, which may be linked to the cortical cytoskeleton. Thus, the alteration of the accumulation of both proteins could lead to the defective control of tube morphology observed in EGFR mutant conditions.

5.2 A role for EGFR in endocytic traffic regulation

We find that EGFR itself can also localise in the endosomes containing Crb and Serp. It has been already shown that upon activation, EGFR is internalised and that the endocytic trafficking machinery regulates its activity. The endocytic trafficking of EGFR ensures, on the one hand, the downregulation of the signal by targeting the receptor to its degradation, and, on the other, its recycling back to the plasma membrane to initiate again the signalling cascade. The decision between being degraded or recycled depends, in turn, on signalling events targeting EGFR itself (for reviews see (Gonzalez-Gaitan 2003) (Jones and Rappoport 2014)). But besides being a cargo, the endocytic trafficking of EGFR can also serve as a platform for signalling. As such, EGFR could activate in the endosomes downstream signalling cascades that reach the nucleus and regulates transcription (e.g. the MAPK pathway), or it could approach EGFR signalling to particular downstream effectors, residing in specific cellular organelles, regulating cytoplasmic targets (Wortzel and Seger 2011) (Yao and Seger 2009). Our results are consistent with a model where EGFR would activate signalling and regulate cytoplasmic targets, maybe through its main signalling cascade the ERK/MAPK pathway. We find that the most canonical nuclear targets of EGFR signalling, i.e. Pnt and Aop/Yan, do not seem to be implicated in the control of tube size, further suggesting that EGFR regulates cytoplasmic targets in this case. However, further analyses need to be carried out to determine the possible contribution of other remaining nuclear targets such as Capicua (Cic) (Astigarraga et al. 2007).

EGFR signalling targets could be in the endosome itself (Stasyk et al. 2007). Actually, it was shown that EGFR could regulate Rab5 activity through the regulation of Rab5 GAP and GEF proteins (Lanzetti et al. 2000, Tall et al. 2001), and that ERK can regulate plasma membrane clathrin-independent recycling (Robertson et al. 2006). In addition, EGFR can phosphorylate Clathrin in a Src-mediated mechanism regulating its redistribution, defining a role for regulation of endocytosis by receptor signalling (Wilde et al. 1999). EGFR can also phosphorylate the endocytic adaptor protein Eps15 (Salcini et al. 1999, Zhou Y. et al. 2014), and can induce E-Cadh macropinocytosis (Bryant et al. 2007). Interestingly, myopic was shown to regulate EGFR signalling (Miura et al. 2008) and to interact with Rab4 (Chen et al. 2012). Furthermore, Rac1, which can be a target of Receptor Tyrosine Kinases (Wertheimer et al. 2012), has been shown to regulate Serp and Crb in the trachea (Sollier et al. 2015).

In summary, while EGFR has been extensively analysed as an endocytic cargo, some reports also point to more direct effects of EGFR signalling upon the endocytic machinery, and therefore our analysis identifies a good system to further explore this mechanism. Although our results suggest that EGFR is required for the proper organisation of Serp/Crb endosomes, promoting the recycling of both proteins to their final destination ensuring proper tube elongation, more work is required to identify the target/s of EGFR regulating endosomal trafficking in the trachea. However, our results suggest that EGFR could directly or indirectly target WASH-promoted actin organisation or the Retromer complex, which is required for WASH recruitment (Fig.69).

5.3 The regulation of Crb localisation in the trachea

Our results provide new insights into Crb accumulation during morphogenesis and the role of its recycling in the process. Crb requires the Retromer complex to recycle to the membrane (Pocha and Wassmer 2011, Zhou B. et al. 2011). The retromer complex is typically implicated in the retrieval of cargoes from the endosomes to the TGN via the retrograde pathway (Gallon and Cullen 2015, Wang and Bellen 2015). However, it was proposed that Rab9 activity, required for the TGN retrieval trafficking in the trachea, did not affect Crb accumulation (Dong et al. 2013). Furthermore, in HeLa cells Crb2 undergoes a rapid recycling to the membrane without accumulating in the TGN (Pocha and Wassmer 2011). Besides this role of the Retromer in retrograde transport, a Retromer-mediated traffic directly from the early endosomes to the plasma membrane was also identified (Temkin et al. 2011). Rab4, which was known to participate in a rapid recycling pathway back to the plasma membrane (Bhuin and Roy 2014), associates with the Retromer tubules for this direct traffic (Temkin et al. 2011). As Crb requires the Retromer, does not undertake the retrograde pathway and we found it in Rab4 endosomes, we propose that it undergoes a fast direct recycling to the plasma membrane regulated by Rab4/Retromer.

Both Serp and Crb require the Retromer complex for recycling, but they seem to undergo different Retromer-dependent pathways. How does the Retromer complex select the cargo? The retromer complex uses the same core machinery for membrane budding and fission. Nevertheless, Retromer interacting proteins, like sorting nexins, provide cargo specificity for each of the specific vesicular trafficking pathways (Burd and Cullen 2014, Gallon and Cullen 2015, Seaman et al. 2013, Wang and Bellen 2015). Interestingly, the nexin Snx27 has been shown to participate in the direct Retromer-regulated pathway to the plasma membrane. Snx27 is unique within nexin family because it contains a PDZ domain that binds to PDZ-binding motifs (PDZbm) in the cytoplasmic tail of cargo proteins (Steinberg et al. 2013, Temkin et al. 2011). Because Crb contains a PDZbm (Flores-Benitez and Knust 2016) and it is recycled through the retromer complex (Pocha and Wassmer 2011, Temkin et al. 2011), we speculated that Snx27 could be involved in this process. We find that CG32758 is the ortholog of Snx27 in *Drosophila*. We are currently investigating the role of this nexin in development. To this end we are generating and gathering the adequate tools to determine Snx27 requirements during *Drosophila* development. We are particularly interested in investigating a possible role of this nexin in Crb trafficking to the plasma membrane, likely in a Rab4/Retromer dependent pathway.

Our results also indicate that during the tracheal development, Crb can accumulate in different subcellular domains of the apical membrane. At early stages it is strongly accumulated in the AFR, in direct contact with the lumen, and later it becomes enriched preferentially in the SAR. This accumulation of Crb in the SAR or more diffusively in the AFR has also been observed in other *Drosophila* ectodermal tissues (Tepass 1996) or in other organisms, as it is the case of mammalian Crb3 that is present both on the apical surface and at the Tight Junctions (Makarova et al. 2003). Our results suggest that the specific subcellular apical localisation may perform specific functions. Actually, we find a correlation between the apical subcellular localisation of Crb and the apical membrane

growth, both in the trachea and in salivary glands. In the trachea, the loss of accumulation of Crb in the SAR observed when EGFR is constitutively active correlates with cells with smaller apical domains. In the salivary glands, the preferential accumulation of Crb in the SAR observed when EGFR activity is downregulated correlates with bigger apical domains. While more experiments are required, our data point to the hypothesis that an enrichment in the SAR drives or favours apical membrane growth.

We find that the late enrichment of Crb in the SAR depends on Rab5-mediated endocytosis, as when it is blocked Crb remains high in all apical domain. Crb is internalised and accumulates in endosomes, which are abundant preceding SAR enrichment, from where a fraction of the internalised protein undertake the degradation pathway and another fraction recycles back to the apical region.

Crb apical recycling could depend on two different endocytic itineraries: 1) A Rab4/Retromer pathway could recycle Crb rapidly to the apical membrane, preferentially to the AFR. 2) A longer loop involving RE-Rab11 would also recycle Crb apically, preferentially to the SAR. Alternatively, our results are also consistent with a temporally regulated model, in which right after internalisation (stages 13 and 14) Crb is recycled by any of the two pathways preferentially to the AFR. As Rab4 involves a shorter loop it could be more relevant in this phase. Later on, from stage 15 onwards, the recycling is preferentially routed to the SAR, with RE-Rab11 being more relevant in this phase (Fig. 69). This involvement of either distinct recycling pathways, or different recycling phases, in Crb sorting may be a general mechanism. Actually, when the endocytosis is prevented in 3D-MDCK cells, Crb3 levels are general increased and it is not able to relocalise from the apical domain to the Tight Junctions (Rodriguez-Fraticelli et al. 2015).

Finally, understanding the molecular mechanisms regulating Crb accumulation in the apical membrane, including its recycling, is a key question given the importance of Crb in all organisms.

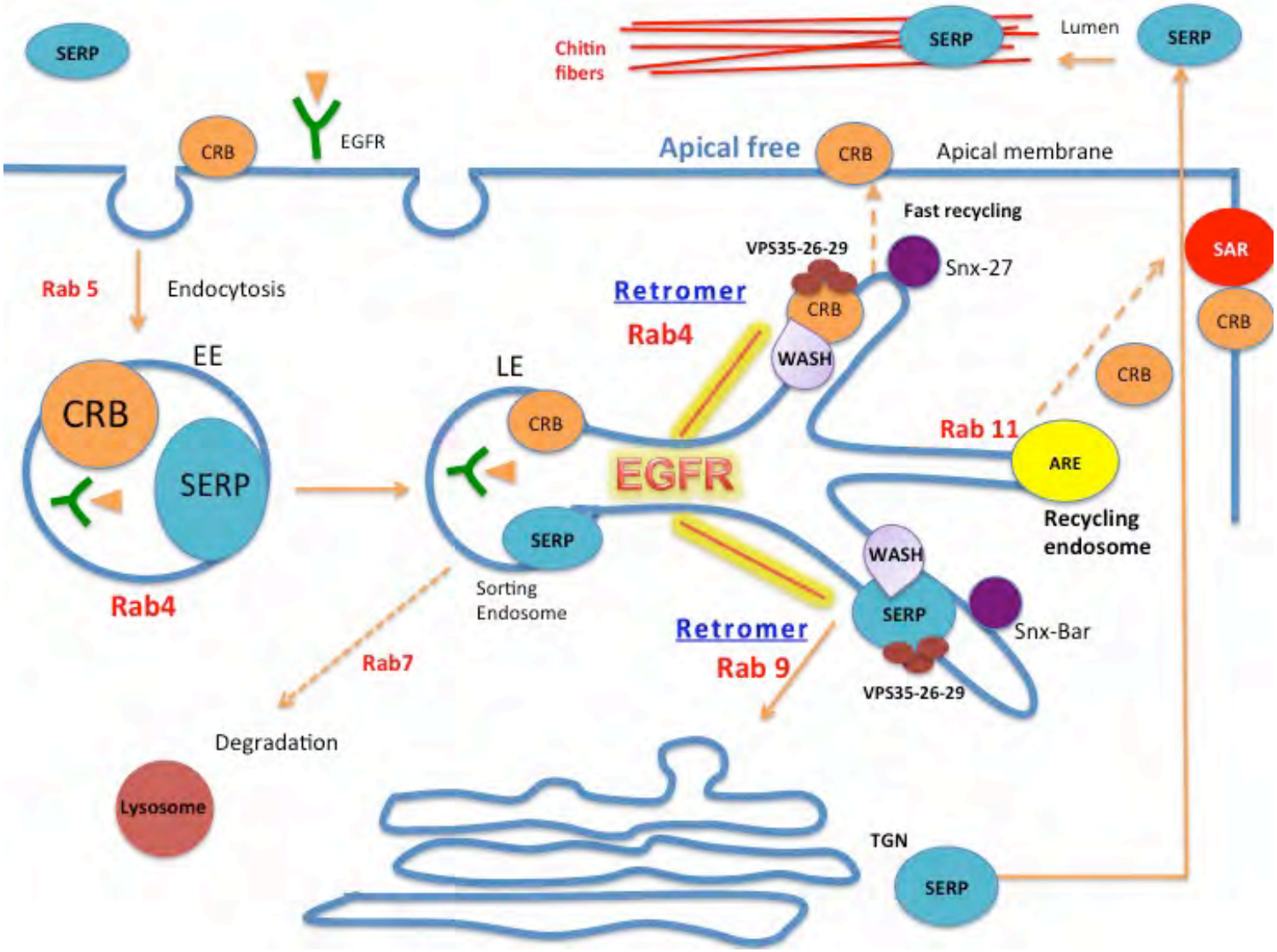

Figure 69. Model of Crb apical recycling and Serp luminal recycling controlled by EGFR activity. Crb and Serp are endocytosed by Rab5 and arrive to common endosomes (EE), sorted into different domains. Meanwhile a fraction of Crb and Serp internalised protein will be degraded into lysosomes, the other fraction will be retrieved from degradation pathways and recycled back to the membrane (Crb) or to the lumen (Serp). Crb apical recycling depend on two different pathways: 1) a Rab4/Retromer recycling to the apical membrane, preferentially to AFR. 2) A longer loop involving RE-Rab11 recycling Crb apically, preferentially to the SAR. Serp is recycled back through the retrograde transport mediated by the Rab9/retromer through TGN to the lumen. EGFR may control the proper sorting of cargoes, particularly the organisation of Serp and Crb in the endosomal membranes, promoting recycling of both proteins to their final destination ensuring proper tube elongation. This endocytic traffic regulation could be directly or indirectly target WASH-promoted actin organisation or the Retromer complex.

5.4 The regulation of Crb anisotropic accumulation in DT cell junctions

Crb is a key regulator of the apical membrane growth, which is involved in tube length control (Laprise et al. 2010). Our results indicate that Crb is not equally distributed in the different cellular junctions in the DT, and that it is more accumulated in the axial/longitudinal cell junctions (LCJ) than in circumferential/vertical ones (CCJ). In agreement with this, FRAP analysis shows a higher recovery of fluorescent protein intensity in LCJ than in CCJ. Because Crb has been proposed to control tube growth through apical membrane expansion (Dong et al. 2014b, Laprise et al. 2010), our results raise the possibility that a planar polarised Crb accumulation promotes a polarised longitudinal/axial (but not circumferential) tube growth. These results are consistent with the idea that during tracheal development there are distinct kinetics for circumferential and axial expansion, which are two independent mechanisms with a different genetic control (Beitel and Krasnow 2000).

The hypothesis that a planar polarised Crb accumulation promotes axial tube elongation is in agreement with the results obtained with Src42A downregulation. When Src42A activity is downregulated in the tracheal tubes, the DT remains shorter than in the control (Forster and Luschnig 2012, Nelson et al. 2012). We find that in addition Crb accumulation is more evenly distributed in all the junctions. Furthermore, FRAP analysis in this $Src42A^{DN}$ conditions leads to a more homogenous Crb recovery in all junctions. These results suggest that Src42A participates in the mechanism driving anisotropic accumulation of Crb in axial/circumferential junctions. This hypothesis perfectly fits with the proposal that Src42A may act as a mechanical sensor that translates the differential longitudinal/circumferential tension of the tube (an inherent property of cylindrical structures) into polarised cell behaviour (Forster and Luschnig 2012). Hence, in response to an intrinsic tubular anisotropy, Src42A would increase Crb traffic/recycling to the LCJ leading to an increased apical surface growth in the longitudinal direction thereby orienting cell elongation and a consequence longitudinal tube growth.

In summary, we propose that, in response to a polarised cylindrical mechanical tension, Src42A contributes to a planar polarisation of Crb accumulation. Src42A would sense extracellular stimuli as previously proposed (Forster and Luschnig 2012, Nelson et al. 2012, Ozturk-Colak et al. 2016) and would translate it into the cell by polarising Crb-mediated apical membrane growth.

5.5 A possible connection between Src42A activity and intracellular trafficking

The constitutive activation of Src42A produces longitudinally elongated tracheal tubes as previously described (Luschnig et al. 2006). This phenotype could be due to an expected increased anisotropic accumulation of Crb in the longitudinal cellular junctions LCJ. Surprisingly, however, we found that Crb was lost from the junctions, as it was strongly decreased in the SAR of DT cells. Two main reasons may account for this observation: First, Src42A activity could need to be planar polarised to drive polarised recycling. The constitutively activation of Src42A would override the required asymmetries blocking recycling. Second, the high activity of Src42A above physiological conditions could lead to a trafficking collapse. As a consequence, membrane proteins undergoing cycles of internalisation and recycling like Crb, or E-Cadh would be clearly affected (Forster and Luschnig 2012), as it is the case. Actually, in agreement with this hypothesis it was shown that regulated levels of Src42A are required for proper tracheal cell organisation (Ozturk-Colak et al. 2016). Furthermore, we also find that Serp accumulation in the lumen, which requires endocytic-retromer trafficking (Dong et al. 2013) , is also severely affected when Src42A is constitutively active.

Altogether the results suggest a role for Src42A in regulating trafficking. Actually, a function for Src42A in trafficking has already been proposed in the literature. Lin *et al.* (Lin et al. 2017) proposed a role for Src42A in modulating Rab7 activity through its tyrosine phosphorylation, thereby regulating membrane trafficking and cell signalling. On the other hand, Src42A mediates cytoskeleton rearrangements and the overactivation of Src42A disorganizes the F-actin rings. The actin filaments act as a track for movement of proteins within endosomal compartments and it has been associated with membrane budding events that contribute to vesicle scission (Arden et al. 2007, Roux et al. 2006, Seaman et al. 2013). Hence, a disruption in F-actin organisation in Src42A constitutive conditions could cause defects in the sorting of multiple membrane proteins and in endosomal maturation (Ohashi et al. 2011). Finally, a recent study shows that excessive Src42A activity in tracheal cells alters the actin bundle organisation, which in turn disrupts the formation of the extracellular chitin matrix (Ozturk-Colak et al. 2016). This alteration of the chitin aECM could result in the defects of Serp luminal accumulation that we observed, as Serp is a binding chitin protein.

Further analyses are required to identify the exact molecular mechanism of Src42A in regulating Serp and Crb accumulation.

6. CONCLUSIONS

6. CONCLUSIONS

1. The modulation of EGFR activity controls tracheal tube elongation at late embryonic stages.

2. EGFR activity prevents excessive DT elongation and regulates the morphology of DT cells.

3. Spi acts as an EGFR ligand that activates the receptor in the tracheal system.

4. Other EGFR ligands such as Vn, Grk and Krn are not required to activate EGFR during tracheal formation.

5. EGFR signal regulates DT elongation through the activation of the canonical RAS-MAPK pathway independently of Pnt and Yan.

6. EGFR activity controls Serp luminal accumulation and Crb accumulation in the DT during tracheal development, providing explanation for the effect of EGFR in tube size.

7. During tracheal development, Crb can accumulate in different subcellular domains of the apical membrane. At early stages, Crb is strongly accumulated in the AFR, whereas later on, it becomes enriched preferentially in the SAR.

8. Crb undergoes a highly dynamic pattern of subcellular localisation, which requires Rab5-dependent endocytosis.

9. After Rab5-mediated endocytosis, a pool of Crb is recycled back to the apical membrane using at least two different pathways, one involving a Rab4/Retromer short-loop and another one involving the Rab11-Recycling endosome route.

10. Crb and Serp traffic together in common sorting endosomes, but they are sorted into different domains.

11. Crb and Serp mutually influence each other's trafficking, either directly or indirectly.

12. Impairing EGFR activity results in the missorting of vesicular cargoes. EGFR is required for the proper endosome sorting of cargoes, particularly Crb and Serp, in the endosomal membranes.

13. EGFR downregulation results in the missorting of Crb and Serp in endosomal membranes.

14. EGFR plays a role in endosome organisation ensuring the proper accumulation of different factors. Among them, it is required for proper WASH-complex accumulation, which promotes actin patches facilitating Retromer-dependant cargo sorting.

15. Crb is not equally distributed among all cell junctions in the DT, being more enriches in LCJ than in CCJ. This transient planar polarisation of Crb at stages 15-16 correlates with an anisotropic growth of tracheal tubes along the longitudinal axis of the DT.

16. In Src42A loss of function conditions Crb is more evenly distributed in all cell junctions.

17. Src42A regulates Crb dynamics in cell junctions contributing to the preferential accumulation of Crb in the LCJ.

18. The constitutive activation of Src42A compromises Crb accumulation at the apical domain as well as Serp accumulation in the lumen.

7. BIBLIOGRAPHY

7. BIBLIOGRAPHY

Adamson, E. D. (1990). "EGF receptor activities in mammalian development." Mol Reprod Dev **27**(1): 16-22.

Affolter, M. and E. Caussinus (2008). "Tracheal branching morphogenesis in Drosophila: new insights into cell behaviour and organ architecture." Development **135**(12): 2055-2064.

Affolter, M. and B. Z. Shilo (2000). "Genetic control of branching morphogenesis during Drosophila tracheal development." Curr Opin Cell Biol **12**(6): 731-735.

Andrew, D. J. and A. J. Ewald (2010). "Morphogenesis of epithelial tubes: Insights into tube formation, elongation, and elaboration." Dev Biol **341**(1): 34-55.

Arden, S. D., C. Puri, J. S. Au, J. Kendrick-Jones and F. Buss (2007). "Myosin VI is required for targeted membrane transport during cytokinesis." Mol Biol Cell **18**(12): 4750-4761.

Arighi, C. N., L. M. Hartnell, R. C. Aguilar, C. R. Haft and J. S. Bonifacino (2004). "Role of the mammalian retromer in sorting of the cation-independent mannose 6-phosphate receptor." J Cell Biol **165**(1): 123-133.

Arkhipov, A., Y. Shan, R. Das, N. F. Endres, M. P. Eastwood, D. E. Wemmer, J. Kuriyan and D. E. Shaw (2013). "Architecture and membrane interactions of the EGF receptor." Cell **152**(3): 557-569.

Armbruster, K. and S. Luschnig (2012). "The Drosophila Sec7 domain guanine nucleotide exchange factor protein Gartenzwerg localizes at the cis-Golgi and is essential for epithelial tube expansion." J Cell Sci **125**(Pt 5): 1318-1328.

Aspenstrom, P., N. Richnau and A. S. Johansson (2006). "The diaphanous-related formin DAAM1 collaborates with the Rho GTPases RhoA and Cdc42, CIP4 and Src in regulating cell morphogenesis and actin dynamics." Exp Cell Res **312**(12): 2180-2194.

Astigarraga, S., R. Grossman, J. Diaz-Delfin, C. Caelles, Z. Paroush and G. Jimenez (2007). "A MAPK docking site is critical for downregulation of Capicua by Torso and EGFR RTK signaling." EMBO J **26**(3): 668-677.

Barr, F. A. (2013). "Review series: Rab GTPases and membrane identity: causal or inconsequential?" J Cell Biol **202**(2): 191-199.

Beitel, G. J. and M. A. Krasnow (2000). "Genetic control of epithelial tube size in the Drosophila tracheal system." Development **127**(15): 3271-3282.

Belenkaya, T. Y., Y. Wu, X. Tang, B. Zhou, L. Cheng, Y. V. Sharma, D. Yan, E. M. Selva and X. Lin (2008). "The retromer complex influences Wnt secretion by recycling wntless from endosomes to the trans-Golgi network." Dev Cell **14**(1): 120-131.

Bhuin, T. and J. K. Roy (2014). "Rab proteins: the key regulators of intracellular vesicle transport." Exp Cell Res **328**(1): 1-19.

Blankenship, J. T., M. T. Fuller and J. A. Zallen (2007). "The Drosophila homolog of the Exo84 exocyst subunit promotes apical epithelial identity." J Cell Sci **120**(Pt 17): 3099-3110.

Bogdan, S. and C. Klambt (2001). "Epidermal growth factor receptor signaling." Curr Biol **11**(8): R292-295.

Boube, M., M. Llimargas and J. Casanova (2000). "Cross-regulatory interactions among tracheal genes support a co-operative model for the induction of tracheal fates in the Drosophila embryo." Mech Dev **91**(1-2): 271-278.

Brand, A. H. and N. Perrimon (1993). "Targeted gene expression as a means of altering cell fates and generating dominant phenotypes." Development **118**(2): 401-415.

Brodu, V. and J. Casanova (2006). "The RhoGAP crossveinless-c links trachealess and EGFR signaling to cell shape remodeling in Drosophila tracheal invagination." Genes Dev **20**(13): 1817-1828.

Brunner, D., K. Ducker, N. Oellers, E. Hafen, H. Scholz and C. Klambt (1994). "The ETS domain protein pointed-P2 is a target of MAP kinase in the sevenless signal transduction pathway." Nature **370**(6488): 386-389.

Bryant, D. M., M. C. Kerr, L. A. Hammond, S. R. Joseph, K. E. Mostov, R. D. Teasdale and J. L. Stow (2007). "EGF induces macropinocytosis and SNX1-modulated recycling of E-cadherin." J Cell Sci **120**(Pt 10): 1818-1828.

Bulgakova, N. A. and E. Knust (2009). "The Crumbs complex: from epithelial-cell polarity to retinal degeneration." J Cell Sci **122**(Pt 15): 2587-2596.

Burd, C. and P. J. Cullen (2014). "Retromer: a master conductor of endosome sorting." Cold Spring Harb Perspect Biol **6**(2).

Butchar, J. P., D. Cain, S. N. Manivannan, A. D. McCue, L. Bonanno, S. Halula, S. Truesdell, C. L. Austin, T. L. Jacobsen and A. Simcox (2012). "New negative feedback regulators of Egfr signaling in Drosophila." Genetics **191**(4): 1213-1226.

Campbell, G. (2002). "Distalization of the Drosophila leg by graded EGF-receptor activity." Nature **418**(6899): 781-785.

Campellone, K. G. and M. D. Welch (2010). "A nucleator arms race: cellular control of actin assembly." Nat Rev Mol Cell Biol **11**(4): 237-251.

Cela, C. and M. Llimargas (2006). "Egfr is essential for maintaining epithelial integrity during tracheal remodelling in Drosophila." Development **133**(16): 3115-3125.

Chavrier, P., J. P. Gorvel, E. Stelzer, K. Simons, J. Gruenberg and M. Zerial (1991). "Hypervariable C-terminal domain of rab proteins acts as a targeting signal." Nature **353**(6346): 769-772.

Chen, D., H. Xiao, K. Zhang, B. Wang, Z. Gao, Y. Jian, X. Qi, J. Sun, L. Miao and C. Yang (2010). "Retromer is required for apoptotic cell clearance by phagocytic receptor recycling." Science **327**(5970): 1261-1264.

Chen, D. Y., M. Y. Li, S. Y. Wu, Y. L. Lin, S. P. Tsai, P. L. Lai, Y. T. Lin, J. C. Kuo, T. C. Meng and G. C. Chen (2012). "The Bro1-domain-containing protein Myopic/HDPTP coordinates with Rab4 to regulate cell adhesion and migration." J Cell Sci **125**(Pt 20): 4841-4852.

Chen, R. E. and J. Thorner (2007). "Function and regulation in MAPK signaling pathways: lessons learned from the yeast Saccharomyces cerevisiae." Biochim Biophys Acta **1773**(8): 1311-1340.

Christoforidis, S., M. Miaczynska, K. Ashman, M. Wilm, L. Zhao, S. C. Yip, M. D. Waterfield, J. M. Backer and M. Zerial (1999). "Phosphatidylinositol-3-OH kinases are Rab5 effectors." Nat Cell Biol **1**(4): 249-252.

Chung, S., M. S. Vining, P. L. Bradley, C. C. Chan, K. A. Wharton, Jr. and D. J. Andrew (2009). "Serrano (sano) functions with the planar cell polarity genes to control tracheal tube length." PLoS Genet **5**(11): e1000746.

de Vreede, G., J. D. Schoenfeld, S. L. Windler, H. Morrison, H. Lu and D. Bilder (2014). "The Scribble module regulates retromer-dependent endocytic trafficking during epithelial polarization." Development **141**(14): 2796-2802.

Derivery, E., C. Sousa, J. J. Gautier, B. Lombard, D. Loew and A. Gautreau (2009). "The Arp2/3 activator WASH controls the fission of endosomes through a large multiprotein complex." Dev Cell **17**(5): 712-723.

Devine, W. P., B. Lubarsky, K. Shaw, S. Luschnig, L. Messina and M. A. Krasnow (2005). "Requirement for chitin biosynthesis in epithelial tube morphogenesis." Proc Natl Acad Sci U S A **102**(47): 17014-17019.

Dominguez, M., J. D. Wasserman and M. Freeman (1998). "Multiple functions of the EGF receptor in Drosophila eye development." Curr Biol **8**(19): 1039-1048.

Dong, B., E. Hannezo and S. Hayashi (2014a). "Balance between apical membrane growth and luminal matrix resistance determines epithelial tubule shape." Cell Rep **7**(4): 941-950.

Dong, B. and S. Hayashi (2015). "Shaping of biological tubes by mechanical interaction of cell and extracellular matrix." Curr Opin Genet Dev **32**: 129-134.

Dong, B., K. Kakihara, T. Otani, H. Wada and S. Hayashi (2013). "Rab9 and retromer regulate retrograde trafficking of luminal protein required for epithelial tube length control." Nat Commun **4**: 1358.

Dong, B., G. Miao and S. Hayashi (2014b). "A fat body-derived apical extracellular matrix enzyme is transported to the tracheal lumen and is required for tube morphogenesis in Drosophila." Development **141**(21): 4104-4109.

Feng, Y., B. Press and A. Wandinger-Ness (1995). "Rab 7: an important regulator of late endocytic membrane traffic." J Cell Biol **131**(6 Pt 1): 1435-1452.

Flores-Benitez, D. and E. Knust (2016). "Dynamics of epithelial cell polarity in Drosophila: how to regulate the regulators?" Curr Opin Cell Biol **42**: 13-21.

Flynn, J. F., C. Wong and J. M. Wu (2009). "Anti-EGFR Therapy: Mechanism and Advances in Clinical Efficacy in Breast Cancer." J Oncol **2009**: 526963.

Forster, D., K. Armbruster and S. Luschnig (2010). "Sec24-dependent secretion drives cell-autonomous expansion of tracheal tubes in Drosophila." Curr Biol **20**(1): 62-68.

Forster, D. and S. Luschnig (2012). "Src42A-dependent polarized cell shape changes mediate epithelial tube elongation in Drosophila." Nat Cell Biol **14**(5): 526-534.

Franch-Marro, X., F. Wendler, S. Guidato, J. Griffith, A. Baena-Lopez, N. Itasaki, M. M. Maurice and J. P. Vincent (2008). "Wingless secretion requires endosome-to-Golgi retrieval of Wntless/Evi/Sprinter by the retromer complex." Nat Cell Biol **10**(2): 170-177.

Freeman, M. (1994). "The spitz gene is required for photoreceptor determination in the Drosophila eye where it interacts with the EGF receptor." Mech Dev **48**(1): 25-33.

Freeman, M. (1996). "Reiterative use of the EGF receptor triggers differentiation of all cell types in the Drosophila eye." Cell **87**(4): 651-660.

Freeman, M., C. Klambt, C. S. Goodman and G. M. Rubin (1992). "The argos gene encodes a diffusible factor that regulates cell fate decisions in the Drosophila eye." Cell **69**(6): 963-975.

Futran, A. S., A. J. Link, R. Seger and S. Y. Shvartsman (2013). "ERK as a model for systems biology of enzyme kinetics in cells." Curr Biol **23**(21): R972-979.

Gabay, L., H. Scholz, M. Golembo, A. Klaes, B. Z. Shilo and C. Klambt (1996). "EGF receptor signaling induces pointed P1 transcription and inactivates Yan protein in the Drosophila embryonic ventral ectoderm." Development **122**(11): 3355-3362.

Gabay, L., R. Seger and B. Z. Shilo (1997). "In situ activation pattern of Drosophila EGF receptor pathway during development." Science **277**(5329): 1103-1106.

Galindo, M. I., S. A. Bishop, S. Greig and J. P. Couso (2002). "Leg patterning driven by proximal-distal interactions and EGFR signaling." Science **297**(5579): 256-259.

Gallon, M. and P. J. Cullen (2015). "Retromer and sorting nexins in endosomal sorting." Biochem Soc Trans **43**(1): 33-47.

Ghabrial, A., S. Luschnig, M. M. Metzstein and M. A. Krasnow (2003). "Branching morphogenesis of the Drosophila tracheal system." Annu Rev Cell Dev Biol **19**: 623-647.

Ghabrial, A. S., B. P. Levi and M. A. Krasnow (2011). "A systematic screen for tube morphogenesis and branching genes in the Drosophila tracheal system." PLoS Genet **7**(7): e1002087.

Ghiglione, C., E. A. Bach, Y. Paraiso, K. L. Carraway, 3rd, S. Noselli and N. Perrimon (2002). "Mechanism of activation of the Drosophila EGF Receptor by the TGFalpha ligand Gurken during oogenesis." Development **129**(1): 175-186.

Gomez, A. R., A. Lopez-Varea, C. Molnar, E. de la Calle-Mustienes, M. Ruiz-Gomez, J. L. Gomez-Skarmeta and J. F. de Celis (2005). "Conserved cross-interactions in Drosophila and Xenopus between Ras/MAPK signaling and the dual-specificity phosphatase MKP3." Dev Dyn **232**(3): 695-708.

Gomez, T. S. and D. D. Billadeau (2009). "A FAM21-containing WASH complex regulates retromer-dependent sorting." Dev Cell **17**(5): 699-711.

Gonzalez-Gaitan, M. (2003). "Signal dispersal and transduction through the endocytic pathway." Nat Rev Mol Cell Biol **4**(3): 213-224.

Gonzalez-Reyes, A., H. Elliott and D. St Johnston (1995). "Polarization of both major body axes in Drosophila by gurken-torpedo signalling." Nature **375**(6533): 654-658.

Gorvel, J. P., P. Chavrier, M. Zerial and J. Gruenberg (1991). "rab5 controls early endosome fusion in vitro." Cell **64**(5): 915-925.

Grant, B. D. and J. G. Donaldson (2009). "Pathways and mechanisms of endocytic recycling." Nat Rev Mol Cell Biol **10**(9): 597-608.

Gruenberg, J. (2001). "The endocytic pathway: a mosaic of domains." Nat Rev Mol Cell Biol **2**(10): 721-730.

Gruenberg, J., G. Griffiths and K. E. Howell (1989). "Characterization of the early endosome and putative endocytic carrier vesicles in vivo and with an assay of vesicle fusion in vitro." J Cell Biol **108**(4): 1301-1316.

Guichard, A., M. Roark, M. Ronshaugen and E. Bier (2000). "brother of rhomboid, a rhomboid-related gene expressed during early Drosophila oogenesis, promotes EGF-R/MAPK signaling." Dev Biol **226**(2): 255-266.

Harterink, M., F. Port, M. J. Lorenowicz, I. J. McGough, M. Silhankova, M. C. Betist, J. R. van Weering, R. G. van Heesbeen, T. C. Middelkoop, K. Basler, P. J. Cullen and H. C. Korswagen (2011). "A SNX3-dependent retromer pathway mediates retrograde transport of the Wnt sorting receptor Wntless and is required for Wnt secretion." Nat Cell Biol **13**(8): 914-923.

Harterink, M., F. Port, M. J. Lorenowicz, I. J. McGough, M. Silhankova, M. C. Betist, J. R. T. van Weering, R. van Heesbeen, T. C. Middelkoop, K. Basler, P. J. Cullen and H. C. Korswagen (2011). "A SNX3-dependent retromer pathway mediates retrograde transport of the Wnt sorting receptor Wntless and is required for Wnt secretion." Nat Cell Biol **13**(8): 914-923.

Hayashi, S. and B. Dong (2017). "Shape and geometry control of the Drosophila tracheal tubule." Dev Growth Differ **59**(1): 4-11.

Hori, K., A. Sen, T. Kirchhausen and S. Artavanis-Tsakonas (2011). "Synergy between the ESCRT-III complex and Deltex defines a ligand-independent Notch signal." J Cell Biol **195**(6): 1005-1015.

Hsu, V. W., M. Bai and J. Li (2012). "Getting active: protein sorting in endocytic recycling." Nat Rev Mol Cell Biol **13**(5): 323-328.

Isaac, D. D. and D. J. Andrew (1996). "Tubulogenesis in Drosophila: a requirement for the trachealess gene product." Genes Dev **10**(1): 103-117.

Jaillais, Y., M. Santambrogio, F. Rozier, I. Fobis-Loisy, C. Miege and T. Gaude (2007). "The retromer protein VPS29 links cell polarity and organ initiation in plants." Cell **130**(6): 1057-1070.

Jayaram, S. A., K. A. Senti, K. Tiklova, V. Tsarouhas, J. Hemphala and C. Samakovlis (2008). "COPI vesicle transport is a common requirement for tube expansion in Drosophila." PLoS One **3**(4): e1964.

Jazwinska, A. and M. Affolter (2004). "A family of genes encoding zona pellucida (ZP) domain proteins is expressed in various epithelial tissues during Drosophila embryogenesis." Gene Expr Patterns **4**(4): 413-421.

Jazwinska, A., C. Ribeiro and M. Affolter (2003). "Epithelial tube morphogenesis during Drosophila tracheal development requires Piopio, a luminal ZP protein." Nat Cell Biol **5**(10): 895-901.

Jin, M. H., K. Sawamoto, M. Ito and H. Okano (2000). "The interaction between the Drosophila secreted protein argos and the epidermal growth factor receptor inhibits dimerization of the receptor and binding of secreted spitz to the receptor." Mol Cell Biol **20**(6): 2098-2107.

Jones, S. and J. Z. Rappoport (2014). "Interdependent epidermal growth factor receptor signalling and trafficking." Int J Biochem Cell Biol **51**: 23-28.

Kerman, B. E., A. M. Cheshire and D. J. Andrew (2006). "From fate to function: the Drosophila trachea and salivary gland as models for tubulogenesis." Differentiation **74**(7): 326-348.

Kim, M., G. H. Cha, S. Kim, J. H. Lee, J. Park, H. Koh, K. Y. Choi and J. Chung (2004). "MKP-3 has essential roles as a negative regulator of the Ras/mitogen-activated protein kinase pathway during Drosophila development." Mol Cell Biol **24**(2): 573-583.

Kim, S.-K. (2011). Chitin, chitosan, oligosaccharides and their derivatives: Biological activities and applications. Boca Raton: CRC Press

Klambt, C. (1993). "The Drosophila gene pointed encodes two ETS-like proteins which are involved in the development of the midline glial cells." Development **117**(1): 163-176.

Klebes, A. and E. Knust (2000). "A conserved motif in Crumbs is required for E-cadherin localisation and zonula adherens formation in Drosophila." Curr Biol **10**(2): 76-85.

Klein, D. E., V. M. Nappi, G. T. Reeves, S. Y. Shvartsman and M. A. Lemmon (2004). "Argos inhibits epidermal growth factor receptor signalling by ligand sequestration." Nature **430**(7003): 1040-1044.

Knust, E. and O. Bossinger (2002). "Composition and formation of intercellular junctions in epithelial cells." Science **298**(5600): 1955-1959.

Kolodkin, A. L., A. T. Pickup, D. M. Lin, C. S. Goodman and U. Banerjee (1994). "Characterization of Star and its interactions with sevenless and EGF receptor during photoreceptor cell development in Drosophila." Development **120**(7): 1731-1745.

Lai, Z. C. and G. M. Rubin (1992). "Negative control of photoreceptor development in Drosophila by the product of the yan gene, an ETS domain protein." Cell **70**(4): 609-620.

Labouesse, M. (2012). "Role of the extracellular matrix in epithelial morphogenesis: a view from C. elegans." Organogenesis **8**(2): 65-70.

Lamb, R. S., R. E. Ward, L. Schweizer and R. G. Fehon (1998). "Drosophila coracle, a member of the protein 4.1 superfamily, has essential structural functions in the septate junctions and developmental functions in embryonic and adult epithelial cells." Mol Biol Cell **9**(12): 3505-3519.

Lanzetti, L., V. Rybin, M. G. Malabarba, S. Christoforidis, G. Scita, M. Zerial and P. P. Di Fiore (2000). "The Eps8 protein coordinates EGF receptor signalling through Rac and trafficking through Rab5." Nature **408**(6810): 374-377.

Laprise, P., S. Beronja, N. F. Silva-Gagliardi, M. Pellikka, A. M. Jensen, C. J. McGlade and U. Tepass (2006). "The FERM protein Yurt is a negative regulatory component of the Crumbs complex that controls epithelial polarity and apical membrane size." Dev Cell **11**(3): 363-374.

Laprise, P., S. M. Paul, J. Boulanger, R. M. Robbins, G. J. Beitel and U. Tepass (2010). "Epithelial polarity proteins regulate Drosophila tracheal tube size in parallel to the luminal matrix pathway." Curr Biol **20**(1): 55-61.

Laprise, P. and U. Tepass (2011). "Novel insights into epithelial polarity proteins in Drosophila." Trends Cell Biol **21**(7): 401-408.

Lee, J. R., S. Urban, C. F. Garvey and M. Freeman (2001). "Regulated intracellular ligand transport and proteolysis control EGF signal activation in Drosophila." Cell **107**(2): 161-171.

Letizia, A., S. Sotillos, S. Campuzano and M. Llimargas (2011). "Regulated Crb accumulation controls apical constriction and invagination in Drosophila tracheal cells." J Cell Sci **124**(Pt 2): 240-251.

Lin, X., J. Zhang, L. Chen, Y. Chen, X. Xu, W. Hong and T. Wang (2017). "Tyrosine phosphorylation of Rab7 by Src kinase." Cell Signal **35**: 84-94.

Llimargas, M. and J. Casanova (1999). "EGF signalling regulates cell invagination as well as cell migration during formation of tracheal system in Drosophila." Dev Genes Evol **209**(3): 174-179.

Llimargas, M., M. Strigini, M. Katidou, D. Karagogeos and J. Casanova (2004). "Lachesin is a component of a septate junction-based mechanism that controls tube size and epithelial integrity in the Drosophila tracheal system." Development **131**(1): 181-190.

Loganathan R., Cheng Y.L., Andrew D.J. (2016) *Organogenesis of the Drosophila Respiratory System*. In: Castelli-Gair Hombría J., Bovolenta P. (eds) Organogenetic Gene Networks. Springer, Cham

Luschnig, S., T. Batz, K. Armbruster and M. A. Krasnow (2006). "serpentine and vermiform encode matrix proteins with chitin binding and deacetylation domains that limit tracheal tube length in Drosophila." Curr Biol **16**(2): 186-194.

Makarova, O., M. H. Roh, C. J. Liu, S. Laurinec and B. Margolis (2003). "Mammalian Crumbs3 is a small transmembrane protein linked to protein associated with Lin-7 (Pals1)." Gene **302**(1-2): 21-29.

Manning, G., & Krasnow, M. A. (1993). Development of the Drosophila tracheal system. In M. Bate & A. Martinez Arias (Eds.), *The development of Drosophila melanogaster* (pp. 609–685). Cold Spring Harbor Press.

Martin-Bermudo, M. D., O. M. Dunin-Borkowski and N. H. Brown (1997). "Specificity of PS integrin function during embryogenesis resides in the alpha subunit extracellular domain." EMBO J **16**(14): 4184-4193.

Martin-Blanco, E. (1998). "Regulatory control of signal transduction during morphogenesis in Drosophila." Int J Dev Biol **42**(3): 363-368.

Massarwa, R., E. D. Schejter and B. Z. Shilo (2009). "Apical secretion in epithelial tubes of the Drosophila embryo is directed by the Formin-family protein Diaphanous." Dev Cell **16**(6): 877-888.

Maxfield, F. R. and T. E. McGraw (2004). "Endocytic recycling." Nat Rev Mol Cell Biol **5**(2): 121-132.

McDonald, J. A., E. M. Pinheiro, L. Kadlec, T. Schupbach and D. J. Montell (2006). "Multiple EGFR ligands participate in guiding migrating border cells." Dev Biol **296**(1): 94-103.

Medina, E., J. Williams, E. Klipfell, D. Zarnescu, G. Thomas and A. Le Bivic (2002). "Crumbs interacts with moesin and beta(Heavy)-spectrin in the apical membrane skeleton of Drosophila." J Cell Biol **158**(5): 941-951.

Miura, G. I., J. Y. Roignant, M. Wassef and J. E. Treisman (2008). "Myopic acts in the endocytic pathway to enhance signaling by the Drosophila EGF receptor." Development **135**(11): 1913-1922.

Mukadam, A. S. and M. N. Seaman (2015). "Retromer-mediated endosomal protein sorting: The role of unstructured domains." FEBS Lett **589**(19 Pt A): 2620-2626.

Murray, J. T., C. Panaretou, H. Stenmark, M. Miaczynska and J. M. Backer (2002). "Role of Rab5 in the recruitment of hVps34/p150 to the early endosome." Traffic **3**(6): 416-427.

Nelson, K. S., Z. Khan, I. Molnar, J. Mihaly, M. Kaschube and G. J. Beitel (2012). "Drosophila Src regulates anisotropic apical surface growth to control epithelial tube size." Nat Cell Biol **14**(5): 518-525.

Nemetschke, L. and E. Knust (2016). "Drosophila Crumbs prevents ectopic Notch activation in developing wings by inhibiting ligand-independent endocytosis." Development **143**(23): 4543-4553.

Neuman-Silberberg, F. S. and T. Schupbach (1993). "The Drosophila dorsoventral patterning gene gurken produces a dorsally localized RNA and encodes a TGF alpha-like protein." Cell **75**(1): 165-174.

Nishimura, M., Y. Inoue and S. Hayashi (2007). "A wave of EGFR signaling determines cell alignment and intercalation in the Drosophila tracheal placode." Development **134**(23): 4273-4282.

Norum, M., E. Tang, T. Chavoshi, H. Schwarz, D. Linke, A. Uv and B. Moussian (2010). "Trafficking through COPII stabilises cell polarity and drives secretion during Drosophila epidermal differentiation." PLoS One **5**(5): e10802.

O'Neill, E. M., I. Rebay, R. Tjian and G. M. Rubin (1994). "The activities of two Ets-related transcription factors required for Drosophila eye development are modulated by the Ras/MAPK pathway." Cell **78**(1): 137-147.

Ochoa-Espinosa, A., M. M. Baer and M. Affolter (2012). "Tubulogenesis: Src42A goes to great lengths in tube elongation." Curr Biol **22**(11): R446-449.

Ohashi, E., K. Tanabe, Y. Henmi, K. Mesaki, Y. Kobayashi and K. Takei (2011). "Receptor sorting within endosomal trafficking pathway is facilitated by dynamic actin filaments." PLoS One **6**(5): e19942.

Okenve-Ramos, P. and M. Llimargas (2014a). "Fascin links Btl/FGFR signalling to the actin cytoskeleton during Drosophila tracheal morphogenesis." Development **141**(4): 929-939.

Okenve-Ramos, P. and M. Llimargas (2014b). "A role for fascin in preventing filopodia breakage in Drosophila tracheal cells." Commun Integr Biol **7**(5).

Ozturk-Colak, A., B. Moussian, S. J. Araujo and J. Casanova (2016). "A feedback mechanism converts individual cell features into a supracellular ECM structure in Drosophila trachea." Elife **5**.

Paul, S. M., M. Ternet, P. M. Salvaterra and G. J. Beitel (2003). "The Na+/K+ ATPase is required for septate junction function and epithelial tube-size control in the Drosophila tracheal system." Development **130**(20): 4963-4974.

Perrimon, N., C. Pitsouli and B. Z. Shilo (2012). "Signaling mechanisms controlling cell fate and embryonic patterning." Cold Spring Harb Perspect Biol **4**(8): a005975.

Petkau, G., C. Wingen, L. C. Jussen, T. Radtke and M. Behr (2012). "Obstructor-A is required for epithelial extracellular matrix dynamics, exoskeleton function, and tubulogenesis." J Biol Chem **287**(25): 21396-21405.

Pfeffer, S. R. (2013). "Rab GTPase regulation of membrane identity." Curr Opin Cell Biol **25**(4): 414-419.

Pocha, S. M. and T. Wassmer (2011). "A novel role for retromer in the control of epithelial cell polarity." Commun Integr Biol **4**(6): 749-751.

Pocha, S. M., T. Wassmer, C. Niehage, B. Hoflack and E. Knust (2011). "Retromer controls epithelial cell polarity by trafficking the apical determinant Crumbs." Curr Biol **21**(13): 1111-1117.

Port, F., M. Kuster, P. Herr, E. Furger, C. Banziger, G. Hausmann and K. Basler (2008). "Wingless secretion promotes and requires retromer-dependent cycling of Wntless." Nat Cell Biol **10**(2): 178-185.

Puthenveedu, M. A., B. Lauffer, P. Temkin, R. Vistein, P. Carlton, K. Thorn, J. Taunton, O. D. Weiner, R. G. Parton and M. von Zastrow (2010). "Sequence-dependent sorting of recycling proteins by actin-stabilized endosomal microdomains." Cell **143**(5): 761-773.

Queenan, A. M., A. Ghabrial and T. Schupbach (1997). "Ectopic activation of torpedo/Egfr, a Drosophila receptor tyrosine kinase, dorsalizes both the eggshell and the embryo." Development **124**(19): 3871-3880.

Rajendran, L., H. J. Knolker and K. Simons (2010). "Subcellular targeting strategies for drug design and delivery." Nat Rev Drug Discov **9**(1): 29-42.

Rebay, I. and G. M. Rubin (1995). "Yan functions as a general inhibitor of differentiation and is negatively regulated by activation of the Ras1/MAPK pathway." Cell **81**(6): 857-866.

Reich, A. and B. Z. Shilo (2002). "Keren, a new ligand of the Drosophila epidermal growth factor receptor, undergoes two modes of cleavage." EMBO J **21**(16): 4287-4296.

Ribeiro, C., A. Ebner and M. Affolter (2002). "In vivo imaging reveals different cellular functions for FGF and Dpp signaling in tracheal branching morphogenesis." Dev Cell **2**(5): 677-683.

Ribeiro, C., M. Neumann and M. Affolter (2004). "Genetic control of cell intercalation during tracheal morphogenesis in Drosophila." Curr Biol **14**(24): 2197-2207.

Robertson, S. E., S. R. Setty, A. Sitaram, M. S. Marks, R. E. Lewis and M. M. Chou (2006). "Extracellular signal-regulated kinase regulates clathrin-independent endosomal trafficking." Mol Biol Cell **17**(2): 645-657.

Rodriguez-Fraticelli, A. E., J. Bagwell, M. Bosch-Fortea, G. Boncompain, N. Reglero-Real, M. J. Garcia-Leon, G. Andres, M. L. Toribio, M. A. Alonso, J. Millan, F. Perez, M. Bagnat and F. Martin-Belmonte (2015). "Developmental regulation of apical endocytosis controls epithelial patterning in vertebrate tubular organs." Nat Cell Biol **17**(3): 241-250.

Roeth, J. F., J. K. Sawyer, D. A. Wilner and M. Peifer (2009). "Rab11 helps maintain apical crumbs and adherens junctions in the Drosophila embryonic ectoderm." PLoS One **4**(10): e7634.

Rogge, R., P. J. Green, J. Urano, S. Horn-Saban, M. Mlodzik, B. Z. Shilo, V. Hartenstein and U. Banerjee (1995). "The role of yan in mediating the choice between cell division and differentiation." Development **121**(12): 3947-3958.

Rojas, R., T. van Vlijmen, G. A. Mardones, Y. Prabhu, A. L. Rojas, S. Mohammed, A. J. Heck, G. Raposo, P. van der Sluijs and J. S. Bonifacino (2008). "Regulation of retromer recruitment to endosomes by sequential action of Rab5 and Rab7." J Cell Biol **183**(3): 513-526.

Roman-Fernandez, A. and D. M. Bryant (2016). "Complex Polarity: Building Multicellular Tissues Through Apical Membrane Traffic." Traffic **17**(12): 1244-1261.

Roux, A., K. Uyhazi, A. Frost and P. De Camilli (2006). "GTP-dependent twisting of dynamin implicates constriction and tension in membrane fission." Nature **441**(7092): 528-531.

Rutledge, B. J., K. Zhang, E. Bier, Y. N. Jan and N. Perrimon (1992). "The Drosophila spitz gene encodes a putative EGF-like growth factor involved in dorsal-ventral axis formation and neurogenesis." Genes Dev **6**(8): 1503-1517.

Sakaidani, Y., T. Nomura, A. Matsuura, M. Ito, E. Suzuki, K. Murakami, D. Nadano, T. Matsuda, K. Furukawa and T. Okajima (2011). "O-linked-N-acetylglucosamine on extracellular protein domains mediates epithelial cell-matrix interactions." Nat Commun **2**: 583.

Salcini, A. E., H. Chen, G. Iannolo, P. De Camilli and P. P. Di Fiore (1999). "Epidermal growth factor pathway substrate 15, Eps15." Int J Biochem Cell Biol **31**(8): 805-809.

Samakovlis, C., G. Manning, P. Steneberg, N. Hacohen, R. Cantera and M. A. Krasnow (1996). "Genetic control of epithelial tube fusion during Drosophila tracheal development." Development **122**(11): 3531-3536.

Schindelin, J., I. Arganda-Carreras, E. Frise, V. Kaynig, M. Longair, T. Pietzsch, S. Preibisch, C. Rueden, S. Saalfeld, B. Schmid, J. Y. Tinevez, D. J. White, V. Hartenstein, K. Eliceiri, P. Tomancak and A. Cardona (2012). "Fiji: an open-source platform for biological-image analysis." Nat Methods **9**(7): 676-682.

Schnepp, B., T. Donaldson, G. Grumbling, S. Ostrowski, R. Schweitzer, B. Z. Shilo and A. Simcox (1998). "EGF domain swap converts a drosophila EGF receptor activator into an inhibitor." Genes Dev **12**(7): 908-913.

Schnepp, B., G. Grumbling, T. Donaldson and A. Simcox (1996). "Vein is a novel component in the Drosophila epidermal growth factor receptor pathway with similarity to the neuregulins." Genes Dev **10**(18): 2302-2313.

Scholz, H., J. Deatrick, A. Klaes and C. Klambt (1993). "Genetic dissection of pointed, a Drosophila gene encoding two ETS-related proteins." Genetics **135**(2): 455-468.

Schottenfeld, J., Y. Song and A. S. Ghabrial (2010). "Tube continued: morphogenesis of the Drosophila tracheal system." Curr Opin Cell Biol **22**(5): 633-639.

Schweitzer, R., R. Howes, R. Smith, B. Z. Shilo and M. Freeman (1995). "Inhibition of Drosophila EGF receptor activation by the secreted protein Argos." Nature **376**(6542): 699-702.

Schweitzer, R., M. Shaharabany, R. Seger and B. Z. Shilo (1995). "Secreted Spitz triggers the DER signaling pathway and is a limiting component in embryonic ventral ectoderm determination." Genes Dev **9**(12): 1518-1529.

Schweitzer, R. and B. Z. Shilo (1997). "A thousand and one roles for the Drosophila EGF receptor." Trends Genet **13**(5): 191-196.

Seaman, M. N. (2004). "Cargo-selective endosomal sorting for retrieval to the Golgi requires retromer." J Cell Biol **165**(1): 111-122.

Seaman, M. N. (2012). "The retromer complex - endosomal protein recycling and beyond." J Cell Sci **125**(Pt 20): 4693-4702.

Seaman, M. N., A. Gautreau and D. D. Billadeau (2013). "Retromer-mediated endosomal protein sorting: all WASHed up!" Trends Cell Biol **23**(11): 522-528.

Seaman, M. N., M. E. Harbour, D. Tattersall, E. Read and N. Bright (2009). "Membrane recruitment of the cargo-selective retromer subcomplex is catalysed by the small GTPase Rab7 and inhibited by the Rab-GAP TBC1D5." J Cell Sci **122**(Pt 14): 2371-2382.

Shilo, B. Z. (2003). "Signaling by the Drosophila epidermal growth factor receptor pathway during development." Exp Cell Res **284**(1): 140-149.

Shilo, B. Z. (2005). "Regulating the dynamics of EGF receptor signaling in space and time." Development **132**(18): 4017-4027.

Shilo, B. Z. (2014). "The regulation and functions of MAPK pathways in Drosophila." Methods **68**(1): 151-159.

Sibilia, M., J. P. Steinbach, L. Stingl, A. Aguzzi and E. F. Wagner (1998). "A strain-independent postnatal neurodegeneration in mice lacking the EGF receptor." EMBO J **17**(3): 719-731.

Simcox, A. A., G. Grumbling, B. Schnepp, C. Bennington-Mathias, E. Hersperger and A. Shearn (1996). "Molecular, phenotypic, and expression analysis of vein, a gene required for growth of the Drosophila wing disc." Dev Biol **177**(2): 475-489.

Sollier, K., H. M. Gaude, F. J. Chartier and P. Laprise (2015). "Rac1 controls epithelial tube length through the apical secretion and polarity pathways." Biol Open **5**(1): 49-54.

Sopko, R. and N. Perrimon (2013). "Receptor tyrosine kinases in Drosophila development." Cold Spring Harb Perspect Biol **5**(6).

Stasyk, T., N. Schiefermeier, S. Skvortsov, H. Zwierzina, J. Peranen, G. K. Bonn and L. A. Huber (2007). "Identification of endosomal epidermal growth factor receptor signaling targets by functional organelle proteomics." Mol Cell Proteomics **6**(5): 908-922.

Steinberg, F., M. Gallon, M. Winfield, E. C. Thomas, A. J. Bell, K. J. Heesom, J. M. Tavare and P. J. Cullen (2013). "A global analysis of SNX27-retromer assembly and cargo specificity reveals a function in glucose and metal ion transport." Nat Cell Biol **15**(5): 461-471.

Sutherland, D., C. Samakovlis and M. A. Krasnow (1996). "branchless encodes a Drosophila FGF homolog that controls tracheal cell migration and the pattern of branching." Cell **87**(6): 1091-1101.

Swanson, L. E. and G. J. Beitel (2006). "Tubulogenesis: an inside job." Curr Biol **16**(2): R51-53.

Tall, G. G., M. A. Barbieri, P. D. Stahl and B. F. Horazdovsky (2001). "Ras-activated endocytosis is mediated by the Rab5 guanine nucleotide exchange activity of RIN1." Dev Cell **1**(1): 73-82.

Temkin, P., B. Lauffer, S. Jager, P. Cimermancic, N. J. Krogan and M. von Zastrow (2011). "SNX27 mediates retromer tubule entry and endosome-to-plasma membrane trafficking of signalling receptors." Nat Cell Biol **13**(6): 715-721.

Tepass, U. (1996). "Crumbs, a component of the apical membrane, is required for zonula adherens formation in primary epithelia of Drosophila." Dev Biol **177**(1): 217-225.

Tepass, U. (2012). "The apical polarity protein network in Drosophila epithelial cells: regulation of polarity, junctions, morphogenesis, cell growth, and survival." Annu Rev Cell Dev Biol **28**: 655-685.

Tepass, U. and E. Knust (1990). "Phenotypic and developmental analysis of mutations at thecrumbs locus, a gene required for the development of epithelia inDrosophila melanogaster." Roux Arch Dev Biol **199**(4): 189-206.

Tepass, U., G. Tanentzapf, R. Ward and R. Fehon (2001). "Epithelial cell polarity and cell junctions in Drosophila." Annu Rev Genet **35**: 747-784.

Tepass, U., C. Theres and E. Knust (1990). "crumbs encodes an EGF-like protein expressed on apical membranes of Drosophila epithelial cells and required for organization of epithelia." Cell **61**(5): 787-799.

Thomas, G. H. (2001). "Spectrin: the ghost in the machine." Bioessays **23**(2): 152-160.

Thomas, S. M. and J. S. Brugge (1997). "Cellular functions regulated by Src family kinases." Annu Rev Cell Dev Biol **13**: 513-609.

Tiklova, K., V. Tsarouhas and C. Samakovlis (2013). "Control of airway tube diameter and integrity by secreted chitin-binding proteins in Drosophila." PLoS One **8**(6): e67415.

Tio, M., C. Ma and K. Moses (1994). "spitz, a Drosophila homolog of transforming growth factor-alpha, is required in the founding photoreceptor cells of the compound eye facets." Mech Dev **48**(1): 13-23.

Tio, M. and K. Moses (1997). "The Drosophila TGF alpha homolog Spitz acts in photoreceptor recruitment in the developing retina." Development **124**(2): 343-351.

Tonning, A., J. Hemphala, E. Tang, U. Nannmark, C. Samakovlis and A. Uv (2005). "A transient luminal chitinous matrix is required to model epithelial tube diameter in the Drosophila trachea." Dev Cell **9**(3): 423-430.

Tootle, T. L., P. S. Lee and I. Rebay (2003). "CRM1-mediated nuclear export and regulated activity of the Receptor Tyrosine Kinase antagonist YAN require specific interactions with MAE." Development **130**(5): 845-857.

Tsarouhas, V., K. A. Senti, S. A. Jayaram, K. Tiklova, J. Hemphala, J. Adler and C. Samakovlis (2007). "Sequential pulses of apical epithelial secretion and endocytosis drive airway maturation in Drosophila." Dev Cell **13**(2): 214-225.

Ullrich, O., S. Reinsch, S. Urbe, M. Zerial and R. G. Parton (1996). "Rab11 regulates recycling through the pericentriolar recycling endosome." J Cell Biol **135**(4): 913-924.

Urban, S., J. R. Lee and M. Freeman (2001). "Drosophila rhomboid-1 defines a family of putative intramembrane serine proteases." Cell **107**(2): 173-182.

Urban, S., J. R. Lee and M. Freeman (2002). "A family of Rhomboid intramembrane proteases activates all Drosophila membrane-tethered EGF ligands." EMBO J **21**(16): 4277-4286.

Urbe, S., L. A. Huber, M. Zerial, S. A. Tooze and R. G. Parton (1993). "Rab11, a small GTPase associated with both constitutive and regulated secretory pathways in PC12 cells." FEBS Lett **334**(2): 175-182.

Uv, A., R. Cantera and C. Samakovlis (2003). "Drosophila tracheal morphogenesis: intricate cellular solutions to basic plumbing problems." Trends Cell Biol **13**(6): 301-309.

van der Sluijs, P., M. Hull, P. Webster, P. Male, B. Goud and I. Mellman (1992). "The small GTP-binding protein rab4 controls an early sorting event on the endocytic pathway." Cell **70**(5): 729-740.

Van Der Sluijs, P., M. Hull, A. Zahraoui, A. Tavitian, B. Goud and I. Mellman (1991). "The small GTP-binding protein rab4 is associated with early endosomes." Proc Natl Acad Sci U S A **88**(14): 6313-6317.

Verges, M., F. Luton, C. Gruber, F. Tiemann, L. G. Reinders, L. Huang, A. L. Burlingame, C. R. Haft and K. E. Mostov (2004). "The mammalian retromer regulates transcytosis of the polymeric immunoglobulin receptor." Nat Cell Biol **6**(8): 763-769.

Wandinger-Ness, A. and M. Zerial (2014). "Rab proteins and the compartmentalization of the endosomal system." Cold Spring Harb Perspect Biol **6**(11): a022616.

Wang, S. and H. J. Bellen (2015). "The retromer complex in development and disease." Development **142**(14): 2392-2396.

Wang, S., S. A. Jayaram, J. Hemphala, K. A. Senti, V. Tsarouhas, H. Jin and C. Samakovlis (2006). "Septate-junction-dependent luminal deposition of chitin deacetylases restricts tube elongation in the Drosophila trachea." Curr Biol **16**(2): 180-185.

Wasserman, J. D. and M. Freeman (1997). "Control of EGF receptor activation in Drosophila." Trends Cell Biol **7**(11): 431-436.

Wertheimer, E., A. Gutierrez-Uzquiza, C. Rosemblit, C. Lopez-Haber, M. S. Sosa and M. G. Kazanietz (2012). "Rac signaling in breast cancer: a tale of GEFs and GAPs." Cell Signal **24**(2): 353-362.

Wichmann, H., L. Hengst and D. Gallwitz (1992). "Endocytosis in yeast: evidence for the involvement of a small GTP-binding protein (Ypt7p)." Cell **71**(7): 1131-1142.

Wilcke, M., L. Johannes, T. Galli, V. Mayau, B. Goud and J. Salamero (2000). "Rab11 regulates the compartmentalization of early endosomes required for efficient transport from early endosomes to the trans-golgi network." J Cell Biol **151**(6): 1207-1220.

Wilde, A., E. C. Beattie, L. Lem, D. A. Riethof, S. H. Liu, W. C. Mobley, P. Soriano and F. M. Brodsky (1999). "EGF receptor signaling stimulates SRC kinase phosphorylation of clathrin, influencing clathrin redistribution and EGF uptake." Cell **96**(5): 677-687.

Wilk, R., I. Weizman and B. Z. Shilo (1996). "trachealess encodes a bHLH-PAS protein that is an inducer of tracheal cell fates in Drosophila." Genes Dev **10**(1): 93-102.

Wilkin, M. B., M. N. Becker, D. Mulvey, I. Phan, A. Chao, K. Cooper, H. J. Chung, I. D. Campbell, M. Baron and R. MacIntyre (2000). "Drosophila dumpy is a gigantic extracellular protein required to maintain tension at epidermal-cuticle attachment sites." Curr Biol **10**(10): 559-567.

Wodarz, A., U. Hinz, M. Engelbert and E. Knust (1995). "Expression of crumbs confers apical character on plasma membrane domains of ectodermal epithelia of Drosophila." Cell **82**(1): 67-76.

Wollert, T., C. Wunder, J. Lippincott-Schwartz and J. H. Hurley (2009). "Membrane scission by the ESCRT-III complex." Nature **458**(7235): 172-177.

Wortzel, I. and R. Seger (2011). "The ERK Cascade: Distinct Functions within Various Subcellular Organelles." Genes Cancer **2**(3): 195-209.

Wu, V. M., J. Schulte, A. Hirschi, U. Tepass and G. J. Beitel (2004). "Sinuous is a Drosophila claudin required for septate junction organization and epithelial tube size control." J Cell Biol **164**(2): 313-323.

Yao, Z. and R. Seger (2009). "The ERK signaling cascade--views from different subcellular compartments." Biofactors **35**(5): 407-416.

Yarnitzky, T., L. Min and T. Volk (1997). "The Drosophila neuregulin homolog Vein mediates inductive interactions between myotubes and their epidermal attachment cells." Genes Dev **11**(20): 2691-2700.

Zelzer, E. and B. Z. Shilo (2000). "Interaction between the bHLH-PAS protein Trachealess and the POU-domain protein Drifter, specifies tracheal cell fates." Mech Dev **91**(1-2): 163-173.

Zhou, B., Y. Wu and X. Lin (2011). "Retromer regulates apical-basal polarity through recycling Crumbs." Dev Biol **360**(1): 87-95.

Zhou, Y., T. Tanaka, N. Sugiyama, S. Yokoyama, Y. Kawasaki, T. Sakuma, Y. Ishihama, I. Saiki and H. Sakurai (2014). "p38-Mediated phosphorylation of Eps15 endocytic adaptor protein." FEBS Lett **588**(1): 131-137.

Zuo, L., E. Iordanou, R. R. Chandran and L. Jiang (2013). "Novel mechanisms of tube-size regulation revealed by the Drosophila trachea." Cell Tissue Res **354**(2): 343-354.

8. APPENDICES

8. APPENDICES

8.1 List of abbreviations

aECM	Apical ExtraCellular Matrix
AFR	Apical Free Region
AJ	Adherens Junctions
aop	Anterior Open
aos	Argos
aPKC	Atypical Protein Complex/Cyclosome
bnl	Branchless
BSA	Bovine Serum Albumine
Btl	Breathless
CDA	Chitin deacetylase Domain
CBD	Chitin Binding Domain
CBP	Chitin Binding Protein
CCJ	Circumferential Cell Junctions
cic	Capicua
COPI	Coat Complex protein I
COPII	Coat Complex protein II
cora	Coracle
crb	Crumbs
CSC	Cargo Selective Complex
cv-c	Crossveinless-c
DAAM	Dishevelled-associated activator of morphogenesis
DB	Dorsal branch
dlg	Disc Large
DP	Dumpy
DT	Dorsal trunk
E-Cadh	E-Cadherin
EE	Early Endosome
EGFR	Epidermal Growth Factor Receptor
EGFR^{DN}	Dominant negative EGFR
EGFR^{CA}	Constitutively activated EGFR
Eps15	Epidermal growth factor receptor pathway substrate 15
ERC	Endocytic recycling compartment
ERK	Extracellular signal Regulated Kinases
ESCRT	Endosomal Sorting Complexes Required for Transport
Exo84	Exocyst 84
FDB	FERM domain binding
FERM	4.1/ezrin/radixin/moesin
FGF	Fibroblast Growth Factor
FGFR	Fibroblast Growth Factor Receptor
Fig.	Figure
FRAP	Fluorescence Recovery After Photobleaching
GAPs	GTPase-activating Proteins
GB	Ganglionic branch
GEFs	Guanine-nucleotide Exchange Factors

GFP	Green Fluorescent Protein
Grb2	Cytoplasmic Growth Factor Receptor Bound protein 2
grk	Gurken
kkv	Krotzkopf Verkehrt
krn	Keren
KSR1	Kinase Suppressor of Ras-1
LCJ	Longitudinal Cell Junctions
LE	Late Endosome
lgl	Lethal Giant Larvae
LT	Lateral trunk
MAPK	Mitogen Activated Protein Kinase
MKP3	MAPK phosphatase 3
MT	Malphigian tubules
mum	*mummy/cystic*
NrxIV	Neurexin IV
Obst-A	Obstructor-A
PDB	PDZ-domain binding
PDZ	PSD-95/Disc-large/ZO-1
PDZbm	PDZ binding motif
Pio	Piopio
PKC	Protein Kinase C
pnt	Pointed
PTB	Phosphotyrosine binding domain
RE	Recycling Endosome
RE-RAB11	Recycling Endosome Rab11
rho	Rhomboid
RhoGap	RhoGTPase-Activating Protein
rll	Rolled
ROIs	Regions Of Interest
RTK	Receptor Tyrosine Kinase
SAR	Subapical Region
scrib	Scribble
SEM	Standard Error of the Mean
serp	Serpentine
SH 1, 2	Src Homology domain 1, 2
SJ	Septate Junctions
SNX	Sorting Nexins
SOS	Son Of Sevenless
spi	Spitz
SP	Spiracular branch
Src42A	Src oncogene at 42 a
Src64B	Src oncogene at 64 b
Src42A^{DN}	Downregulation form of Src42A
Src42A^{CA}	Constitutitvely active form of Src42A
stg	Stage
TC	Transverse connective
TGF-α	Transforming growth factor-α
TGN	Trans-Golgi network
trh	Trachealess

VB	Visceral branch
verm	Vermiform
vn	Vein
vps	Vacuolar Protein Sorting
vvl	Ventral Veinless
WASH	Wiskott-Aldrich Syndrome Protein and SCAR Homolog
Wnt	Wingless
wt	*wild-type*
YFP	Yellow Fluorescent Protein
yrt	Yurt
ZA	Zonula Adherens
ZP	Zona Pellucida
β-gal	beta-galactosidase
βH	β_H spectrin

8.2 Movie legends

Movie 1. Crb apical subcellular accumulation. Embryo carrying *Crb^{GFP}* visualised from a lateral view using a Zeiss Lsm780 Confocal and Multiphoton System with 63x Oil objective and a 2 zoom. Images were taken every 2 minutes during 2,30 hours in 20 Z-sections of 0,5µm thick from early stage 14 to stage 15. Note that at early stages Crb is accumulated in the AFR of DT cells (Yellow arrow). As development proceeds, Crb becomes enriched in the SAR (red arrow).

Movie 2. Rab4 and Crb accumulation. Stage 14 embryos carrying *Rab4^{EYFP}* and *Crb^{Cherry}* were visualised from a lateral view using a Zeiss Lsm780 Confocal and Multiphoton System with 63x Oil objective and a 2,5 zoom. Images were taken continuously in one single Z-section 0,5µm thick during 2 minutes. Note that many Crb vesicles are also positive for Rab4 (white arrow).

Movie 3 and Movie 4. Serp and Crb vesicle traffiking. Stage 14 embryos carrying *btlG4-UAS-serp-CBD-GFP and Crb^{Cherry}* were visualised from a lateral view using a Zeiss Lsm780 Confocal and Multiphoton System with 63x Oil objective and a 2,5 zoom. Images were taken continuously in one single Z-section 0,5µm thick during 3,5 minutes (movie 3) and 6 minutes (movie 4). Note that Crb and Serp vesicles are highly dynamic.

Movie 5 and Movie 6. FRAP assay. FRAP experiments were carried out in stage 14 embryos carrying *btl*Gal4;*Crb^{GFP}-C* (i.e Control) (movie 5A: Axial, movie5B: Circumferential) and *btl*Gal4;*Crb^{GFP}-C*/UAS-Src42A^{DN} (i.e mutant) (movie 6A: Axial, movie6B: Circumferential) visualised from a lateral view, using a Zeiss Lsm780 Confocal and Multiphoton System with 63x Oil objective and a 1,5 zoom. After 10 pre-bleach scans, bleaching was performed at the regions-of-interest (ROIs) selected for each type of junctions (Axial/Circumferential). Post-bleach scans were obtained immediately after bleaching in 4 Z-sections of 1µm thick at every 10 seconds and during 10-20 minutes. Note that in control conditions, Crb protein is more prone to recycle and/or traffic in the axial junctions (LCJ) than in the circumferential (CCJ), whereas in Src42A^{DN} embryos, these differences decreased.

8.3 Summary

The tracheal (respiratory) system of the *Drosophila* embryo is a network of interconnected epithelial tubes that supplies and exchanges the gas to maintain the homeostasis of the entire organism. Maintaining a controlled tube diameter and fitting tube length are two mor requirements for proper tube function.

The Epidermal growth factor receptor (EGFR), a Tyrosine Kinase Receptor (RTK), triggers one of the principal conserved signalling pathways operating in development and homeostasis. EGFR is known to be use reiteratively for organ and tissue formation in the fruitfly. One of the aims of this work was to gain new insights into the activity of EGFR during *Drosophila* development. We focused on the requirements of EGFR during the formation of the tracheal system. EGFR was previously known to be required for different aspects of tracheal development, such as for invagination, branching and epithelial integrity. In this work, we identify a new requirement for EGFR during tracheal formation in controlling the length of the tracheal tubes.

We found that EGFR regulates the size of the Dorsal trunk (DT), the main branch of the *Drosophila* tracheal network. The constitutively activation of EGFR ($EGFR^{CA}$) displays shorter tubes whereas a downregulation of EGFR ($EGFR^{DN}$) activity leads to an overelongated and convoluted DT. This phenotype correlates with cell shape regulation, resulting in more cuboidal cells in the case of $EGFR^{CA}$ and more elongated cells in $EGFR^{DN}$.

This work shows that EGFR act as a hub to coordinate cell intrinsic and extrinsic tube elongation mechanisms. This role is performed through the regulation of the luminal deposition of the extracellular matrix regulator Serpentine (Serp) (extrinsic factor) and of the apical determinant Crumbs (Crb) in the DT (intrinsic factor). In EGFR downregulation conditions the accumulation of both proteins is altered, and this may lead to the defective control of tube size observed. We show that Crb and Serp are loaded in common endosomes, which require EGFR activity for the proper organisation, ensuring delivery of both cargoes to their final destination. The regulation of endosomal sorting of cargoes could be one of the molecular mechanisms downstream of EGFR, and therefore could regulate different morphogenetic and pathological EGFR-mediated events.

We also report that during tracheal development Crb undergoes a complex pattern of recycling, which involves internalisation and different sorting pathways that ensures its apical subcellular accumulation. We propose that Crb recycles using the Rab11-Recycling Endosome route to accumulate preferentially to the Subapical Region (SAR) and a Rab4/Retromer short-loop from the endosome to the plasma membrane to enrich in the Apical free region (AFR).

Concerning the accumulation of Crb in the SAR, our results indicate that Crb is not equally distributed in all cellular junctions, but instead it is more clearly accumulated in longitudinal cell junctions (LCJ) than in circumferential cell junctions (CCJ). Crb has been proposed to control tube length through apical membrane expansion, so we hypothesize that Crb promotes a polarised longitudinal/axial tube growth. Because Src42A was previously proposed to mediate polarised cell shape changes in DT cells by regulating membrane growth in the longitudinal/axial axis, we evaluated a possible Crb/Src42A

interaction. We find that in loss of function conditions for Src42A, in which the DT remains shorter, Crb is more evenly distributed in all cellular junctions. The results suggest that Src42A may contribute to Crb preferential accumulation in the LCJ. FRAP experiments point to a role of Src42A in controlling the dynamics of Crb protein accumulation in junctions.

Conversely, in conditions of constitutive activation of Src42A, where there is an overelongation of the DT, we find that Crb is lost from all junctions. In addition, Serp accumulation in the lumen is also severely affected. Altogether, these results suggest a possible role for Src42A in regulating trafficking.

8.4 Resumen en castellano

El sistema traqueal embrionario de *Drosophila* está compuesto por una red de tubos epiteliales interconectados, los cuales necesitan una regulación constante tanto del diámetro como de la longitud para su correcto funcionamiento.

Durante el desarrollo traqueal, el receptor de EGF (Epidermal Growth Factor Receptor) está implicado en la regulación de la invaginación e integridad epitelial de las diferentes ramas traqueales. Uno de los principales objetivos de este trabajo es obtener nuevos conocimientos sobre la implicación de EGFR en el desarrollo traqueal. Nuestros datos indican que EGFR regula la longitud del tronco dorsal (DT), ya que en embriones con una disminución de su actividad ($EGFR^{DN}$), la longitud del DT se ve afectada produciendo una elongación de éste.

Asimismo, cuando alteramos la actividad de EGFR, observamos que la localización apical de Crumbs (Crb) y la acumulación luminal de Serpentine (Serp), dos proteínas que regulan el crecimiento del DT, se ven afectadas. La alteración en la acumulación de ambas proteínas desencadena un defecto en el control de la elongación del tubo, tal y como se observa en embriones $EGFR^{DN}$. Observamos que Crb y Serp localizan en endosomas comunes que necesitan de la actividad de EGFR para organizarse correctamente y transportar las proteínas a su destino final. Además, nuestros resultados demuestran que Crb sufre un complejo proceso de transporte y reciclaje durante el desarrollo traqueal.

En estadios tardíos de la embriogénesis, Crb se localiza en la región Subapical (SAR) pero lo hace de manera anisotrópica: Crb presenta mayor acumulación en las uniones longitudinales (LCJ) que en las circunferenciales (CCJ). Cuando disminuimos la actividad de Src42A, un regulador axial del crecimiento del tubo, Crb se distribuye homogéneamente, pero en condiciones de sobreactividad, Crb desaparece de esas uniones. Nuestros resultados indican que Src42A contribuye a una mayor acumulación de Crb en las LCJ regulando su dinámica, y sugieren una posible implicación de Src42A en el reciclaje de proteínas.

8.5 Published papers

The following published paper is attached.

- "EGFR controls Drosophila tracheal tube elongation by intracellular trafficking regulation." Olivares-Castineira, I. and M. Llimargas (2017). PLoS Genet **13**(7): e1006882.

PLOS GENETICS

RESEARCH ARTICLE

EGFR controls *Drosophila* tracheal tube elongation by intracellular trafficking regulation

Ivette Olivares-Castiñeira, Marta Llimargas*

Developmental Biology Department, Institut de Biologia Molecular de Barcelona, CSIC, Parc Científic de Barcelona, Barcelona, Spain

* mlcbmc@ibmb.csic.es

OPEN ACCESS

Citation: Olivares-Castiñeira I, Llimargas M (2017) EGFR controls *Drosophila* tracheal tube elongation by intracellular trafficking regulation. PLoS Genet 13(7): e1006882. https://doi.org/10.1371/journal.pgen.1006882

Editor: Norbert Perrimon, Harvard Medical School, Howard Hughes Medical Institute, UNITED STATES

Received: March 16, 2017

Accepted: June 21, 2017

Published: July 5, 2017

Data Availability Statement: All relevant data are within the paper and its Supporting Information files.

Funding: This work was supported by Ministerio de Economía y Competitividad of the Spanish Government (BFU2012-39509-C02, BFU2015-68098-P and Programme Consolider CSD2007-00008), and from AGAUR of the Generalitat de Catalunya (2009 SGR1333). IOC is supported by a FPI fellowship from Ministerio de Economía y Competitividad (BES-2013-065462). The funders

Abstract

Development is governed by a few conserved signalling pathways. Amongst them, the EGFR pathway is used reiteratively for organ and tissue formation, and when dysregulated can lead to cancer and metastasis. Given its relevance, identifying its downstream molecular machinery and understanding how it instructs cellular changes is crucial. Here we approach this issue in the respiratory system of *Drosophila*. We identify a new role for EGFR restricting the elongation of the tracheal Dorsal Trunk. We find that EGFR regulates the apical determinant Crb and the extracellular matrix regulator Serp, two factors previously known to control tube length. EGFR regulates the organisation of endosomes in which Crb and Serp proteins are loaded. Our results are consistent with a role of EGFR in regulating Retromer/WASH recycling routes. Furthermore, we provide new insights into Crb trafficking and recycling during organ formation. Our work connects cell signalling, trafficking mechanisms and morphogenesis and suggests that the regulation of cargo trafficking can be a general outcome of EGFR activation.

Author summary

The control of organ size and shape is a critical aspect of morphogenesis, as miss-regulation can lead to pathologies and malformations. The tracheal system of *Drosophila* is a good model to investigate this issue as tube size is strictly regulated. In addition, tracheal system development represents also an excellent system to study the molecular mechanisms employed by signalling pathways to instruct cells to form tubular structures. Here we describe that EGFR, which triggers one of the principal conserved pathways acting reiteratively during development and homeostasis, is required to restrict tube elongation. We find that EGFR regulates the accumulation and subcellular localisation of Crumbs and Serpentine, two factors previously known to regulate tube length. We show that Crumbs and Serpentine are loaded in common endosomes, which require EGFR for proper organisation, ensuring delivery of both cargoes to their final destination. We also report that during tracheal development the apical determinant Crumbs undergoes a complex pattern of recycling, which involves internalisation and different sorting

had no role in study design, data collection and analysis, decision to publish, or preparation of the manuscript.

Competing interests: The authors have declared that no competing interests exist.

pathways. Our analysis identifies EGFR as a hub to coordinate both cell intrinsic properties, namely Crumbs-dependant apical membrane growth, and extrinsic mechanisms, Serpentine-mediated extracellular matrix modifications, which regulate tube elongation. We suggest that the regulation of the endocytic traffic of specific cargoes could be one of the molecular mechanisms downstream of the EGFR, and therefore could regulate different morphogenetic and pathological EGFR-mediated events.

Introduction

Understanding how organs form and are maintained is a major goal in developmental biology. The *Drosophila* tracheal system is an excellent model to analyse the morphogenesis of branched tubular organs. Tubular structures are present in all organisms and accomplish basic functions of gas and liquid transport [1,2]. Embryonic tracheal development involves a morphogenetic phase where the tubular structure is formed [3]. In parallel, there is a maturation phase where the tubes attain their final size and shape and become physiologically active, able to transport oxygen [4]. The control of tube size and shape is key, as loss of regulation can lead to pathologies and malformations [2,5]. Diametric/circumferential growth of tracheal tubes occurs at stage 14 and correlates with a pulse of secretion that ensures apical membrane growth and secretion of contents into the lumen [4,6]. This secreted luminal material, which includes chitin, chitin-associated proteins and ZP proteins like Pio-Pio and Dumpy, forms an apical extracellular matrix (aECM) that organises into an elastic filament [7,8]. This filament plays an important role in the control of the size and stability of the tracheal tubes [9,10]. Longitudinal/axial growth of tracheal tubes occurs in a continuous manner after diametric expansion. It depends on intrinsic cell properties such as Crumbs-dependant (Crb) apical membrane growth [7,11] and pSrc-dependant polarised cell shape changes [12,13]. In addition, it also depends on extrinsic mechanical forces exerted by the aECM that counteracts and restricts tube elongation. In particular, it was shown that the chitin filament needs to be properly organised and modified by chitin-associated proteins like the chitin deacetylases Vermiform (Verm) and Serpertine (Serp) to prevent excessive growth [14,15]. While we have some hints into how these intrinsic cell properties and the aECM crosstalk and are balanced to control the final tube size [7,16] we still don't have a complete picture of how it works.

Work from different labs has identified roles in tracheal formation of several conserved signalling pathways that regulate development and homeostasis in multicellular organisms. The Epidermal Growth Factor Receptor (EGFR), a Tyrosine Kinase Receptor (RTK), triggers one of these conserved signalling pathways. EGFR is critical during embryonic development controlling important aspects such as migration, differentiation, proliferation, cell growth and survival [17,18]. In addition, miss-regulation of EGFR activity has been associated with cancer and metastasis, and is a target for therapies [19]. EGFR is used in a reiterated manner during the development of different organs in *Drosophila*, such as in the eye (for a review see [20]). Interestingly, EGFR also displays different requirements during tracheal formation, being required at different steps: for invagination [21–24], branching [25,26] and epithelial integrity [27]. Given the relevance of EGFR, it is important to investigate the exact molecular mechanism/s downstream of EGFR that lead to these different outcomes, and understand how they then instruct the cellular changes.

The endocytic pathway uptakes cargoes (membrane proteins, ligands, lipids or extracellular material) and return them back to the membrane or the extracellular space, ensuring their correct recycling or relocalisation. After endocytosis, internalised cargoes arrive to sorting

endosomes, from where they are sorted to the final destination through different specific routes. Membrane cargoes destined to degradation will be targeted to intraluminal vesicles (ILV), which will fill the multivesicular bodies, previous to delivery to the lysosome. Alternatively, cargoes can either undergo retrograde transport to the TransGolgi Network (TGN), accessing the secretory pathway, or they can recycle to the plasma membrane using a direct or an indirect (through the recycling endosome, RE) route [28,29]. Each of these trafficking steps in the endocytic pathway is associated and mediated by different Rab proteins. For instance, while Rab5 mediates internalisation and targeting to early endosomes (EE), Rab4 and Rab35 are associated with a short loop recycling pathway back to the plasma membrane [30,31]. Cargo retrieval to the TGN or to the membrane usually relies on the presence of sorting signals in the cargoes that are recognised by coat complexes. This interaction facilitates the partition of cargoes into different discrete domains in the sorting endosome and the subsequent formation of distinct transport intermediates delivered to the final destination. One of these coat complexes is the Retromer complex, which rescues cargoes from degradation using the retrograde transport or direct delivery to plasma membrane. The Retromer associates with different proteins, like sorting nexins, providing specificity for cargo and trafficking itinerary [32–35]. In addition, the Retromer associates with the WASH complex, an actin-polymerisation promoting complex that generates discrete actin patches that facilitate cargo sorting, Retromer tubule formation and fission [34].

Here we identify a new tracheal requirement of EGFR signalling in regulating tracheal axial growth. Downregulation of the pathway leads to overelongated tubes. We find that EGFR acts on the proper accumulation and subcellular localisation of different factors known to participate in the control of tube length, namely the apical determinant Crb and the chitin deacetylase Serp. A detailed analysis of this regulation shows that these two proteins traffic together in common sorting endosomes, from which they will reach their final destination. Serp was shown to undergo retrograde transport using the Rab9-Retromer complex machinery to recycle to the lumen [36]. Here we find that, in the trachea, Crb also undergoes a complex pattern of recycling. Our data indicates that after Rab5-mediated internalisation, Crb accumulates in Serp/Crb endosomes from which a fraction of the internalised protein is targeted to degradation and another fraction is recycled back to the apical domain, using Rab11 and Retromer/Rab4 routes. Dominant negative mutations of EGFR affect the organisation of the Crb/Serp sorting endosomes, likely affecting the correct trafficking of both cargoes. Our results also suggest that Serp and Crb influence each others' recycling, raising the possibility that they are not only cargo but also direct or indirect regulators of endocytic trafficking. Our analysis identifies EGFR signalling as a hub to coordinate both cell intrinsic properties and extrinsic mechanisms that regulate tube elongation. EGFR is a key signalling pathway that participates in many different processes during normal development and pathogenic conditions, and we suggest that the regulation of the endocytic traffic of specific cargoes could be one of the molecular mechanisms used.

Results

The modulation of EGFR activity controls tube growth

Previous analysis identified roles of the EGFR pathway in regulating invagination and the integrity of the tracheal branches [23,27]. In addition to this requirement, we noticed that at late embryonic stages the size and shape of the tracheal tubes were abnormal when EGFR was downregulated ($EGFR^{DN}$) or constitutively activated ($EGFR^{CA}$) in tracheal cells. In particular, we found a highly convoluted Dorsal Trunk (DT) in $EGFR^{DN}$ mutants and a shorter one in $EGFR^{CA}$ (Fig 1A–1C, S1A–S1C Fig). We quantified this phenotype by measuring the tubes of

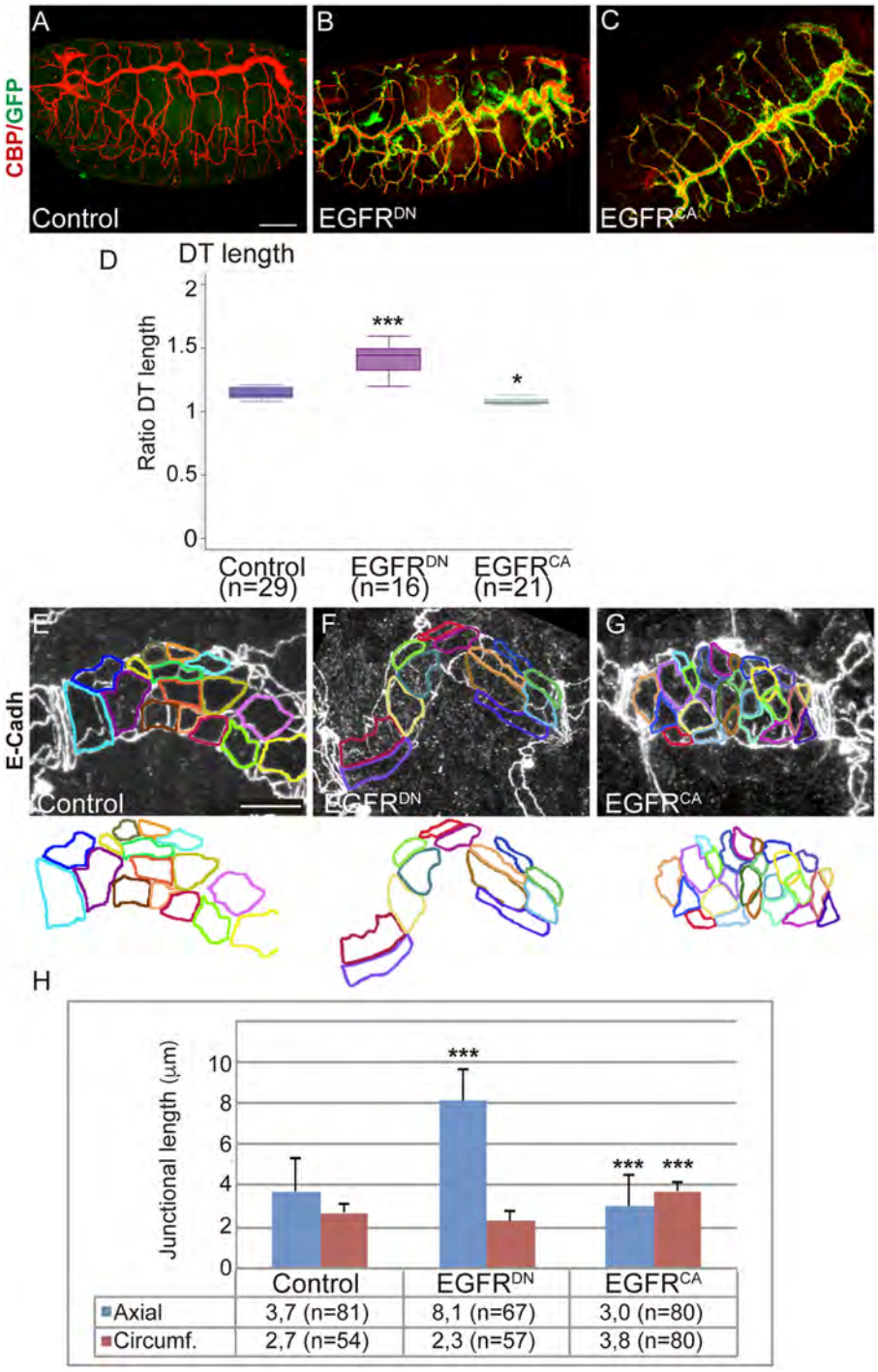

Fig 1. EGFR controls the elongation of the DT. (A-C) Lateral views of stage 16 embryos stained for GFP (green) and CBP (red, lumen).Compare the elongated DT when EGFR is downregulated (*btlGal4-UASsrcGFP-UASEGFR^{DN}*) to control (*UAS-EGFR^{DN}*) and to EGFR overactivation (*btlGal4-UASsrcGFP-UASEGFR^{CA}*). Scale bar 50 μm (D) Box plot for Ratio DT quantification (length of the tube/linear length) of the different experimental conditions of stage 16 embryos. n, number of embryos analysed. The single (*) and triple (***) asterisks represent P<0.05 and P<0.001, respectively, compared with the control by Student's t-test. (E-G) Details of 1 single tracheal metamere of stage 16 embryos stained for E-Cadh to visualise the apical cell shape. The apical outline is highlighted in colours. Note the axial elongation in EGFR^{DN} mutant cells and the circumferential expansion in EGFR^{CA}. Scale bar 7,5 μm (H) Quantification of the length of the axial and circumferential junctions. n, number of cells analysed from 3

different embryos per genotype. Triple asterisks (***) represent a significant difference from the control by Student's t-test (P<0.001).

https://doi.org/10.1371/journal.pgen.1006882.g001

$EGFR^{DN}$ and $EGFR^{CA}$ mutants at stage 16. We measured the length of the DT, of Dorsal Branch 5 (DB5), of Transverse Connective 5 (TC5), and the diameter of the DT in metamere 7–8. The quantification indicated a clear elongation of the DT when the receptor is downregulated (the DT of $EGFR^{DN}$ is 22,6% longer than the sibling control embryos), and a mild reduction (3%) in $EGFR^{CA}$ (Fig 1D), while the embryo length did not change (S1G Fig). This correlated with a subtle diametrical enlargement of the tubes in $EGFR^{CA}$ embryos (S1F Fig). Length of the rest of the branches was unchanged (S1D and S1E Fig), indicating a specific role of the EGFR in regulating the proportion of the multicellular DT.

To characterise the nature of the elongation we analysed cell number to determine if an increase could cause an enlarged DT in $EGFR^{DN}$ mutants. We found comparable numbers of cells in metamere 7–8 DT region in mutants and control (25,5 cells in control embryos, n = 4 embryos, and 26 cells in $EGFR^{DN}$, n = 3 embryos). We then analysed cell shape of DT cells, as it is documented that cell morphology impinges on tube size and shape [12,13]. We observed that cells were elongated along the anterioposterior axis in $EGFR^{DN}$ mutants (Fig 1F). By contrast, cells in $EGFR^{CA}$ embryos were abnormally oriented diametrically (Fig 1G). We measured the length of the axial cell junctions and of the circumferential junctions in control and mutant embryos. We detected a significant bias towards an enlargement of the axial junctions in $EGFR^{DN}$ and a significant bias towards a reduction in $EGFR^{CA}$ (Fig 1H). Modulation of the activity of Breathless, Btl, another RTK with critical roles in tracheal formation (reviewed in [3]), did not affect tube size and cell shape (S1H–S1K Fig), indicating that EGFR effects were specific.

Altoghether these results indicate that the EGFR activity prevents the excessive DT elongation and regulates the morphology of DT cells.

EGFR controls Serp accumulation in the aECM

During embryonic development the lumen of tracheal tubes is filled transiently with an aECM composed of chitin and chitin associated proteins. This matrix plays a key role in controlling tube size and shape [9,10]. The chitin binding protein Serp specifically restricts excessive tube elongation by regulating the structural properties of this chitin filament [14,15]. Hence, in the absence of Serp the tracheal tubes overelongate, showing a phenotype similar to that of the EGFR downregulation. This prompted us to analyse a possible relationship between EGFR and Serp.

Serp is first detected in the cytoplasm of tracheal cells at stage 13. From stage 14, and until stage 16, Serp is secreted and accumulates in the lumen of the tubes (Fig 2A–2C; S2A–S2C Fig, pink arrows), colocalising with the chitin filament [14]. In addition, Serp also accumulates from early stages in the apical membrane of the tracheal cells, lining the lumen (Fig 2B and 2C; S2B and S2C Fig blue arrows). We analysed Serp accumulation when $EGFR^{DN}$ was expressed in the trachea. Serp was detected in the tracheal cells at early stages (Fig 2D) and in the apical membrane (Fig 2E and 2F blue arrowhead), as in the control. However, we detected a decrease of Serp accumulation in the lumen at late stages (Fig 2F). This was especially clear when we expressed $EGFR^{DN}$ in the posterior part of the tracheal system (Fig 2G and 2H).

The expression of $EGFR^{CA}$ has a mild effect on Serp accumulation, which seems to start accumulating in the lumen slightly earlier than in the control, while at later stages this luminal accumulation remains strong (Fig 2I; S2D–S2F Fig).

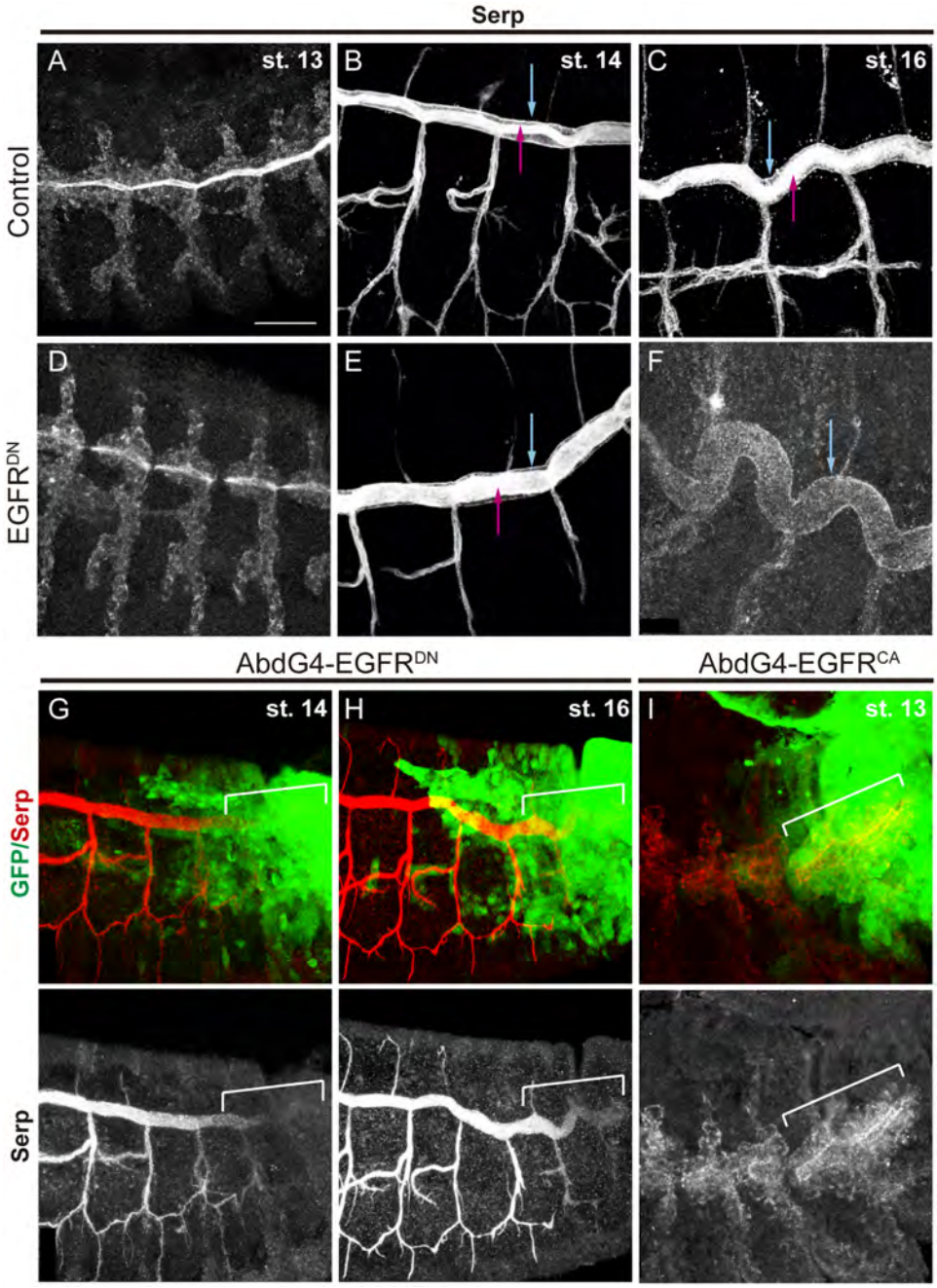

Fig 2. EGFR regulates the luminal accumulation of Serp. (A-F) Lateral views of embryos stained with Serp antibody at the indicated stages. From early stages Serp can be detected in the lumen (pink arrows) and in the apical membrane of tracheal cells (blue arrows). When EGFR is downregulated, Serp accumulation in the lumen decreases strongly with time, but remains detectable in the apical membrane (blue arrow in F). (G-I) Lateral views of embryos at the indicated stages carrying *AbdGal4-UASGFP* stained with Serp antibody (red or white) and GFP (green). Note the difference of Serp luminal accumulation in the Abd domain (marked by a white bracket) in the different EGFR mutant conditions. Scale bar 25 μm.

https://doi.org/10.1371/journal.pgen.1006882.g002

As Serp has been shown to control tube elongation and we find that EGFR controls Serp luminal accumulation, we propose that EGFR controls tube size at least in part by regulating Serp accumulation.

EGFR controls Crb accumulation in the DT

Besides the key role of the aECM, the activity of *crb* also correlates with tube elongation. Overexpression of *crb* [11] or an increased *crb* activity [7] leads to an overproduction of apical membrane that results in overelongated tubes. In line with these reports, we previously showed that Crb levels are downregulated at late stages [37], consistent with the idea that Crb is finely regulated to prevent excessive growth.

Hence, we analysed Crb accumulation in EGFR mutant conditions. In embryos expressing $EGFR^{DN}$ in the trachea, Crb normally localised apically throughout all tracheal development. However, we detected a bright and sharp accumulation of Crb compared to the control (Fig 3A and 3B; S3A–S3H Fig). To verify this observation we quantified the levels of Crb at stage 16 in the DT and normalised the value to the levels in Malphigian Tubules (MT) for each embryo (see Materials and Methods). We found that in $EGFR^{DN}$ embryos the levels of Crb in the trachea are higher than in control sibling embryos (Fig 3D). When we quantified Crb levels in $EGFR^{CA}$ conditions we also detected higher levels of Crb as compared to wild type (Fig 3C and 3D; S3I–S3L Fig).

In spite of the apparently similar phenotype of increased Crb levels in $EGFR^{DN}$ and $EGFR^{CA}$, a closer evaluation indicated differences. In stage 16 control embryos we found Crb sharply localised and defined in the Subapical Region (SAR). The SAR corresponds to the most apicolateral region of the membrane, connecting adjacent epithelial cells (Fig 3H, red). In addition, we also detected some Crb accumulated in the most apical membrane, that we name Apical Free Region (AFR), which is in direct contact with the tracheal lumen (Fig 3H, yellow). Accumulation of Crb in the SAR outlines the cell contour, as it does the accumulation of E-Cadherin (E-Cadh), which accumulates in the Adherens Junctions (AJ) (Fig 3E and 3H, green), positioned just below the SAR. In $EGFR^{DN}$ mutant conditions we found Crb well defined in the SAR (Fig 3F; S3N Fig). In contrast, in $EGFR^{CA}$ mutant conditions, the accumulation of Crb in the SAR appeared blurred and faint, while Crb seemed very conspicuous in the AFR (Fig 3G; S3O Fig). This abnormal accumulation was particularly conspicuous in certain regions of the DT, randomly distributed but more frequent in the posterior region. These regions with more delocalised Crb accumulation in the SAR correlated with cell surfaces elongated circumferentially and with a circumferential enlargement of the tube (arrow in Fig 3G). To evaluate this observation we quantified the ratio of Crb levels in SAR versus AFR in individual cells of control and mutant EGFR conditions. The analysis indicated that while the ratio was not very different from the control in $EGFR^{DN}$ mutants (suggesting that Crb is increased in all apical regions), it was significantly different in $EGFR^{CA}$, with less enrichment of Crb in the SAR (Fig 3L).

Altogether our results indicate that EGFR activity regulates Crb levels in the DT. Because Crb has been shown to promote apical membrane growth at late stages of tracheal formation, we propose that EGFR triggers its function through the regulation of Crb levels. In addition, our results also show that Crb can accumulate in different subcellular domains in the apical membrane of tracheal cells.

Crb subcellular accumulation depends on its endocytic trafficking

Our results suggested that Crb can localise in different apical domains in a regulated manner. We further investigated this subcellular accumulation of Crb at different stages. We used the

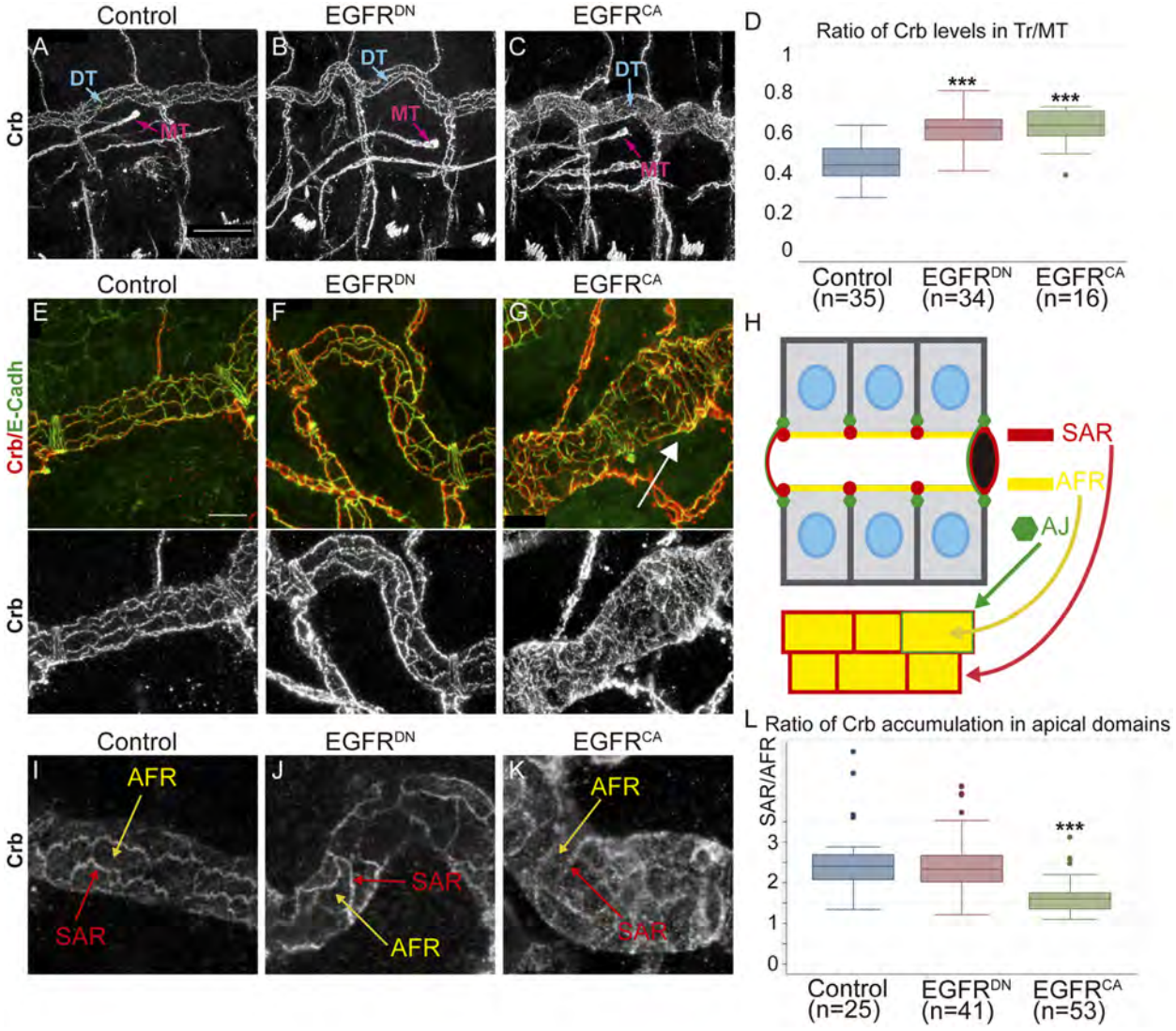

Fig 3. EGFR regulates the accumulation of Crb. (A-C) Lateral views of stage 16 embryos of indicated genotypes stained for Crb. Panels show the DT of 3 tracheal metameres and a MT to compare Crb levels. MT do not express EGFR constructs. Scale Bar 25 μm (D) Quantification of Crb levels. The ratio significantly increases in EGFR mutants, indicating higher levels of Crb in the DT. n, number of embryos analysed. Triple asterisks (***) represent a significant difference from the control by Student's t-test (P<0.001) (E-G) Details of 1 single tracheal metamere of stage 16 embryos of indicated genotypes stained for E-Cadh (green) and Crb (red, white). Scale bar 7,5 μm (H) Diagram representing a fragment of the DT in a sagital and a 2D-planar apical view. The apical region of the tracheal cells faces the lumen of the tube (black hole). Crb accumulates in the apical free region (AFR, yellow), in direct contact with the lumen, and in the Subapical region (SAR, red), contacting two adjacent cells. E-Cadh accumulates basal to the SAR in AJs (green) (I-K) Details of 1 single tracheal metamere of stage 16 embryos of indicated genotypes stained for Crb. Panels show an example used to evaluate Crb subcellular accumulation in the AFR (yellow arrows) and the SAR (red arrows). (L) Quantification of the ratio of Crb accumulation in apical region. Note that when EGFR is overactivated Crb enrichment in the SAR is decreased. n, number of DT cells analysed from 5 control, 9 $EGFR^{DN}$ and 11 $EGFR^{CA}$ embryos. Triple asterisks (***) represent a significant difference from the control by Student's t-test (P<0.001).

https://doi.org/10.1371/journal.pgen.1006882.g003

pattern of E-Cadh, which reveals the cell outline homogeneously throughout all tracheal development (Figs 3H and 4A–4E), to compare to Crb. We observed that at stages 13–14 Crb is mainly localised in the AFR region, with not much enrichment in the SAR (Fig 4A and 4B). However, as development proceeds we detected a progressive enrichment of Crb in the SAR (Fig 4C and 4D; S1 Video). By st 16–17 Crb appears neatly accumulated and can be perfectly

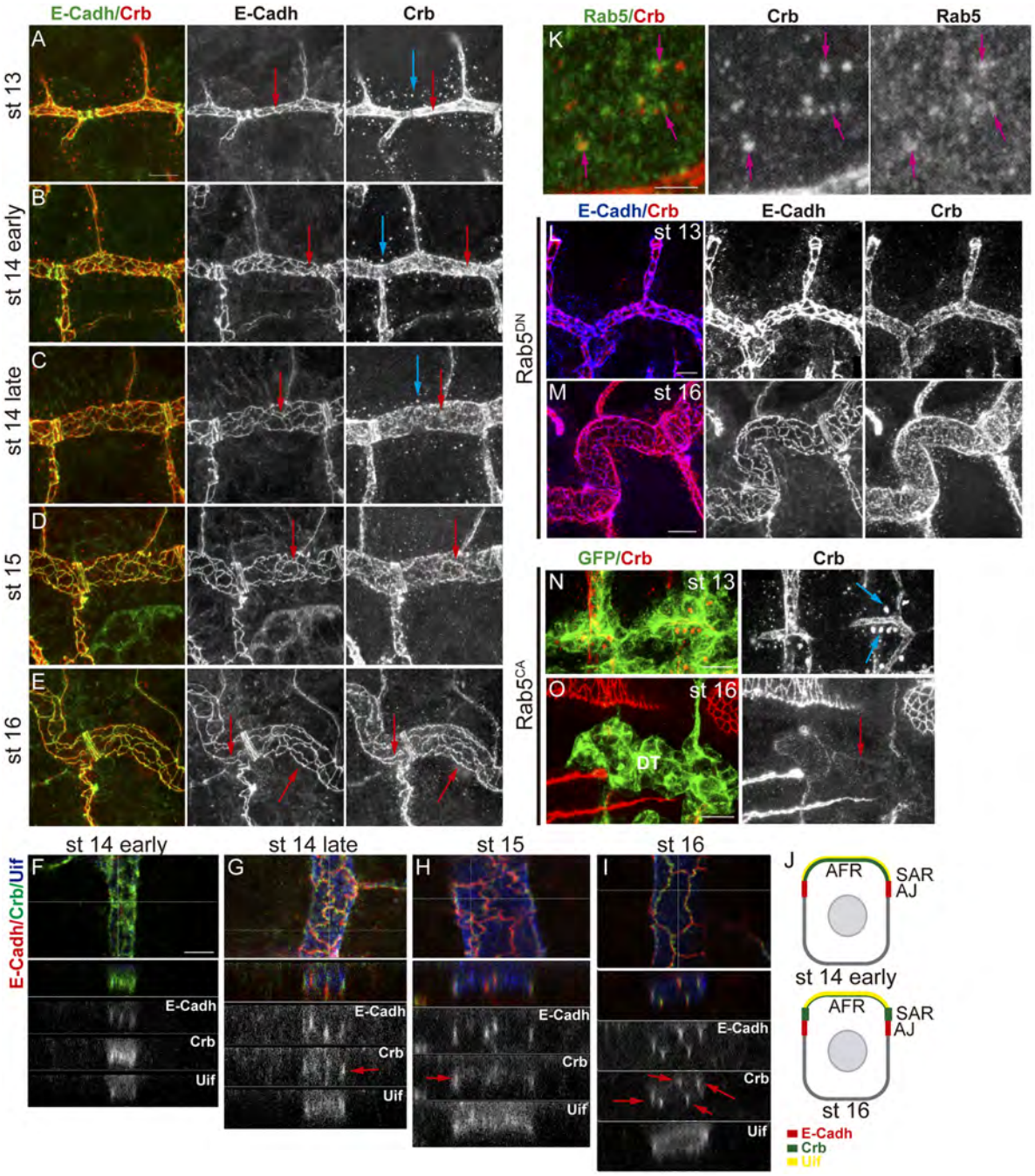

Fig 4. Subcellular accumulation of Crb during tracheal development. (A-E) Lateral views of wild type embryos at indicated stages stained for E-Cadh (green, white) and Crb (red, white), showing 1–2 tracheal metameres. At early stages, while E-Cadh is already detectable in the junctional area (red arrows), Crb mostly accumulates in the AFR. Crb accumulation becomes enriched in the SAR as development proceeds (E). At early stages, abundant vesicles containing Crb are detected (blue arrows), and they decrease as development proceeds. Scale bar 7,5 μm (F-I) Z-reconstructions of the DT of embryos at the indicated stages stained for E-Cadh (red, white), Crb (green, white) and Uif (blue, white). Horizontal line in the upper panel indicates the position of the Z-reconstruction. E-Cadh always localise to the AJs, in the apicolateral membrane, visualised as lines spanning the AJs. Uif localises in the most apical membrane. Note the evolution of Crb pattern that becomes more enriched in the SAR (red arrows, partially colocalising with E-Cadh) as development proceeds. Scale bar 5 μm (J) Diagram representing a Z-section of a DT cell at early and late stages. The apical region of the tracheal cells facing the lumen (AFR) accumulates Uif (yellow). E-Cadh accumulates in AJs (red). Crb (green) first accumulates more in the Uif region and later becomes enriched in the SAR. (K) Wild type embryo stained with

Rab5 (green, white) and Crb (red, white) antibodies. Many Crb vesicles co-stain with Rab5 (pink arrows). Scale bar 2,5 μm (L,M) Lateral views of embryos with downregulated Rab5 activity at the indicated stages stained for E-Cadh (blue, white) and Crb (red, white) showing 1–2 tracheal metameres. At early stages Crb vesicles are absent (G), and at late stages (H) Crb is not enriched in the SAR. Scale bar G 5 μm, H 7,5 μm (N,O) Lateral views of embryos with activated Rab5 activity at the indicated stages stained for GFP (green) and Crb (red, white) showing 2 tracheal metameres. At early stages huge Crb vesicles are detected (blue arrows in I), but at late stages (J) Crb is almost absent mainly from the DT region. Scale bar I 7,5 μm, J 10 μm.

https://doi.org/10.1371/journal.pgen.1006882.g004

distinguished in the SAR (Fig 4E). This evolution of Crb subcellular accumulation in the apical region, which can also be observed in Z-sections (Fig 4F–4J), correlated with a stage specific accumulation of Crb in intracellular vesicles. These Crb vesicles were abundant and clearly detected at stages 13–14 (Fig 4A, 4B and 4C blue arrows), and decreased by late st 14 or st 15, being less frequent at st 16 (Fig 4D and 4E). The inverse correlation between the presence of Crb vesicles prior to its enrichment in the SAR raised the possibility that these two events are related.

We investigated the nature of these vesicles. Diameter quantification indicated that they are around 0,5–0,6 μm (n = 21 vesicles, from 3 different embryos), consistent with being endosomes [38]. To determine their nature we double stained for different Rab proteins, which identify different intracellular trafficking vesicles [30,31]. Rab5 mediates traffic from the plasma membrane to EE and serves as marker for EE. We found that the Crb vesicles are rich in Rab5, further suggesting that these are endosomes (Fig 4K). To confirm this we expressed a dominant negative form of Rab5 in the trachea to block endocytosis. We found that the 0,5–0,6 μm Crb vesicles typically found at stages 13–14 disappeared (Fig 4L; S4A Fig). Interestingly, we also found that when endocytosis was blocked, Crb remained high in the AFR and did not become enriched in the SAR at late stages (Fig 4M), suggesting a dynamic recycling of Crb at different apical domains dependent on internalisation. The expression of a constitutively active Rab5 protein induced the formation of enormous Crb endosomes at early stages (Fig 4N). At later stages, Crb was almost absent from the trachea, particularly from the DT (Fig 4O), suggesting that most Crb accumulating in the big endosomes is targeted to degradation.

Altogether the results indicate that Crb undergoes a highly dynamic pattern of subcellular localisation throughout tracheal development, refining at the SAR at late stages. This pattern requires Rab5-dependent endocytosis.

Crb apical localisation and recycling pathways

Our results suggested that during tracheal development Crb is endocytosed and likely recycled back to the SAR. It has been shown in other tissues that different endosomal sorting pathways control Crb trafficking regulating its activity. While a fraction of the pool of internalised Crb protein undergoes degradation [8], Crb is also recycled back to the apical membrane through Rab11/ [39] Exo84 [40] or the Retromer complex [41,42] dependent pathways. We asked whether any of these pathways is required for Crb trafficking and recycling during tracheal development.

We analysed the contribution of the RE-Rab11 dependent trafficking on Crb accumulation. We found that the downregulation of Rab11 activity (expressing a dominant negative construct in the trachea) produced defects in Crb accumulation. At early stages we did not detect defects and Crb was enriched in the AFR and found in endosomes as in the wild type (S4B and S4C Fig). However, at late stages Crb was not specially enriched in the SAR as much as it is in normal conditions, whereas E-Cadh was still detected in the junctional area (Fig 5A and 5B). We quantified the ratio of Crb accumulation in the SAR versus the AFR and found it to be significantly different from the control, being biased towards a depletion in the SAR (Fig 5C).

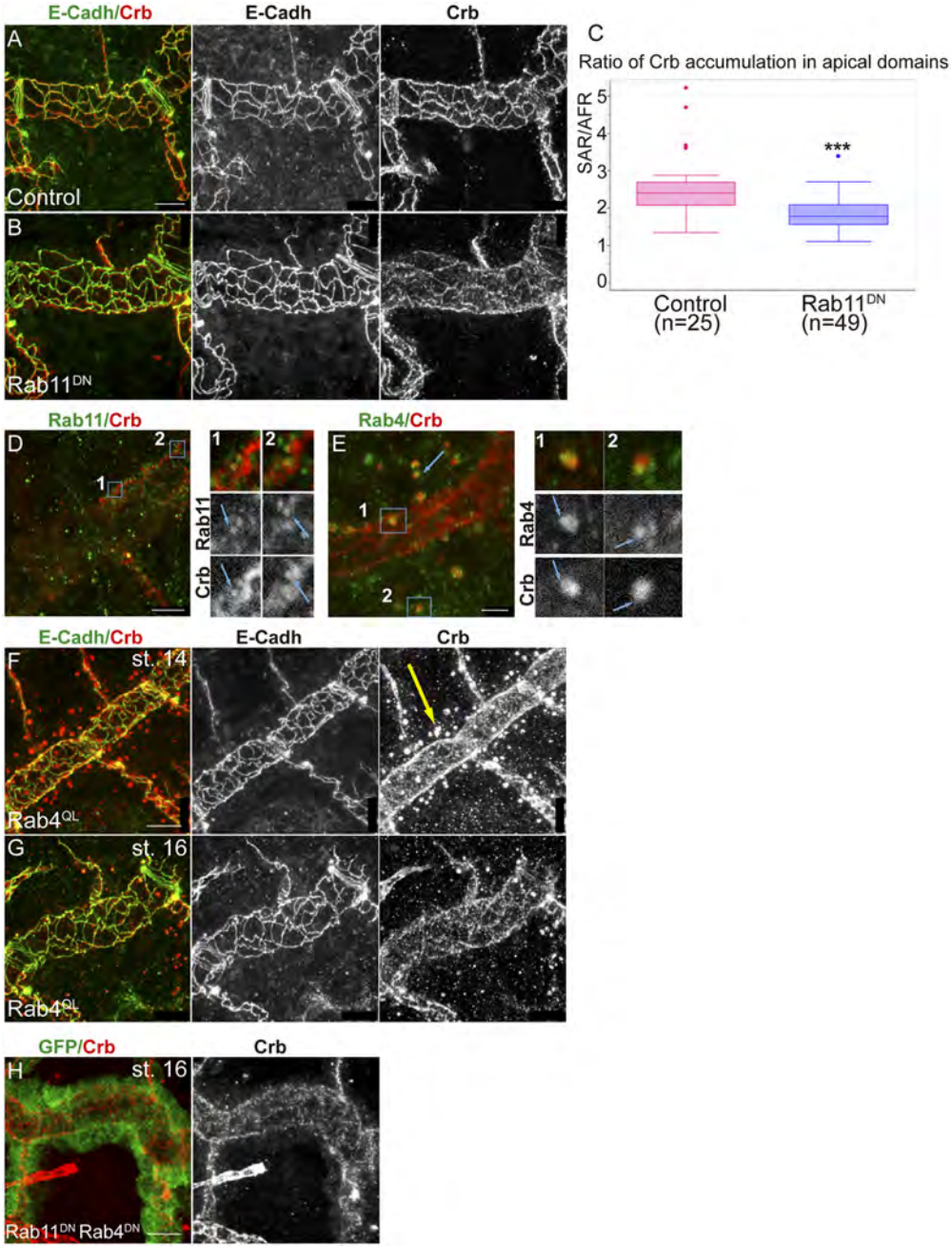

Fig 5. Trafficking of Crb through the endocytic pathway. (A,B) Lateral views of stage 16 embryos stained for Crb (red, white) and E-Cadh (green, white) showing 1 tracheal metamere. Note the pattern of accumulation of Crb when Rab11 is downregulated in the trachea. Scale bars 7,5 μm (C) Quantification of the ratio of accumulation of Crb in different apical regions. When Rab11 is downregulated Crb enrichment in the SAR is decreased. n, number of DT cells analysed from 5 control and 11 $Rab11^{DN}$ embryos. Triple asterisks (***) represent a significant difference from the control by Student's t-test ($P<0.001$) (D,E) Single confocal sections to show the colocalisation of Crb and Rab11 (using anti-Rab11, D) or Rab4 (using $Rab4^{EYFP}$, E). Panels marked with 1 and 2 correspond to the insets shown in D and E. (D) Note the presence of small Crb vesicles, in contact with the junctional area, marked with Rab11 at late stages (stage 15, blue arrows in 1 and 2). (E) Most endosomes present at early stages containing Crb are marked with Rab4. Rab4 and Crb colocalise in regions of these endosomes (blue arrows in 1 and 2). Scale bar D 5 μm, E 2,5 μm (F-H) Lateral views of embryos expressing the indicated transgenes in the trachea stained for Crb (red, white) and E-Cadh (green, white) (except H, stained for GFP, green), showing 1–2 tracheal metameres. Note that Crb accumulates in big

endosomes at early stages when Rab4 is constitutively activated (yellow arrow in F), and decreases at later stages (G) or when both Rab11 and Rab4 are downregulated (H). Scale bars 7,5 μm.

https://doi.org/10.1371/journal.pgen.1006882.g005

This result suggested a role for the RE route for Crb recycling in the trachea. In agreement with this we detected Rab11-REs containing Crb. These were not the endosomes detected at early stages, as they were smaller (0,28 μm, n = 6 recycling endosomes from 2 different embryos), detected at later stages, and typically close to cell junctions (Fig 5D). Altogether these results are consistent with a role of Rab11 in recycling Crb, particularly to the SAR junctional area.

To further characterise the abundant Crb endosomes present at early stages we used tagged Rab proteins. We found that these endosomes were rich in Rab4. A close look showed that Rab4-YFP-tagged protein decorated the Crb endosomes (Fig 5E, S2 Video), suggesting that a pool of Crb protein accumulates in the lumen of the endosome, likely to be directed to degradation. We also detected some puncta of Crb/Rab4 colocalisation, suggesting a Rab4-mediated recycling (Fig 5E1 and 5E2). It has been shown that Rab4 participates in a short loop endocytic pathway to recycle cargoes back to the membrane [30], and that it can associate with Retromer tubules [43]. The Retromer complex has been shown to participate in Crb recycling [41,42]. In light of this evidence, our results suggested that Crb could recycle using a Rab4/Retromer-dependent pathway. In agreement with this hypothesis we found that when Rab4 is constitutively active, bigger vesicles containing Crb are detected, and they are present until late embryonic stages (Fig 5F, yellow arrow). This correlates with a poorer enrichment of Crb in the SAR at late stages (Fig 5G), suggesting a hypothetical route of Crb recycling mainly to the AFR involving Rab4/Retromer. Interestingly, in $EGFR^{DN}$ mutants we detected an advanced enrichment of Crb in the SAR as compared to control (S5 Fig). A dominant negative form of Rab4 expressed in the trachea did not produce clear defects (S4D and S4F Fig).

Altogether our results are consistent with a model where, after Rab5-mediated internalisation, a pool of Crb would be retrieved from the degradation pathway to undertake different recycling routes. One of them would involve the Rab4/Retromer complex and would ensure the fast recycling directly to the apical, preferentially the AFR. A slower/longer recycling route, involving Rab11-RE, would traffic Crb from the endosome to the apical membrane, mainly in the SAR. In agreement with a role of both routes in Crb recycling we found that downregulating both of them leads to a strong decrease of Crb in apical regions, particularly in the DT (Fig 5H).

Serp and Crb localise in common sorting endosomes

Serp has been shown to undergo a specific recycling that maintains its luminal content, which is necessary to restrict tube elongation. Serp recycling requires Rab9, the Retromer complex and WASH to mediate its retrograde trafficking to the lumen through the TGN [36]. Similarly, here we describe that Crb trafficking is also regulated to maintain its apical localisation. We analysed the relative subcellular localisation of the two proteins in tracheal cells.

We found very often that Crb and Serp partially co-localise, indicating that they localise in a common endosome. This common localisation increased as development proceeds and reached a peak at stage 14 (Fig 6A and 6B). Quantifications in embryos at stage 14 indicated that 66% of vesicles contained both Crb and Serp, 15% contained only Crb and 18% contained only Serp ($Crb/Serp_e$, Crb_e and $Serp_e$, respectively, in Fig 6A. n = 194 vesicles from 5 different embryos; S6A–6C' and S6D Fig). From stage 15 onwards Crb endosomes decreased or became smaller while Serp endosomes were maintained (Fig 6C). As mentioned, Serp and Crb do not

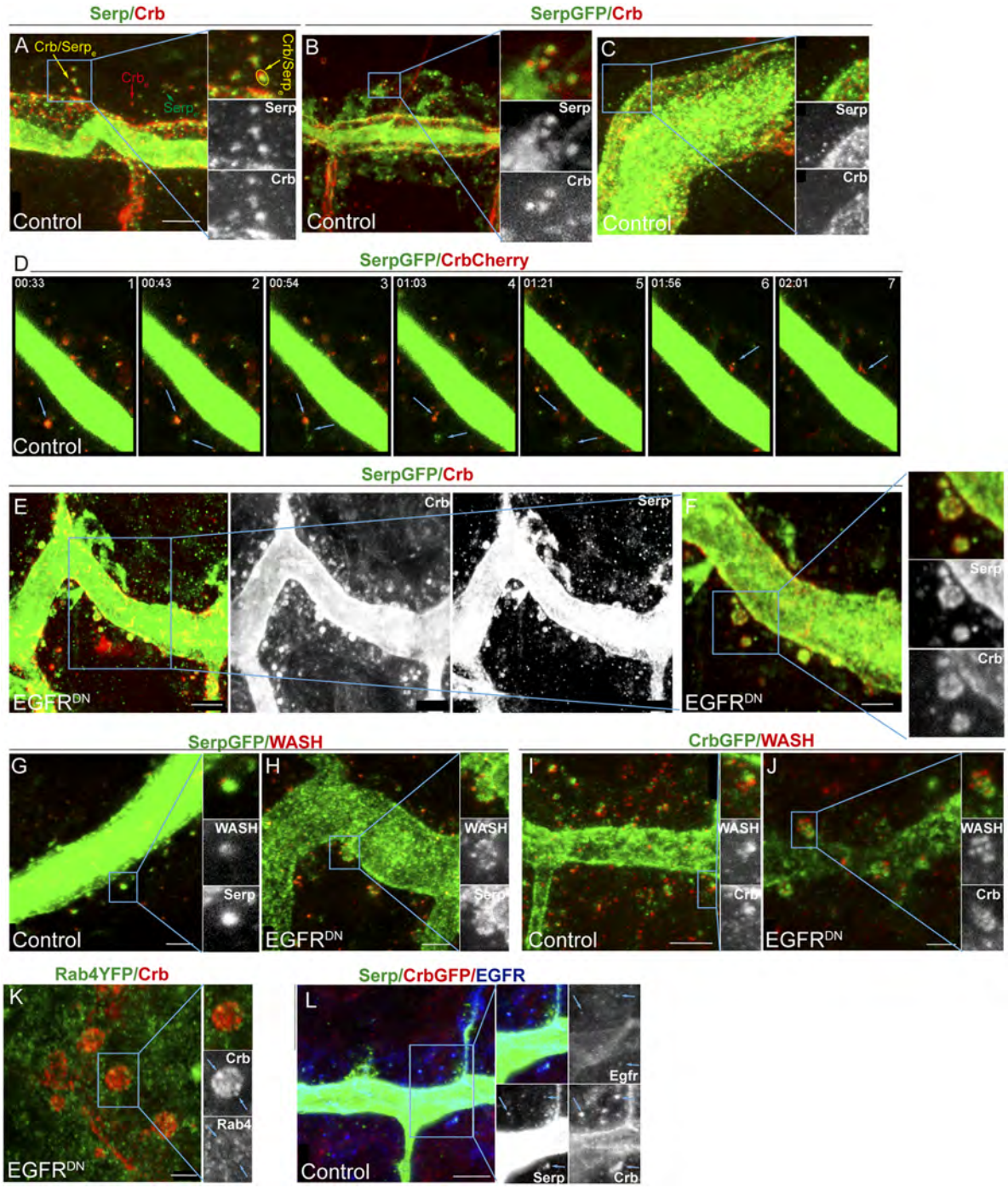

Fig 6. Crb and Serp accumulate in common endosomes, which require EGFR activity. (A-C) Lateral views of WT (A) or *btlGal4-UASSerp-CBD-GFP* (B,C) embryos stained for Crb (red, white) and Serp/GFP (green, white). At stage 14 (A,B) many endosomes accumulate both Serp and Crb (Crb/$Serp_e$), but endosomes containing only Serp or Crb ($Serp_e$ and Crb_e, respectively) are also found. In Crb/$Serp_e$ the two proteins are sorted into different endosomal domains (insets) but they colocalise in a region. At stage 16 (C) Serp endosomes are still abundant. Scale bar 5 μm (D) Time-lapse images of tracheal cells carrying *btlGal4-UASSerp-CBD-GFP* and Crb^{Cherry}. Crb/Serp endosomes are highly dynamic. Bottom arrows point to an endosome from which Serp is sorted, joining another Serp containing vesicle (2–5). A fraction of Crb protein is also sorted and the rest fades (4–5). Upper arrows in 6–7 point to a Crb tubulation. (E-F) Lateral views of stage 14 embryos carrying *btlGal4-UASSerp-CBD-GFP* and $EGFR^{DN}$ stained for GFP (green, white) and Crb (red, white). Endosomes are bigger and Serp and Crb are abnormally localised, missorted and intermingled.

The cargoes often accumulate at the endosome surface (insets in F). Scale bar E 5 μm, F 2,5 μm (G-J) Lateral views of stage 14 embryos carrying *btlGal4-UASSerp-CBD-GFP* (G,H) or Crb^{GFP} (I,J) stained for GFP (green, white) and WASH (red, white). In control embryos typically one or two punctae are detected per Crb/Serp endosome. In $EGFR^{DN}$ embryos WASH accumulates in more punctae forming a rosette around the endosome. Scale bar G,H,J 2,5 μm, I 5μm (K) Lateral view of a stage 14 embryo expressing $EGFR^{DN}$ in the trachea and carrying $Rab4^{EYFP}$ to visualise Rab4 accumulation. Rab4 is less nicely accumulated and frequent Crb/Rab4 punctae are detected (arrows in inset). Scale bar 2,5 μm (L) Lateral view of a stage 14 embryo carrying Crb^{GFP} and stained for GFP (red, white), Serp (green, white) and EGFR (blue, white). EGFR itself is found very often in Serp/Crb containing endosomes (blue arrows). Scale bar 5μm.

https://doi.org/10.1371/journal.pgen.1006882.g006

perfectly colocalise but rather they seem sorted into different regions of a common endosome (insets in Fig 6A and 6B and yellow arrow in A; S6A'–S6C' and S6D Fig). Image analysis and co-localisation quantification indicated around a 60% of co-localisation of Serp/Crb signal in common sorting endosomes (n = 118 endosomes, from 5 different embryos). This result indicates that Crb and Serp are partitioned into different discrete domains in a common sorting endosome.

Live imaging using Serp-GFP and Crb^{Cherry} showed a highly dynamic pattern of vesicle trafficking (Fig 6D; S6G–S6I Fig and S3 and S4 Videos). We could clearly detect endosomes containing both Crb and Serp, very often sorted in different regions. We could observe examples where Crb/Serp endosomes fused or evolved rendering Serp and Crb distinct vesicles (arrows in Fig 6D1–6D4), examples where Crb endosomes seemed to disapear (likely reflecting protein degradation, arrows in Fig 6D4 and 6D5), or examples where Crb or Serp localised in (distinct) tubulations or smaller vesicles (likely reflecting retrieval for recycling, arrow in Fig 6D7).

These results show that Crb and Serp traffic together in common sorting endosomes and are sorted into different domains, consistent with the hypothesis that they use different retrieval pathways to recycle to their final destination.

EGFR is required for the proper organisation of Serp-Crb endosomes

Because EGFR regulates both Crb apical localisation and Serp luminal accumulation, and because both Crb and Serp accumulation depend on their recycling and localise in common sorting endosomes, we investigated the requirement of EGFR in their trafficking.

In $EGFR^{DN}$ conditions Crb/Serp endosomes were still found, indicating that internalisation was not impaired. This was confirmed by a live endocytosis assay [4] that showed presence of internalised rhodamine-labelled dextran in control and EGFR mutant conditions (S7 Fig). However, Crb/Serp endosomes displayed an abnormal aspect (Fig 6E and 6F; S6E and S6F Fig). Endosomes were bigger in general, measuring around 1,3 μm in diametre (n = 27 endosomes, from 6 different embryos). In the control Crb and Serp normally accumulate in a well-defined region in the endosome, usually differently sorted (Fig 6A and 6B). In $EGFR^{DN}$ conditions their accumulation was more diffuse and both proteins were found intermingled, although generally still differently sorted. Crb and Serp were often detected at the surface of the endosome, rather than in the lumen (Fig 6E and 6F), suggesting that more protein is retrieved from the degradation pathway. This would be consistent with the fact that we detect higher levels of Crb (Fig 3D). Hence, our results show that impairing EGFR activity results in the missorting of both cargoes, consistent with the hypothesis that EGFR is required for the proper sorting of cargoes, particularly Crb and Serp, in endosomal membranes.

The Retromer plays a key role in Serp and Crb recycling. We asked whether EGFR somehow controls Retromer activity. The Retromer recruits the actin nucleator WASH complex, which generates discrete actin patches in the endosomes. We analysed WASH accumulation with respect Crb and Serp in normal and EGFR mutant conditions. We found one or

occasionally two WASH punctae partially colocalising with Serp and Crb in wild type embryos (Fig 6G and 6I). In $EGFR^{DN}$ mutant conditions the pattern of WASH accumulation was clearly different. We detected many more small punctae of WASH in the endosomes, often forming a rosette, with Serp or Crb abnormally sorted and intermingled (Fig 6H and 6J). This suggests a role for the EGFR in regulating WASH dynamics on the endosome. We also analysed the accumulation of other markers of the Serp/Crb endosomes, like Rab4. We found that Rab4 was not nicely and strongly decorating Crb endosomes as in the control (Fig 5E). Instead Rab4 accumulation was weaker and diffuse, and we could detect punctae of Crb/Rab4 colocalisation more frequently than in control embryos (Fig 6K). Altogether our results indicate that during tracheal development, EGFR is required to organise the sorting endosome containing Serp and Crb, likely regulating their proper sorting.

Interestingly, we found that EGFR itself also traffics in the same sorting endosomes containing Serp and Crb (Fig 6L, S6J–S6L Fig). Image analysis indicated a 40–50% of co-localisation of EGFR/Serp/Crb or EGFR/Crb or EGFR/Serp signal in common endosomes (n = 109 endosomes, from 7 different embryos). This result raises the possibility that EGFR directly influences the traffic of endosomes in which the receptor is loaded.

Serp and Crb recycling mutually influence each other

Because Crb and Serp localise in common sorting endosomes, and because their recycling is regulated by common mechanisms, we wondered whether the recycling of one of the cargoes could influence the other.

In *crb* mutants apico-basal polarity is strongly affected, but a rudimentary tracheal system is still formed [44]. We analysed Serp accumulation in *crb* null mutants. *crb* mutants still deposit chitin (Fig 7A yellow arrow), indicating the capacity of these cells to organise in a tube, to localise apically the machinery for chitin deposition, and to secrete material into a luminal compartment. Serp accumulation in the luminal spaces was largely decreased or absent, and only occasionally we found Serp colocalising with CBP (Fig 7A blue arrow). Furthermore, when we overexpressed *crb* in the tracheal tissue we detected the expected apicalisation of the membranes, with accumulation of CBP around the cells and the formation of an abnormal lumen compartment. This indicates that all the machinery necessary to produce chitin is able to localise at the membrane, even if it is mislocalised. Strikingly, Serp was completely absent in the lumen of these embryos (Fig 7B). These results suggest that Crb regulates the accumulation of Serp in a specific manner.

In *serp* mutants Crb is found in apparently normal endosomes at stage 13–14. At later stages Crb is also found enriched in the SAR, however, this enrichment is slightly less conspicous as compared to the sibling control embryos (Fig 7C and 7D). This result suggested a possible role for *serp* in Crb recycling. To further explore this possibility we analysed Crb accumulation in the absence of *serp* in sensitised conditions, in particular in EGFR downregulation conditions. We found a strong phenotype, with the presence of large Crb-containing endosomes at early and late stages (st 14 and 16) (Fig 7E and 7F yellow arrows). Enrichment of Crb in the apical domain was hardly detected at late stages (Fig 7F blue arrowhead). These results raise the possibility that Serp plays a direct or indirect role in endocytic trafficking affecting Crb recycling.

In summary, our results would be consistent with the hypothesis that Serp and Crb are endocytic cargoes that in turn also regulate (directly or indirectly) the endocytic trafficking.

Discussion

In this work we identify a novel role for EGFR in the regulation of the length of the tracheal tubes. Downregulation of EGFR leads to the overelongation of the main tracheal trunk. We

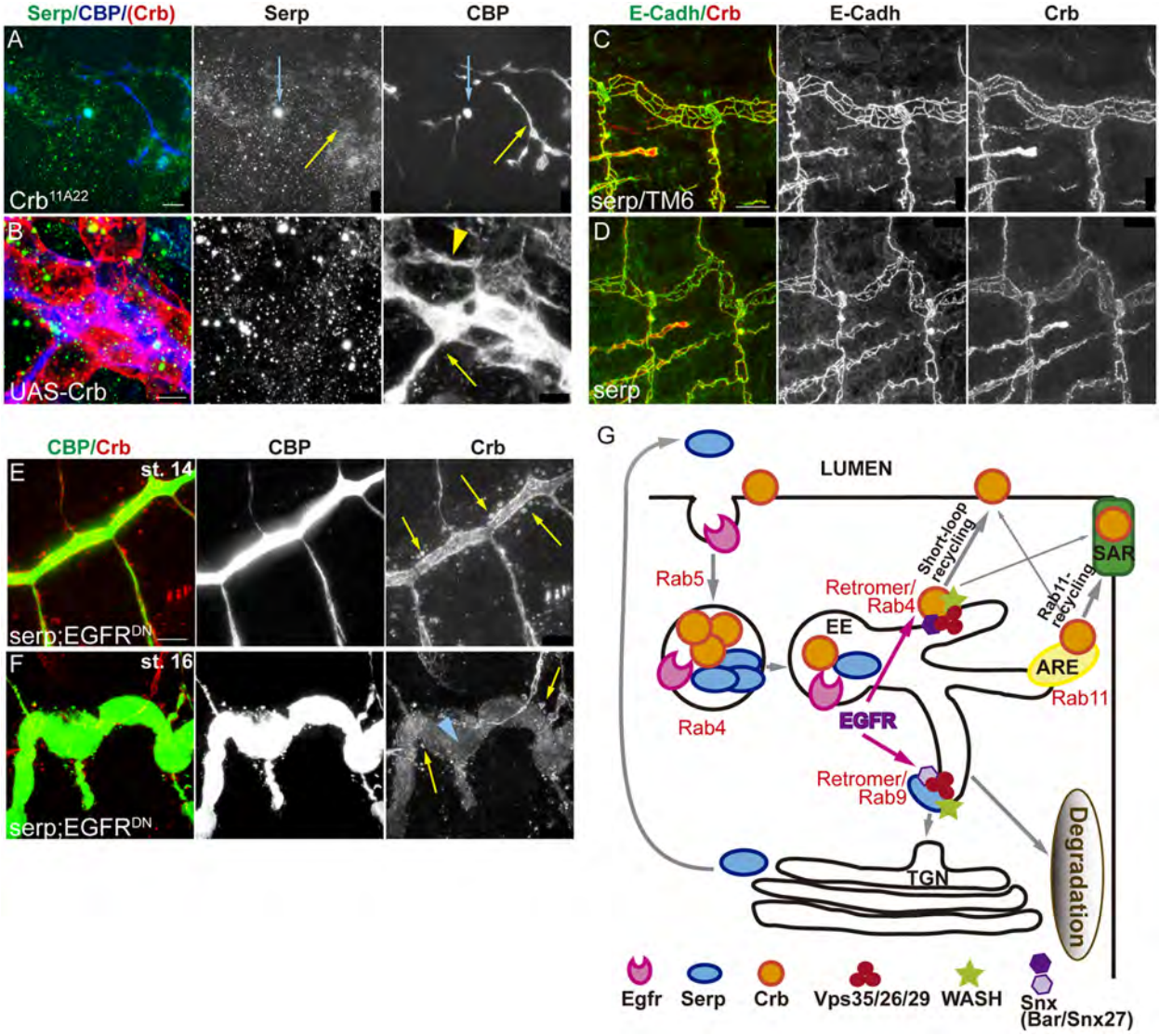

Fig 7. Crb and Serp require each other for proper recycling. (A,B) Lateral views of embryos lacking (A) or overexpressing *crb* (B). (A) In spite of *crb* absence, chitin (visualised with CBP) is deposited in the malformed lumen (yellow arrow), but Serp is only occasionally detected there (blue arrow). (B) When *crb* is overexpressed in trachea it accumulates around the cells, indicating apicalisation. Chitin is deposited extracellularly, in the apical (yellow arrow) and the basal surfaces (yellow arrowhead) but Serp is completely absent. Scale bar A 10 μm, B 5μm (C,D) Lateral views showing 2 tracheal metameres of stage 16 embryos stained for Crb (red, white) and E-Cadh (green, white). Note that Crb staining in the SAR is slightly compromised when *serp* is absent (D), compared to control (C). Scale bar C 10 μm (E,F) Lateral views showing a portion of the DT when *serp* is absent and *EGFR* is downregulated. Note the presence of large Crb vesicles (yellow arrows) at all stages and the depletion of Crb in the apical domain of late embryos (blue arrowhead). Scale bar E 7,5 μm (G) Model. Crb and Serp are endocytosed and arrive to common endosomes, sorted into different domains. A fraction of Crb and Serp internalised protein will be retrieved from the degradation pathway and will be recycled back to the membrane (Crb) or to the lumen (Serp). Serp undergoes retrograde transport using the Rab9-Retromer. Crb uses the Rab11-RE and the Rab4/Retromer routes to recycle back to the apical membrane. EGFR is required for the organisation of Serp/Crb endosomes, promoting the recycling of both cargoes to their final destination ensuring proper tube elongation.

https://doi.org/10.1371/journal.pgen.1006882.g007

find that EGFR regulates the accumulation and subcellular localisation of different factors known to participate in the control of tube length, in particular the apical determinant Crb and the chitin deacetylase Serp. Our results show that these two proteins traffic together in common sorting endosomes. EGFR affects the organisation of these Crb/Serp endosomes,

likely impairing the correct delivery of both cargoes to their final destination. As a consequence, tube length is abnormally attained. Our results also show that these two cargoes are partitioned into different discrete domains within this common sorting endosome, consistent with the hypothesis that they use different retrieval pathways to recycle. In agreement with this it was shown that Serp undergoes retrograde transport using the Rab9-Retromer complex machinery to recycle to the lumen [36]. Here we find that, in the trachea, Crb also undergoes a complex pattern of recycling. Crb is first internalised in a temporal regulated manner. After internalisation part of the Crb pool is retrieved from the degradation pathway and would undertake different recycling routes (i.e the Rab4/Retromer short loop and the Rab11-RE route) to return to the membrane. This recycling pattern correlates with a temporally regulated localisation of Crb in different subcellular domains in the apical membrane: before and during internalisation Crb is high in the AFR, while internalisation promotes an enrichment of Crb the SAR (Model Fig 7G). Hence, our work identifies EGFR signalling as a hub to coordinate both cell intrinsic properties (Crb-mediated apical membrane growth) and extrinsic mechanisms (Serp modification of the aECM) that regulate tube elongation. We suggest that the regulation of the endocytic traffic of specific cargoes could be one of the molecular mechanisms downstream of the EGFR signal, and therefore could regulate different morphogenetic and pathological EGFR-mediated events.

A role for EGFR in endocytic traffic regulation

We find that EGFR itself can also localise in the endosomes containing Crb and Serp. It has been already shown that upon activation, EGFR is internalised and that its activity is regulated by endocytic traffic. The endocytic trafficking of EGFR ensures, on the one hand, the downregulation of the signal by targeting the receptor to degradation, or its recycling back to the plasma membrane. The decision between being degraded or recycled depends, in turn, on signalling events targeting EGFR itself (for reviews see [45,46]). But besides being a cargo, the endocytic trafficking of EGFR can also serve as a platform for signalling. As such, EGFR could activate in the endosome downstream signalling cascades that reach the nucleus and regulate transcription (e.g. the MAPK pathway), or it could approach EGFR signalling to particular downstream effectors, residing in specific cellular organelles, regulating cytoplasmic targets [47,48].

Our results are consistent with a model where EGFR would activate signalling and regulate cytoplasmic targets, perhaps through its main signalling cascade, the ERK/MAPKinase pathway. EGFR signalling targets could be in the endosome itself [49]. Actually, it was shown that EGFR can regulate Rab5 activity through the regulation of Rab5 GAP and GEF proteins [50,51], and that ERK can regulate plasma membrane clathrin-independent recycling [52]. In addition, EGFR can phosphorylate Clathrin in a Src-mediated mechanism regulating its redistribution [53], can also phosphorylate the endocytic adaptor protein Eps15 [54,55], and can induce E-Cadh macropinocytosis [56]. Interestingly, myopic was shown to regulate EGFR signalling [57] and to interact with Rab4 [58]. Furthermore, Rac1, which can be a target of Receptor Tyrosine Kinases [59], has been shown to regulate Serp and Crb in the trachea [60]. In summary, while EGFR has been extensively analysed as an endocytic cargo, some reports also point to more direct effects of EGFR signalling upon the endocytic machinery, and therefore our analysis identifies a good system to further explore this mechanism. More work is required to identify the target of EGFR regulating endosomal trafficking in the trachea, however, our results suggest that EGFR could directly or indirectly target WASH-promoted actin organisation or the Retromer complex, which is required for WASH recruitment.

Tube elongation

The elongation of the tracheal tubes depends largely on the proper organisation of an aECM, which acts as a viscoelastic matrix that restricts excessive elongation [7,14,15]. On the other hand, Crb-dependant apical membrane growth [7,11] and pSrc-regulated cell shape changes [12,13] also control tube length. How the aECM instructs the underlying tracheal epithelium to adjust its apical enlargement is not fully understood, although mechanical or signalling events, or a combination of both, may be required. Nevertheless, it is likely that the cell intrinsic mechanisms (i.e. apical membrane expansion and/or cell shape changes) and cell extrinsic mechanisms (i.e. aECM) are coordinated rather than being two independent mechanisms controlling the same morphogenetic event. Indeed, some reports propose that the aECM may be anchored to the apical cell membrane through connecting proteins such as ZP proteins [7,8,61–63]. In such case, it still remains to be explained if these proteins transduce the signal to regulate Crb-mediated apical membrane growth.

Our observation that one single signalling pathway, EGFR, controls both intrinsic and extrinsic tube elongation mechanisms provides an explanation to further understand the coordination of these mechanisms. Furthermore, our results suggest that the trafficking of Crb and Serp may influence each other, adding an extra layer of coordination to the system. Actually, a role for Crb in regulating endocytic trafficking has been already proposed [64]. Indeed, several reports indicate that polarity proteins are both cargoes and regulators of endocytic recycling [65]. Crb seems to control Serp trafficking in the trachea, and accordingly we find that when overexpressed, Serp is lost from the lumen, maybe because the excess of Crb saturates all Retromer complex precluding Serp recycling. In turn, Serp can also influence Crb trafficking, particularly in sensitised backgrounds. While Serp has been proposed to act as a chitin deacetylase [14,15], it cannot be ruled out that it also plays a role in endocytic trafficking. Further experiments are required to determine whether Crb and Serp exert a direct instructive role by controlling specific endocytic regulator/s, or an indirect one by altering the trafficking homeostasis, by competing for common trafficking factors or by stimulating compensatory trafficking pathways.

The interdependence of different tube length regulators may mask the exact contribution of each one to tube enlargement. Hence, a clear correlation of tube size with excess or absence of different tube length regulators may be difficult to be established. In agreement with this it has been shown that both the absence of Serp and its overexpression gives rise to extralong tubes [15].

The regulation of Crb localisation in the trachea

Our work provides insights into Crb accumulation during morphogenesis and the role of recycling in the process. Crb requires the Retromer complex for recycling [41,42]. The Retromer complex is typically implicated in the retrieval of cargoes from endosomes to TGN via the retrograde pathway [33,35]. However, it was proposed that Rab9, required for TGN trafficking in the trachea, did not affect Crb accumulation [36]. Furthermore, in HeLa cells Crb2 undergoes a rapid recycling to the membrane without accumulating in the TGN [41]. Besides this role of Retromer in retrograde transport, a Retromer-mediated traffic directly from endosomes to the plasma membrane was also identified [43]. Rab4, which was known to participate in a rapid recycling pathway back to the membrane [30], associates with Retromer tubules for this direct traffic [43]. As Crb requires Retromer, does not undertake the retrograde pathway and is found in Rab4 endosomes, we propose that it undergoes a rapid direct recycling to the apical membrane regulated by Rab4/Retromer.

Both Serp and Crb require the Retromer complex for recycling, but they seem to undergo different Retromer-dependent pathways. How does the complex select the cargo? Retromer interacting proteins, like sorting nexins, might provide cargo specificity loading distinct transport intermediates, which nevertheless use the same core machinery for membrane budding and fission [32–35]. Interestingly, the nexin Snx27 has been shown to participate in the direct Retromer pathway to the plasma membrane. Snx27 is unique because it contains a PDZ domain that binds to PDZ-binding motifs (PDZbm) in cargo proteins [43,66]. Because Crb contains a PDZbm [67] and it is recycled through the retromer complex [41,42], we speculated that Snx27 could be involved in this process. We find that CG32758 is the ortholog of Snx27 in *Drosophila*. While more experiments are required to draw definitive conclusions, our preliminary data point to the participation of Snx27-CG32758 in Crb trafficking to plasma membrane, likely in a Rab4/Retromer dependent pathway.

Finally, our results indicate that during tracheal development Crb can concentrate in different subdomains of the apical membrane. At early stages it is strongly concentrated in the AFR, in direct contact with the lumen, and later it becomes enriched preferentially in the SAR. Accumulation of Crb in the SAR or more diffusely in the AFR has also been observed in other *Drosophila* ectodermal tissues [68] or in other organisms, as it is the case of mammalian Crb3 that is present both on the apical surface and at Tight Junctions [69]. Whether the specific subcellular apical localisation of Crb performs different functions (e. g. in the case of the trachea, SAR accumulation directing tube elongation while AFR accumulation maintaining apicobasal polarity) is an interesting issue that remains to be investigated. We find that the late enrichment of Crb in the SAR depends on Rab5-mediated endocytosis, as when it is blocked Crb remains high in all apical domain. Crb is internalised and accumulates in endosomes, which are abundant preceding SAR enrichment, from where a fraction of the internalised protein follows the degradation pathway and another fraction recycles back to the apical region. Crb apical recycling could depend on two different endocytic itineraries: A Rab4/Retromer pathway could recycle Crb rapidly to the apical membrane, preferentially to the AFR, while a longer loop involving Rab11-RE would also recycle Crb apically, preferentially to the SAR. Alternatively, our results are also consistent with a temporally regulated model, in which right after internalisation (stages 13 and 14) Crb is recycled by any of the two pathways preferentially to the AFR. As Rab4 involves a shorter loop it could be more relevant in this phase. In a later cellular context (from stage 15) the recycling is preferentially routed to the SAR. The involvement of these two recycling pathways, or different recycling phases, in Crb sorting may be a general mechanism. Actually, when endocytosis is prevented in 3D-MDCK cells Crb3 levels are increased and it is not able to relocalise from the apical domain to the Tight Junctions [70]. Understanding the molecular mechanisms regulating Crb accumulation, including its recycling, is a key question given the importance of Crb in organisms.

Materials and methods

Drosophila strains

The following stocks are described in Flybase: *y* ^{1}*w* ^{118} (wild type, WT), *UAS-Egfr*^{DN}, *UAS-Egfr*^{CA} (*UAS-Egfr*$^{\lambda top}$), *UAS-btl*^{DN}, *UAS-btl*^{CA} (*UAS-λbtl*), *UAS-Rab5*^{DN} (*UAS-Rab5*^{S43N}), *UAS-Rab5*^{CA} (*UAS-Rab5*^{Q88L}), *UAS-Rab4*^{DN}*-YFP* (*UAS-Rab4*^{S22N}*-YFP*), *UAS-Rab4*^{CA} (*UAS-RAB4*^{Q67L}), *Rab4*^{EYFP}, *UAS-Rab11*^{DN}*-YFP* (*UAS-Rab4*^{S25N}*-YFP*), *UAS-Crb*^{FL} (gift from E. Knust), *Crb*^{11A22}. *serp*^{RB} mutants and *UAS-Serp-CBD-GFP* were kindly provided by S. Luschnig. Knock in alleles *Crb*^{GFP}*-c* and *Crb*^{Cherry} were kindly provided by Y. Hong.

For overexpression in the trachea from invagination onwards we used *btlGal4* or *btlGal4-UAS-Src-GFP* (to mark tracheal cells with Src membrane protein). *AbdBGal4* was used to drive expression in the posterior part of the embryo.

Immunofluorescent stainings and dextran injections

Immunostainings were performed on embryos fixed in 4% formaldehyde for 20 minutes, except for E-Cadh stainings, for which embryos were fixed for 10 minutes. The following primary antibodies were used: mouse anti-EGFR Extracellular domain (1:500) from Sigma; mouse anti-Crb (Cq4) (1:20), rat anti-E-Cadh (DCAD2) 1:100 and mouse anti-Wash P3 (1:50) from Developmental Studies Hybridoma Bank, DSHB; rabbit anti-Serp (1:300) generously provided by S. Luschnig; rabbit anti-Rab11 (1:2000) and guinea pig anti-Rab5 (1:1000) were generously provided by T. Tanaka; guinea-pig anti-Uif (1:500) generously provided by R. Ward; rabbit or goat anti-GFP (1:600) from Molecular Probes and Roche used to visualise both GFP and YFP-tagged proteins; chicken anti-ßgal (1:300) from Abcam. Alexa Fluor 488, 555, 647 (Invitrogen) or Cy2-, Cy3-, Cy5-Conjugated secondary antibodies (Jackson ImmunoResearch) were used at 1:300 in PBT 0.5% BSA. CBP (Chitin Binding Protein) was visualised as a secondary antibody at 1:300. Rhodamine-labelled 10 KDa dextran injections were used for an in vivo endocytosis assay and were performed as described in [4].

Image acquisition

Fluorescence confocal images of fixed embryos were obtained with a Leica TCS-SPE system. Unless otherwise indicated, images shown are maximum projections of Z stack sections (0.2–0.4 μm). Images were imported into Fiji and Photoshop, and assembled into figures using Illustrator.

Time lapse movies

Dechorionated embryos were mounted and lined up on a Menzel-Gläser cover slips with oil 10-S Voltalef (VWR) and covered with a membrane (YSI membrane kit). Life imaging was performed on a Zeiss Lsm780 Confocal and Multiphoton System. For Movie 1 a 950 nm Multiphoton laser MaiTai HP DS was used. For movies 2–4 a 488 /514 nm Argon laser was used. In all movies we used an oil 63x/1.4 NA objective. To visualize time-lapse movies, maximal intensity projections are shown.

Morphometric analyses

Tube size. Confocal projections were used to analyse the length of the embryonic dorsal trunk (DT) stained with CBP in stage 16 embryos. We traced two paths using the freehand line selection tool of Fiji software between the junction DT/Transverse Connective (TC) from metamere 4 to 9, one following DT curvature and a straight one. DT length was expressed as the ratio between the real path and the straight line. A ratio of 1 reflects a straight DT.

Cell junction lengths. Cell junctions were classified according to the angles (tube axis set to 0˚), considering axial junctions those oriented 0˚±30˚ and circumferential junctions 90˚ ±30˚. The freehand line selection tool of Fiji software was used to measure the length of the junctions.

Crb intensity levels. Projections of confocal sections that include MT and a piece of DT were used for the analysis. $EGFR^{DN}/EGFR^{CA}$ transgenes were expressed in the tracheal cells by means of *btlGal4* but not in the MT. We measured the levels in pixels in each structure using the freehand line selection tool of Fiji, tracing a line including the whole tube (line with 60 for

DT and line with 10 for MT). Fluorescence intensity of Crb in the DT was normalised to the Crb levels in MT in each embryo. We compared the ratio of Crb levels in the trachea/MT among the experimental conditions and the internal control wild type embryos.

Crb subcellular accumulation. We quantified the total levels of Crb (using the Sum Fluorescent Intensity in Fiji) in different apical subcellular domains. We selected individual cells from the region of the DT between metameres 7 and 9, and generated projections of few sections to include only the whole cell or a small number of them. We quantified Crb in SAR by outlining the cell contour (using E-Cadh to visualise it) and Crb in AFR by drawing a freehand section inside. We express the subcellular accumulation as the ratio between SAR/AFR.

Crb Serp colocalization. Colocalisation analysis was performed using the ImageJ plugin Colocalisation highlighter, considering colocalisation when the ratio of fluorescence intensities between red and green channels was above 0.5. Those fluorescence intensities above the threshold appear in a binary image colour as white (colocalised points). From this mask, we selected manually each colocalised vesicle by wand tool in Fiji and added it in the ROI Manager. Thereafter, to analyse the colocalisation, a ratio between the number of pixels (integrated density) of one channel that colocalises with the marker in the other channel and the total number of pixels above the threshold measured for each channel was measured.

Analysis of cargoes/endosome. For each region of DT analysed, we counted in each stack the number of endosomes containing both Crb and Serp, Crb alone or Serp alone. We analysed the proportion of each type of vesicle.

Cell number. To count cell number, embryos were stained with anti-Uif, anti-laminin A and DAPI to label apical and basement membrane, and the nuclei of tracheal cells. To analyse the cell number, we counted in each stack the nuclei from the region of the DT between metameres 7 and 8 in stage 15–16 embryos. Images were obtained with Leica DMI6000 TCS-SP5 laser confocal microscope 63x/1.4 NA oil using 405 nm diode laser.

Quantifications and statistics

Total number of cells/embryos is provided in text and figures. Error bars indicate standard error (s.e.). *P*-values were obtained with an unpaired two-tailed Student's *t*-test using STATA 12.1 software. $^{*}P<0.05$, $0.001<^{**}P<0.01$, $^{***}P<0.001$.

Supporting information

S1 Fig. Quantification of tube size. (A-C) Lateral views of stage 16 embryos stained for GFP (green) and CBP (red) to visualise the lumen. Compare the elongated DT when EGFR is downregulated (*btlGal4-UASsrcGFP-UA SEGFR*^{DN}) to control (*UAS-EGFR*^{DN}) and to EGFR overactivation (*btlGal4-UASsrcGFP-UAS EGFR*^{CA}). Scale bar 50 μm. (D-G) Quantification of the length of the Dorsal Branch (DB) and the Transverse Connective (TC) of metamere 5 (D and E respectively), the Dorsal Trunk (DT) diameter measured in the region between tracheal metameres 7 and 8 (F) and the total length of the embryo measured from the most anterior to most posterior region (G). The measures are shown in (A). Note that only the diameter of the DT of EGFR^{CA} mutants is significantly different from the control, with a $P<0.05$ by Student's t-test. n refers to the number of embryos analysed. (H-K) Effects of Btl activity modulation. (H,J) Lateral views of stage 16 embryos stained for GFP (green) and CBP (red) to visualise the lumen. (I,K) Lateral views showing 2 tracheal metameres of stage 16 embryos stained with E-Cadh to visualise apical cell shape. The downregulation (*btlGal4-UASsrcGFP-UASbtl*^{DN}) or the constitutive activation of *btl* (*btlGal4-UASsrcGFP-UASbtl*^{CA}) does not give rise to tube elongation or cell shape defects. In contrast, defects of lack of terminal branching and fusion

are detected when *btl* is downregulated (arrows in H) and excess of terminal branching and missguidances are detected when *btl* is constitutively activated (arrows in J). Scale bar H 50 μm, I 10 μm.
(TIF)

S2 Fig. Accumulation of Serp in EGFR^{CA}. (A-F) Lateral views of control embryos and embryos carrying *btlGal4-UAS-EGFR^{CA}* at the indicated stages. Embryos are stained with Serp antibody. Serp is detected in the lumen (pink arrows) and in the apical membrane of tracheal cells (blue arrows). When EGFR is constitutively activated high levels of Serp are detected in the lumen. Scale bars A,F 10 μm, B-E 25 μm.
(TIF)

S3 Fig. Accumulation of Crb in EGFR mutants. (A-L) Lateral views of representative stage 16 control embryos or embryos expressing the indicated transgenes in the trachea (using *btlGal4*) stained for Crb. Panels include the DT of 3 tracheal metameres and a MT to compare Crb levels. Note that MT do not express EGFR constructs. Scale bar 25 μm. (M-O) Details of 1 single tracheal metamere of stage 16 embryos of the indicated genotypes stained for E-Cadh (green, white) to visualise the apical domain and Crb (red, white). Scale bar 7,5 μm.
(TIF)

S4 Fig. Accumulation of Crb in Rab mutants. (A,F) Lateral views of embryos of the indicated genotypes stained for Crb (red, white) and E-Cadh (green, white) or CBP (green, white) showing 1–2 tracheal metamere. Stages are indicated. (A) shows the last tracheal metamere, in contact with the spiracle. *btlGal4* expression limit is marked by a blue line. Note that while Crb vesicles are absent in the tracheal region, they are still detected in the spiracle (blue arrows). (A-D) Note that at early stages the pattern of Crb accumulation is similar to control when Rab11 or Rab4 are downregulated. (E,F) At late stages Crb is sharply accumulated in the SAR in Rab4^{DN} mutants. Scale bars A,E 10μm, B 5μm and F 7,5μm.
(TIF)

S5 Fig. Accumulation of Crb in EGFR mutants. (A-H) Lateral views of representative stage 14 control embryos or embryos expressing EGFR^{DN} in the trachea stained for E-Cadh (green, white) and Crb (red, white). Note that in EGFR^{DN} mutants the enrichment of Crb in the SAR is more conspicuous at this stage as compared to control embryos. Scale bar 7,5 μm.
(TIF)

S6 Fig. Accumulation of Crb, Serp and EGFR and EGFR requirement. (A-C') Lateral views of stage 14 WT embryos stained for Crb (red) and Serp (green). Each image in A,B,C corresponds to a single confocal stack. Panels marked with 1 and 2 correspond to the insets shown in A-C. Below, the same image is shown with a co-localisation point mask visualised in white. Note that many endosomes accumulate both Serp and Crb, but endosomes containing only Serp or Crb are also found. In endosomes containing both Crb and Serp, the two proteins are sorted into different endosomal domains, colocalising in a region (insets). Scale bar 5 μm. (D) Shows a scheme to represent the different type of vesicles found (Crb/Serp$_e$, Serp$_e$ and Crb$_e$). Crb and Serp partially colocalise (white). (E,F) Lateral views of st 14 embryos expressing EGFR^{DN} in tracheal cells. Endosomes are different from control, and Serp (E) and Crb (F) accumulate abnormally. Scale bar E 2,5 μm, F 5 μm. (G,H) Lateral views of *Crb^{Cherry}* embryos at stage 16. The embryos show a normal tracheal pattern (visualised with CBP in G) and normal cell organisation (visualised with E-Cadh in H). Scale bar G 50 μm, H 10 μm. (I) Lateral view of a stage 14 embryo carrying *btlGal4-UASserp-CBD-GFP* stained for Serp (red, white)

and GFP (green, white) showing 1 tracheal metamere. Note that Serp and GFP largely colocalise, indicating that Serp-CBD-GFP recapitulates Serp accumulation. Occasionally we find endosomes containing only endogenous Serp protein (red arrow in I) or Serp-CBD-GFP (green arrow in I; note that Serp antibody does not recognise Serp-CBD-GFP protein, [14]). Scale bar 5 μm. (J-L) Lateral views of stage 14 embryos stained for EGFR, Serp and/or GFP (in embryos carrying Crb^{GFP} in J,L). EGFR itself is found very often in Serp and/or Crb containing endosomes (white arrows). Scale bar J 5μm, K,L 2,5μm.
(TIF)

S7 Fig. (A-C) Time-lapse images of stage 17 embryos carrying *btlGal4-UASSerp-CBD-GFP* injected with rhodamine-labelled dextran in the different genetic backgrounds indicated. Intracellular dextran punctae largely co localise with Serp-CBD-GFP containing endosomes, indicating internalisation. Note that dextran internalisation is detected in downregulation and constitutively active conditions for EGFR. Also note that Serp-CBD-GFP/Dextran containing endosomes are abnormally big compared with the control when EGFR is downregulated (pink arrows in B). Scale bar 5 μm.
(TIF)

S1 Video. Crb apical subcellular accumulation. Embryo carrying Crb^{GFP} visualised from a lateral view using an inverted Zeiss Lsm780 confocal with 63x Oil objective and a 2 zoom. Images were taken every 2 minutes during 2,30 hours in 20 Z-stack of 0,5μm, from early stage 14 to stage 15. Note that at early stages Crb is detected in the AFR of DT cells (yelow arrow). As development proceeds Crb becomes enriched in the SAR (red arrows).
(AVI)

S2 Video. Rab4 and Crb accumulation. Stage 14 embryo carrying $Rab4^{EYFP}$ *and* Crb^{Cherry} visualised from a lateral view using an inverted Zeiss Lsm780 confocal with 63x Oil objective and a 2,5 zoom. Images were taken continuously in one single Z-stack during two minutes. Note that many Crb vesicles are also positive for Rab4 (white arrows).
(AVI)

S3 Video. Serp and Crb accumulation. Stage 14 embryo carrying *btlGal4-UAS-Serp-CBD-GFP and* Crb^{Cherry} visualised from a lateral view using an inverted Zeiss Lsm780 confocal with 63x Oil objective and a 2,5 zoom. Images were taken continuously in a single Z-stack during 3,5 min. Crb and Serp are highly dynamic, and move around the cell.
(AVI)

S4 Video. Serp and Crb accumulation. Stage 14 embryo carrying *btlGal4-UAS-Serp-CBD-GFP and* Crb^{Cherry} visualised from a lateral view using an inverted Zeiss Lsm780 confocal with 63x Oil objective and a 2,5 zoom. Images were taken continuously in a single Z-stack during 6 min. Crb and Serp are highly dynamic, and move around the cell.
(AVI)

Acknowledgments

We thank E. Fuentes and N. Martín for excellent technical help, and E. Rebollo from the MIP-IBMB-PCB facility for imaging expertise. We acknowledge the Developmental Studies Hybridoma Bank and the Bloomington Stock Centre for fly lines and antibodies. We thank S. Luschnig, E. Knust, T. Tanaka and Y. Hong for reagents and flies. Thanks also go to the members of the Llimargas lab for helpful discussions and J. Casanova, M. Furriols, S. Araújo, A. Letizia and M.I. Geli for critically reading the manuscript.

Author Contributions

Conceptualization: IOC ML.

Formal analysis: IOC.

Funding acquisition: ML.

Investigation: IOC ML.

Project administration: ML.

Supervision: ML.

Visualization: IOC ML.

Writing – original draft: ML.

Writing – review & editing: ML.

References

1. Baer MM, Chanut-Delalande H, Affolter M (2009) Cellular and molecular mechanisms underlying the formation of biological tubes. Curr Top Dev Biol 89: 137–162. https://doi.org/10.1016/S0070-2153(09)89006-6 PMID: 19737645
2. Lubarsky B, Krasnow MA (2003) Tube morphogenesis: making and shaping biological tubes. Cell 112: 19–28. PMID: 12526790
3. Ghabrial A, Luschnig S, Metzstein MM, Krasnow MA (2003) Branching morphogenesis of the Drosophila tracheal system. Annu Rev Cell Dev Biol 19: 623–647. https://doi.org/10.1146/annurev.cellbio.19.031403.160043 PMID: 14570584
4. Tsarouhas V, Senti KA, Jayaram SA, Tiklova K, Hemphala J, et al. (2007) Sequential pulses of apical epithelial secretion and endocytosis drive airway maturation in Drosophila. Dev Cell 13: 214–225. https://doi.org/10.1016/j.devcel.2007.06.008 PMID: 17681133
5. Song Y, Eng M, Ghabrial AS (2013) Focal defects in single-celled tubes mutant for Cerebral cavernous malformation 3, GCKIII, or NSF2. Dev Cell 25: 507–519. https://doi.org/10.1016/j.devcel.2013.05.002 PMID: 23763949
6. Forster D, Armbruster K, Luschnig S (2010) Sec24-dependent secretion drives cell-autonomous expansion of tracheal tubes in Drosophila. Curr Biol 20: 62–68. https://doi.org/10.1016/j.cub.2009.11.062 PMID: 20045324
7. Dong B, Hannezo E, Hayashi S (2014) Balance between apical membrane growth and luminal matrix resistance determines epithelial tubule shape. Cell Rep 7: 941–950. https://doi.org/10.1016/j.celrep.2014.03.066 PMID: 24794438
8. Dong B, Hayashi S (2015) Shaping of biological tubes by mechanical interaction of cell and extracellular matrix. Curr Opin Genet Dev 32: 129–134. https://doi.org/10.1016/j.gde.2015.02.009 PMID: 25819978
9. Devine WP, Lubarsky B, Shaw K, Luschnig S, Messina L, et al. (2005) Requirement for chitin biosynthesis in epithelial tube morphogenesis. Proc Natl Acad Sci U S A 102: 17014–17019. https://doi.org/10.1073/pnas.0506676102 PMID: 16287975
10. Tonning A, Hemphala J, Tang E, Nannmark U, Samakovlis C, et al. (2005) A transient luminal chitinous matrix is required to model epithelial tube diameter in the Drosophila trachea. Dev Cell 9: 423–430. https://doi.org/10.1016/j.devcel.2005.07.012 PMID: 16139230
11. Laprise P, Paul SM, Boulanger J, Robbins RM, Beitel GJ, et al. (2010) Epithelial Polarity Proteins Regulate Drosophila Tracheal Tube Size in Parallel to the Luminal Matrix Pathway. Curr Biol 20: 55–61. https://doi.org/10.1016/j.cub.2009.11.017 PMID: 20022244
12. Forster D, Luschnig S (2012) Src42A-dependent polarized cell shape changes mediate epithelial tube elongation in Drosophila. Nat Cell Biol 14: 526–534. https://doi.org/10.1038/ncb2456 PMID: 22446736
13. Nelson KS, Khan Z, Molnar I, Mihaly J, Kaschube M, et al. (2012) Drosophila Src regulates anisotropic apical surface growth to control epithelial tube size. Nat Cell Biol 14: 518–525. https://doi.org/10.1038/ncb2467 PMID: 22446737
14. Luschnig S, Batz T, Armbruster K, Krasnow MA (2006) serpentine and vermiform encode matrix proteins with chitin binding and deacetylation domains that limit tracheal tube length in Drosophila. Curr Biol 16: 186–194. https://doi.org/10.1016/j.cub.2005.11.072 PMID: 16431371

15. Wang S, Jayaram SA, Hemphala J, Senti KA, Tsarouhas V, et al. (2006) Septate-junction-dependent luminal deposition of chitin deacetylases restricts tube elongation in the Drosophila trachea. Curr Biol 16: 180–185. https://doi.org/10.1016/j.cub.2005.11.074 PMID: 16431370

16. Ozturk-Colak A, Moussian B, Araujo SJ, Casanova J (2016) A feedback mechanism converts individual cell features into a supracellular ECM structure in Drosophila trachea. Elife 5.

17. Shilo BZ (2003) Signaling by the Drosophila epidermal growth factor receptor pathway during development. Exp Cell Res 284: 140–149. PMID: 12648473

18. Shilo BZ (2014) The regulation and functions of MAPK pathways in Drosophila. Methods 68: 151–159. https://doi.org/10.1016/j.ymeth.2014.01.020 PMID: 24530508

19. Zeng F, Harris RC (2014) Epidermal growth factor, from gene organization to bedside. Semin Cell Dev Biol 28: 2–11. https://doi.org/10.1016/j.semcdb.2014.01.011 PMID: 24513230

20. Malartre M (2016) Regulatory mechanisms of EGFR signalling during Drosophila eye development. Cell Mol Life Sci 73: 1825–1843. https://doi.org/10.1007/s00018-016-2153-x PMID: 26935860

21. Brodu V, Casanova J (2006) The RhoGAP crossveinless-c links trachealess and EGFR signaling to cell shape remodeling in Drosophila tracheal invagination. Genes Dev 20: 1817–1828. https://doi.org/10.1101/gad.375706 PMID: 16818611

22. Kondo T, Hayashi S (2013) Mitotic cell rounding accelerates epithelial invagination. Nature 494: 125–129. https://doi.org/10.1038/nature11792 PMID: 23334416

23. Llimargas M, Casanova J (1999) EGF signalling regulates cell invagination as well as cell migration during formation of tracheal system in Drosophila. Dev Genes Evol 209: 174–179. PMID: 10079360

24. Nishimura M, Inoue Y, Hayashi S (2007) A wave of EGFR signaling determines cell alignment and intercalation in the Drosophila tracheal placode. Development 134: 4273–4282. https://doi.org/10.1242/dev.010397 PMID: 17978004

25. Llimargas M, Casanova J (1997) ventral veinless, a POU domain transcription factor, regulates different transduction pathways required for tracheal branching in Drosophila. Development 124: 3273–3281. PMID: 9310322

26. Wappner P, Gabay L, Shilo BZ (1997) Interactions between the EGF receptor and DPP pathways establish distinct cell fates in the tracheal placodes. Development 124: 4707–4716. PMID: 9409686

27. Cela C, Llimargas M (2006) Egfr is essential for maintaining epithelial integrity during tracheal remodelling in Drosophila. Development 133: 3115–3125. https://doi.org/10.1242/dev.02482 PMID: 16831830

28. Grant BD, Donaldson JG (2009) Pathways and mechanisms of endocytic recycling. Nat Rev Mol Cell Biol 10: 597–608. https://doi.org/10.1038/nrm2755 PMID: 19696797

29. Hsu VW, Bai M, Li J (2012) Getting active: protein sorting in endocytic recycling. Nat Rev Mol Cell Biol 13: 323–328. https://doi.org/10.1038/nrm3332 PMID: 22498832

30. Bhuin T, Roy JK (2014) Rab proteins: the key regulators of intracellular vesicle transport. Exp Cell Res 328: 1–19. https://doi.org/10.1016/j.yexcr.2014.07.027 PMID: 25088255

31. Wandinger-Ness A, Zerial M (2014) Rab proteins and the compartmentalization of the endosomal system. Cold Spring Harb Perspect Biol 6: a022616. https://doi.org/10.1101/cshperspect.a022616 PMID: 25341920

32. Burd C, Cullen PJ (2014) Retromer: a master conductor of endosome sorting. Cold Spring Harb Perspect Biol 6.

33. Gallon M, Cullen PJ (2015) Retromer and sorting nexins in endosomal sorting. Biochem Soc Trans 43: 33–47. https://doi.org/10.1042/BST20140290 PMID: 25619244

34. Seaman MN, Gautreau A, Billadeau DD (2013) Retromer-mediated endosomal protein sorting: all WASHed up! Trends Cell Biol 23: 522–528. https://doi.org/10.1016/j.tcb.2013.04.010 PMID: 23721880

35. Wang S, Bellen HJ (2015) The retromer complex in development and disease. Development 142: 2392–2396. https://doi.org/10.1242/dev.123737 PMID: 26199408

36. Dong B, Kakihara K, Otani T, Wada H, Hayashi S (2013) Rab9 and retromer regulate retrograde trafficking of luminal protein required for epithelial tube length control. Nat Commun 4: 1358. https://doi.org/10.1038/ncomms2347 PMID: 23322046

37. Letizia A, Sotillos S, Campuzano S, Llimargas M (2011) Regulated Crb accumulation controls apical constriction and invagination in Drosophila tracheal cells. J Cell Sci 124: 240–251. https://doi.org/10.1242/jcs.073601 PMID: 21172808

38. Gruenberg J (2001) The endocytic pathway: a mosaic of domains. Nat Rev Mol Cell Biol 2: 721–730. https://doi.org/10.1038/35096054 PMID: 11584299

39. Roeth JF, Sawyer JK, Wilner DA, Peifer M (2009) Rab11 helps maintain apical crumbs and adherens junctions in the Drosophila embryonic ectoderm. PLoS One 4: e7634. https://doi.org/10.1371/journal.pone.0007634 PMID: 19862327

40. Blankenship JT, Fuller MT, Zallen JA (2007) The Drosophila homolog of the Exo84 exocyst subunit promotes apical epithelial identity. J Cell Sci 120: 3099–3110. https://doi.org/10.1242/jcs.004770 PMID: 17698923

41. Pocha SM, Wassmer T, Niehage C, Hoflack B, Knust E (2011) Retromer controls epithelial cell polarity by trafficking the apical determinant Crumbs. Curr Biol 21: 1111–1117. https://doi.org/10.1016/j.cub.2011.05.007 PMID: 21700461

42. Zhou B, Wu Y, Lin X (2011) Retromer regulates apical-basal polarity through recycling Crumbs. Dev Biol 360: 87–95. https://doi.org/10.1016/j.ydbio.2011.09.009 PMID: 21958744

43. Temkin P, Lauffer B, Jager S, Cimermancic P, Krogan NJ, et al. (2011) SNX27 mediates retromer tubule entry and endosome-to-plasma membrane trafficking of signalling receptors. Nat Cell Biol 13: 715–721. https://doi.org/10.1038/ncb2252 PMID: 21602791

44. Tepass U, Theres C, Knust E (1990) crumbs encodes an EGF-like protein expressed on apical membranes of Drosophila epithelial cells and required for organization of epithelia. Cell 61: 787–799. PMID: 2344615

45. Gonzalez-Gaitan M (2003) Signal dispersal and transduction through the endocytic pathway. Nat Rev Mol Cell Biol 4: 213–224. https://doi.org/10.1038/nrm1053 PMID: 12612640

46. Jones S, Rappoport JZ (2014) Interdependent epidermal growth factor receptor signalling and trafficking. Int J Biochem Cell Biol 51: 23–28. https://doi.org/10.1016/j.biocel.2014.03.014 PMID: 24681003

47. Wortzel I, Seger R (2011) The ERK Cascade: Distinct Functions within Various Subcellular Organelles. Genes Cancer 2: 195–209. https://doi.org/10.1177/1947601911407328 PMID: 21779493

48. Yao Z, Seger R (2009) The ERK signaling cascade—views from different subcellular compartments. Biofactors 35: 407–416. https://doi.org/10.1002/biof.52 PMID: 19565474

49. Stasyk T, Schiefermeier N, Skvortsov S, Zwierzina H, Peranen J, et al. (2007) Identification of endosomal epidermal growth factor receptor signaling targets by functional organelle proteomics. Mol Cell Proteomics 6: 908–922. https://doi.org/10.1074/mcp.M600463-MCP200 PMID: 17293594

50. Lanzetti L, Rybin V, Malabarba MG, Christoforidis S, Scita G, et al. (2000) The Eps8 protein coordinates EGF receptor signalling through Rac and trafficking through Rab5. Nature 408: 374–377. https://doi.org/10.1038/35042605 PMID: 11099046

51. Tall GG, Barbieri MA, Stahl PD, Horazdovsky BF (2001) Ras-activated endocytosis is mediated by the Rab5 guanine nucleotide exchange activity of RIN1. Dev Cell 1: 73–82. PMID: 11703925

52. Robertson SE, Setty SR, Sitaram A, Marks MS, Lewis RE, et al. (2006) Extracellular signal-regulated kinase regulates clathrin-independent endosomal trafficking. Mol Biol Cell 17: 645–657. https://doi.org/10.1091/mbc.E05-07-0662 PMID: 16314390

53. Wilde A, Beattie EC, Lem L, Riethof DA, Liu SH, et al. (1999) EGF receptor signaling stimulates SRC kinase phosphorylation of clathrin, influencing clathrin redistribution and EGF uptake. Cell 96: 677–687. PMID: 10089883

54. Salcini AE, Chen H, Iannolo G, De Camilli P, Di Fiore PP (1999) Epidermal growth factor pathway substrate 15, Eps15. Int J Biochem Cell Biol 31: 805–809. PMID: 10481267

55. Zhou Y, Tanaka T, Sugiyama N, Yokoyama S, Kawasaki Y, et al. (2014) p38-Mediated phosphorylation of Eps15 endocytic adaptor protein. FEBS Lett 588: 131–137. https://doi.org/10.1016/j.febslet.2013.11.020 PMID: 24269888

56. Bryant DM, Kerr MC, Hammond LA, Joseph SR, Mostov KE, et al. (2007) EGF induces macropinocytosis and SNX1-modulated recycling of E-cadherin. J Cell Sci 120: 1818–1828. https://doi.org/10.1242/jcs.000653 PMID: 17502486

57. Miura GI, Roignant JY, Wassef M, Treisman JE (2008) Myopic acts in the endocytic pathway to enhance signaling by the Drosophila EGF receptor. Development 135: 1913–1922. https://doi.org/10.1242/dev.017202 PMID: 18434417

58. Chen DY, Li MY, Wu SY, Lin YL, Tsai SP, et al. (2012) The Bro1-domain-containing protein Myopic/HDPTP coordinates with Rab4 to regulate cell adhesion and migration. J Cell Sci 125: 4841–4852. https://doi.org/10.1242/jcs.108597 PMID: 22825871

59. Wertheimer E, Gutierrez-Uzquiza A, Rosemblit C, Lopez-Haber C, Sosa MS, et al. (2012) Rac signaling in breast cancer: a tale of GEFs and GAPs. Cell Signal 24: 353–362. https://doi.org/10.1016/j.cellsig.2011.08.011 PMID: 21893191

60. Sollier K, Gaude HM, Chartier FJ, Laprise P (2015) Rac1 controls epithelial tube length through the apical secretion and polarity pathways. Biol Open 5: 49–54. https://doi.org/10.1242/bio.015727 PMID: 26700724

61. Jazwinska A, Affolter M (2004) A family of genes encoding zona pellucida (ZP) domain proteins is expressed in various epithelial tissues during Drosophila embryogenesis. Gene Expr Patterns 4: 413–421. https://doi.org/10.1016/j.modgep.2004.01.003 PMID: 15183308

62. Jazwinska A, Ribeiro C, Affolter M (2003) Epithelial tube morphogenesis during Drosophila tracheal development requires Piopio, a luminal ZP protein. Nat Cell Biol 5: 895–901. https://doi.org/10.1038/ncb1049 PMID: 12973360

63. Sakaidani Y, Nomura T, Matsuura A, Ito M, Suzuki E, et al. (2011) O-linked-N-acetylglucosamine on extracellular protein domains mediates epithelial cell-matrix interactions. Nat Commun 2: 583. https://doi.org/10.1038/ncomms1591 PMID: 22158438

64. Nemetschke L, Knust E (2016) Drosophila Crumbs prevents ectopic Notch activation in developing wings by inhibiting ligand-independent endocytosis. Development 143: 4543–4553. https://doi.org/10.1242/dev.141762 PMID: 27899511

65. Roman-Fernandez A, Bryant DM (2016) Complex Polarity: Building Multicellular Tissues Through Apical Membrane Traffic. Traffic.

66. Steinberg F, Gallon M, Winfield M, Thomas EC, Bell AJ, et al. (2013) A global analysis of SNX27-retromer assembly and cargo specificity reveals a function in glucose and metal ion transport. Nat Cell Biol 15: 461–471. https://doi.org/10.1038/ncb2721 PMID: 23563491

67. Flores-Benitez D, Knust E (2016) Dynamics of epithelial cell polarity in Drosophila: how to regulate the regulators? Curr Opin Cell Biol 42: 13–21. https://doi.org/10.1016/j.ceb.2016.03.018 PMID: 27085003

68. Tepass U (1996) Crumbs, a component of the apical membrane, is required for zonula adherens formation in primary epithelia of Drosophila. Dev Biol 177: 217–225. https://doi.org/10.1006/dbio.1996.0157 PMID: 8660889

69. Makarova O, Roh MH, Liu CJ, Laurinec S, Margolis B (2003) Mammalian Crumbs3 is a small transmembrane protein linked to protein associated with Lin-7 (Pals1). Gene 302: 21–29. PMID: 12527193

70. Rodriguez-Fraticelli AE, Bagwell J, Bosch-Fortea M, Boncompain G, Reglero-Real N, et al. (2015) Developmental regulation of apical endocytosis controls epithelial patterning in vertebrate tubular organs. Nat Cell Biol 17: 241–250. https://doi.org/10.1038/ncb3106 PMID: 25706235